



MONASH University

Comparing and combining the anti-fibrotic effects of various current and emerging treatments in mouse models of kidney disease.

Matthew Shen

Bachelor of Science (Honours)

A thesis submitted for the degree of
Doctor of Philosophy
at Monash University in 2019
Department of Pharmacology

Copyright notice

I certify that I have made all reasonable efforts to secure copyright permissions for third-party content included in this thesis and have not knowingly added copyright content to my work without the owner's permission.

Table of Contents

Abstract	9
Declaration	11
Acknowledgements	12
Research output	14
Abbreviations	17
Chapter 1	20
1.0 Introduction	21
1.1 The anatomy and physiology of the kidneys	22
1.1.1 Function of the renin-angiotensin system (RAS) and Ang II	25
1.2 Kidney response to injury and disease	27
1.2.1 Normal tissue repair after injury.....	27
1.2.2 Chronic or severe injury leads to loss of kidney function	27
1.2.3 Mediators involved in tissue repair and fibrosis.....	28
1.2.3.1 Collagen.....	28
1.2.3.2 Matrix metalloproteinases (MMPs) & Tissue inhibitor of MMPs (TIMPs).....	31
1.2.3.3 Transforming growth factor (TGF)- β 1.....	34
1.2.4 Ang II receptors and implications for fibrosis	38
1.2.4.1 AT ₁ receptors and fibrosis.....	40
1.2.4.2 AT ₂ receptors and its anti-fibrotic role.....	41
1.2.4.3 AT ₄ receptor (IRAP) and its disease role.....	43
1.3 Current anti-fibrotic treatments	44
1.3.1 Other treatments for CKD	46
1.4 Novel treatments that will be investigated in this thesis	47
1.4.1 AT ₂ receptor agonists as novel anti-fibrotic treatments.....	47
1.5 IRAP as a novel anti-fibrotic target	50
1.5.1 Mechanistic actions of Ang IV	50
1.5.2 Synthetic IRAP inhibitors.....	52
1.5.3 HFI-419	54
1.6 Relaxin as a novel anti-fibrotic treatment strategy	55
1.6.1 History of relaxin.....	55
1.6.2 Relaxin family peptide receptors (RXFPs)	58

1.6.3 Relaxin as a drug-based therapy	59
1.6.4 Angiogenic effects of relaxin.....	62
1.6.5 Vasodilator effects of relaxin	63
1.6.6 Anti-inflammatory effects of relaxin.....	63
1.6.7 Anti-fibrotic actions of relaxin	64
1.6.8 Endothelial-to-mesenchymal transition-inhibitory effects of relaxin.....	65
1.6.9 Anti-fibrotic mechanism of relaxin	66
1.6.10 B7-33, a single-chain derivative of relaxin.....	69
1.7 Stem cells as treatments for CKD.....	70
1.7.1 Immunomodulatory effects of stem cells.....	71
1.7.2 Anti-apoptotic effects of stem cells	72
1.7.3 Angiogenic effects of stem cells.....	73
1.7.4 Stem cells alone and in combination in treating chronic diseases	73
1.7.5 Human amniotic epithelial cells (hAECs)	74
1.7.5 Limitation of stem cell-based therapies	75
1.8 Exosomes	76
1.9 Aims and Hypothesis.....	77
1.10 References	79
Chapter 2	109
2.0 Materials & Methods	110
2.1 Relaxin.....	110
2.2 Animals.....	110
2.3 High salt model	111
2.4 Unilateral ureteric obstruction (UUO) model.....	111
Figure 2.1 UUO surgery.....	112
2.5 Body weight & blood pressure measurements	112
2.6 Osmotic mini-pump implantation.....	112
2.7 Animal cull and tissue collection.....	113
Figure 2.2 Kidney collection and allocation for analysis	114
2.8 Tissue sectioning and morphometry	115
2.9 Immunohistochemistry.....	115
2.10 Immunofluorescence	117

2.11 Imaging and analysis	117
2.12 Protein analysis	119
2.12.1 Protein extraction	119
2.12.2 Protein assay	119
2.13 Gelatin zymography	120
2.14 Western blotting	121
2.14.1 PVDF Membrane stripping for reprobing	122
2.15 Hydroxyproline assay	123
2.16 Plasma urea.....	124
2.17 Statistical analysis	124
2.18 References	125
Chapter 3.....	126
3.1 Introduction	127
3.2 Materials and methods.....	129
Materials	129
3.2.1 Animals.....	129
3.2.2 Experimental design.....	129
3.2.3 Tissue collection.....	131
3.2.4 Kidney histopathology	132
3.2.5 Immunohistochemistry and Immunofluorescence.....	132
3.2.6 Morphometric analysis	132
3.2.7 Hydroxyproline assay	133
3.2.8 Gelatin zymography	133
3.2.9 Plasma urea.....	133
3.2.10 Statistical analysis	133
3.3 Results.....	134
3.3.1 The effects of HS and the treatments investigated on systolic blood pressure.	134
3.3.2 The effects of HS and the treatments investigated on measures of renal inflammation.	136
3.3.3 The effects of HS and the treatments investigated on glomerulosclerosis.	139
3.3.4 The effects of HS and the treatments investigated on interstitial and total renal collagen (fibrosis).	141
3.3.5 The effects of HS and the treatments investigated on TGF- β 1 staining.....	143

3.3.6 The effects of HS and the treatments investigated on myofibroblast differentiation and vascular rarefaction.	145
3.3.7 The effects of HS and the treatments investigated on gelatinase expression.	148
3.3.8 The effects of HS and the treatments investigated on TIMP-1 expression.	150
3.3.9 The effects of HS and the treatments investigated on plasma urea levels.	152
3.4 Discussion.....	154
3.5 References	161
Chapter 4.....	168
4.1. Introduction	169
4.2. Materials and methods.....	172
Materials	172
4.2.1 Animals.....	172
4.2.2 Experimental design.....	172
4.2.3 Tissue collection.....	174
4.2.4 Kidney histopathology	175
4.2.5 Immunohistochemistry and Immunofluorescence.....	175
4.2.6 Morphometric analysis	175
4.2.7 Hydroxyproline assay	176
4.2.8 Gelatin zymography	176
4.2.9 Western blotting	176
4.2.10 Plasma urea.....	177
4.2.11 Statistical analysis	177
4.3. Results	178
4.3.1 The effects of HS and the treatments investigated on systolic blood pressure and body weight.	178
4.3.2 The effects of HS and the treatments investigated on measures of renal inflammation.	180
4.3.3 The effects of HS and the treatments investigated on glomerulosclerosis.	183
4.3.4 The effects of HS and the treatments investigated on interstitial and total renal collagen (fibrosis).	185
4.3.5 The effects of HS and the treatments investigated on vascular rarefaction of peritubular capillaries.	188
4.3.6 The effects of HS and the treatments investigated on TGF- β 1 staining.	190
4.3.7 The effects of HS and the treatments investigated on renal myofibroblast accumulation. ...	192
4.3.8. The effects of HS and the treatments investigated on renal gelatinase expression levels. ...	194

4.3.9 The effects of HS and the treatments investigated on TIMP-1 expression.	196
4.3.10 The effects of HS and the treatments investigated on plasma urea levels.	198
4.4. Discussion.....	200
4.4.1 Renoprotective effects of the current standard of care treatments against HS-induced pathology.	200
4.4.2 Effects of novel treatments.....	202
4.4.3 Effects of combination treatments.	204
4.4.4 Conclusion	206
4.5. References	207
Chapter 5.....	214
5.1 Introduction	215
5.2 Methods	218
Materials	218
5.2.1 Animals.....	218
5.2.2 Experimental model and treatments.....	218
5.2.3 Tissue collection	221
5.2.4 Kidney histopathology	222
5.2.5 Immunohistochemistry and immunofluorescence.....	222
5.2.6 Morphometric analysis	222
5.2.7 Hydroxyproline assay	223
5.2.8 Gelatin zymography	223
5.2.9 Western blotting.....	224
5.2.10 Statistical analysis	224
5.3 Results	225
5.3.1 The effects of UUO and the treatments investigated on measures of renal inflammation.	225
5.3.2 The effects of UUO and the treatments investigated on interstitial and total renal collagen deposition (fibrosis).	228
5.3.3 The effects of UUO and the treatments investigated on KIM-1 staining.	230
5.3.4 The effects of UUO and the treatments investigated on renal peritubular capillary density.	232
5.3.5 The effects of UUO and the treatments investigated on renal TGF- β 1 staining.	234
5.3.6 The effects of UUO and the treatments investigated on renal myofibroblast differentiation.	236
5.3.7 The effects of UUO and the treatments investigated on MMP-2 expression.	238

5.3.8 The effects of UUO and the treatments investigated on TIMP-1 expression.....	240
Table 5.3.1: MMP-2/TIMP-1 ratio.....	242
5.4. Discussion.....	244
5.4.1 Therapies targeting the RAS in the setting of obstructive nephropathy.	244
5.4.2 Therapies targeting RXFP1 in the setting of obstructive nephropathy.	248
5.4.3 The therapeutic effects of exosomes and combination treatments in the setting of obstructive nephropathy.	250
4.4 Limitations and conclusion.	252
5.5 References	254
Chapter 6.....	262
6.0 General discussion	263
6.1 Summary of thesis.....	264
6.2 The limited renoprotection offered by candesartan or perindopril in normotensive disease settings.....	266
6.3 Novel treatments with alternative receptor targets provide better anti-fibrotic efficacy.....	268
6.5 Limitations and future directions.....	275
6.4 Final remarks.....	277
6.5 References	278
7.0 Appendix	288

Abstract

Renal fibrosis (scarring) is a hallmark of chronic kidney disease and is characterised by aberrant collagen production over dysregulated collagen degradation. The failure to resolve fibrosis induces severe organ dysfunction leading to end-stage renal failure. Currently-used pharmacological therapies that target the vasoconstricting effects of angiotensin II mainly offer symptomatic (anti-hypertensive) management of disease progression, but slow-acting tissue remodelling effects. Eventually, dialysis or kidney transplantation are often required to maintain renal function, both of which are financially exhausting and impact significantly on quality of life. The limited anti-fibrotic efficacy of currently-used treatments suggests a need for alternative treatments that directly target collagen turnover. This thesis aimed to compare and combine the anti-fibrotic effects of various novel and existing therapies in high salt diet (HS)- or unilateral ureteric obstructed (UUO)-induced murine models of normotensive kidney disease.

In Chapter 3, the renoprotective effects of the RXFP1 peptide hormone-agonist, relaxin (RLX; 0.5mg/kg/day), were compared and combined with either an AT₂R agonist, (CGP; 1.44 mg/kg/d), or AT₁ receptor blocker, candesartan cilexetil (CAND; 2mg/kg/day), in an 8-week model of HS (5% NaCl)-induced renal damage in male FVB/N mice. All treatments were administered from weeks 5-8 of the 8-week model, either by osmotic mini-pump (RLX, CGP) or drinking water (CAND) (n=8 mice/group). HS diet-fed mice underwent increased renal inflammation, glomerulosclerosis, interstitial and total collagen deposition, TGF- β 1 expression, myofibroblast differentiation, vascular rarefaction and plasma urea levels (renal dysfunction), compared to mice fed a normal salt (0.5% NaCl) diet (all $P < 0.05$ vs NS group). The kidney fibrosis in these mice was reduced to the greatest extent by RLX, while CGP had a greater effect in reducing renal inflammation and the contribution of inflammation to fibrosis; and both drugs demonstrated improved anti-fibrotic efficacy over CAND. Combining CAND with RLX compromised the renoprotective effects of RLX alone, while combining CGP with RLX retained the anti-inflammatory effect of CGP and anti-fibrotic effects of RLX; with RLX or CGP alone and both drugs combined being able to normalise plasma urea levels in the model studied.

Using the same 8-week HS model and treatment period employed in Chapter 3, in Chapter 4 the

renoprotective effects of RLX (0.5mg/kg/day) were compared to the IRAP inhibitor, HFI-419 (HFI; 0.72mg/kg/day), CAND (2mg/kg/day) or the ACE inhibitor, perindopril (PERIN; 4mg/kg/day) in male C57B6J mice. The effects of HFI were also combined with CAND, PERIN or RLX at the doses used individually; with all treatments being administered either by osmotic mini-pump (RLX, HFI) or drinking water (CAND, PERIN) (n=5-8 mice/group). Once again, HS-fed mice underwent significantly increased renal inflammation, fibrosis, vascular rarefaction and plasma urea levels compared to mice fed a normal salt (0.5% NaCl) diet (all $P < 0.05$ vs NS group). The renal fibrosis in this model was equivalently reduced by RLX or HFI alone or both combined, and to a greater extent than PERIN, and then over CAND. However, at the dose of PERIN administered, it induced hypotension and exacerbated renal failure. Combining HFI with CAND also compromised the renoprotective effects of HFI alone; whereas combining HFI with PERIN or RLX maintained the anti-fibrotic effects of either drug administered alone, respectively.

In Chapter 5, the preventative effects of RLX (0.5mg/kg/day), its single-chain derivative, B7-33 (0.25mg/kg/day; equivalent dose to RLX when corrected for molecular weight), HFI (0.72mg/kg/day), the AT₂R agonist, β -pro⁷-Ang III (BPRO; 0.1mg/kg/day), human amnion epithelial cells (hAECs; 1×10^6 cells) combined with RLX, hAEC-derived exosomes (EXO; 25 μ g), EXO+RLX were compared to that of PERIN (1mg/kg/day), in male C57B6J mice (n=6 mice/group). When the same end-point measures were performed (as per the HS model), UUO-injured mice had significantly increased renal damage, inflammation, fibrosis and vascular rarefaction by day 7 post-injury compared to their SHAM-control counterparts (all $P < 0.05$ vs SHAM group). The combined effects of EXO+RLX demonstrated optimal renoprotection over the other individual and combination therapies investigated, all of which demonstrated improved anti-fibrotic efficacy over the effects of PERIN.

In conclusion, this thesis has identified more effective anti-fibrotic therapies that can be used to treat fibrosis-induced CKD, including agonists that target the RXFP1 or AT₂ receptors, inhibitors of IRAP or the combined effects of EXO+RLX. In comparison, this thesis has confirmed the limited anti-fibrotic efficacy offered by ARBs or ACEi that can lower blood pressure.

Declaration

This thesis contains no material which has been accepted for the award of any other degree or diploma at any university or equivalent institution and that, to the best of my knowledge and belief, this thesis contains no material previously published or written by another person, except where due reference is made in the text of the thesis.

Signature:

Print Name: Matthew Shen

Date: 01-Jul-19

Acknowledgements

The reason I started my PhD journey was to personally see how chronic diseases could affect organ function and the quality of life for the elderly, hoping that I could contribute to making a change and finding a cure in some form or another. Towards the end of my PhD, I felt a little more secure that I was able to take a step in the right direction and would like to acknowledge all the incredible people that helped me close the gap towards my goal.

First and foremost, to everyone I've met during my years as a PhD student, whether it's through work or social activities, thank you all for being a part of this journey.

I want to express my sincere gratitude to my supervisor, Associate Professor Chrishan Samuel, and my co-supervisor, Professor Robert Widdop, for the continuous support of my PhD studies and related research, for their patience, motivation, and immense knowledge. Their guidance helped me throughout the research projects undertaken and writing of this thesis. I could not have imagined having a better advisory team for my PhD. To Chrishan, thank you for taking me on as an honours year, showing me how things are done, provide positive criticisms and putting up with all the SHENanigans I've pulled. Thank you for all the time and patience you provided me with and for giving me an opportunity to work in your lab. I would also like to thank Rob for letting me be a part of the department and a member of your lab as well, the fortnightly lab meetings that helped me keep on track, learn about new papers, receive validations and suggestions necessary for my experiments.

To Dr Tracey Gaspari, your constant cheerful and helpful attitude was always great to have around when working. Thank you so much for your life advice and for letting me bombard you with questions about HFI-419. To Dr Simon Royce, thank you for sharing your expertise in IHC with me, providing me with an opportunity to demonstrate in your Pathology unit and for not throwing me out of the buggy on our conference trip in Los Cabos. To Yan Wang, thank you so much for showing me how to do IF, WB and being a volunteer for my protocol videos. To Dr Brooke Huuskes, your constant positivity, optimism and energy were always a delight to be around. Thanks for teaching me how to perform the UUO surgery. Special thanks to Camila Cohen

and members of the Monash Histology Platforms for offering your histological services to help quantify my results.

I am also grateful to the teaching staff, Liz, Barb, Klaudia and Jen, for providing me with the opportunity to demonstrate throughout several semesters while conducting my PhD studies, as it was often a refreshing way to retreat from my lab work.

To the past and present graduate students: Peshy, John, Keshia, Ray, Emma, Kaki, Chao, Felipe, Vivian, Richard, May, and Tommy, each of you had helped and supported me in your own way and made this arduous journey tolerable. Thank you for all the social activities organized such as snow trips, D&D, games night, dinners etc. I would like to especially thank Maggie for starting this four-year exercise in sustained suffering with me and encouraging me to push on towards completion.

Finally, I would like to thank my family for their continuous encouragement throughout my years of study. This accomplishment would not have been possible without them. For any relatives who would read this acknowledgement page...for the last time, pharmacology is not pharmacy...so stop asking me to dispense drugs.

Scholarship acknowledgement

This research was supported by a Biomedical Discovery Institute Departmental Scholarship and an Australian Government Research Training Program (RTP) Scholarship.

Research output

Conference Abstracts

Shen M, Han A, Royce SG, Wang Y, Jones ES, Widdop RE, Samuel CS (2015) "Comparing the anti-fibrotic actions of an angiotensin AT1 receptor blocker and AT2 receptor agonist versus relaxin in a high-salt diet model of renal fibrosis." APSA-ASCEPT Joint Scientific Meeting, Hobart, TAS.

**Oral and Poster presentation*

Samuel CS, Royce SG, Huuskes BM, Patel KP, **Shen M**, Widdop RE, Ricardo SD, Hewitson TD (2015) "Serelaxin as an anti-fibrotic therapy: comparisons to current and other emerging treatments" 7th International conference on Relaxin and Related Peptides, Malaysia.

**Oral presentation presented by CS Samuel*

Shen M, Han A, Royce SG, Wang Y, Jones ES, Widdop RE, Samuel CS (2016) "Comparing the anti-fibrotic actions of an AT1 receptor blocker and AT2 receptor agonist and relaxin in a high-salt diet model of renal fibrosis." Biomed Link, Melbourne, VIC.

**Poster*

Shen M, Han A, Wang Y, Royce SG, Jones ES, Widdop RE, Samuel CS (2016) "Comparing the anti-fibrotic effects of serelaxin, CGP42112 and candesartan cilexetil in a high salt-induced mouse model of kidney disease." AAS-HBPRCA-AVBS Joint Annual Scientific Meeting, Hobart, TAS.

**Oral presentation*

Wang Y, **Shen M**, Han A, Jones ES, Widdop RE, Samuel CS (2016) "Comparing the anti-fibrotic effects of serelaxin, CGP42112 and candesartan cilexetil in a high salt-induced mouse model of heart disease." AAS-HBPRCA-AVBS Joint Annual Scientific Meeting, Hobart, TAS.

**Oral presentation by Wang Y*

Samuel CS, **Shen M**, Shastry A, Gaspari T, Widdop RE (2017) "Comparing the anti-fibrotic effects of the IRAP inhibitor, HFI-419, to a clinically used angiotensin receptor blocker and ACE inhibitor in a high salt-induced mouse model of kidney fibrosis." IRAP Conference, Paris, France.

**Oral presentation by Samuel CS*

Shen M, Shastry A, Wang Y, Gaspari T, Widdop RE, Samuel CS (2017) "Comparing the anti-fibrotic effects of emerging treatments: Serelaxin and the IRAP inhibitor, HFI-419 to a clinically-used ARB and ACE inhibitor in a high salt-induced mouse model of kidney disease." APSA-ASCEPT Joint Scientific Meeting, Brisbane, QLD.

**Oral presentation*

Shen M, Shastry A, Wang Y, Gaspari T, Widdop RE, Samuel CS (2018) "Comparing and combining the anti-fibrotic effects of serelaxin to the IRAP inhibitor, HFI-419, and to that of a clinically-used angiotensin receptor blocker and ACE inhibitor in a high salt-induced mouse model of kidney disease" 8th International Conference on Relaxin and Related Peptides, Los Cabos, Mexico.

**Oral presentation*

Gaspari T, **Shen M**, Wang Y, Shastry A, Siew Yeen C, Samuel CS, Widdop RE (2018) "Comparing anti-fibrotic effects of the Irapi inhibitor, HFI-419 to an angiotensin receptor blocker and Ace inhibitor in a high salt-induced mouse model of kidney disease." ISH Hypertension Scientific Meeting, Beijing, China.

**Oral presentation by Gaspari T*

Shen M, Chelvaretnam S, Huuskes BM, Gaspari T, Widdop RE, Samuel CS (2018) "Serelaxin enhances the renoprotective effects of human amnion epithelial cell-derived exosomes in a murine model of obstructive nephropathy." ASCEPT Annual Scientific Meeting, Adelaide, SA.

**Oral presentation*

Publications during PhD

Royce, SG, **Shen, M**, Patel, KP, Huuskes, BM, Ricardo, SD, Samuel, CS (2015). Mesenchymal stem cells and serelaxin synergistically abrogate established airway fibrosis in an experimental model of chronic allergic airways disease. *Stem Cell Res.* **15**: 495–505.

Royce, SG, Tominaga, AM, **Shen, M**, Patel, KP, Huuskes, BM, Lim, R, *et al.* (2016). Serelaxin improves the therapeutic efficacy of RXFP1-expressing human amnion epithelial cells in experimental allergic airway disease. *Clin. Sci.* **130**: 2151–2165.

Ng, HH, **Shen, M**, Samuel, CS, Schlossmann, J, Bennett, RG (2019). Relaxin and extracellular matrix remodeling: Mechanisms and signaling pathways. *Mol Cell Endocrinol.* **487**: 59-65.

Chow, BSM, Kocan, **M, Shen, M**, Wang, Y, Han, L, Chew, JY, Wang, C, Bosnyak, S, Mirabito-Colafella, KM, Barsha, G, Wigg, B, Johnstone, EKM, Hossain, MA, Pfleger, KDG, Denton, KM, Widdop, RE, Summers, RJ, Bathgate, RAD, Hewitson, TD, Samuel, CS (2019). AT1R-AT2R-RXFP1 Functional Crosstalk in Myofibroblasts: Impact on the Therapeutic Targeting of Renal and Cardiac Fibrosis. *J Am Soc Nephrol.* **30**: 1-18. doi: 10.1681/ASN.2019060597.

Abbreviations

ACE	angiotensin converting enzyme
ACEi	angiotensin converting enzyme inhibitor
AKI	acute kidney injury
Ang I	angiotensin I
Ang II	angiotensin II
Ang III	angiotensin III
Ang IV	angiotensin IV
ANOVA	analysis of variance
AP-1	activator protein-1
ARB(s)	angiotensin receptor blocker(s)
AT ₁ R	angiotensin II type 1 receptor
AT ₂ R	angiotensin II type 2 receptor
bFGF	basic fibroblast growth factor
BP	blood pressure
C21	compound 21
CCR	C-C motif chemokine receptor
CD31	cluster of differentiation 31
CGP	CGP42112
CKD	chronic kidney disease
CTGF	connective tissue growth factor
CVD	cardiovascular disease
CXCR	C-X-C motif chemokine receptor
DAB	3,3'-diaminobenzidine
DAPI	4'6'-diamidine-2-phenylindole
DPX	di-N-butyl phthalate in xylene
ECM	extracellular matrix
EGFR	epidermal-growth factor receptor

EMT	epithelial-mesenchymal transition
EndMT	endothelial-mesenchymal transition
eNOS	endothelial nitric oxide synthase
ERK1/2	extracellular signal-regulated kinase ½
ESC(s)	embryonic stem cell(s)
ESKD	end-stage kidney disease
EXO	stem cell-derived exosomes
GFR	glomerular filtration rate
GPCR(s)	G-protein-coupled receptor (s)
H2 relaxin	human gene-2 relaxin
hAEC(s)	human amniotic epithelial cell(s)
HP	hydroxyproline assay
i.r.	intrarenal injection
i.v.	intravenous injection
IF	immunofluorescence
IHC	immunohistochemistry
IL	interleukin
iPSC(s)	induced pluripotent stem cell(s)
IRAP	insulin regulated aminopeptidase
JNK	cJun N-terminal kinase
LDLa	low-density lipoprotein A
LGR	leucine-rich repeat containing G protein coupled receptor
LRR	leucine-rich repeats
Lys-Bk	lys-bradykinin
MAPK	mitogen-activated protein kinases
MMP(s)	matrix metalloproteinase(s)
mRNA	messenger ribonucleic acid
MSC(s)	mesenchymal stem cell(s)
NADPH	nicotinamide adenine dinucleotide phosphate

NF- κ B	nuclear factor kappa B
NO	nitric oxide
NOS	nitric oxide synthase
OCT	optimal cutting temperature
PBS	phosphate buffered saline
PDGF	platelet-derived growth factor
PFA	paraformaldehyde
pSmad	phosphorylated Smad
RAS	renin-angiotensin system
RLX	relaxin/Serelaxin
ROS	reactive oxygen species
RXFP	relaxin family peptide receptor
s.c.	subcutaneous delivery
SDS	sodium dodecyl sulphate
SEM	standard error of the mean
Smad	mothers against decapentaplegic homolog
TBS-T	Tris-buffered saline in Tween 20
TGF- β	transforming growth factor-beta
TIMP(s)	tissue inhibitor of matrix metalloproteinase(s)
TNF- α	tumour necrosis factor-alpha
T β R-I	TGF- β receptor type I
T β R-II	TGF- β receptor type II
UUO	unilateral ureteral/ureteric obstruction
VEGF	vascular endothelial growth factor
WB	western blot
α -SMA	alpha-smooth muscle actin

Chapter 1

General Introduction

1.0 Introduction

Chronic kidney disease (CKD) is increasingly being recognized as a global health issue. Worldwide, the number of deaths caused by CKD had increased by 82% from 1990 to 2010, ranking CKD from 27th to 18th place on the leading disease mortality list within the 2010 Global Burden of Disease study (Lozano *et al.*, 2012). Taking the degree of tissue injury to disease mortality into consideration, CKD was ranked second only to HIV and AIDS, with life lost due to premature mortality (82%) being the third highest behind HIV and AIDS (96%) and diabetes (93%) (Lozano *et al.*, 2012; Jha *et al.*, 2013). In Australia alone, CKD contributes to 14% of all deaths and 1 in 10 adults have CKD symptoms (Australian Bureau of Statistics, 2013, Chadban *et al.*, 2003). Financially, in 2004-2005, the total healthcare expenditure for CKD in Australia exceeded \$900 million – 1.7% of the healthcare budget with patients in Victoria paying an average of \$1,300 in out-of pocket expenses annually excluding substantial costs associated with self-management (Essue *et al.*, 2013). The progression of CKD ultimately results in the deterioration of kidney function and an increased risk of developing cardiovascular disease (CVD). Both CKD and CVD share a common hallmark, fibrosis, the accumulation of extracellular matrix (ECM), and in particular, collagen deposition eventually leading to end-stage renal failure (ESRF) (Weber, 2000; Edwards *et al.*, 2015; Longo *et al.*, 2015).

Fibrosis refers to the organ scarring that results from an aberrant wound healing response to kidney injury and is a significant contributor to renal dysfunction and failure. It is characterized by excessive extracellular matrix (ECM), and in particular, collagen accumulation is a pathological feature of CKD (Hewitson, 2009) and CVD (Kong *et al.*, 2014), irrespective of etiology. Numerous studies have shown that fibroblasts and other phenotypically similar mesenchymal cells are the predominant source of ECM, with *de novo* expression of α -smooth muscle actin (α -SMA) in these cells indicative of their differentiation into activated myofibroblasts (Darby and Hewitson, 2007). Despite fibrosis representing a significant health burden, there are currently no effective strategies that directly ameliorate its progression.

Current therapies for renal fibrosis offer symptomatic management of disease progression rather than effective treatment of kidney scarring. For example, angiotensin converting enzyme inhibitors (ACEi) and angiotensin receptor blockers (ARB) mainly lower blood pressure (BP) in treated patients by blocking the vasoconstricting effects of angiotensin II (Ang II) (Boor *et al.*, 2007), aldosterone receptor blockers mainly lower the increased blood volume and BP that is caused by abnormal levels of aldosterone (Coats, 2001), while statins act to lower cholesterol levels in the blood (Balakumar *et al.*, 2012). Although these therapies have been reported to demonstrate modest anti-fibrotic actions, they only delay end-stage organ failure by a couple of months (Schelbert *et al.*, 2014). Furthermore, these therapies can be associated with several side-effects when chronically administered. Hence, patients who progress to CKD and ESRF often require intensive medical support by dialysis or kidney transplantation, which places an enormous economic burden upon the patient and the healthcare system (Essue *et al.*, 2013). Therefore, novel pharmacological treatments that effectively attenuate fibrosis are greatly needed. This thesis aims to investigate the anti-fibrotic actions of several peptides- and stem cell-based therapies in experimental models of kidney disease that are associated with renal fibrosis.

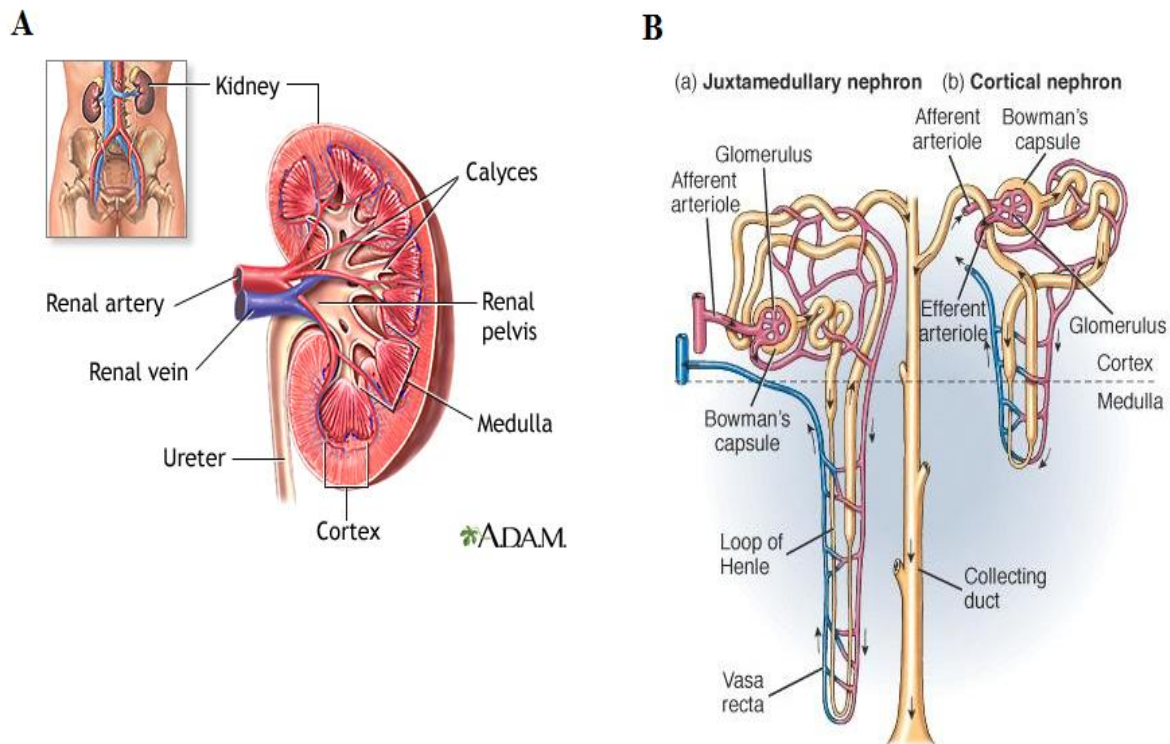
Before detailing the various novel anti-fibrotic treatments and strategies that will be investigated in this thesis, an understanding of how the kidney functions normally and after it has been affected by fibrosis will initially be outlined.

1.1 The anatomy and physiology of the kidneys

The kidneys are bean-shaped organs located retroperitoneally in the lower ribs of mammals. Kidneys are tasked to maintain body fluid balance and filter out toxic metabolic waste products from the blood by independent units known as nephrons (Bennett and Grunfeld, 1995; Sherwood, 2007). Each nephron is the structural and functional unit of the kidney and is made up of vascular components (including the afferent arteriole, glomerulus, efferent arteriole, peritubular capillaries) and tubular components (including the Bowman's capsule, loop of Henle, proximal tubule, distal tubule and the collecting duct) (Lemley and Kriz, 1991; Sherwood, 2007). Situated within the spaces between the vascular and tubular components are the interstitial compartment

that facilitates intrarenal fluid exchange, structural scaffolding and microvasculature compliance (Figure 1.1). Together, thousands of nephrons are interlinked by connective tissue that is located from the renal cortex to the renal medulla to maintain several kidney functions (Lemley and Kriz, 1991). It is estimated that an adult human kidney contains between 300,000 to 1.8 million nephrons, however, once nephrons are formed during birth, no new nephrons are created (Hartman *et al.*, 2007). Aside from disease states, ageing alone can cause progressive nephron loss, however, should be considered as separate to nephron loss from pathological conditions (Denic *et al.*, 2017). Due to filtration being highly energy demanding when any reduction in the supply of oxygen to the kidney is compromised, nephron loss can be predicted (Yang *et al.*, 2011). While nephrons do have some capacity for regeneration in acute experimental injury models and clinical settings of ischemia reperfusion injury, once a threshold is reached, the kidney undergoes irreversible damage and can progress into chronic kidney disease (Hoffmann *et al.*, 2002; Cochrane, 2005).

Figure 1.1:



The anatomy of the kidney – (A) the kidneys are located retroperitoneally in mammals. At the cortex of the kidneys is where thousands of nephrons are interlinked. (B) Nephrons are the individual units responsible for proper kidney function. Each nephron has vascular components (highlighted in red and blue) and tubular components (highlighted in yellow). Reproduced from <https://www.nlm.nih.gov/medlineplus/ency/imagepages/1101.htm>

1.1.1 Function of the renin-angiotensin system (RAS) and Ang II

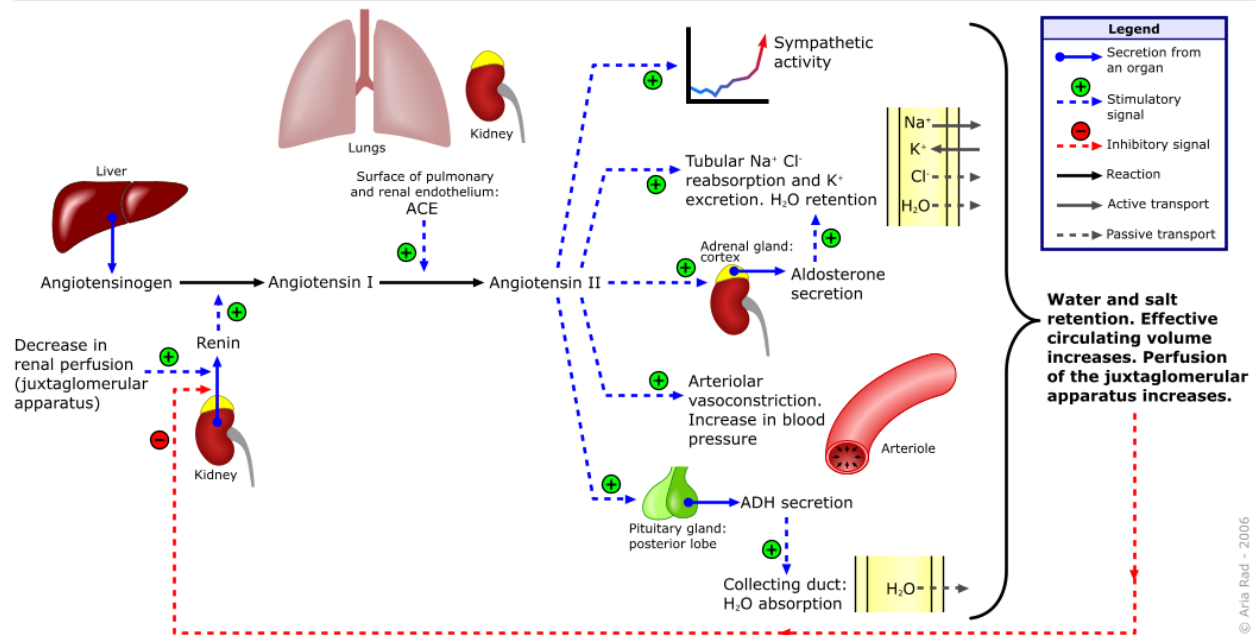
One key function of the kidneys is to maintain blood pressure by a central feedback system known as the pressure-natriuresis, whereby increasing renal perfusion pressure leads to increased sodium excretion with decreased sodium reabsorption (Granger *et al.*, 2002; Crowley and Coffman, 2014). The specific mechanism for tubular reabsorption and response to the renal perfusion pressure relies on the regulation of medullary blood flow, renal interstitial hydrostatic pressure and modulation of renal autocooids such as nitric oxide, prostaglandins, kinins and mostly Ang II (Granger *et al.*, 2002).

The renin-angiotensin system (RAS) is a multistep cascade which plays an integral role in maintaining pressure-natriuresis via the vasoconstricting peptide hormone, Ang II (Mezzano *et al.*, 2001; Crowley *et al.*, 2006). When renal injury results in a drop in blood pressure and reduced renal flow, renin, an aspartyl protease produced from the juxtaglomerular granular cells within the nephrons act on angiotensinogen secreted by the liver to undergo proteolytic cleavage to form angiotensin I (Ang I) (Silverthorn *et al.*, 2013). Subsequently, Ang I then stimulates angiotensin converting enzyme (ACE) from the surface of the renal endothelium to bind and convert Ang I into Ang II (Silverthorn *et al.*, 2013). Once upregulated, Ang II can stimulate various factors for sodium retention and increase arterial pressure (Figure 1.2). The RAS is often activated in response to pathological conditions associated with CVDs with decreased cardiac output, and to CKDs with renal injury that results in the stimulation of Ang II production to counteract the decreased blood pressure associated with injury (Silverthorn *et al.*, 2013).

Ang II is, however, a pleiotropic hormone (Mehta and Griendling, 2007). Studies have shown that during pathological conditions, Ang II binds to angiotensin type 1 (AT₁) receptors to promote renal growth factor in activating inflammatory cells, stimulating fibroblast proliferation and up-regulating the production of TGF- β 1 during tissue injury, which can result in further organ damage (Mezzano *et al.*, 2001; Sayeski and Bernstein, 2001).

Figure 1.2:

Renin-angiotensin-aldosterone system



Schematic illustration of the Renin-angiotensin system (RAS). RAS, also known as the renin-angiotensin-aldosterone system, is a multistep cascade which plays an integral role in salt retention and blood pressure regulation via the peptide hormone, angiotensin II which is converted from angiotensin I and its precursor angiotensinogen. Ang II promotes vasoconstriction, cell proliferation and inflammation, hypertrophy, oxidative stress and fibrosis by acting through the AT1 receptor. Reproduced from (Rad, 2006).

1.2 Kidney response to injury and disease

1.2.1 Normal tissue repair after injury

Following injury to the kidney, the body's innate immune system triggers a wound-healing response to counteract the insult (Wynn and Ramalingam, 2013). This initially results in an inflammatory reaction occurring within the tissue, which in turn, results in an influx of inflammatory cells to the site of damage. These inflammatory cells secrete and release various pro-inflammatory cytokines such as tumour necrosis factor (TNF)- α , interleukin (IL)-1, IL-4 and IL-13 (Becker and Hewitson, 2000; Atkins, 2002) as well as pro-fibrotic factors such as transforming growth factor (TGF)- β 1, connective tissue growth factor (CTGF) and platelet-derived growth factor (PDGF). The pro-inflammatory cytokines signal the recruitment and migration of matrix-producing fibroblasts to the site of injury to further the wound healing process. The pro-fibrotic factors, most notably TGF- β 1, then stimulate the differentiation of fibroblasts (which are normally low producers of ECM proteins, which act to maintain a slow and steady state of tissue turnover) into activated myofibroblasts, which (in contrast to fibroblasts) synthesize prodigious amounts of matrix proteins, such as collagen and fibronectin. Myofibroblasts can also produce matrix metalloproteinases (MMPs) and their natural inhibitors, the tissue inhibitors of metalloproteinases (TIMPs), which regulate the extent of matrix degradation (Angelica and Fong, 2013). Collagen aids in tissue repair as it provides a structural scaffold to accelerate wound healing. MMPs and TIMPs work together to maintain collagen homeostasis where MMPs breakdown collagen/fibronectin, while TIMPs regulate the activity of the MMPs. This balance of collagen production vs elimination keeps the structural scaffold of the organ during healing. After tissue repair is completed, myofibroblasts usually undergo apoptosis (Visse and Nagase, 2003) and are cleared from the repaired organ.

1.2.2 Chronic or severe injury leads to loss of kidney function

Although the kidneys are able to restore their structure and function in response to acute or minor injuries, the reparative effects of the organ are diminished when it is subjected to chronic

or severe injuries (Sherwood, 2007). Thus, repetitive insults, as in disease states, will cause structural damage and eventually, a loss of renal function (when that damage cannot be restored).

In the aftermath of a chronic renal injury via metabolic (diabetes), immunological (glomerulonephritis) and/or mechanical (hypertension) disease, aberrant wound healing occurs and persists (Edgley *et al.*, 2012). An excessive amount of the local pro-fibrotic mediator, TGF- β 1, is up-regulated after prolonged injury, consequently causing excessive collagen synthesis by activation of SMAD 2/3 signalling, which also down-regulates MMP activity (Derynck and Zhang, 2003; Liu, 2006). Thus, the prolonged stimulation of TGF- β 1 results in the continued activation of myofibroblasts (which instead of undergoing apoptosis, continue to secrete large amounts of ECM proteins), with a disrupted equilibrium of ECM homeostasis leading to extensive collagen accumulation and collagen-induced tissue scarring (fibrosis) (Eddy *et al.*, 2012). If the resulting fibrosis remains untreated or is poorly controlled, the progressive damage to the affected organ (such as the kidneys) becomes irreversible; and as a result, the organ will progressively deteriorate and ultimately fail to function (Liu, 2006).

1.2.3 Mediators involved in tissue repair and fibrosis

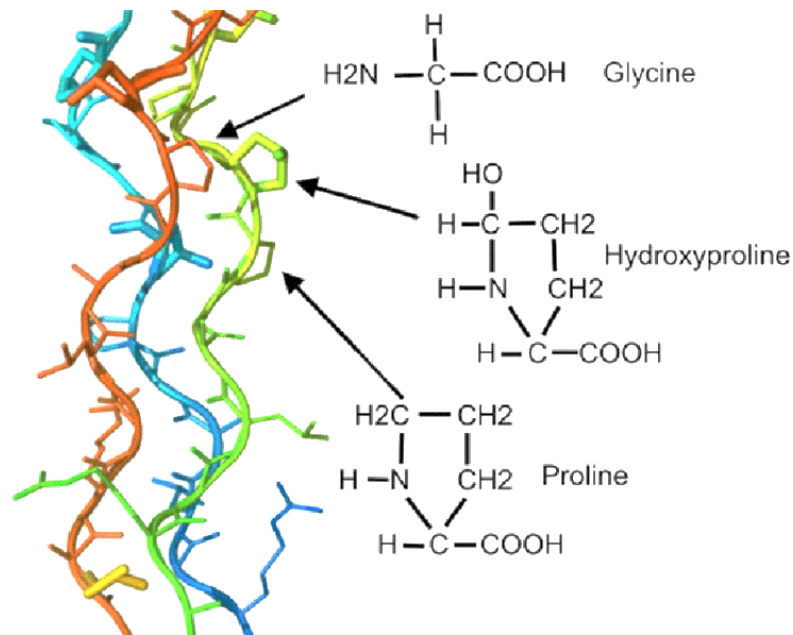
Tissue repair involves the coordination between various proteins and cytokines. In particular, collagen, MMPs, TIMPs and TGF- β 1 are critical for normal tissue repair. The following section will go over these four key elements in detail.

1.2.3.1 Collagen

Collagen is the most common protein-framework for all multi-cellular organisms, and is a rigid triple-stranded helical protein produced by myofibroblasts containing three alpha (α)-polypeptide chains composed of three amino acids: glycine, proline and hydroxyproline (Brodsky and Ramshaw, 1997) (Figure 1.3). Hydroxyproline is a unique amino acid found in collagen, making up ~12-20% of its protein structure and is seldom detected in other protein compositions within mammals (Brodsky and Persikov, 2005; Ricard-Blum, 2011). To date, there are eight major collagen families (Table 1.1) with the fibril-forming and basement membrane families often associated with the pathogenesis of fibrosis in the kidneys (Gelse *et al.*, 2003; Ricard-Blum, 2011).

Specifically, 70% of the kidneys are composed of components containing collagen IV while collagen types I and III are also found in CKDs accompanying renal tubulointerstitial fibrosis (Samuel *et al.*, 2005; Samuel and Hewitson, 2009).

Figure 1.3:



Collagen triple helix structure - the collagen protein is composed of 3 intertwined helices with two identical chains ($\alpha 1$) and one chain with a slightly different composition ($\alpha 2$). Each chain has a common motif in amino acid sequence, commonly including glycine, proline and hydroxyproline-repeats. The helices are stabilized by steric repulsion between proline rings and further stabilized by hydrogen bonding and covalent cross links of other chains. Adapted from (Berillis, 2015).

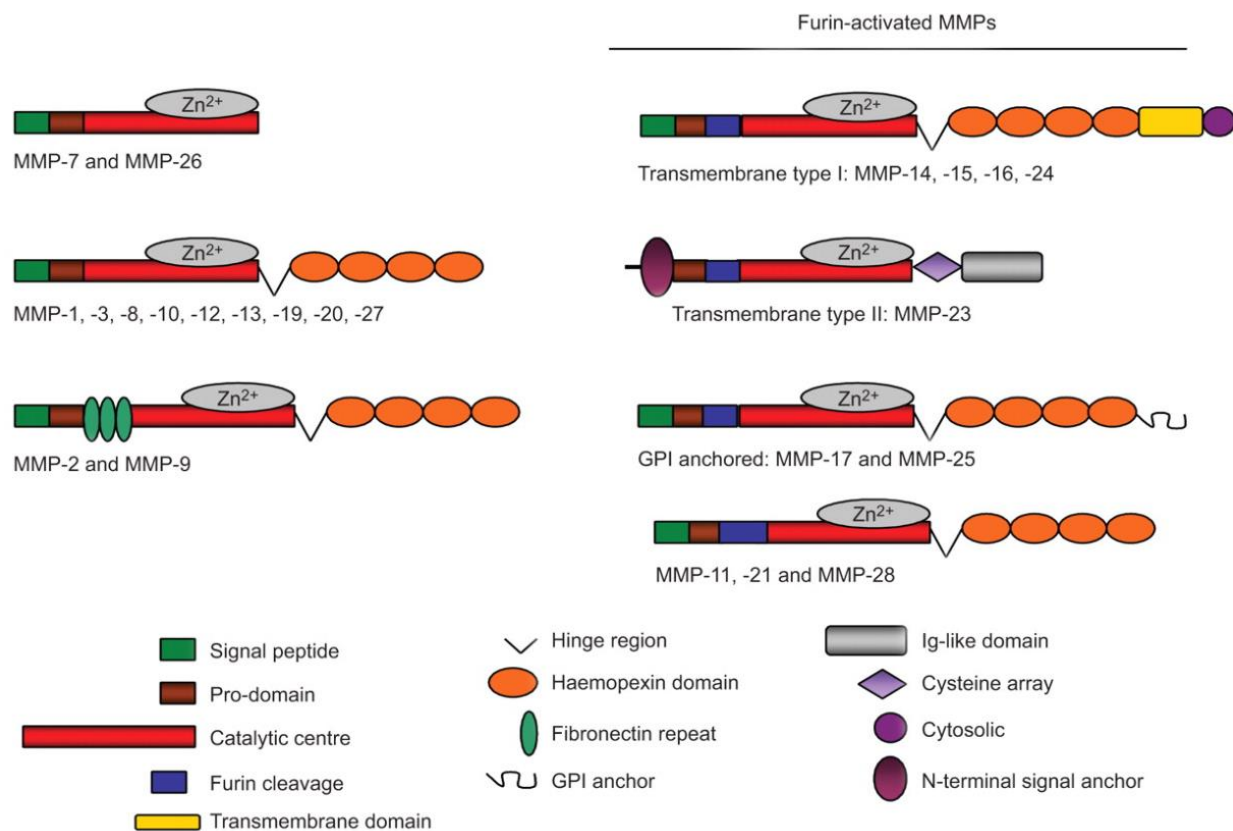
Table 1.1: Major collagen family and their distribution. Adapted from (Gelse *et al.*, 2003).

Collagen Family	Collagen Types	Distribution
Fibril-forming	I	Bone, dermis, tendon, ligaments, cornea, lungs, kidney, heart, nerves, uterus, liver, spleen
	II	Cartilage, vitreous body, nucleus pulposus
	III	Skin, vessel wall, reticular fibers of most tissues (lungs, liver, spleen etc.)
	V	Lung, cornea, bone, fetal membranes; together with type I collagen
	XI	Cartilage, vitreous body
Basement membrane	IV	Basement membranes
Microfibrillar	VI	Widespread: dermis, cartilage, placenta, lungs, vessel wall, intervertebral disc
Anchoring fibrils	VII	Skin, dermal- epidermal junctions; oral mucosa, cervix
Network-forming	VIII	Endothelial cells, Descemet's membrane
	X	Hypertrophic cartilage
Fibril-associated (FACIT)	IX	Cartilage, vitreous humor, cornea
	XII	Perichondrium, ligaments, tendon
	XIV	Dermis, tendon, vessel wall, placenta, lungs, liver
	XIX	Human rhabdomyosarcoma
	XX	Corneal epithelium, embryonic skin, sternal cartilage, tendon
	XXI	Blood vessel wall
Transmembrane	XIII	Epidermis, hair follicle, endomysium, intestine, chondrocytes, lungs, liver
	XVII	Dermal- epidermal junctions
Multiplexins	XV	Fibroblasts, smooth muscle cells, kidney, pancreas
	XVI	Fibroblasts, amnion, keratinocytes
	XVIII	Lungs, liver

1.2.3.2 Matrix metalloproteinases (MMPs) & Tissue inhibitor of MMPs (TIMPs)

As mentioned previously (in section 1.2.1), both MMPs and TIMPs are important regulators of collagen degradation, especially in the context of fibrosis. MMPs act as rate-limiting enzymes for ECM molecules which are important for creating cellular environments in development and tissue repair, particularly involving collagen (Visse and Nagase, 2003). MMPs are categorised into six families (Table 1.2) based on their substrate specificities. However, all MMPs have similar structures (Figure 1.4), including: i) a N-terminal signalling peptide which directs the secretion of MMPs into the extracellular space, ii) a pro-domain which contains a highly conserved cysteine switch motif that controls the activation state of the MMP and leaves it in an inactive conformation until removed, and iii) a catalytic centre which controls the proteolytic activity of the enzyme (Nagase *et al.*, 2006; Loffek *et al.*, 2010). From the six families, two main families of MMPs contribute to collagen degradation in the kidneys. These include the collagenases (MMP-1, MMP-8, MMP-13), which function to cleave interstitial collagens I, III and V at specific sites within the α -chains that constitute the collagen triple helix, into 3/4 and 1/4 fragments; and the gelatinases (consisting of gelatinase A (MMP-2) and gelatinase B (MMP-9), respectively), which readily digest the collagenase-digested collagen fragments into gelatin (denatured collagen) (Allan *et al.*, 1995; Visse and Nagase, 2003). In the kidneys, macrophages, fibroblasts, as well as tubular, mesangial, endothelial and epithelial cells contribute to MMP synthesis by activating serine proteases which cleave MMP pre-cursors, zymogens into its active form (Nagase, 1997). Once activated, MMPs function to aid in the angiogenesis, morphogenesis and removal of necrotic tissues during injury repair (Visse and Nagase, 2003; Nagase *et al.*, 2006). During kidney repair, renal fibroblasts promote the generation of collagenases and gelatinases. Both collagenases and gelatinases aid in the degradation of excessive collagen during inflammation and recovery to prevent further disease states (Nagase *et al.*, 2006; Ahmed, 2009).

Figure 1.4:



Structural features of matrix metalloproteinases (MMPs) – all MMPs contain a i) N-terminal signal peptide which directs the secretion of MMPs into the extracellular space, ii) a pro-domain which controls the activation state of the enzyme, and iii) a catalytic centre which controls the proteolytic activity of the enzyme. MMPs -7, -26 and -23 lack a C-terminal haemopexin domain which facilitates the binding to their inhibitors (TIMPs). Outside these common structural domains, different MMP subgroups have characteristics features. For example, MMP-2 and -9 uniquely contain 3 fibronectin repeats within their catalytic domain. Others have furin recognition site before their catalytic domain. Reproduced from (Loffek et al., 2010).

Table 1.2: Classification of matrix metalloproteinases (MMPs), substrate and renal distribution.
Adapted from (Visse and Nagase, 2003; Ahmed, 2009).

Family	MMP	Substrate	Renal Distribution
Collagenases	MMP-1	Collagen I, II, III, V, VII, VIII, X, XI, aggrecan, fibronectin gelatin, non-ECM proteins	Mesangial, endothelial, fibroblasts, macrophages
	MMP-8		
	MMP-13	Collagen I, II, III, V, VII, VIII, X, XI, aggrecan, fibronectin gelatin, non-ECM proteins Collagen I, II, III, IV, V, IX, X, XI, XIV aggrecan, fibronectin gelatin, non-ECM proteins	Neutrophils Fibroblasts
Gelatinases	MMP-2	Collagen I, II, III, V, VII, VIII, X, XI, aggrecan, fibronectin gelatin, laminin Collagen IV, V, VII, XI, XIV, aggrecan, gelatin	Mesangial, glomerular, epithelial, endothelial, fibroblasts, macrophages Same as MMP-2
	MMP-9		
Stromelysins	MMP-3	Collagen II, III, IV, V, VII, X, XI, fibronectin, gelatin, laminin	Mesangial, fibroblasts
	MMP-10	Collagen IV, aggrecan, fibronectin, laminin, elastin	Fibroblasts
	MMP-11	Collagen IV, aggrecan, fibronectin, gelatin, laminin	N.D.
Matrilysins	MMP-7	Collagen IV, aggrecan, fibronectin, gelatin, laminin, elastin	Mesangial, uterine, macrophages
	MMP-26	Collagen IV, fibronectin, gelatin	N.D.
Membrane-type	Transmembrane: MMP-14	Collagen I, II, III, fibronectin, gelatin, laminin	Mesangial, fibroblasts
	MMP-15	Collagen I, II, III, fibronectin, gelatin, laminin	N.D.
	MMP-16		N.D.
	MMP-24	Fibronectin, gelatin, laminin	N.D.
	GPI anchor: MMP-17	Collagen III, fibronectin, gelatin, laminin	N.D.

	MMP-25	Fibrin Gelatin	N.D.
Others	MMP-12	Collagen IV, fibronectin, elastin	N.D.
	MMP-19	Collagen IV, gelatin, elastin, fibrillin, aggrecan	N.D.
	MMP-20	Aggrecan	N.D.
	MMP-21	Aggrecan	N.D.
	MMP-23	Gelatin, casein, fibronectin	N.D.
	MMP-27	Gelatin	N.D.
	MMP-28	Unknown	N.D.

N.D. denotes not determined

On the other hand, TIMPs are the endogenous inhibitors of MMPs, and non-covalently bind onto the N-terminus domain of the specific MMPs that they inhibit (Visse and Nagase, 2003). To date, there are four known TIMPs which have been identified in vertebrates and their expression/activity are influenced by the presence of various cytokines and growth factors (Loffek *et al.*, 2010). Studies have extensively shown changes in TIMP levels directly influence the activity of all MMPs and are highly implicated in renal fibrosis (Eddy, 1996). Specifically, TIMP-1 inhibits MMP-1, MMP-13 and MMP-9 (and can also weakly inhibit MMP-2), while TIMP-2 is the primary inhibitor of MMP-2. Under normal physiological conditions, MMP activation is regulated via TIMPs with a ratio that favours ECM degradation. However, in pathological states such as fibrosis, a decrease in the activation of MMPs and higher TIMP levels leads to less degradation of ECM components (Visse and Nagase, 2003).

1.2.3.3 Transforming growth factor (TGF)- β 1

In CKD, numerous cytokines and growth factors are upregulated and involved in disease progression, including Ang II, interleukin-1 (IL-1), tumour necrosis factor (TNF)- α , platelet-derived growth factor (PDGF) and TGF- β 1 (Borthwick *et al.*, 2013). Of these cytokines, TGF- β 1 plays a

predominant role in promoting collagen accumulation in renal fibrosis. Thus, all the treatments assessed in this thesis will examine their effects against TGF- β 1 in relation to fibrosis.

TGF- β 1 is part of a large family of cytokines that have been thoroughly studied as the most influential inducers of fibrogenesis following organ injury and disease (Liu, 2006; Farris and Colvin, 2012). The pro-fibrotic effects of TGF- β 1 include: promoting the differentiation of fibroblasts into activated myofibroblasts, stimulating myofibroblast-induced synthesis of ECM components and inhibiting MMP activity while upregulating TIMP activity, thereby reducing ECM degradation via Smad 2/3 signalling (Figure 1.5)(Cheng and Grande, 2002; Liu, 2006; Hewitson *et al.*, 2007). TGF- β 1 can also promote epithelial cell (EMT)- and endothelial cell (EndMT)-to-mesenchymal cell transition. Although TGF- β has 3 isoforms: TGF- β 1, TGF- β 2 and TGF- β 3; TGF- β 1 is largely implicated as the primary pro-fibrotic stimulus with increased expression of its type I and II receptors being reported during chronic renal injury (Cheng and Grande, 2002). Even though TGF- β 1 is associated with fibrosis, it also serves as a pleiotropic cytokine for several normal physiological functions. It has been shown to be an anti-inflammatory mediator, promote growth and wound healing, neuron and ganglion cell protection as well as regulate other cytokines for the proliferation of epithelial cells (Cheng and Grande, 2002; Derynck and Zhang, 2003; Liu, 2006; Walshe *et al.*, 2011). Thus, if TGF- β 1 is completely inhibited, it can result in severe inflammatory responses and possible cancer growth due to unregulated cell proliferation.

Nevertheless, the overexpression of TGF- β 1 and its receptors has been associated with the progression of fibrosis and related organ damage (Cheng and Grande, 2002). TGF- β 1 can be produced by inflammatory macrophages, mesangial cells and myofibroblasts, and is often accompanied by the presence of other cytokines, in particular Ang II which has also been shown to promote pro-fibrotic effects through TGF- β 1-dependent and independent pathways (Cheng and Grande, 2002; Farris and Colvin, 2012).

TGF- β 1 can contribute to renal fibrosis through several signalling pathways. TGF- β 1 signal transduction first occurs after it binds to its receptors, which are composed of two distinct

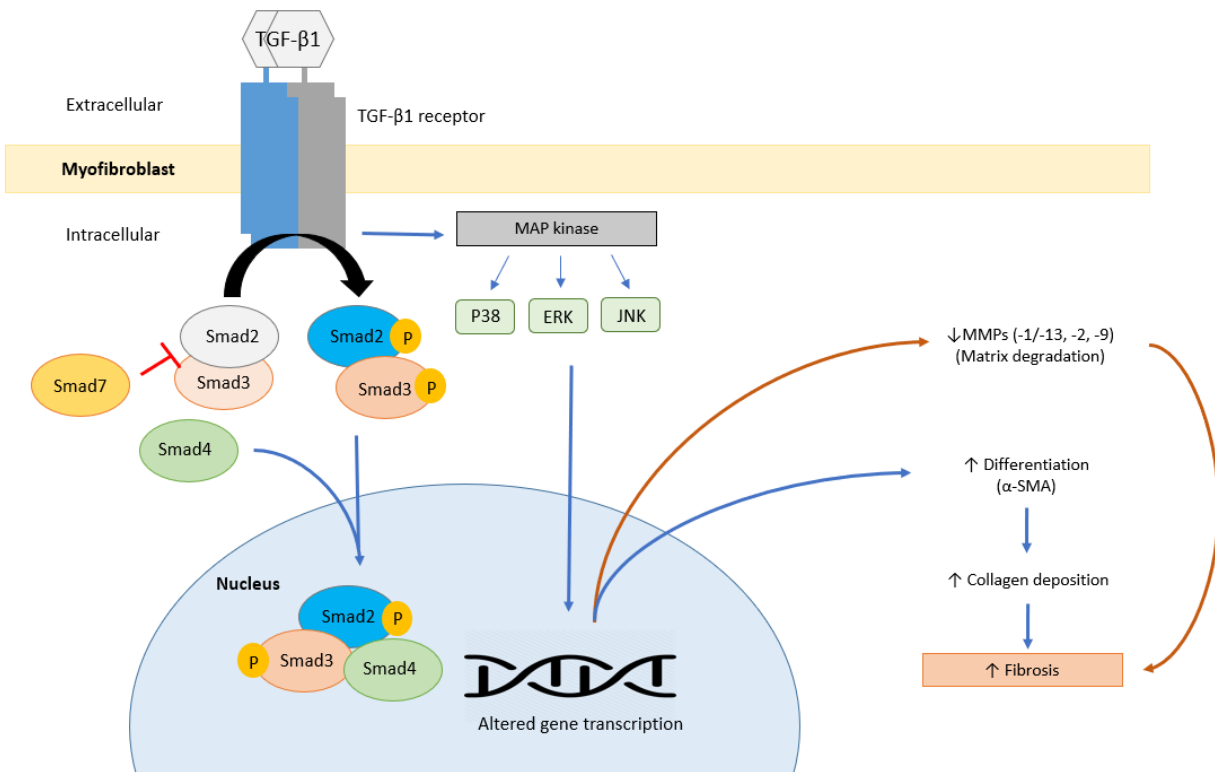
transmembrane proteins, type I (T β R-I) and type 2 (T β R-II), which form a heteromeric receptor complex (Attisano and Wrana, 2002; Derynck and Zhang, 2003). If TGF- β 1 is absent, each receptor exists as a homodimer in an inactive state (Attisano and Wrana, 2002; Zhang, 2009). Only when TGF- β 1 binds to the T β R-II receptor does it stimulate the dimerization of T β R-II with T β R-I to form a functional receptor complex to initiate downstream signalling (Attisano and Wrana, 2002; Derynck and Zhang, 2003; Zhang, 2009).

TGF- β 1 signalling primarily occurs through Smad-dependent signalling, but can also occur through mitogen-activated protein kinases (MAPK) (Derynck and Zhang, 2003), which will be discussed later. The former signalling pathway involves the intracellular proteins, Smads 2, 3 and 4 mediating the matrix remodelling effects of TGF- β 1 in the kidneys (Zhang, 2009). As illustrated in Figure 1.5, once TGF- β 1 binds to its receptor complex, it stimulates the phosphorylation of Smad2 and Smad3 which complex together and translocate towards the cell nucleus, to activate transcription factors that stimulate collagen and fibronectin production: which forms the basis of fibrosis (Liu, 2006; Samuel and Hewitson, 2009). On their translocation towards the nucleus, phosphorylated Smad2/3 oligomerizes with Smad4 to form a Smad2/3/4 complex, which then translocates and interacts with nuclear factor kappa B (NF- κ B) and activated protein (AP)-1 to promote the differentiation of fibroblasts into myofibroblasts as well as the synthesis and deposition of collagen and fibronectin (Li *et al.*, 2015). On the other hand, Smad7 within the pathway acts as an inhibitory protein to prevent phosphorylation and activation of Smad2 at TGF- β 1 receptors and also recruits ubiquitin ligases (Smurf 1 and 2) to induce proteasomal degradation of Smad complexes when there is an overexpression and/or activity of TGF- β 1 (Derynck and Zhang, 2003). However, in disease states during fibrogenesis, Smad7 and related endogenous inhibitors are often down-regulated, resulting in a further increase in TGF- β 1/Smad2/3/4-mediated rise in gene transcription of various ECM proteins (Derynck and Zhang, 2003; Li *et al.*, 2015).

Outside Smad2/3/4, TGF- β 1 can signal through a number of MAPK, including P38 MAPK, extracellular signal-regulated kinase (ERK) and/or cJun N-terminal kinase (JNK), which have also

been implicated in promoting ECM production (Derynck and Zhang, 2003). In particular, p38 MAPK has been shown to be involved in the promotion of various collagens, while JNK has been shown to be involved in the promotion of fibronectin (Choi *et al.*, 2012). MAPK activation has also been shown to result in the activation/phosphorylation of Smads suggesting possible crosstalk of these pathways to increase TGF- β 1 responses (Derynck and Zhang, 2003; Zhang, 2009; Li *et al.*, 2015). Furthermore, the inclusion of MAPK activity contributes to regulating TGF- β 1-induced EMT and/or EndMT, which is essentially tubular cells acquiring a mesenchymal phenotype and re-differentiate into myofibroblasts to increase collagen production (Zhang, 2009). In addition, accumulating literature has also found that the pro-fibrotic properties of TGF- β 1 can also be regulated by other factors including Ang II. Hence treatments that target the involvement of Ang II will also be examined and discussed in this thesis (Kagami *et al.*, 1994; Mezzano *et al.*, 2001; Widdop *et al.*, 2003; Rodrigues Díez *et al.*, 2010; Wang *et al.*, 2017b)

Figure 1.5:



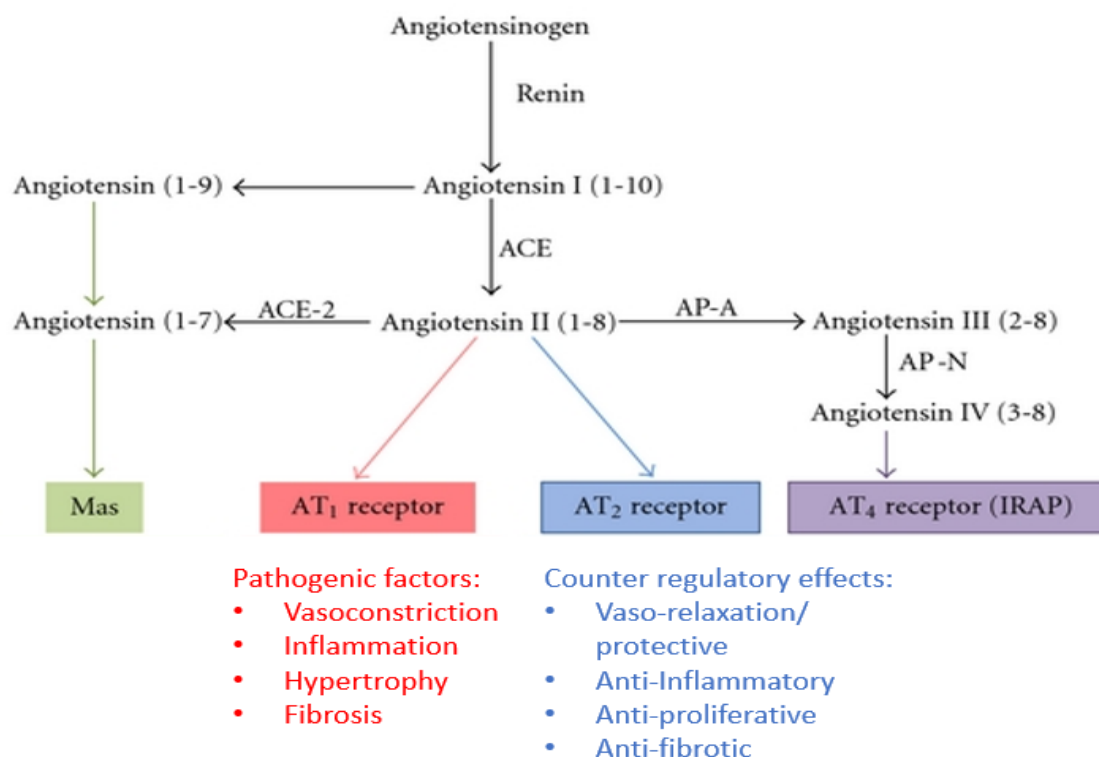
Schematic illustration of TGF-β1 signal transduction in myfibroblasts. Once TGF-β1 binds to the TβR-II and TβR-I heteromeric receptors, intracellular Smad 2/3 become phosphorylated and subsequently form a heteromeric complex with Smad4, which translocates to the cell nucleus to regulate various transcription factors (ie. Nuclear factor kappa-light-chain-enhancer of activated B cells (NF-κB), activator protein-1) and promotion of myfibroblast differentiation (which can be detected by α-SMA) leading to collagen production and inhibit MMP production. Other Smads such as Smad7, can negate TGF-β1 signalling by inhibiting the phosphorylation of Smad2. In addition, several non-Smad pathways may also be activated, including p38 MAPK, JNK and ERK; which contribute to fibrosis independently or through cross-talk with the Smad2/3/4 complex. Adapted from (Chow et al., 2014; Li et al., 2015).

1.2.4 Ang II receptors and implications for fibrosis

As mentioned above in Section 1.1.1, Ang II is also a pleiotropic hormone in which its activity is dependent on the type of receptor it stimulates. Aside from its up-regulation and activation in

response to a drop in blood pressure or organ damage, Ang II has also been shown to be a potent growth factor during pathological conditions, promoting fibrogenesis via acting on AT₁ receptors (De Gasparo *et al.*, 2000). In contrast, Ang II can also bind to AT₂ receptors with similar affinity, which elicits opposing and beneficial effects (Figure 1.6)(De Gasparo *et al.*, 2000; Mezzano *et al.*, 2001). To date, there are currently four known Ang II receptor subtypes within the RAS, with AT₁ and AT₂ receptors being the most widely studied in relation to the actions of Ang II in pathological conditions (De Gasparo *et al.*, 2000). Only the relevance of the AT₁, AT₂ and AT₄ receptors will be discussed further, as this thesis will compare various drugs that specifically target these receptors.

Figure 1.6:



Schematic illustration of the RAS and receptors that Ang II and its metabolites can target. Ang II mainly acts on AT₁ receptors to mediate various actions that eventually contribute to the pathogenesis of CKDs and CVDs. During diseased states, Ang II can also bind to up-regulated AT₂ receptors, which provides counter regulatory effects and suppression of its actions at AT₁ receptors. Ang II can also be broken down to Ang III and Ang IV, the latter of which can interact with AT₄ receptors, now recognised as the enzyme, IRAP. Adapted from (Guimond and Gallo-Payet, 2012).

1.2.4.1 AT₁ receptors and fibrosis

AT₁ receptors are G-protein coupled receptors (GPCRs) which mainly mediate the vasoconstricting, pro-inflammatory, hypertrophic and pro-fibrotic actions of Ang II. In humans, AT₁ receptors are encoded by a single gene, whereas in rodents there are two homologous AT₁ receptor genes which encode for AT_{1A} and AT_{1B} subtypes of AT₁ receptors (Sayeski *et al.*, 1998). Nevertheless, both subtypes only differ in their tissue localization with their binding and signalling being identical to their human counterpart (Sayeski *et al.*, 1998). In the kidneys, AT₁

receptors are expressed abundantly within the glomerulus, proximal tubule, cortex and interstitium (De Gasparo *et al.*, 2000). During renal injury, AT₁ receptors activate the inflammatory process by direct chemotaxis and production of pro-inflammatory and pro-fibrotic mediators such as MCP-1 and TGF- β 1, respectively (De Gasparo *et al.*, 2000; Mezzano *et al.*, 2001). Upon activation of AT₁ receptors, the receptor triggers a signalling sequence involving the increased production of nicotinamide adenine dinucleotide phosphate (NADPH) oxidase-mediated reactive oxygen species (ROS), transactivation of epidermal-growth factor receptor (EGFR) and the activation of MAPK signaling to promote the actions of TGF- β 1 (De Gasparo *et al.*, 2000). From there, TGF- β 1 can continue to act as a positive feedback to Ang II activity and follow through to increase collagen production, which forms the basis of renal fibrosis.

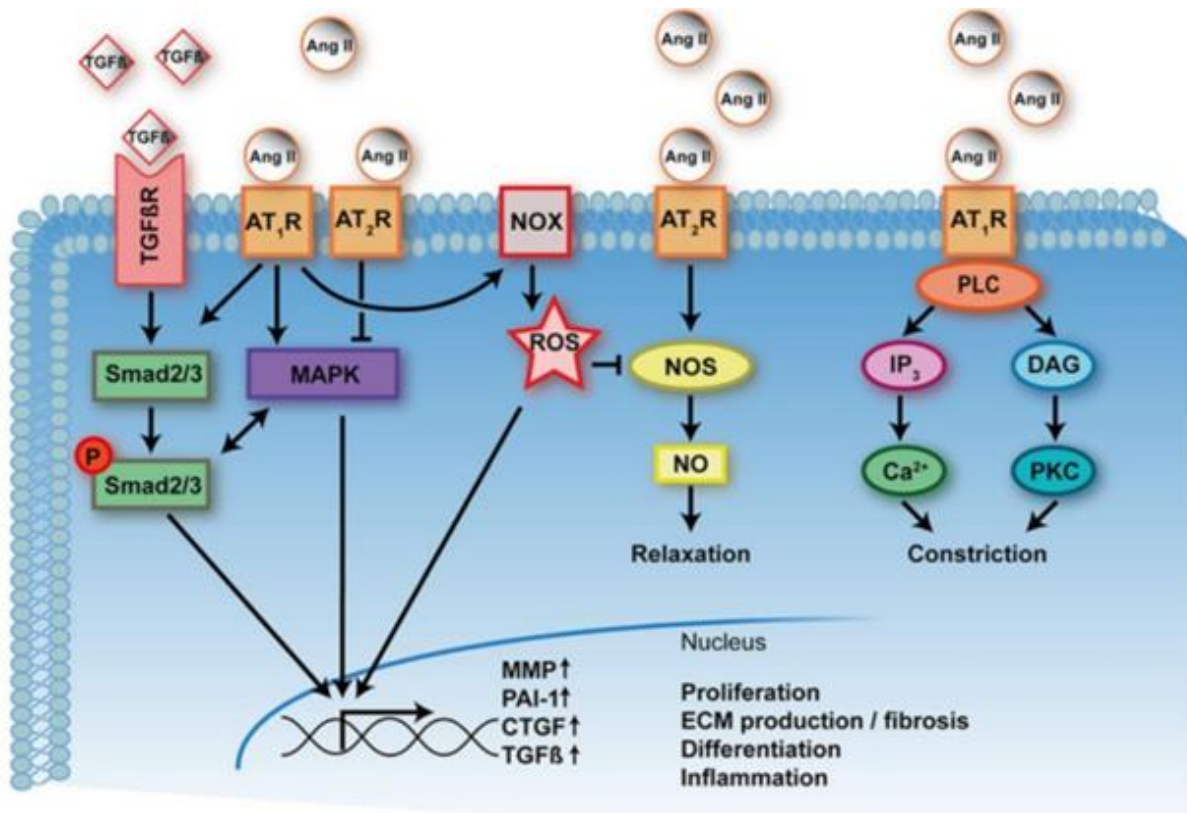
1.2.4.2 AT₂ receptors and its anti-fibrotic role.

On the other hand, although AT₂ receptors are GPCRs and are structurally similar to other GPCRs, the signalling pathways associated with its activation are not fully understood (Mezzano *et al.*, 2001; Jones *et al.*, 2008) (Figure 1.7). Moreover, unlike the abundance of AT₁ receptor expression within adult kidneys, AT₂ receptors are consistently detected in low abundance within glomerular mesangial cells, preglomerular arteries and tubular interstitium in adults (from being highly expressed in embryonic and fetal tissues), but significantly up-regulated during tissue injury or diseased states (De Gasparo *et al.*, 2000). Nevertheless, activation of AT₂ receptors have been shown to elicit organ-protection through anti-inflammatory, anti-hypertrophic, anti-fibrotic, vasodilatory, and pro-apoptotic properties (Arima and Ito, 2000; De Gasparo *et al.*, 2000).

Studies have shown that activation of AT₂ receptor can initiate at least three classical signalling pathways, involving nitric oxide (NO)/cGMP, protein phosphatases and phospholipase A2 signalling (Mezzano *et al.*, 2001). By signalling through nitric oxide and increased cGMP production, activation of the AT₂ receptor attenuates the vasoconstrictor and hypertrophic effects produced by the AT₁ receptor (Morrissey and Klahr, 1999; Mezzano *et al.*, 2001). Furthermore, as NO/cGMP have been found to suppress Smad2/3 phosphorylation (Saura *et al.*, 2005), AT₂ receptor-dependent NO/cGMP signalling can also inhibit the pro-fibrotic actions of the

AT₁ receptor/TGF-β1 axis. This implicates a regulatory role of AT₂ receptors acting to antagonize the effects mediated by AT₁ receptors (Yang *et al.*, 2012). This was further confirmed by additional studies conducted on AT₂ receptor knockout mice which showed increased AT₁ receptor activity associated with elevated blood pressure and collagen deposition (fibrosis). Similar findings were obtained when AT₂ receptor activity was pharmacologically blocked with a specific AT₂ receptor antagonist, PD123319 (Morrissey and Klahr, 1999). Taken together, these findings demonstrate both AT₁ and AT₂ receptors elicit opposing responses from Ang II activation. It is likely that Ang II binds to the higher levels of AT₁ receptors that are normally expressed in adult tissues (compared to that of AT₂ receptor expression), but that following tissue injury/disease, can also bind to AT₂ receptors, following their up-regulation. Studies have shown that these up-regulated AT₂ receptors may bind to AT₁ receptors to form a heterodimer complex to inhibit AT₁ receptor signalling (AbdAlla *et al.*, 2001).

Figure 1.7:



Schematic illustration of the actions of angiotensin II binding to either the AT₁R and AT₂R. Upon binding of Ang II to AT₁ receptors, this can result in increased extracellular matrix production via multiple intracellular signalling pathways including promotion of the TGF-β1/TGF-βR/Smad2/3 pathway, increased growth factor signalling and the activation of MAPKs through the increase in NADPH-mediated ROS production. In contrast, upon binding of Ang II to AT₂ receptors, this acts as a counter-regulatory action to AT₁ receptor activation, resulting in vasorelaxation and reduced matrix accumulation via inhibition of MAPK, and increased nitric oxide/cGMP signalling. Adapted from (Te Riet et al., 2015; Yu and Jeremy, 2018).

1.2.4.3 AT₄ receptor (IRAP) and its disease role.

In addition to targeting the AT₂ receptor, recent attention has also turned to therapeutically targeting the AT₄ receptor for fibrosis regression, which is also known as the insulin regulated aminopeptidase (IRAP) as its co-localization with glucose transport GLUT4 and plays an important

role in insulin action (Albiston *et al.*, 2001; Keller, 2004). This receptor, which is now recognized as an enzyme, is a single transmembrane integral protein made up of 916 amino acids with an extracellular catalytic site (Albiston *et al.*, 2001). It was found to have high binding affinity to angiotensin IV (Ang IV), a fragment generated from Ang II being cleaved by Aminopeptidase A to form Ang III which is further cleaved by Aminopeptidase B and N (De Gasparo *et al.*, 2000). Although first discovered in adipocytes, IRAP has now been identified in several organ tissues including the brain, heart, kidney, adrenal glands and placenta (Keller *et al.*, 1995; Chai *et al.*, 2004). Within the kidneys, the distribution of IRAP receptors are in the proximal tubules, glomerulus, loop of Henle, collecting ducts and renal fibroblasts (Harding *et al.*, 1994; Chai *et al.*, 2004). IRAP expression was found to be increasingly expressed in the aged heart and kidneys of 2 year-old mice, in mice with various form of heart and kidney disease, and specifically localised on myofibroblasts (unpublished findings; reported in the PhD Thesis of Huey Wen Lee, Monash Pharmacology). IRAP has been shown to regulate blood flow, increase hypertrophy and increase sodium reabsorption in the kidneys analogous to AT₁ receptors (De Gasparo *et al.*, 2000). It has also been implicated with possible roles in regulating the inflammatory process as it can be found in macrophages, dendritic cells, B and T cells (Saveanu and Van Endert, 2012). In the past, studies conducted in the heart reported upregulation of IRAP during CVDs and inhibition of the enzyme leads to vaso-protective effects via inhibition of IRAP's catalytic site and increasing the bioavailability of cardio protective IRAP substrates including lys-bradykinin, vasopressin and oxytocin (Moeller *et al.*, 1999; Wallis *et al.*, 2007; Vinh *et al.*, 2008; Vanderheyden, 2009). One of IRAP's substrate, lys-bradykinin (lys-Bk) has been shown to decrease TGF- β 1 levels and promote nitric oxide (NO) levels in several disease states including renal ischemia (Hartman, 1995; Kakoki *et al.*, 2007; Vanderheyden, 2009). Thus, potential inhibition of IRAP may be a promising anti-fibrotic lead.

1.3 Current anti-fibrotic treatments

The current intervention for CKD patients with chronic fibrosis-related disease pathology is dialysis or organ transplant (Liu, 2006; Amer and Griffin, 2014; Tromp *et al.*, 2015). Not only are both procedures invasive and expensive, neither target the factors that drive fibrosis. Aside from

organ support and transplantation, there have been use of pharmacological interventions in the market to prevent organ failure from fibrosis (Liu, 2006) (Table 1.3). Most target the angiotensin (Ang) II and/or aldosterone pathway, which is involved in the activation of AT₁ receptors to promote gene expression of TGF-β1 and reduce MMP levels, as mentioned previously. The two classes of drugs that have been frequently used are ACEi and ARBs. ARBs bind selectively and non-competitively to block the activation of AT₁ receptors, while ACEi act up-stream of ARBs by inhibiting the conversion of angiotensin I to Ang II (Crowley *et al.*, 2006). Both have beneficial effects as ARBs have been found to be more tolerable for patients with angioedema than using ACEi, while ACEi are hypothesized to be more effective than ARBs with the additional benefit of increasing the retention of renal protective mediators such as prostaglandins, bradykinin and NO (Liu, 2006; Kakoki *et al.*, 2007). Despite the current use of both ARBs and ACEis, both treatments have only shown moderate changes in reversing fibrosis through clinical studies over a 10 month period (Schelbert *et al.*, 2014), but can exacerbate cardiac and renal failure when administered together (Chan *et al.*, 2011). Thus, the limited efficacy of such therapeutics for long-term treatment raises the need to find new effective alternatives to reverse kidney fibrosis.

Table 1.3: Current treatments used for CKD.

Class of drug	Examples of clinical agents used
Angiotensin converting enzyme (ACE) inhibitors	Perindopril / Enalapril / Ramipril / Lisinopril / Captopril (Strippoli <i>et al.</i> , 2012)
Angiotensin receptor blockers (ARBs)	Candesartan / Telmisartan / Losartan / Irbesartan / Olmesartan / Valsartan (Strippoli <i>et al.</i> , 2012)
Mineralocorticoid receptor blockers (MRBs)	Cyclophosphamide / Spironolactone / Eplerenone (Davide <i>et al.</i> , 2014)
Statins	Atorvastatin / Lovastatin / Pitavastatin / Pravastatin / Rosuvastatin (Hart and Bakris, 2007)
TGF-β1 inhibitors	Tranilast / Pirfenidone (Klinkhammer <i>et al.</i> , 2017)
Loop and thiazide diuretics	Furosemide / Torsemide (Vasavada <i>et al.</i> , 2003) Chlorthalidone / Hydrochlorothiazide / Bendroflumethiazide (Sinha and Agarwal, 2015)

Beta blockers	Atenolol / Metoprolol / Carvedilol (Hart and Bakris, 2007)
----------------------	--

1.3.1 Other treatments for CKD

Aside from drugs that are used to target the vasoconstricting, pro-inflammatory and pro-fibrotic effects of Ang II, statins, are a class of lipid-lowering drugs that are used to lower high cholesterol levels in patients with CVD and diabetes, which often accompany CKD. Patients with diabetes-induced CKD frequently exhibit elevated low-density lipoprotein cholesterol (LDL-C), which when built-up, can result in atherosclerosis. In regards to fibrosis, statins have been shown to inhibit Ang II-mediated Smad activation, thereby reducing vascular damage (Rodriguez Díez *et al.*, 2010) and having PPAR-activating properties that reduce inflammation, oxidative stress and fibrosis (Balakumar *et al.*, 2012). However, studies have shown conflicting effects of statins within the kidneys. In regards to the early stages of CKD, statins are able to reduce risks of CVD progression and eventual fibrosis (Palmer *et al.*, 2012). On the other hand, studies have shown that high-dose of statins can lead to further progression of CKD within the first 120 days of treatment (Dormuth *et al.*, 2013). Thus, statins are not currently-used as effective anti-fibrotics for CKD patients, but are used more for preventing and treating the development of CVDs.

Another class of treatment for CKD is the use of mineralocorticoid receptor blockers (MRBs), which have anti-proteinuric actions most suitable for diabetic nephropathy (Volk *et al.*, 2011), as well as moderate anti-hypertensive properties (Jain *et al.*, 2009). MRBs, especially spironolactone and eplerenone have shown success at reducing mortality and managing complications in CVDs (Coats, 2001). Within the kidneys, studies have shown that MRBs can reverse established renal fibrosis and vascular inflammation (Lam *et al.*, 2006). The effects of these drugs, however, are mostly conducted as an adjunct therapy to ACEi and ARBs, while the direct mechanisms involved with their protective effects are yet to be fully elucidated (Mavrakanas *et al.*, 2014). Of all the current treatments being used, the African-American Study on Kidney Disease and Hypertension (AASK), a clinical trial conducted in 2002 which used various antihypertensive drugs including

MRBs to treat hypertensive kidney disease (Wright *et al.*, 2002) found no additional benefit of slowing the progression of nephrosclerosis by reducing of blood pressure alone. Furthermore, this study found that MRBs were not as effective as the ACEi examined in slowing the decline of kidney function (Wright *et al.*, 2002). Hence, novel treatments or strategies are needed to provide a more effective means of reducing or reversing the fibrosis associated with CKD.

1.4 Novel treatments that will be investigated in this thesis

1.4.1 AT₂ receptor agonists as novel anti-fibrotic treatments

As mentioned in section 1.2.4.2, AT₂ receptors are detected in low abundance during normal kidney function in adults, however, they are significantly upregulated during tissue injury and disease states (De Gasparo *et al.*, 2000). This receptor thus, provides a therapeutic target for potential anti-fibrotic treatments strategy that can bind and activate it during kidney injury, to promote AT₂ receptor-mediated renal protection. Aside from the endogenous ligand Ang II, other agonists have been developed and used for their vasodilatory, anti-inflammatory, anti-fibrotic, anti-hypertrophic properties (Namsolleck *et al.*, 2014). Currently, the two AT₂ receptor agonists used in research are CGP42112 (CGP) and its non-peptide counterpart, compound 21 (C21). Studies on rat isolated mesenteric arteries have shown CGP to evoke vasodilatory actions through possible crosstalk of AT₂ receptors with AT₁ receptors, as seen in combination with the AT₁ receptor blocker, candesartan, to preserve long term vasorelaxation (Barber *et al.*, 1999; Widdop *et al.*, 2002). The key molecular mechanisms involved in the anti-inflammatory actions of AT₂ agonists appear to associated with their ability to inhibit of NF- κ B activity and reduce oxidative stress (Namsolleck *et al.*, 2014). This was also seen using C21, which dose-dependently reduced TNF- α -induced IL-6 levels, while also inhibiting the pro-inflammatory effects mediated by AT₁ receptors on NF- κ B activation (Rompe *et al.*, 2010). These anti-inflammatory properties of C21 have also been concomitantly shown with anti-fibrotic actions in a model of renal disease using clipped kidneys which caused inflammation, generation of reactive oxygen species (ROS) and kidney fibrosis, whereby it reduced infiltration of inflammatory markers and TGF- β 1 levels, while enhancing the production of NO and cGMP (Matavelli *et al.*, 2011). Furthermore, in experimental models of myocardial infarction (MI) the use of C21 was shown to be protective,

counteracting the contribution of the AT₁ receptor to tissue injury, inflammation and adverse remodelling, which resulted in decreased infarct collagen content and improved atrial stiffness (Kaschina *et al.*, 2008; Lauer *et al.*, 2013). Outside the several studies mentioned above, Table 1.4 collectively details other studies documenting the organ protective roles of AT₂ receptors agonists. As seen, there is widely more research conducted on C21 and its anti-fibrotic or related actions over that of CGP. Hence, the lack of studies on the antifibrotic effects of CGP prompted further examination and assessment of its properties in Chapter 3 in comparison to other investigated novel treatments.

Table 1.4: Summary of various organ protective effects evoked by treatments with AT₂ receptor agonists. Adapted from (Wang *et al.*, 2017b).

Models used	Effects of AT ₂ R stimulation	Reference
Spontaneously hypertensive rats (SHR)	CGP42112 was examined over 4 days: no effect on mean arterial pressure (MAP); however, coadministration with candesartan ↓ MAP; CGP4212 effects were blocked by PD123319	(Barber <i>et al.</i> , 1999)
Atherosclerosis model using Apolipoprotein E-deficient (ApoE^{-/-}) mice	CGP42112 for 4 weeks: ↑endothelial function; ↓atherosclerotic lesion progression and mediated plaque stability partly due to an ↑nitric oxide bioavailability.	(Kljajic <i>et al.</i> , 2013)
Myocardial infarction (MI) in Wistar rats MI in Wistar rats: MI	C21 for 7 days post-MI: Improved MI-impaired cardiac dysfunction; ↓ fibrosis; ↓inflammation (mRNA cytokines); and apoptosis (caspase 3, Fas ligand) in the peri-infarct zone; C21 effects were blocked by PD123319. C21 for 6 weeks post-MI: Improved MI-impaired cardiac dysfunction (echocardiography); ↓cardiac interstitial fibrosis and LV TGF-β1 expression	(Kaschina <i>et al.</i> , 2008) (Lauer <i>et al.</i> , 2014)
Stroke-prone SHR (SP-SHR) rats	C21 for 6 weeks: Prevented vascular fibrosis (coronary and aorta) and stiffness (mesenteric); ↓ vascular inflammation and oxidative stress (aorta); ↓ cardiac interstitial and perivascular myocardial collagen;	(Rehman <i>et al.</i> , 2012)

	unchanged cardiac MMP2/9; ↓ renal inflammatory/T cell infiltration.	
L-NAME-treated Wistar rats	C21 for 6 weeks with L-NAME: Partially prevented vascular wall stiffening and fibrosis.	(Paulis <i>et al.</i> , 2015)
Pulmonary hypertension via monocrotaline (MCT) in Sprague Dawley rats	C21 for 2 weeks; started 2 weeks after MCT: Improved MCT-impaired RV function; ↓ lung and RV fibrosis; ↓ pro-fibrotic and pro-inflammatory cytokines in lungs (mRNA); C21 effects were blocked by PD123319 or MasR antagonist	(Bruce <i>et al.</i> , 2015)
SP-SHR rats on a high salt diet	C21 for the duration of 8-weeks high salt: delayed brain lesions and delayed proteinuria; ↓ glomerulosclerosis, renal fibrosis, and macrophage infiltration; ↓ epithelium/mesenchymal differentiation	(Gelosa <i>et al.</i> , 2009)
Doxorubicin-induced renal toxicity in Wistar rats	C21 for 4 weeks post-doxorubicin: Renal fibrosis unchanged; ↓ oxidative stress and restored glomerular density	(Hrenák <i>et al.</i> , 2013)
Streptozotocin (STZ) in ApoE^{-/-} mice with diabetic nephropathy	C21 for 20 weeks post-STZ; ↓ glomerulosclerosis, mesangial expansion, albuminuria; inhibited many markers of oxidative stress, inflammation, and fibrosis; ↑ MMP2/9	(Koulis <i>et al.</i> , 2015)
Human proximal tubular cells	CGP42112 ↓ TGF-βRII protein expression; effects were blocked by PD123319 and L-NAME.	(Guo <i>et al.</i> , 2016)

Based on the studies conducted with CGP and C21, additional AT₂ receptor agonists with improved selectivity for the receptor, such as β-Pro⁷Ang III have been developed (Del Borgo *et al.*, 2015). Although Ang II is widely acknowledged as the major peptide which exerts its effect on AT₁ and AT₂ receptors, the heptapeptide Ang III exerts similar effects to that of Ang II, however, is less potent at AT₁ receptors and has shown favourable selectivity to AT₂ receptor binding (Bouley *et al.*, 1998; Cesari *et al.*, 2002; Bosnyak *et al.*, 2011). Furthermore, a few studies published by Padia *et al.*, have shown that Ang III, not Ang II, was the preferred AT₂ receptor ligand in terms of the kidney's natriuretic response (Padia *et al.*, 2006, 2008). In the past, it had been shown by Jones *et al.*, that a single β-amino acid substitution to the peptide sequence of Ang II conferred a shift in AT₂ receptor over AT₁ receptor binding (Jones *et al.*, 2011). As such, β-amino acid substitutions were also conducted on each of the Ang III residues, where it was found

that β -Pro⁷Ang III had greater than 20,000-fold selective binding to the AT₂ receptor over the AT₁ receptor, and to a greater extent than CGP42112, which was at 18,000-fold selective for the AT₂R (Del Borgo *et al.*, 2015). Additionally, the use of β -Pro⁷Ang III evoked similar AT₂ receptor-mediated cardioprotective effects such as vasorelaxation in mouse thoracic aortae and lowered mean arterial pressure in SHR during AT₁ receptor blockade *in vivo* (Del Borgo *et al.*, 2015). Seeing as AT₂ receptor agonists are cardio-protective, this thesis aims to compare the reno-protective effects of CGP42112 and β -Pro⁷Ang III, to a number of other anti-fibrotics, in experimental models of CKD.

1.5 IRAP as a novel anti-fibrotic target

Although Ang IV is a fragment of Ang II, it has been shown to act like a pleiotropic peptide as well, with its primary function residing in the brain and being associated with memory acquisition and recall (De Gasparo *et al.*, 2000). The Ang IV/IRAP system is also associated with blood flow regulation, mediated by an increase in endothelial nitric oxide synthase (eNOS) and improved NO bioavailability to promote vasodilation (Patel *et al.*, 1998; Vinh *et al.*, 2008). Furthermore, Ang IV can inhibit sodium reabsorption and hence, promotes natriuresis which is beneficial to reduce hypervolemia that accompanies hypertension and CKD (Hamilton *et al.*, 2001). In addition, Ang IV also has anti-hypertrophic effects. Studies have reported that Ang IV blocks increases in RNA and protein synthesis associated with Ang II binding to AT₁ receptors within chick cardiocytes (Baker *et al.*, 1992). Also, the application of an AT₄ receptor antagonist (divalinal-Ang IV) to rats resulted in significantly increased collagen accumulation and left ventricular hypertrophy. These results point to a protective role of Ang IV against collagen accumulation in hypertrophied hearts (Baker *et al.*, 1992; De Gasparo *et al.*, 2000). Taken together, the beneficial properties of Ang IV make it an ideal candidate for treating fibrosis within the injured kidneys.

1.5.1 Mechanistic actions of Ang IV

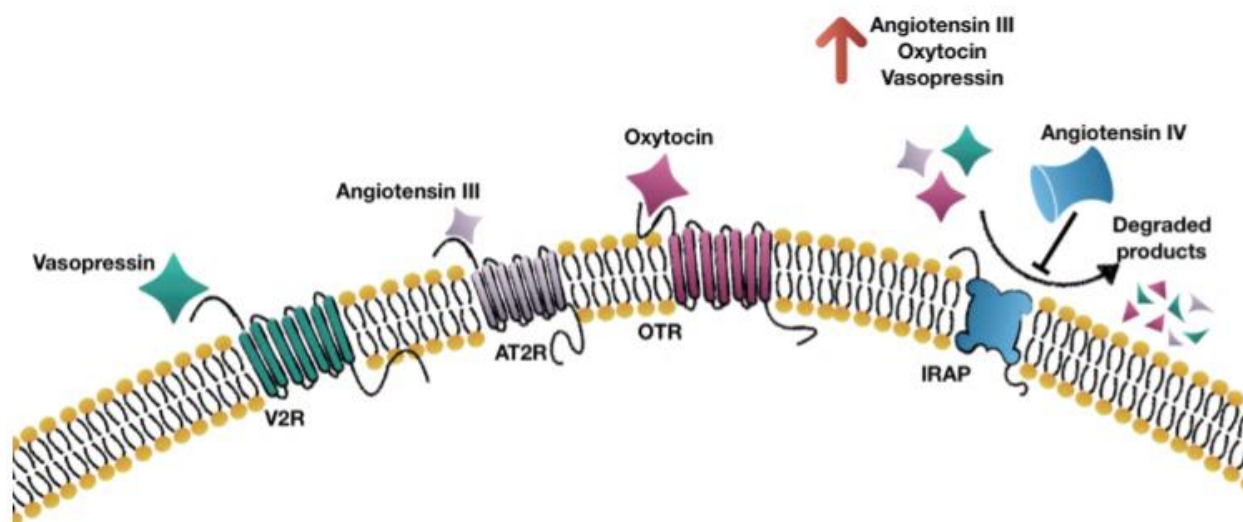
The exact mechanisms of how Ang IV mediates its effects after binding to IRAP are still unclear. Briefly, there are three general IRAP-mediated mechanisms which are hypothesized: 1) binding of AT₄ receptor ligands cause the accumulation of IRAP substrates by preventing their

degradation by IRAP; 2) IRAP is co-localized with glucose transporter GLUT4, and binding by AT₄ receptor ligands may prolong the cell surface localisation of IRAP as well as GLUT4 thereby resulting in increased glucose uptake which may mediate the biological effects of Ang IV; and 3) If the cellular effects are mediated via binding of Ang IV to IRAP, it can be considered a classical receptor (Vanderheyden, 2009). With respect to a classical receptor function, studies have shown that AT₄ receptor ligands are capable of activating several signalling pathways including calcium, MAPK kinases, NF- κ B and cGMP production (Vanderheyden, 2009). The main hypothesis regarding Ang IV and IRAP ligand-mechanisms of action appear to be associated with the inhibition of IRAP's catalytic activity leading to the increase in availability of IRAP substrates including lys-Bk, vasopressin, Ang III and oxytocin (Figure 1.8).

By inhibiting the breakdown of lys-Bk (as mentioned in section 1.2.4.3), the substrate decreases TGF- β 1 levels and promote nitric oxide (NO) levels (Hartman, 1995; Kakoki *et al.*, 2007; Vanderheyden, 2009). While vasopressin can act on its receptor V2R, it plays a crucial role in the regulation of water reabsorption in the renal collecting ducts and hence, inhibition of IRAP may impact on renal functional outcomes (Masuda *et al.*, 2003). In the kidneys, Ang II can be metabolised by aminopeptidase A (APA) to form angiotensin III (Ang III) (Wright *et al.*, 1990), which is also a substrate of IRAP that can bind to AT₂ receptors and elicit organ protective effects as discussed in section 1.2.4.2 and 1.4.1, while also controlling vasopressin release (Zini *et al.*, 1996; Chen and Huang, 2000). Lastly, another major IRAP substrate is oxytocin which is known for its uterine contractile effects and anti-diuretic effects (Li *et al.*, 2008; Borrow and Cameron, 2012). Oxytocin additionally has been found to also decrease fibrosis and inflammation via the reduction of NADPH-dependent IL-6 activity (Plante *et al.*, 2015). Administration of oxytocin has been found to increase IRAP translocation and alleviate renal injury against ischemia/reperfusion-induced oxidative damage (Tugtepe *et al.*, 2007; Plante *et al.*, 2015).

Hence by inhibiting the breakdown of IRAP activity, the bioavailability of these substrates increases, where they act on their receptor targets to produce their protective effects. However, a limitation of Ang IV is that it has a short half-life.

Figure 1.8:



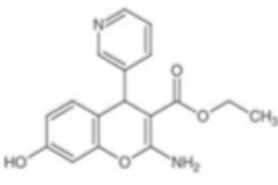
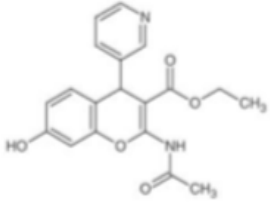
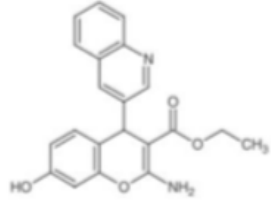
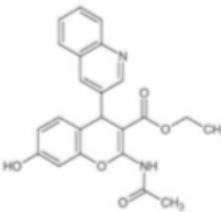
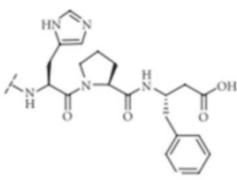
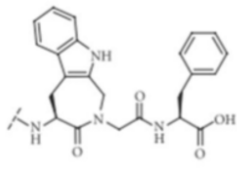
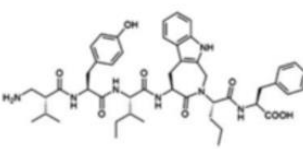
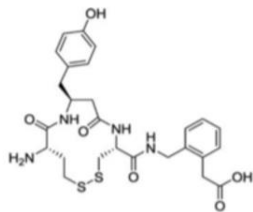
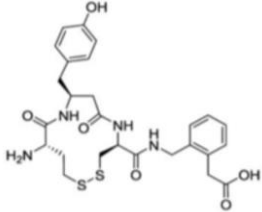
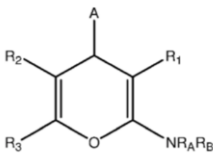
The possible mechanisms by which Ang IV and IRAP ligands mediate their organ protective effects. Ang IV and IRAP ligands inhibits the catalytic activity of IRAP thereby promoting the accumulation of IRAP substrates such as vasopressin, angiotensin III and oxytocin, which in turn bind on their respective receptors each contributing to various organ protective functions. Adapted from (Master Thesis of Sharenja Chelvaretnam).

1.5.2 Synthetic IRAP inhibitors

As Ang IV has a short half-life due to its degradation by aminopeptidases (Chai *et al.*, 2004), this likely limits the clinical potential of Ang IV peptide-based therapeutics. Attention has thus, turned to chemically-produced IRAP inhibitors to inhibit the detrimental effects of IRAP activity (Sardinia *et al.*, 1994; Chai *et al.*, 2004; Albiston *et al.*, 2008). The initial development of IRAP inhibitors were based on the homology model of the IRAP catalytic domain via *in silico* screening, modifications and characterisation, which led to the development of HFI-142 analogues from the Howard Florey Institute, Australia (Albiston *et al.*, 2008). Following chemical modifications of its side-chains, three lead synthetic IRAP inhibitors were developed: HFI-419, HFI-435 and HFI-437 (Albiston *et al.*, 2008), all with K_i values within the nanomolar range (see Table 1.5A).

Subsequently around a similar time, two classes of IRAP inhibitors were also developed involving: i) β -homo-amino acid substitution of Ang IV resulting in AL-11, AL-40 and IVDE77 (Lukaszuk *et al.*, 2008, 2009; Nikolaou *et al.*, 2013) (see Table 1.5B); and ii) based on the N-terminal amino acid of the cyclic substrates oxytocin and vasopressin, contributing to the synthesis of 13-membered macrocyclic compounds termed HA08 and HA09 (Andersson *et al.*, 2010) (see Table 1.5C), with HA08 documented as the highest affinity IRAP inhibitor to date (Diwakarla *et al.*, 2016). Of note, the K_i of the HFI series are comparable to that of the HA series since both inhibition of IRAP catalytic activity were performed in the presence of Zn^{2+} . On the other hand, the K_i values for the AL and IVDE series were determined by radioligand binding assays performed in the absence of the co-factor Zn^{2+} , hence a direct comparison between the various classes of IRAP inhibitors developed to date cannot be made (Lukaszuk *et al.*, 2008, 2009; Nikolaou *et al.*, 2013). Lastly, using the same *in silico* screening process as the HFI series, a second series of IRAP inhibitors have been developed by Professor Phillip Thompson at the Monash Institute of Pharmaceutical Sciences. SJM-4-164, although having a lower affinity for IRAP compared to HFI-419 (see Table 1.5D), offers better solubility ($>1\text{mg/ml}$) and similar renal protective effects as HFI-419 in reversing age-induced cardiac fibrosis in mice when administered at an equivalent dose of 0.72mg/kg/day (unpublished findings; reported in the Master Thesis of Sharenja Chelvaretnam, Monash Pharmacology).

Table 1.5: Developed synthetic IRAP inhibitors from different classes and their respective K_i .

<p>A</p>  <p>HFI-142 $K_i=2\mu\text{M}$</p>	 <p>HFI-419 $K_i=0.48\mu\text{M}$</p>	 <p>HFI-435 $K_i=0.36\mu\text{M}$</p>	 <p>HFI-437 $K_i=0.02\mu\text{M}$</p>
<p>B</p>  <p>AL-11 $K_i=16.6\text{nM}$</p>	 <p>AL-40 $K_i=8.5\text{nM}$</p>	 <p>IVDE77 $K_i=1.71\text{nM}$</p>	
<p>C</p>  <p>HA08 $K_i=3.3\text{nM}$</p>	 <p>HA09 $K_i=0.242\mu\text{M}$</p>	<p>D</p>  <p>Where R_1, R_2, R_3, R_A, R_B and A represent various sidechains.</p> <p>SJM-4-164 $K_i=1.0\mu\text{M}$</p>	

1.5.3 HFI-419

Of the available synthetic IRAP inhibitors, HFI-419 was found to optimally inhibit IRAP activity. It has relatively high affinity, a good solubility profile and is more stable than other peptide inhibitors of IRAP (Albiston *et al.*, 2008). Its K_i value of $0.48\mu\text{M}$, determined by its ability to inhibit IRAP from cleaving the IRAP substrate Leu-4-methylcoumaryl 7-amide ($25\mu\text{M}$ of Leu-MCA) is comparable to the K_i value of $0.11\mu\text{M}$ for Ang IV to inhibit IRAP (Lew *et al.*, 2003). Furthermore, an additional advantage of HFI-419 is its high specificity for IRAP, with no affinity for glucose-6-phosphatase, aminopeptidase N, ACE1, leukotriene A4 hydrolase, ER-associated

aminopeptidases (ERAP)-1 and 2 or other ATR subtypes (Albiston *et al.*, 2008). HFI-419 was first modified from its synthetic precursor molecule, HFI-142, by altering the 2-amino terminal end via acetylation resulting in enhanced stability (Albiston *et al.*, 2008). Studies utilising HFI-419 demonstrated similar effects to Ang IV within the brain in improving memory (Albiston *et al.*, 2008). In a study published on the effects of HFI-419 within the brain, although intravenous (I.V.) administration of HFI-419 resulted in its disappearance 30 minutes post-administration, it immediately increased the active metabolite HFI-142, its precursor, in the plasma (Mountford *et al.*, 2014). Further neurological assessment showed I.V. administration of HFI-419 resulted in greater plasma concentrations of HFI-142 which were detectable up to 240 minutes post-administration, which implied a longer-term benefit of using HFI-419 to treat neurological disorders (Mountford *et al.*, 2014). In the hope of translating the therapeutic potential of HFI-419 for organ protection, preliminary studies have indicated that HFI-419 can effectively reverse cardiac fibrosis and vascular remodelling in aged (2-year-old) and Ang II-injured mice where it reduced LV TGF- β 1 expression levels, myofibroblast differentiation and aberrant ECM degradation (unpublished findings; reported in the PhD Thesis of Huey Wen Lee, Monash Pharmacology). Thus, in this PhD project, HFI-419 was selected to be evaluated for its anti-fibrotic potential against experimental kidney disease, as it was readily available and had been studied in other disease settings (so the findings from this thesis could be compared to previously conducted studies by others).

1.6 Relaxin as a novel anti-fibrotic treatment strategy

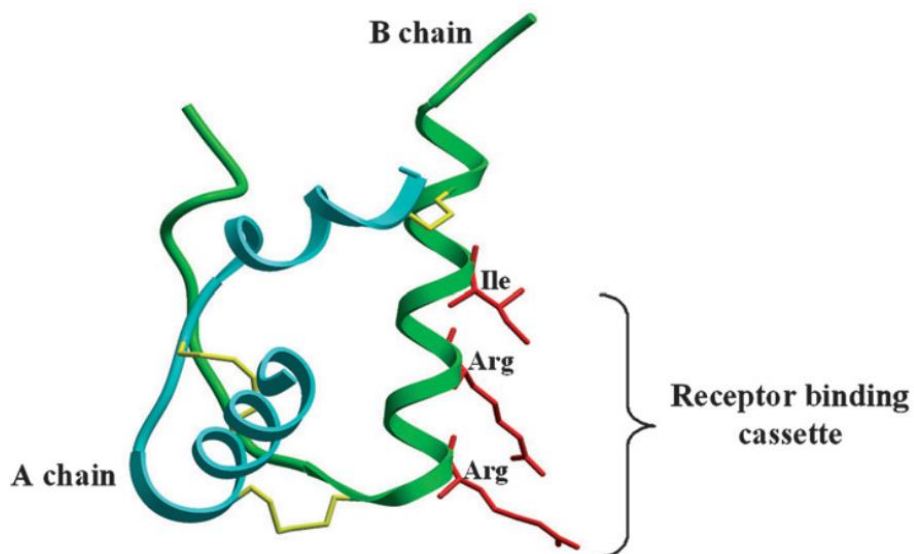
1.6.1 History of relaxin

Relaxin is an endogenous peptide hormone that was first identified by Fredrick Hisaw in 1926, for its ability to play an important role in relaxing the pelvic ligaments of female mammals during pregnancy to facilitate parturition (Hisaw, 1926). Relaxin is predominantly produced in the corpus luteum (ovary) of pregnant mammals and is also produced in smaller concentrations within the prostate and/or testes of the male reproductive tract (Weiss *et al.*, 1976) and the heart of both genders (Dschietzig *et al.*, 2001). In the late 1950s, studies that exploited the use of relaxin as a therapeutic agent for treating human patients used impure preparations of porcine relaxin

(Releasin). Releasin was found to be able to prevent premature birth by inhibiting uterine contractility, soften the cervix to reduce the duration of childbirth and also increased skin elasticity in patients with progressive systemic sclerosis (as reviewed in (Sherwood, 2004)). However, clinical studies with Releasin in the mid-1960s were discontinued due to the lack of its consistency, safety and failure to meet the requirements of the United States Food and Drug Administration (FDA) (Evans, 1959; Erikson and Unemori, 2001). Over the years, research on relaxin has significantly improved its synthesis (by chemical or recombinant means) and purification (Sherwood and O'Byrne, 1974), the discovery of additional forms of relaxin (Bathgate *et al.*, 2002, 2003) and the identification of GPCRs that serve as relaxin receptors (Hsu *et al.*, 2002). Over time, studies have demonstrated the consistent pleotropic actions of relaxin that serve to reverse several pathological conditions in various organs to highlight its therapeutic potential (reviewed in (Bathgate *et al.*, 2013, 2018; Samuel *et al.*, 2017; Sarwar *et al.*, 2017; Jelinic *et al.*, 2018)).

Relaxin belongs to a family of seven peptide hormones in humans, consisting of three relaxin peptides: human gene-1 (H1), gene-2 (H2) and gene-3 (H3) relaxin, and four insulin-like (INSL) peptides: INSL-3, -4, -5, -6. These two-chain peptide hormones, linked by disulphide bonds (Figure 1.9), share structural similarity to insulin and the insulin-like growth factors (IGFs) (Wilkinson *et al.*, 2005; Samuel *et al.*, 2007). The A chain of relaxin contains two α -helical segments that play an important role in ensuring peptide stability (Hossain *et al.*, 2008), while the B chain contains a receptor binding motif Arg-X-X-X-Arg-X-X-Ile/Val in the middle of its structure which is essential for relaxin-receptor binding and bioactivity (Sherwood, 2004; Bathgate *et al.*, 2006a). However, unlike insulin and IGFs which bind and activate tyrosine kinase receptors, the relaxin peptides bind and act through GPCRs (Bathgate *et al.*, 2006a). Most other mammals including rodents only have two relaxin peptides: relaxin-1 and relaxin-3 (equivalent to H2 and H3 relaxin, respectively) and INSL-3, -5 and -6. H2 relaxin is the major stored and circulating form of human relaxin (Bathgate *et al.*, 2006a), is bioactive in mice (Bathgate *et al.*, 2006; Samuel *et al.*, 2007), and will be the form of relaxin studied in this PhD project.

Figure 1.9:



Structure of relaxin. Crystal structure of a mature relaxin, with its constituent A (blue) and B (green) chains linked together by 2 inter-chain and 1 intra-chain disulphide (yellow) bonds. The A chain is responsible for peptide stability, while the B chain is made up of several conserved residues with receptor-binding motif. Reproduced from (Samuel and Hewitson, 2007).

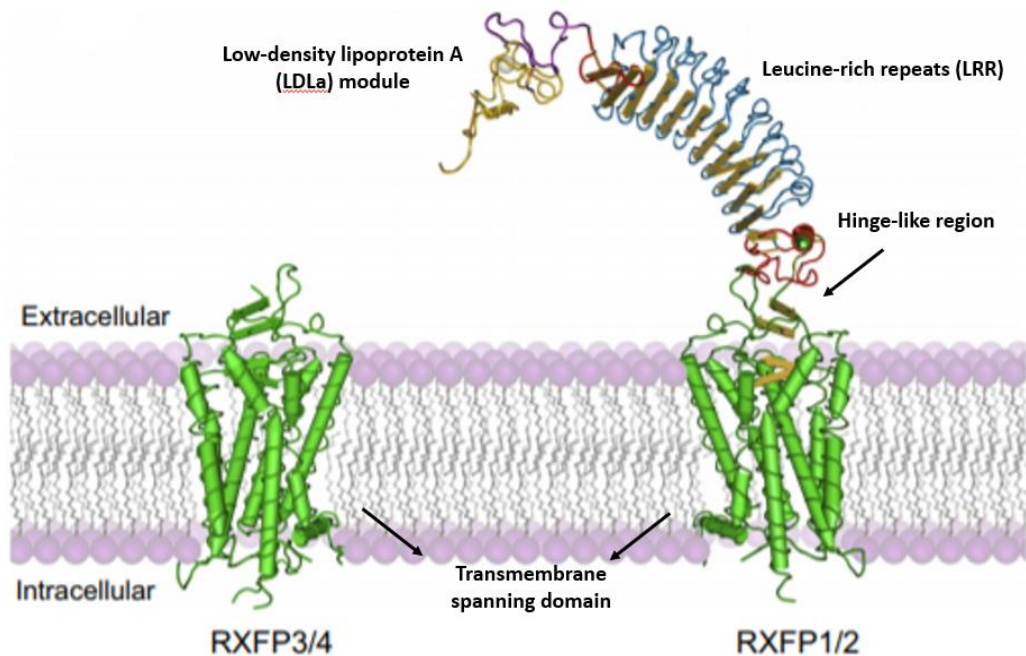
H2 relaxin is composed of a 24-25 amino acid long A-chain and 29 amino acid long B-chain connected by 3 disulphide bonds and has been shown to bind to the class A GPCR, Relaxin Family Peptide Receptor 1 (RXFP1). This occurs between a conserved arginine-arginine-isoleucine binding domain on the B-chain of relaxin and the extracellular loops of RXFP1. RXFP1 has been identified in several reproductive tissues, brain, heart, kidneys and lungs (Hsu *et al.*, 2002; Bathgate *et al.*, 2006a; Hossain *et al.*, 2016). Through this receptor, H2 relaxin has demonstrated rapidly-occurring anti-fibrotic actions in several organs including the kidneys (Samuel *et al.*, 2003). Consistent with this, relaxin- (Samuel *et al.*, 2003) and RXFP1- (Samuel *et al.*, 2009) deficient mice undergo an age-related progression of fibrosis, suggesting that relaxin-RXFP1 axis is an important endogenous regulator of collagen accumulation (the basis of fibrosis).

1.6.2 Relaxin family peptide receptors (RXFPs)

In contrast to relaxin being discovered in 1926, the relaxin receptors were not discovered until 75 years later (Hsu *et al.*, 2002). Prior to their finding, relaxin was thought to bind and activate tyrosine kinase receptors that were similarly bound and activated by insulin and the insulin-like growth factors (IGFs); given the structural similarity of relaxin and insulin/IGFs. It was the advancement of genome sequencing that led to the identification of GPCRs as receptors that could be bound by relaxin family peptides. This in turn, led to the de-orphanisation of four receptors (RXFP1-4) belonging to two distinct subclasses of the family A of GPCRs; leucine-rich repeat (LRR)-containing GPCRs (RXFP1 and RXFP2) and small peptide receptor-like GPCRs (RXFP3 and RXFP4) (Hsu *et al.*, 2002; Liu *et al.*, 2003; Bathgate *et al.*, 2006b; Van Der Westhuizen *et al.*, 2007) (Figure 1.10).

Of relevance to this thesis, the cognate receptor for H2 relaxin is RXFP1 as previously mentioned which is widely found in rodent and human heart and kidneys. Although relaxin does weakly bind and activate RXFP2 receptors, its organ-protective effects are primarily mediated via RXFP1 (Hsu *et al.*, 2002; Mookerjee *et al.*, 2009). In terms of receptor structure, RXFP1 (and RXFP2) are different compared to RXFP3 and RXFP4 (Figure 1.10). In addition to containing the seven transmembrane-spanning domain which is typically associated with GPCRs, RXFP1 contains a ten extracellular repeats (which has now been recognised as the main site of relaxin binding to RXFP1) and an N-terminal low-density lipoprotein A (LDLa) module (which directs RXFP1 signaling upon relaxin binding to the receptor) (Bathgate *et al.*, 2006b).

Figure 1.10:



Relaxin family peptide receptors. This diagram illustrates the structural differences between RXFP1 (and RXFP2) compared to RXFP3 and RXFP4. All four known relaxin receptors contain the seven transmembrane spanning domains that are typical of GPCRs, however RXFP1 (and RXFP2) are distinguished from other GPCRs by having several extracellular LRRs and an LDLa module which regulates relaxin signalling upon binding to its receptor. Adapted from (Bathgate et al., 2013).

1.6.3 Relaxin as a drug-based therapy

Although relaxin was initially discovered for its pregnancy-associated actions, these actions were primarily found to be associated with its ability to regulate collagen turnover. As aberrant collagen accumulation forms the basis of fibrosis, it has since been extensively studied for its potential anti-fibrotic properties. Numerous studies to date, have shown the anti-fibrotic effects of human recombinant relaxin also known as Serelaxin (RLX; based on the H2 relaxin sequence) in the heart, kidney, liver, lungs, skin and tendons amongst other tissues, and against several etiologies. Male relaxin knockout (RLX-KO) mice undergo an age-related increase in kidney collagen deposition, proteinuria and creatine levels, which could be reversed by exogenous

administration of RLX (Samuel *et al.*, 2004b). RLX was also seen to improve glomerular filtration rate and renal plasma flow while reducing renal vascular resistance in Munich Wistar rats with chronic nephrosis (Danielson, 2006). As seen in Table 1.6 (below), several studies have demonstrated numerous beneficial effects of RLX within models of CKD. Among relaxin's recognized therapeutic actions during pathological renal conditions by reducing fibrosis, countless studies have also shown relaxin is also able promote angiogenesis, vasodilation and protect against inflammation resulting in a promising treatment with broad organ protection capabilities (Sherwood, 2004; Samuel *et al.*, 2007; Samuel and Hewitson, 2009; Bei *et al.*, 2017). While these actions of relaxin will be further discussed, its anti-fibrotic properties in particular will be discussed in greater detail as it is the main feature of relaxin that will be examined in the thesis. Additionally, our lab has recently shown relaxin to having more rapidly-occurring anti-fibrotic efficacy compared to the ACEi, enalapril, in an experimental model of heart disease (Samuel *et al.*, 2014); and the corticosteroid, methylprednisolone in the airways/lung of a chronic allergic airways disease model (Royce *et al.*, 2013). Hence this thesis will investigate and compare the anti-fibrotic effects of serelaxin to a number of other therapies.

Table 1.6: Effects of relaxin-deficiency and RLX on kidney disease models.

CKD models	Effect	References
Aging	<p>Male RLX-KO mice had ↑collagen deposition, ↑proteinuria, ↑creatinine; which was reversed with RLX treatment.</p> <p>In Munich Wistar rats with chronic nephrosis, RLX ↑glomerular filtration rate, ↑effective renal plasma flow, ↓effective renal vascular resistance, ↑MMPs, ↓collagen deposition</p>	<p>(Samuel <i>et al.</i>, 2004b)</p> <p>(Danielson, 2006)</p>
Hypertension	<p>In 10 month-old male SHR, RLX ↓collagen deposition, ↓α-SMA expression (myofibroblast differentiation), ↑MMPs</p> <p>Ang II-injected SD rats administered with RLX via minipump ↓blood pressure, ↓NO metabolite, ↓ROS, ↑albumin excretion</p>	<p>(Lekgabe <i>et al.</i>, 2005)</p> <p>(Sasser <i>et al.</i>, 2011)</p>
Salt diet	<p>In Dahl salt sensitive/resistant rats given 8% NaCl diet, RLX ↓TGF-β levels, ↑nNOS and ↑eNOS expression, ↓Blood pressure, ↓α-SMA expression (myofibroblast differentiation)</p>	<p>(Yoshida <i>et al.</i>, 2012)</p>
Unilateral ureteral obstruction (UUO)	<p>In UUO-injured mice, RLX ↓tubulointerstitial fibrosis, ↓Collagen I, III, IV deposition, ↑MMPs, ↓α-SMA expression (myofibroblast differentiation)</p> <p>RLX ↓collagen deposition, ↓TGF-β1 expression, ↑MMPs, ↓α-SMA expression (myofibroblast differentiation), ↑stem cell proliferation and migration</p>	<p>(Hewitson <i>et al.</i>, 2007)</p> <p>(Huuskes <i>et al.</i>, 2015)</p>

Renal toxicity	In bromoethylamine-injured rats, RLX ↓TGF-β1 levels, ↓interstitial fibrosis, ↓creatinine, ↑glomerular filtration rate	(Garber <i>et al.</i> , 2001a)
Acute inflammation	In Anti-GBM diseased rats, RLX ↓TGF-β1 levels, ↑fibronectin degradation, ↓focal glomerulosclerosis, ↓interstitial fibrosis	(McDonald <i>et al.</i> , 2003)
Renal mass reduction	In rats with sub-total renal ablation, RLX ↓glomerulosclerosis, ↓collagen IV deposition, ↑creatinine clearance In rats with sub-total renal infarction, RLX ↓systolic blood pressure, ↓glomerulosclerosis, ↓collagen IV deposition, ↑creatinine clearance	(Garber <i>et al.</i> , 2003) (Garber <i>et al.</i> , 2003)

1.6.4 Angiogenic effects of relaxin

In the event of kidney injury, the kidneys themselves will undergo various events endogenously to attempt to recover from the insult. However, this process requires a sufficient blood supply that may be lost during injury. Consistent with the renal reparative functions of relaxin, studies to date have demonstrated that continuous infusion of relaxin promotes the formation of new blood vessels and the reversal of vascular rarefaction. This occurs through a relaxin-induced up-regulation of factors such as basic fibroblast growth factor (bFGF) (Lewis *et al.*, 2001) and vascular endothelial growth factor (VEGF) (Unemori *et al.*, 2000). Of note, a loss of capillaries associated with the pathology of renal fibrosis was reversed upon the administration of exogenous VEGF administration (Kang *et al.*, 2001), suggesting that a relaxin-induced increase in VEGF plays an important role during tissue repair. Relaxin was also found to stimulate α -SMA-stained smooth muscle blood vessel density and Glut-1-stained endothelial blood vessel density in the setting of myocardial infarction-induced heart failure (Samuel *et al.*, 2011).

1.6.5 Vasodilator effects of relaxin

Aside from its angiogenic effects, relaxin has also been shown to promote renal vasodilation and hyperfiltration to ensure that sufficient blood facilitates the wound healing process following injury to the kidney (Conrad, 2010). It has been shown that chronic administration of porcine or recombinant human relaxin increase GFR, renal plasma flow and decreases vascular resistance (Conrad and Novak, 2004; Conrad *et al.*, 2004). The likely mechanisms of relaxin's vasodilator properties are thought to involve the NO-dependent pathway, whereby relaxin can breakdown endothelin-1, a potent vasoconstrictor, into its inactive precursor, ET₁₋₃₂ via upregulating matrix metalloproteinases (MMP)-2 and -9 (will be discussed later). This subsequently activates endothelin type-B (ET_B) receptors and iNOS-mediated NO production (Fernandez-Patron *et al.*, 1999; Conrad, 2010) to promote vasodilation. The vasodilatory effects of relaxin have been demonstrated in various organs, where in the kidney it has been found to reduce myogenic reactivity in an endothelium-dependent manner in rodent small renal arteries (McGuane *et al.*, 2011; Novak *et al.*, 2015) and human subcutaneous arteries (McGuane *et al.*, 2011). Relaxin has also been found to promote vasodilation in the renal arteries of rats with hypertension (Van Drongelen *et al.*, 2013).

1.6.6 Anti-inflammatory effects of relaxin

Excerpt from **Appendix**.

Several studies have shown that relaxin inhibits the infiltration of various immune cells into injured/damaged organs, which produce various pro-inflammatory and pro-fibrotic factors to initiate the wound-healing response to injury, but which over prolonged periods contribute to the stimulation of excess extracellular matrix (ECM) secretion (Wynn and Ramalingam, 2012). Unresolved inflammation followed by dysregulated wound healing can lead to fibrosis-induced organ failure. Relaxin has been shown to i) reduce the cellular content of inflammatory cells within several tissues including neutrophils, basophils, mast cells, endothelial cells and macrophages (Bani *et al.*, 1997, 2002; Garber *et al.*, 2001b; Nistri *et al.*, 2003, 2008; Beiert *et al.*, 2018), the latter of which being a source of TGF- β 1. Furthermore, relaxin ii) decreases granule exocytosis and mast cell degranulation to reduce pro-inflammatory and allergic cytokines such as histamine, leukotrienes and serotonin (Masini *et al.*, 1997). Relaxin can also iii) inhibit the

endothelial adhesiveness to neutrophils and the infiltration of macrophages which are crucial for the recruitment and migration of inflammatory cells to the site of injury (Nistri *et al.*, 2003; Hewitson *et al.*, 2007; Martin *et al.*, 2018), and iv) inhibit toll-like receptor (TLR)4 signalling and promote tissue-repairing M2 macrophage polarization (Chen *et al.*, 2017). Moreover, relaxin v) inhibits NL3P3 inflammasome activity, which is known to produce interleukin (IL)-1 β activity (Raleigh *et al.*, 2017) and also plays a role in vi) inhibiting NF-kB signalling, crucial in regulating many inflammatory genes (Martin *et al.*, 2018). Aside from its effects on inflammatory cell infiltration H2 relaxin has additionally been shown to vii) reduce the pro-fibrotic influence of cytokines or mediators such as TGF- β 1 (Unemori and Amento, 1990; Unemori *et al.*, 1996; Samuel *et al.*, 2004a; Heeg *et al.*, 2005; Mookerjee *et al.*, 2009; Bennett *et al.*, 2013; Wang *et al.*, 2016, 2017a; Martina *et al.*, 2017), IL-1 β (Unemori and Amento, 1990; Pini *et al.*, 2016; Beiert *et al.*, 2017), IL-6 (Yoshida *et al.*, 2014; Beiert *et al.*, 2017, 2018; Wang *et al.*, 2017a), monocyte chemoattractant protein (MCP)-1 (Brecht *et al.*, 2011; Wang *et al.*, 2017a), and tumour necrosis factor α (TNF α)(Brecht *et al.*, 2011; Yoshida *et al.*, 2013, 2014), amongst others.

1.6.7 Anti-fibrotic actions of relaxin

Excerpt from **Appendix**.

Following injury, inflammatory cells recruit ECM-producing fibroblasts to the site of injury, to synthesize various ECM proteins (such as collagens I, III, IV, V, fibronectin, laminin etc). In their resting state, these fibroblasts produce very low levels of ECM proteins to maintain a slow and steady state of tissue turnover. However, when they are activated by factors such as TGF- β 1, IL-1 β and angiotensin II (Ang II), which is derived from activation of the renin-angiotensin system (Weber *et al.*, 1993; Suzuki *et al.*, 2003; Bataller *et al.*, 2005), they undergo proliferation and activation into activated myofibroblasts, which produce large amounts of ECM components. Prolonged and/or chronic injury can then lead to continuous myofibroblast-induced fibrosis progression (Wynn and Ramalingam, 2012). In conjunction with the increased ECM accumulation during fibrosis, factors such as TGF- β 1 and Ang II suppress ECM-degrading enzymes such as matrix metalloproteinases (MMPs) to facilitate the breakdown of this increased ECM, by promoting the ability of tissue inhibitors of metalloproteinases (TIMPs) to inhibit MMP activity.

Relaxin has been found to i) consistently inhibit TGF- β 1, IL-1 β and/or Ang II-mediated fibroblast proliferation and/or differentiation into myofibroblasts, regardless of etiology (Unemori and Amento, 1990; Unemori *et al.*, 1996; Bennett *et al.*, 2003; Samuel *et al.*, 2004a, 2011; Heeg *et al.*, 2005; Lekgabe *et al.*, 2005; Mookerjee *et al.*, 2009; Hewitson *et al.*, 2010; Sassoli *et al.*, 2013; Fallowfield *et al.*, 2014; Huuskes *et al.*, 2015). Furthermore, relaxin has also been found to ii) inhibit myofibroblast contractility as part of its anti-fibrotic actions (Huang *et al.*, 2011). These combined actions of relaxin lead to iii) reduced myofibroblast-induced ECM (primarily collagen and fibronectin) synthesis and deposition (Unemori and Amento, 1990; Unemori *et al.*, 1996; Bennett *et al.*, 2003; Samuel *et al.*, 2004a, 2011; Heeg *et al.*, 2005; Lekgabe *et al.*, 2005; Hewitson *et al.*, 2010; Lee *et al.*, 2011; Sassoli *et al.*, 2013; Royce *et al.*, 2015; Cernaro *et al.*, 2017). Furthermore, relaxin has been found to iv) promote MMP expression and activity and/or inhibit v) TIMP activity to induce the degradation of aberrant ECM protein accumulation (Unemori and Amento, 1990; Unemori *et al.*, 1996; Williams *et al.*, 2001; Heeg *et al.*, 2005; Lekgabe *et al.*, 2005; Hewitson *et al.*, 2010; Samuel *et al.*, 2011; Huuskes *et al.*, 2012; Sassoli *et al.*, 2013; Royce *et al.*, 2015; Kang *et al.*, 2017).

1.6.8 Endothelial-to-mesenchymal transition-inhibitory effects of relaxin

Excerpt from **Appendix**.

In addition to directly stimulating the differentiation of fibroblasts into myofibroblasts, TGF- β 1 can stimulate epithelial and endothelial cells to acquire a mesenchymal phenotype in which they de-differentiate, migrate and subsequently re-differentiate into myofibroblasts to secrete large amounts of matrix proteins to promote wound healing; commonly known as EMT and EndMT, respectively (Klahr and Morrissey, 2002; Barnes and Gorin, 2011; Du *et al.*, 2012). During an aberrant wound healing process, however, these transitioned epithelial and endothelial cells remain as myofibroblasts and continue to produce ECM components such as collagen and fibronectin. In the murine kidney, it was shown that 10% of endothelial cells undergo EndMT and 5% of epithelial cells undergo EMT, contributing to myofibroblast-induced renal fibrosis (LeBleu *et al.*, 2013). Moreover, in a murine model of cardiac fibrosis, it was revealed that 27-33% of all cardiac fibroblasts were of endothelial origin using a Cre-lox genetic marking system to identify

cells that express Tie1 (an endothelial marker) (Zeisberg *et al.*, 2007). Furthermore, in EndMT, phenotypes of endothelial cells, such as CD31 and VE-cadherin expression are often replaced by specific properties of mesenchymal cells like vimentin and α -SMA expression (Kovacic *et al.*, 2012). Evidence over the years have demonstrated that EndMT contributes to a critical role in pressure overload-induced pathological fibrosis.

Recent studies have shown that relaxin can inhibit EndMT within the heart and kidney of isoprenalin-induced cardiomyopathy in rodents (Cai *et al.*, 2017; Zheng *et al.*, 2017). Zhou *et al.* found that relaxin could improve cardiac function in rats with myocardial fibrosis, by reducing EndMT and interstitial collagens I and III, while increasing the microvascular density of the heart (Zhou *et al.*, 2015). It was also found that relaxin could inhibit TGF- β 1-induced mobility of endothelial cells through a Notch-1-dependent pathway, and increasing expression of CD31 while decreasing vimentin content of human umbilical vein endothelial cells (HUVECs) *in vitro* (Zhou *et al.*, 2015). In a separate study, relaxin was found to reduce cardiac fibrosis *in vivo* via the inhibition of EndMT, and by increasing vascular endothelial cadherin and CD31 levels while suppressing vimentin and α -sma levels in HUVECs (Cai *et al.*, 2017) *in vitro*. These combined findings suggest that relaxin can inhibit myofibroblast-mediated aberrant ECM synthesis and deposition at multiple levels.

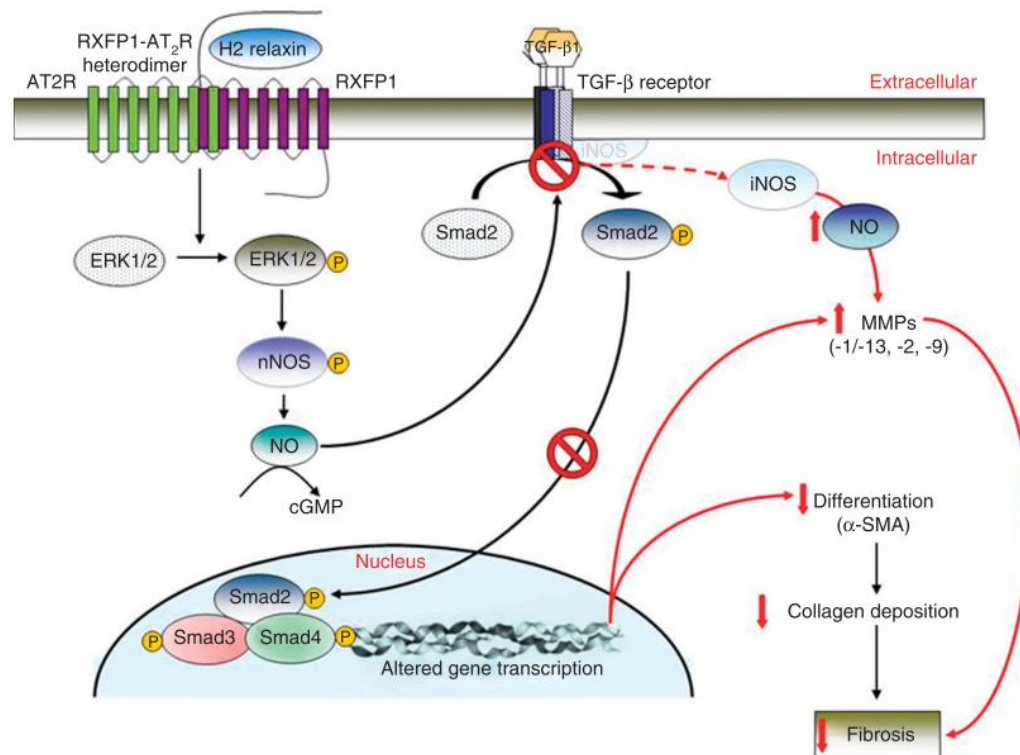
1.6.9 Anti-fibrotic mechanism of relaxin

Excerpt from **Appendix**.

Mechanistically, relaxin has been shown to signal through RXFP1 on myofibroblasts to stimulate Gs and G_{OB} proteins (Mookerjee *et al.*, 2009), and through an extracellular signal-regulated kinase phosphorylation p-ERK1/2 and neuronal nitric oxide (NO) synthase (nNOS)-mediated NO-soluble guanylate cyclase (sGC)-cyclic guanosine monophosphate (cGMP)-dependent pathway to suppress TGF- β 1 signal transduction and activity at the level of Smad2 phosphorylation (Mookerjee *et al.*, 2009; Chow *et al.*, 2014; Sarwar *et al.*, 2015; Wang *et al.*, 2016). This then results in a decrease in TGF- β 1-induced myofibroblast differentiation and hence, myofibroblast-mediated ECM/collagen synthesis; a decrease in TGF- β 1-induced suppression of MMP (MMP-2, MMP-9, MMP-1/-13) activity (Chow *et al.*, 2012); and a decrease in TGF- β 1-induced TIMP activity

and inhibition of ECM degradation. In cardiac myofibroblasts, relaxin has also been found to signal through Notch-1 and suppress Smad3 phosphorylation to inhibit the pro-fibrotic actions of TGF- β 1 (Sassoli *et al.*, 2013; Martina *et al.*, 2017). Interestingly, these signal transduction mechanisms of relaxin in myofibroblasts appears to require the presence of the AT₂ receptors, which could occur through an interaction between RXFP1 and the AT₂R (Chow *et al.*, 2014) [see Figure 1.11]. As a result of this interaction, the anti-fibrotic effects of relaxin can be abrogated by co-administration of an AT₂R antagonist (PD123319) or when relaxin is administered to AT₂R knockout mice (Chow *et al.*, 2014). As the AT₂R can inhibit both the expression and activation of the AT₁R, relaxin may also signal through the RXFP1:AT₂R axis to indirectly inhibit the pro-fibrotic effects of Ang II via the Ang II–AT₁R–TGF- β 1 interaction (Nakajima *et al.*, 1995; Yang *et al.*, 2012).

Figure 1.11:



Schematic illustration of relaxin's signal transduction mechanisms to inhibit TGF-β1. Once H2 relaxin (RLX) binds to RXFP1 on myfibroblasts, it can signal through RXFP1 and possible heterodimers that can form between RXFP1 and AT₂ receptors and through a pERK1/2-nNOS-NO-cGMP-dependent pathway to inhibit intracellular Smad2 phosphorylation and translocation. This disrupts the ability of Smad2 to interact with pSmad3 and eventually Smad4, resulting in the disruption of TGF-β1 signal transduction. In turn, this affects TGF-β1-induced myfibroblast differentiation and myfibroblast-mediated collagen deposition (the basis of fibrosis). Reproduced from (Chow et al., 2014).

Overall, the widely studied organ-protective effects of relaxin as described above, places relaxin and/or other RXFP1-agonists as promising novel therapies to be investigated and compared against current and other novel treatments in this thesis.

1.6.10 B7-33, a single-chain derivative of relaxin

Although various studies have demonstrated the efficacy of relaxin as a rapidly-acting anti-fibrotic and vasodilator, there are certain limitations to its use as a long-term clinical therapy. Aside from its short half-life, relaxin is costly to chemically or recombinantly produce, owing to its two chain structure that requires appropriate linking by disulphide bonds (Hossain and Wade, 2014). Another potential limitation of relaxin is associated with its ability to activate cAMP in many cells, which can promote increased heart rate, tumour progression (Silvertown *et al.*, 2007; Feng *et al.*, 2009) and mortality (Teerlink, 2009). To overcome these limitations, Hossain and colleagues (Hossain *et al.*, 2016) developed a cost-effective single B-chain relaxin derivative, B7-33 which retained the anti-fibrotic effects of relaxin without its tumorigenic potential. B7-33 was created by truncating the first 6 residues from the N-terminus of the relaxin B-chain, and elongating the C-terminus of the native relaxin B-chain (B1-29) with the residues lysine-arginine-serine and leucine (Hossain *et al.*, 2016). This led to B7-33 being highly positively charged (compared to the native B-chain of relaxin), which made it more water soluble for ease of *in vivo* delivery. It specifically bound to RXFP1 and stimulated pERK1/2 activity to a similar extent as H2 relaxin, but only weakly activated cAMP in comparison. Subsequent studies comparing the effects of B7-33 to H2 relaxin demonstrated that at equimolar concentrations to relaxin in heart and lung disease murine models of fibrosis-induced disease, B7-33 decreased interstitial and total collagen deposition (fibrosis) to a similar extent as H2 relaxin and also promoted MMP expression and activity to its two-chained precursor (Hossain *et al.*, 2016). Furthermore, in the same study, using a mouse model of prostate tumour growth, B7-33 administration was found not to exacerbate RM1 cell-induced tumour growth whereas H2 relaxin did (Hossain *et al.*, 2016). In terms of the vasoprotective effects of B7-33, a separate study examined B7-33 in an *ex vivo* model of preeclampsia and found that equimolar doses of B7-33 replicated the same vascular benefits as H2 relaxin in rat mesenteric arteries and prevented endothelial dysfunction in mouse mesenteric arteries (Marshall *et al.*, 2017). Thus, B7-33 has emerged as a new relaxin-like peptidomimetic that is cheaper to produce, but without promoting tumour growth (so is potentially safer as a therapy), and offers equivalent anti-fibrotic effects to that of relaxin in the

heart and lungs. Hence, this thesis examined the effects of B7-33, in comparison to relaxin in treating CKD in a UUO-induced model of interstitial renal disease (Chapter 5).

1.7 Stem cells as treatments for CKD

Stem cells are biological undifferentiated cells characterized by their self-renewal capabilities and their ability to differentiate into various specialized cell lineages to contribute to the reconstruction and homeostasis of tissues (Moore and Lemischka, 2006). Stem cells can be either classified as multipotent, stem cells (ie. mesenchymal stem cells (MSCs)) which are semi-differentiated found within adult tissues (Moore and Lemischka, 2006). Alternatively, pluripotent stem cells, exist in the form of (but not exclusive to) embryonic stem cells (ESCs) and induced pluripotent cells (iPSCs) (Takahashi and Yamanaka, 2006). Pluripotent stem cells have the capability to differentiate into any cell-type of all three germ layers (ectoderm, endoderm and mesoderm) while multipotent stem cells are restricted in their differentiation to either one or two germ layers as they are obtained from adult tissue (Kolios and Moodley, 2013). Although pluripotent stem cells like ESCs have an advantage over adult stem cells in being able to differentiate into more cell types, major ethical concerns and political controversies revolve around the extraction and use of ESCs as therapy. This is due to the extraction of these cells occurring at a time when babies are being born and in some cases involving the destruction of human embryos (Lo and Parham, 2009). One method around the ethical problem is reprogramming somatic cells to becoming iPSCs for stem cell research. However like ESCs, iPSCs may have tumorigenic potential, limiting their use as a safe treatment for kidney disorders that eventuate to CKD (Thomson *et al.*, 1998; Lo and Parham, 2009). On the other hand, adult stem cells are more easily isolated from relevant tissue sources, are non-tumorigenic and in several cases are non-immunogenic (hence, do not provoke an immune response when administered to other species including rodents). Bone marrow-derived MSCs contain all these characteristics, contributing to their wide use in experimental studies and clinical trials (Wise and Ricardo, 2012). These MSC have been used in several registered MSC-based clinical trials (Polymeri *et al.*, 2016).

Aside from the differentiation capacity of MSCs, these cells have also been shown to act via

paracrine signalling to regulate and promote a number of different cellular responses including cell survival, proliferation, migration and gene expression (Hocking and Gibran, 2010). It is the differentiation capabilities of stem cells that contributes to regeneration of damaged tissue while the paracrine signalling of these cells contributes to regulation of local cellular responses to tissue injury. These combined attributes make the use of stem cells, particularly MSCs, an attractive therapy in regenerative medicine. Numerous studies using MSCs have already shown these stem cells to be effective at ameliorating tissue damage in major organs including the heart, brain, kidney, lung, liver, eye and skin (Morigi *et al.*, 2004; Amado *et al.*, 2005; Ma *et al.*, 2006; Sasaki *et al.*, 2008; Honmou *et al.*, 2011; Royce *et al.*, 2015). With such promising data demonstrating broad applicability and efficacy, this has led to the rapid development of numerous stem cell-based therapies in pre-clinical and clinical trials aimed at treating various acute and chronic diseases including diabetes mellitus, cirrhosis, myeloid leukaemia, heart failure, pulmonary fibrosis etc. (Kolios and Moodley, 2013). The main reparative paracrine properties of MSCs, although not limited to, include their anti-inflammatory, anti-apoptotic and angiogenic effects, which will be discussed further below.

1.7.1 Immunomodulatory effects of stem cells

A consistently reported paracrine effect of stem cells is their anti-inflammatory properties. Upon kidney injury, macrophages and neutrophils migrate to the site of injury and release various pro-inflammatory cytokines, chemokines and reactive oxygen species (ROS) in addition to the recruitment of adaptive immune cells i.e. mast cells, natural killer cells, B and T lymphocytes. Under normal physiological conditions, intravenous (i.v.) administration of MSCs, will migrate towards the lungs and then into bone marrow where they can reside for an extended duration of time (Devine *et al.*, 2001). However, upon injury, the i.v.-administered stem cell immediately migrate to the lungs and then migrate towards injured tissues driven by chemokines released from the inflamed injured site (Honczarenko *et al.*, 2006). Although the homing properties of stem cells are yet to be fully elucidated, current studies show whole repertoires of chemokine receptors present on stem cells including C-C chemokine receptor type 1 (CCR1), CCR4, CCR7 C-X-C chemokine receptor type 5 (CXCR5), stromal cell-derived factor-1/CXCR4 and CD44 (Honczarenko *et al.*, 2006; Zhu *et al.*, 2006; Ponte *et al.*, 2007; Ringe *et al.*, 2007; Panja *et al.*,

2017). The fact that stem cells can express a variety of chemokine receptors suggests they can home to an assortment of inflamed tissues during injury. Once at the site of injury, stem cells shift pro-inflammatory cells (ie. monocytes, macrophages) to an anti-inflammatory state by decreasing TNF- α , IL-1 β and/or interferon- γ , which subsequently reduce inflammatory responses (Ortiz *et al.*, 2003; Togel *et al.*, 2005). This in turn, decreases T-cell-induced responses via communication with dendritic cells, suppressing the activity of natural killer cells, and suppressing dendritic cell function for immunosuppression to allow administered stem cells to evade the immune system (Wu *et al.*, 2005). The latter is likely aided by the reduction of antigen presentation to naïve T-cells which also allows for a reduction in host rejection of introduced stem cells (Wu *et al.*, 2005). In addition, stem cells also promote a Th-2 dominant immune response, which is generally anti-inflammatory in nature (Aggarwal and Pittenger, 2005; Wise and Ricardo, 2012). Furthermore, they also additionally secrete soluble factors including IL-1, IL-10 and prostaglandin E2 (PGE2) which diminish the effects of neutrophils and monocytes in being able to release chemokines and cytokines that contribute to tissue inflammation (Bouffi *et al.*, 2010).

1.7.2 Anti-apoptotic effects of stem cells

Another property of stem cells are their anti-apoptotic effects. In the kidneys, insults to tissues such as exposure to toxins, sepsis or ischemia can lead to ROS accumulation, also referred to as oxidative stress (Bussolati *et al.*, 2008). These elevated levels of free radicals coupled with apoptotic proteins cause apoptotic cell death and/or necrosis of tubular cells and podocytes (Wise and Ricardo, 2012). MSC administration has been found to reduce oxidative stress and apoptosis in animal models following both ischemia-reperfusion and cisplatin-induced injury (Chen *et al.*, 2011; Wise and Ricardo, 2012). The latter studies induced acute kidney injury by increasing apoptotic proteins such as Bax and decreasing anti-apoptotic proteins such as Bcl-2. Administration of MSCs downregulated Bax and upregulated Bcl-2, leading to an anti-apoptotic response (Cao *et al.*, 2010; Qi and Wu, 2013).

1.7.3 Angiogenic effects of stem cells

Thirdly, stem cells can stimulate angiogenesis and limit vascular rarefaction. Revascularization plays a critical role in wound healing as it provides nutrient delivery (King *et al.*, 2014). Some stem cells have been shown to differentiate into endothelial cells, stimulate the activity of endothelial progenitor cells, and increase gene expression of proangiogenic factors such as VEGF and angiopoietin. Furthermore, stem cells can up-regulate expression and activity of CXCR4, a receptor that is correlated with angiogenesis and which acts as a chemoattractant as mentioned earlier (Leu *et al.*, 2010; Zacharek *et al.*, 2010). In humans following acute myocardial infarct, administration of stem cells in the heart followed by nine days of revascularization was associated with improvements in ejection fraction, infarct size and myocardial perfusion which were attributed to myocardial regeneration and neovascularization by administered stem cells (Strauer *et al.*, 2002). Within the kidneys, a study using COL4A3-deficient mice injected with MSCs showed the prevention of perivascular capillaries loss and improved recovery of the damaged kidney (Ninichuk *et al.*, 2006).

1.7.4 Stem cells alone and in combination in treating chronic diseases

Amidst the favourable outcomes following the use of stem cells in acute kidney injury and other short-term animal disease models (Wise and Ricardo, 2012), the therapeutic efficacy of stem cells has been less promising in long-term exacerbated/chronic diseases (Dolgachev *et al.*, 2009). This potentially is attributed to the extensive fibrosis that occurs within chronically-damaged tissues which has been shown to impair stem cell survival, migration, proliferation and integration with resident tissue cells (Knight *et al.*, 2010; Eun *et al.*, 2011; Van Dijk *et al.*, 2011). In this setting, kidney studies have shown that the glomerular reparative capacity of MSCs are less impressive and hence, ongoing damage to glomerular cells can result in the progressive loss of nephrons, leading to the expansion of the interstitium and further development of fibrosis (Wise and Ricardo, 2012). Thus, this drove the idea of using a combination therapy with an anti-fibrotic treatment to reduce fibrosis associated with CKD, thereby creating a more favourable environment for stem cell-based therapies to elicit their organ-protective effects. Recent efforts involved the combination of MSCs with relaxin in a mouse model of obstructive nephropathy which showed significantly improved anti-fibrotic and tissue-reparative effects over the effects

of MSCs alone (Huuskens *et al.*, 2015). This combination therapy was further supported by results investigated in chronic lung disease models with established fibrosis, where again the combined effects of MSCs with relaxin, or human amnion epithelial cells with relaxin, reduced established fibrosis and associated airway reactivity to a greater extent than either therapy alone (Royce *et al.*, 2015, 2016).

1.7.5 Human amniotic epithelial cells (hAECs)

While all stem cell lineages have some promise as therapeutics, recent studies into human amniotic epithelial cells (hAECs) have shown that these cells contain several important advantages over other stem cells (Table 1.7). As gestational tissue such as the placenta and amniotic fluid are often discarded upon birth, placental stem cells including hAECs can be easily and non-invasively isolated from discarded placental tissue (Murphy and Atala, 2013). Like MSCs, they share comparable paracrine properties and effects without the need for invasive procedures for extraction (Broughton *et al.*, 2013; Mehanni *et al.*, 2013). Furthermore, they are pluripotent and avoid the ethical concerns, immunogenic and tumorigenic effects seen with ESCs or iPSCs (Broughton *et al.*, 2013; Yang *et al.*, 2018). Recently our lab and colleagues tested the reparative efficacy of MSCs, hAECs and their combined effects with relaxin in a mouse model of chronic allergic airway disease (Royce *et al.*, 2016). The results obtained showed synergistic improvements using hAECs with relaxin over that of the either treatment alone in being able to reduce established airway inflammation, fibrosis and reactivity (Royce *et al.*, 2016). This demonstrated the feasibility and improved efficacy of co-administering hAECs with relaxin in respiratory disease models. However, the effects of hAECs and relaxin have not been evaluated in experimental kidney disease.

Table 1.7: Beneficial characteristics of hAECs over four major cell lineages. Adapted from (Broughton *et al.*, 2013).

<u>Benefits</u>	ESCs	BMSCs	iPSCs	hAECs
Readily available	X	✓	✓	✓
Do not require invasive extraction	✓	X	✓	✓
Pluripotent properties	✓	X	✓	✓
Differentiate into functional neural tissue	✓	X	✓	✓
Non-immunogenic	X	* ✓	X	✓
<u>Immunomodulatory properties</u>	✓	✓	✓	✓
Non-tumorigenic	X	✓	X	✓

* Autologous transplantation only.

1.7.5 Limitation of stem cell-based therapies

Despite the promising findings of this combination therapeutic approach, there are still some drawbacks to using combination therapies involving stem cells. Stem cells can exhibit donor-dependent variability and require cell culture maintenance to achieve sufficient amounts of cells for therapeutic use. Furthermore, they cannot be frozen and thawed for immediate use and again require cell culture maintenance and expansion, thereby prolonging the amount of time taken for their therapeutic administration, which can also involve the risk of freeze/thawing and cell cultured-induced loss of function (Moll *et al.*, 2014). The number of stem cells that can physically be injected into murine models needs to be capped at 1-2 million cells/mouse; as administration

of >2 million cells/mouse can induce respiratory problems leading to death, due to the clumping and accumulation of cells that get trapped within the lung, which can induce the risk of embolism formation and/or prevent the migration of cells to injured tissue sites (Kikuchi *et al.*, 2002; Kyriakou *et al.*, 2008; Moodley *et al.*, 2010). This, however, is less of a problem for the use of stem cells in treating human disease, as the human airways are much larger and deeper than their murine counterparts. Moreover, studies have shown that stem cells are rapidly cleared from the damaged organ within 3-7 days of administration (Huuskens *et al.*, 2015). Interestingly, as their protective effects remain active long after they have been eliminated, it has been proposed that microvesicles derived from stem cells, known as exosomes are likely released and mediate the therapeutic and reparative properties of stem cell well after the cells are cleared from the damaged organs they are administered into (Ng *et al.*, 2015).

1.8 Exosomes

Recently exosomes have been identified as new paracrine factors released by various cell types including dendritic cells, B-lymphocytes, various epithelial, endothelial and stem cells (Van Balkom *et al.*, 2011). They can be isolated by cell culture supernatant and collected from a variety of sources including the amnion (Keller *et al.*, 2007; Motedayyen *et al.*, 2017). Stem cell-derived exosomes are microvesicles that have the diameter of ~50-100nm (1-300th-1/500th the size of their parental stem cells) and contain various lipids, proteins and non-coding RNAs all of which hold the same reparative properties of their parent cell (Valadi *et al.*, 2007; Urbanelli *et al.*, 2015). This shift in direction from stem cells to their secretory vesicles was first spurred by studies demonstrating that culture medium conditioned by MSCs produced similar therapeutic benefits when administered in rodent models of myocardial infarction, lung injury and later, kidney injury (Gnecci *et al.*, 2005; Bruno *et al.*, 2009; Goolaerts *et al.*, 2014). Subsequently, homogenous preparations of exosomes which were equivalent to ~10% of the conditioned medium dosage was shown to reduce infarct size of an ex vivo mouse model of myocardial ischemia/reperfusion (Lai *et al.*, 2010). Thus, this prompted further research and application of stem cell-derived exosomes for their therapeutic capabilities.

Currently, there are 3 main theories on the possible mechanisms of how exosomes elicit their effects on target cells: 1) they adhere to the target cell surface through adhesion molecules and receptors present leading to downstream signalling; 2) the exosomes may directly fuse into the target cell to release its contents; or 3) the exosomes may incorporate into target cells after endocytosis and then be processed in an endosomal pathway which is better supported in the literature (Valadi *et al.*, 2007; Van Balkom *et al.*, 2011).

In terms of benefits over stem cells, exosomes have significant advantages including 1) they are non-tumorigenic as they lack intrinsic self-renewal mechanisms (Lener *et al.*, 2015); 2) because of their smaller size, they are less likely to form an embolism and become trapped in the lungs, and as a result, the therapeutic impact of several million cells (that can't be physically administered to mice) can be delivered in the form of exosomes (Kordelas *et al.*, 2014). 3) Once isolated and stored frozen, they can be thawed for immediate use without the need for cell culture maintenance (Kordelas *et al.*, 2014). Moreover, exosomes exert their protective effects through similar mechanisms as the parent stem cell from which they are released, suggesting that exosomes potentially mediate the cell-to-cell signalling between stem cells and target cells (Xin *et al.*, 2013).

Regarding CKD, whereas the viability and survivability of stem cells are reduced in the presence of fibrosis in chronic disease models (Eun *et al.*, 2011), exosomes are not as sensitive towards environmental factors as they inherently lack cellular activity (Lener *et al.*, 2015). However, the ability for exosomes to migrate to sites of tissue injury could potentially be inhibited by fibrosis. Hence, the addition of an anti-fibrotic agent such as relaxin could also improve the migration of and therapeutic potential of exosomes – which will be investigated in this thesis.

1.9 Aims and Hypothesis

Recent studies have started to compare the anti-fibrotic effects of RLX to the clinically used ACEi, enalapril, in an experimental model of cardiac fibrosis (Samuel *et al.*, 2014); and to bone marrow-derived mesenchymal stem cells (MSCs) in an experimental model of tubulointerstitial renal fibrosis (Huuskes *et al.*, 2015). In both studies, relaxin demonstrated improved anti-fibrotic

efficacy over enalapril or MSCs alone and augmented the actions of both therapies to reduce fibrosis, when added in combination with either of them. These projects aim to extend those studies, by comparing and combining the anti-fibrotic effects of RLX to other front-line treatments (ARB and ACEi), as well other emerging anti-fibrotic (AT₂ receptor agonists; IRAP inhibitor; hAEC derived exosomes) – in high salt or unilateral ureteric obstruction-induced experimental kidney disease models in mice.

Hypotheses: That 1) relaxin will demonstrate at least similar, if not improved anti-fibrotic efficacy over a clinically-used ARB (candesartan cilexetil); ACE inhibitor (perindopril); AT₂ receptor agonist (CGP42112 or β -Pro⁷Ang III); IRAP inhibitor (HFI-419); and hAEC derived exosomes; further confirming its potential as an anti-fibrotic therapy of the future. 2) The combined effects of relaxin and the various therapies it is combined with will offer greater anti-fibrotic efficacy compared to either therapy alone.

Aims: The following aims will be addressed in this PhD thesis:

Aim 1: To compare and combine the anti-fibrotic effects of relaxin to an ARB (candesartan cilexetil) and an AT₂ receptor agonist (CGP42112) in a high salt (5% NaCl)-induced murine model of kidney disease;

Aim 2: To compare and combine the anti-fibrotic effects of relaxin to an ACEi (perindopril) and an IRAP inhibitor (HFI-419) in the high salt (5% NaCl)-induced murine model of kidney disease; and

Aim 3: To compare and combine the anti-fibrotic effects of relaxin to various peptide- and cell-based treatments in a UUO-induced murine model of interstitial kidney disease.

Completion of these studies should lead to the identification of mono- or combination therapies that have improved anti-fibrotic efficacy over current standard of care medications.

1.10 References

- AbdAlla, S, Lothar, H, Abdel-tawab, AM, Quitterer, U (2001). The angiotensin II AT2 receptor is an AT1 receptor antagonist. *J Biol Chem* **276**: 39721–39726.
- Aggarwal, S, Pittenger, MF (2005). Human mesenchymal stem cells modulate allogeneic immune cell responses. *Blood* **105**: 1815–22.
- Ahmed, AKH (2009). Matrix Metalloproteinases and Their Inhibitors in Kidney Scarring: Culprits or Innocents. *J. Heal. Sci.* **55**: 473–483.
- Albiston, AL, McDowall, SG, Matsacos, D, Sim, P, Clune, E, Mustafa, T, *et al.* (2001). Evidence That the Angiotensin IV (AT4) Receptor Is the Enzyme Insulin-regulated Aminopeptidase. *J. Biol. Chem.* **276**: 48623–48626.
- Albiston, AL, Morton, CJ, Ng, HL, Pham, V, Yeatman, HR, Ye, S, *et al.* (2008). Identification and characterization of a new cognitive enhancer based on inhibition of insulin-regulated aminopeptidase. *FASEB J.* **22**: 4209–17.
- Allan, JA, Docherty, AJ, Barker, PJ, Huskisson, NS, Reynolds, JJ, Murphy, G (1995). Binding of gelatinases A and B to type-I collagen and other matrix components. *Biochem. J.* **309**: 299–306.
- Amado, LC, Saliaris, AP, Schuleri, KH, John, M St., Xie, J-S, Cattaneo, S, *et al.* (2005). Cardiac repair with intramyocardial injection of allogeneic mesenchymal stem cells after myocardial infarction. *Proc. Natl. Acad. Sci.* **102**: 11474–11479.
- Amer, H, Griffin, MD (2014). Modulating kidney transplant interstitial fibrosis and tubular atrophy: is the RAAS an important target? *Kidney Int.* **85**: 240–3.
- Andersson, H, Demaegdt, H, Vauquelin, G, Lindeberg, G, Karl, A, Hallberg, M (2010). Disulfide Cyclized Tripeptide Analogues of Angiotensin IV as Potent and Selective Inhibitors of. *J. Med. Chem.* **53**: 8059–8071.
- Angelica, MD, Fong, Y (2013). The myofibroblast matrix: implications for tissue repair and fibrosis. *J. Pathol.* **229**: 298–309.
- Arima, S, Ito, S (2000). Angiotensin II type 2 receptors in the kidney : evidence for endothelial-

cell-mediated renal vasodilatation. 448–451.

Atkins, RC (2002). Inflammatory cytokines in glomerulonephritis. *Nephrology* **7**: 2–6.

Attisano, L, Wrana, J (2002). Signal Transduction by the TGF- β Superfamily. *Science* (80-.). **296**: 1646–1647.

Baker, KJ, Booz, GW, Dostal, DE (1992). Cardiac actions of angiotensin II: role of an intracardiac renin-angiotensin system. *Annu. Rev. Physiol.* **54**: 227–241.

Balakumar, P, Kathuria, S, Taneja, G, Kalra, S, Mahadevan, N (2012). Is targeting eNOS a key mechanistic insight of cardiovascular defensive potentials of statins? *J. Mol. Cell. Cardiol.* **52**: 83–92.

Balkom, BWM Van, Pisitkun, T, Verhaar, MC, Knepper, MA (2011). Exosomes and the kidney: Prospects for diagnosis and therapy of renal diseases. *Kidney Int.* **80**: 1138–1145.

Bani, D, Ballati, L, Masini, E, Bigazzi, M, Sacchi, TB (1997). Relaxin counteracts asthma-like reaction induced by inhaled antigen in sensitized guinea pigs. *Endocrinology* **138**: 1909–1915.

Bani, D, Baronti, R, Vannacci, A, Bigazzi, M, Bani Sacchi, T, Mannaioni, PF, *et al.* (2002). Inhibitory effects of relaxin on human basophils activated by stimulation of the Fc ϵ receptor. The role of nitric oxide. *Int. Immunopharmacol.* **2**: 1195–1204.

Barber, MN, Sampey, DB, Widdop, RE (1999). AT(2) receptor stimulation enhances antihypertensive effect of AT(1) receptor antagonist in hypertensive rats. *Hypertension* **34**: 1112–1116.

Barnes, JL, Gorin, Y (2011). Myofibroblast differentiation during fibrosis: Role of NAD(P)H oxidases. *Kidney Int.* **79**: 944–956.

Bataller, R, Sancho-Bru, P, Gines, P, Brenner, DA (2005). Liver Fibrogenesis: A New Role for the Renin-Angiotensin System. *Antioxid. Redox Signal.* **7**: 1346–1355.

Bathgate, R a D, Halls, M, Westhuizen, E Van Der, Callander, G, Kocan, M, Summers, RJ (2013). Relaxin family peptides and their receptors. *Physiol. Rev.* **93**: 405–480.

Bathgate, R, Hsueh, A, Sheerwood, O (2006a). *Physiology and molecular biology of the relaxin peptide family* (Elsevier).

Bathgate, RA, Ivell, R, Sanborn, B, Sherwood, O, Summers, R (2006b). International Union of Pharmacology LVII: Recommendations for the Nomenclature of Receptors for Relaxin Family Peptides. *Pharmacol. Rev.* **58**: 7–31.

Bathgate, RAD, Kocan, M, Scott, DJ, Hossain, MA, Good, S V., Yegorov, S, *et al.* (2018). The relaxin receptor as a therapeutic target – perspectives from evolution and drug targeting. *Pharmacol. Ther.* **187**: 114–132.

Bathgate, RAD, Samuel, CS, Burazin, TCD, Gundlach, AL, Tregear, GW (2003). Relaxin : new peptides , receptors and novel actions. *Trends Endocrinol. Metab.* **14**: 207–213.

Bathgate, RAD, Samuel, CS, Burazin, TCD, Layfield, S, Claasz, AA, Reytomas, IGT, *et al.* (2002). Human Relaxin Gene 3 (H3) and the Equivalent Mouse Relaxin. *J. Biol. Chem.* **277**: 1148–1157.

Becker, GJ, Hewitson, TD (2000). The role of tubulointerstitial injury in chronic renal failure. *Curr. Opin. Nephrol. Hypertens.* **9**: 133–8.

Beiery, T, Knappe, V, Tiyerili, V, Stöckigt, F, Effelsberg, V, Linhart, M, *et al.* (2018). Chronic lower-dose relaxin administration protects from arrhythmia in experimental myocardial infarction due to anti-inflammatory and anti-fibrotic properties. *Int. J. Cardiol.* **250**: 21–28.

Beiery, T, Tiyerili, V, Knappe, V, Effelsberg, V, Klein, S, Schierwagen, R, *et al.* (2017). Relaxin reduces susceptibility to post-infarct atrial fibrillation in mice due to anti-fibrotic and anti-inflammatory properties. *Biochem. Biophys. Res. Commun.* **490**: 643–649.

Bennett, RG, Heimann, DG, Singh, S, Simpson, RL, Tuma, DJ (2013). Relaxin decreases the severity of established hepatic fibrosis in mice. *Liver Int.* 416–426.

Bennett, RG, Kharbanda, KK, Tuma, DJ (2003). Inhibition of markers of hepatic stellate cell activation by the hormone relaxin. *Biochem. Pharmacol.* **66**: 867–874.

Bennett, W, Grunfeld, J-P (1995). Clinical Nephrology. *Curr. Opin. Nephrol. Hypertens.* **4**: 111–113.

Berillis, P (2015). Marine Collagen: Extraction and Applications. In Research Trends in Biochemistry, Molecular Biology and Microbiology, pp 1–13.

Boor, P, Šebeková, K, Ostendorf, T, Floege, J (2007). Treatment targets in renal fibrosis. *Nephrol. Dial. Transplant.* **22**: 3391–3407.

Borgo, M Del, Wang, Y, Bosnyak, S, Khan, M, Walters, P, Spizzo, I, *et al.* (2015). β -Pro7Ang III is a novel highly selective angiotensin II type 2 receptor (AT2R) agonist, which acts as a vasodepressor agent via the AT2R in conscious spontaneously hypertensive rats. *Clin. Sci.* **129**: 505–513.

Borrow, AP, Cameron, NM (2012). Hormones and Behavior The role of oxytocin in mating and pregnancy. *Horm. Behav.* **61**: 266–276.

Borthwick, LA, Wynn, TA, Fisher, AJ (2013). Cytokine mediated tissue fibrosis. *Biochim. Biophys. Acta - Mol. Basis Dis.* **1832**: 1049–1060.

Bosnyak, S, Jones, ES, Christopoulos, A, Aguilar, M-I, Thomas, WG, Widdop, RE (2011). Relative affinity of angiotensin peptides and novel ligands at AT1 and AT2 receptors. *Clin. Sci.* **121**: 297–303.

Bouffi, C, Bony, C, Courties, G, Jorgensen, C, Noël, D (2010). IL-6-dependent PGE2 secretion by mesenchymal stem cells inhibits local inflammation in experimental arthritis. *PLoS One* **5**:

Bouley, R, Pérodin, J, Plante, H, Řihakova, L, Bernier, SG, Maletínská, L, *et al.* (1998). N- and C-terminal structure-activity study of angiotensin II on the angiotensin AT2receptor. *Eur. J. Pharmacol.* **343**: 323–331.

Brecht, A, Bartsch, C, Baumann, G, Stangl, K, Dschietzig, T (2011). Relaxin inhibits early steps in vascular inflammation. *Regul. Pept.* **166**: 76–82.

Brodsky, B, Persikov, A V (2005). Molecular structure of the collagen triple helix. *Adv. Protein Chem.* **70**: 302–333.

Brodsky, B, Ramshaw, JAM (1997). The collagen triple-helix structure. *Matrix Biol.* **15**: 545–554.

Broughton, BRS, Lim, R, Arumugam, T V., Drummond, GR, Wallace, EM, Sobey, CG (2013). Post-

stroke inflammation and the potential efficacy of novel stem cell therapies: focus on amnion epithelial cells. *Front. Cell. Neurosci.* **6**: 1–9.

Bruce, E, Shenoy, V, Rathinasabapathy, A, Espejo, A, Horowitz, A, Oswald, A, *et al.* (2015). Selective activation of angiotensin AT₂ receptors attenuates progression of pulmonary hypertension and inhibits cardiopulmonary fibrosis. *Br. J. Pharmacol.* **172**: 2219–2231.

Bruno, S, Grange, C, Deregibus, MC, Calogero, RA, Saviozzi, S, Collino, F, *et al.* (2009). Mesenchymal stem cell-derived microvesicles protect against acute tubular injury. *J. Am. Soc. Nephrol.* **20**: 1053–1067.

Bussolati, B, Tetta, C, Camussi, G (2008). Contribution of stem cells to kidney repair. *Am. J. Nephrol.* **28**: 813–822.

Cai, J, Chen, X, Chen, X, Chen, L, Zheng, G, Zhou, H, *et al.* (2017). Anti-Fibrosis Effect of Relaxin and Spironolactone Combined on Isoprenaline-Induced Myocardial Fibrosis in Rats via Inhibition of Endothelial-Mesenchymal Transition. *Cell. Physiol. Biochem.* **41**: 1167–1178.

Cao, H, Qian, H, Xu, W, Zhu, W, Zhang, X, Chen, Y, *et al.* (2010). Mesenchymal stem cells derived from human umbilical cord ameliorate ischemia/reperfusion-induced acute renal failure in rats. *Biotechnol. Lett.* **32**: 725–732.

Cernaro, V, Medici, MA, Bianco, F, Santoro, D, Lacquaniti, A, Romeo, A, *et al.* (2017). Opposite actions of urotensin II and relaxin - 2 on cellular expression of fibronectin in renal fibrosis : A preliminary experimental study. *Clin. Exp. Pharmacol. Physiol.* **44**: 1069–1071.

Cesari, M, Rossi, G, Pessina, A (2002). Biological properties of the angiotensin peptides other than angiotensin II: implications for hypertension and cardiovascular diseases. *J Hypertens* **20**: 793–799.

Chadban, SJ, Briganti, EM, Kerr, PG, Dunstan, DW, Welborn, T a, Zimmet, PZ, *et al.* (2003). Prevalence of kidney damage in Australian adults: The AusDiab kidney study. *J. Am. Soc. Nephrol.* **14**: S131–S138.

Chai, SY, Fernando, R, Peck, G, Ye, SY, Mendelsohn, FAO, Jenkins, TA, *et al.* (2004). The

angiotensin IV/AT4 receptor. *Cell. Mol. Life Sci.* **61**: 2728–2737.

Chan, K, Ikizler, T, Gamboa, JL, Yu, C, Hakim, RM, Brown, NJ (2011). Combined angiotensin-converting enzyme inhibition and receptor blockade associate with increased risk of cardiovascular death in hemodialysis patients. *Kidney Int* **80**: 978–985.

Chen, C, Huang, W (2000). Pressor and Renal Effects of Intracerebroventricularly Administered Angiotensins II and III in Rats. *Kidney Blood Press. Res.* **23**: 95–105.

Chen, L, Sha, M, Li, D, Zhu, Y, Wang, X (2017). Relaxin abrogates renal interstitial fibrosis by regulating macrophage polarization via inhibition of Toll-like receptor 4 signaling. *Oncotarget* **8**: 21044–21053.

Chen, YT, Sun, CK, Lin, YC, Chang, LT, Chen, YL, Tsai, TH, *et al.* (2011). Adipose-Derived Mesenchymal Stem Cell Protects Kidneys against Ischemia-Reperfusion Injury through Suppressing Oxidative Stress and Inflammatory Reaction. *J. Transl. Med.* **9**: 1–17.

Cheng, J, Grande, J (2002). Transforming growth factor- β signal transduction and progressive renal disease. *Exp Biol Med* **227**: 943–956.

Choi, ME, Ding, Y, Kim, S II (2012). TGF- β Signaling via TAK1 Pathway: Role in Kidney Fibrosis. *Semin. Nephrol.* **32**: 244–252.

Chow, BS, Kocan, M, Bosnyak, S, Sarwar, M, Wigg, B, Jones, ES, *et al.* (2014). Relaxin requires the angiotensin II type 2 receptor to abrogate renal interstitial fibrosis. *Kidney Int* **86**: 75–85.

Chow, BSM, Chew, EGY, Zhao, C, Bathgate, RAD, Hewitson, TD, Samuel, CS (2012). Relaxin signals through a RXFP1-pERK-nNOS-NO-cGMP-dependent pathway to up-regulate matrix metalloproteinases: The additional involvement of iNOS. *PLoS One* **7**: 1–9.

Coats, AJS (2001). Exciting new drugs on the horizon - Eplerenone, a selective aldosterone receptor antagonist (SARA). *Int. J. Cardiol.* **80**: 1–4.

Cochrane, AL (2005). Renal Structural and Functional Repair in a Mouse Model of Reversal of Ureteral Obstruction. *J. Am. Soc. Nephrol.* **16**: 3623–3630.

Conrad, KP (2010). Unveiling the Vasodilatory Actions and Mechanisms of Relaxin. *Hypertension* **56**: 2–9.

Conrad, KP, Debrah, DO, Novak, J, Danielson, LA, Shroff, SG (2004). Relaxin modifies systemic arterial resistance and compliance in conscious, nonpregnant rats. *Endocrinology* **145**: 3289–3296.

Conrad, KP, Novak, J (2004). Emerging role of relaxin in renal and cardiovascular function. *Am. J. Physiol. Integr. Comp. Physiol.* **287**: R250–R261.

Crowley, SD, Coffman, TM (2014). The inextricable role of the kidney in hypertension. *J. Clin. Invest.* **124**: 2341–2347.

Crowley, SD, Gurley, SB, Herrera, MJ, Ruiz, P, Griffiths, R, Kumar, AP, *et al.* (2006). Angiotensin II causes hypertension and cardiac hypertrophy through its receptors in the kidney. *Proc. Natl. Acad. Sci. U. S. A.* **103**: 17985–17990.

Danielson, LA (2006). Relaxin Improves Renal Function and Histology in Aging Munich Wistar Rats. *J. Am. Soc. Nephrol.* **17**: 1325–1333.

Darby, IA, Hewitson, TD (2007). Fibroblast Differentiation in Wound Healing and Fibrosis. *Int. Rev. Cytol.* **257**: 143–179.

Davide, B, C, PS, D, NS, FM, SG (2014). Aldosterone antagonists for preventing the progression of chronic kidney disease. *Cochrane Database Syst. Rev.*

Denic, A, Lieske, J, Chakkera, H, Poggio, E, Alexander, M, Singh, P, *et al.* (2017). The Substantial Loss of Nephrons in Healthy Human Kidneys with Aging. *J Am Soc Nephrol* **28**: 313–320.

Derynck, R, Zhang, YE (2003). Smad-dependent and Smad-independent pathways in TGF-beta family signalling. *Nature* **425**: 577–584.

Devine, SM, Bartholomew, AM, Mahmud, N, Nelson, M, Patil, S, Hardy, W, *et al.* (2001). Mesenchymal stem cells are capable of homing to the bone marrow of non-human primates following systemic infusion. *Exp. Hematol.* **29**: 244–255.

- Dijk, A Van, Naaijken, BA, Jurgens, WJFM, Nalliah, K, Sairras, S, Pijl, RJ van der, *et al.* (2011). Reduction of infarct size by intravenous injection of uncultured adipose derived stromal cells in a rat model is dependent on the time point of application. *Stem Cell Res.* **7**: 219–229.
- Diwakarla, S, Nylander, E, Grönbladh, A, Vanga, SR, Khan, YS, Gutiérrez-de-terán, H, *et al.* (2016). Binding to and Inhibition of Insulin-Regulated Aminoamidase by Macrocyclic Disulfides Enhances Spine Density. *Mol. Pharmacol.* **89**: 413–424.
- Dolgachev, VA, Ullenbruch, MR, Lukacs, NW, Phan, SH (2009). Role of stem cell factor and bone marrow-derived fibroblasts in airway remodeling. *Am. J. Pathol.* **174**: 390–400.
- Dormuth, CR, Hemmelgarn, BR, Paterson, JM, James, MT, Teare, GF, Raymond, CB, *et al.* (2013). Use of high potency statins and rates of admission for acute kidney injury: multicenter, retrospective observational analysis of administrative databases. *Bmj* **346**: f880.
- Drongelen, J Van, Koppen, A Van, Pertijs, J, Gooi, JH, Sweep, FCGJ, Lotgering, FK, *et al.* (2013). Impaired effect of relaxin on vasoconstrictor reactivity in spontaneous hypertensive rats. *Peptides* **49**: 41–48.
- Dschietzig, T, Richter, C, Bartsch, C, Laule, M, Armbruster, FP, Baumann, G, *et al.* (2001). The pregnancy hormone relaxin is a player in human heart failure. *FASEB J.* **15**: 2187–2195.
- Du, X, Shimizu, A, Masuda, Y, Kuwahara, N, Arai, T, Kataoka, M, *et al.* (2012). Involvement of matrix metalloproteinase-2 in the development of renal interstitial fibrosis in mouse obstructive nephropathy. *Lab. Investig.* **92**: 1149–1160.
- Eddy, A (1996). Molecular insights into renal interstitial fibrosis. *J. Am. Soc. Nephrol.* **7**: 2495–2508.
- Eddy, AA, Lopez-Guisa, JM, Okamura, DM, Yamaguchi, I (2012). Investigating mechanisms of chronic kidney disease in mouse models. *Pediatr Nephrol* **27**: 1233–1247.
- Edgley, AJ, Krum, H, Kelly, DJ (2012). Targeting fibrosis for the treatment of heart failure: A role for transforming growth factor- β . *Cardiovasc. Ther.* **30**: 30–40.
- Edwards, NC, Moody, WE, Yuan, M, Hayer, MK, Ferro, CJ, Townend, JN, *et al.* (2015). Diffuse

interstitial fibrosis and myocardial dysfunction in early chronic kidney disease. *Am. J. Cardiol.* **115**: 1311–1317.

Erikson, MS, Unemori, EN (2001). Relaxin clinical trials in systemic sclerosis. In *Relaxin 2000*, pp 373–381.

Essue, BM, Wong, G, Chapman, J, Li, Q, Jan, S (2013). How are patients managing with the costs of care for chronic kidney disease in Australia? A cross-sectional study. *BMC Nephrol.* **14**: 1–9.

Eun, L, Song, H, Choi, E, Lee, T, Moon, D, Hwang, D, *et al.* (2011). Implanted bone marrow-derived mesenchymal stem cells fail to metabolically stabilize or recover electromechanical function in infarcted hearts. *Tissue Cell* **43**: 238–245.

Evans, J (1959). Relaxin (releasin) therapy in diffuse progressive scleroderma; a preliminary report. *AMA Arch Derm* **79**: 150–158.

Fallowfield, JA, Hayden, AL, Snowdon, VK, Aucott, RL, Stutchfield, BM, Mole, DJ, *et al.* (2014). Relaxin Modulates Human and Rat Hepatic Myofibroblast Function and Ameliorates Portal Hypertension InVivo. *Hepatology* **59**: 1492–1504.

Farris, AB, Colvin, RB (2012). Renal interstitial fibrosis. *Curr. Opin. Nephrol. Hypertens.* **21**: 289–300.

Feng, S, Agoulnik, IU, Li, Z, Han, HD, Lopez-Berestein, G, Sood, A, *et al.* (2009). Relaxin/RXFP1 Signaling in Prostate Cancer Progression. *Ann. N. Y. Acad. Sci.* **1160**: 379–380.

Fernandez-Patron, C, Radomski, M, Davidge, S (1999). Vascular matrix metalloproteinase-2 cleaves big endothelin-1 yielding a novel vasoconstrictor. *Circ. Res.* **85**: 906–911.

Garber, S, Mirochnik, Y, Brecklin, C, Unemori, E, Singh, A, Slobodskoy, L, *et al.* (2001a). Relaxin decreases renal interstitial fibrosis and slows progression of renal disease. *Kidney Int* **59**: 804–809.

Garber, SL, Mirochnik, Y, Brecklin, C, Slobodskoy, L, Arruda, JAL, Dunea, G (2003). Effect of relaxin in two models of renal mass reduction. *Am. J. Nephrol.* **23**: 8–12.

Garber, SL, Mirochnik, Y, Brecklin, CS, Unemori, EN, Singh, AK, Slobodskoy, L, *et al.* (2001b). Relaxin decreases renal interstitial fibrosis and slows progression of renal disease. *Kidney Int.* **59**: 876–882.

Gasparo, M De, Catt, K, Inagami, T, Wright, J, Unger, T (2000). International Union of Pharmacology . XIII . The Angiotensin II Receptors. *Pharmacol. Rev.* **52**: 415–472.

Gelosa, P, Pignieri, A, Fändriks, L, Gasparo, M de, Hallberg, A, Banfi, C, *et al.* (2009). Stimulation of AT₂ receptor exerts beneficial effects in stroke-prone rats: focus on renal damage. *J. Hypertens.* **27**: 2444–2451.

Gelse, K, Pöschl, E, Aigner, T (2003). Collagens - Structure, function, and biosynthesis. *Adv. Drug Deliv. Rev.* **55**: 1531–1546.

Gnecci, M, He, H, Liang, OD, Melo, LG, Morello, F, Mu, H, *et al.* (2005). Paracrine action accounts for marked protection of ischemic heart by Akt-modified mesenchymal stem cells. *Nat. Med.* **11**: 367–368.

Goolaerts, A, Pellan-Randrianarison, N, Larghero, J, Vanneaux, V, Uzunhan, Y, Gille, T, *et al.* (2014). Conditioned media from mesenchymal stromal cells restore sodium transport and preserve epithelial permeability in an in vitro model of acute alveolar injury. *Am J Physiol Lung Cell Mol Physiol* **306**: 975–985.

Granger, JP, Alexander, BT, Llinas, M (2002). Mechanisms of pressure natriuresis. *Curr. Hypertens. Rep.* **4**: 152–159.

Guimond, MO, Gallo-Payet, N (2012). The angiotensin II type 2 receptor in brain functions: An update. *Int. J. Hypertens.* **2012**: E1–E18.

Guo, H, Liao, X, Liu, Q, Zhang, L (2016). Angiotensin II Type 2 Receptor Decreases Transforming Growth Factor- β Type II Receptor Expression and Function in Human Renal Proximal Tubule Cells. *PLoS One* **11**: e0148696.

Hamilton, TA, Handa, RK, Harding, JW, Wright, JW (2001). A role for the angiotensin IV/AT₄ system in mediating natriuresis in the rat. *Peptides* **22**: 935–944.

- Harding, JW, Wright, JW, Swanson, GN, Hanesworth, JM, Krebs, LT (1994). AT4 receptors: Specificity and distribution. *Kidney Int.* **46**: 1510–1512.
- Hart, P, Bakris, G (2007). Should beta-blockers be used to control hypertension in people with chronic kidney disease? *Semin Nephrol* **27**: 555–564.
- Hartman, HA, Lai, HL, Patterson, LT (2007). Cessation of Renal Morphogenesis in Mice. *Dev Biol* **310**: 379–387.
- Hartman, JC (1995). The role of bradykinin and nitric oxide in the cardioprotective action of ACE inhibitors. *Ann. Thorac. Surg.* **60**: 789–792.
- Heeg, MHJ, Koziolk, MJ, Vasko, R, Schaefer, L, Sharma, K, Müller, GA, *et al.* (2005). The antifibrotic effects of relaxin in human renal fibroblasts are mediated in part by inhibition of the Smad2 pathway. *Kidney Int.* **68**: 96–109.
- Hewitson, TD (2009). Renal tubulointerstitial fibrosis: common but never simple. *Am. J. Physiol. Physiol.* **296**: F1239–F1244.
- Hewitson, TD, Ho, WY, Samuel, CS (2010). Antifibrotic Properties of Relaxin : In Vivo Mechanism of Action in Experimental Renal Tubulointerstitial. *Endocrinology* **151**: 4938–4948.
- Hewitson, TD, Mookerjee, I, Masterson, R, Zhao, C, Tregear, GW, Becker, GJ, *et al.* (2007). Endogenous relaxin is a naturally occurring modulator of experimental renal tubulointerstitial fibrosis. *Endocrinology* **148**: 660–669.
- Hisaw, F (1926). Experimental relaxation of the pubic ligament of the guinea pig. *Exp. Biol. Med.* **23**: 661–663.
- Hocking, AM, Gibran, NS (2010). Mesenchymal stem cells: paracrine signaling and differentiation during cutaneous wound repair. *Exp Cell Res* **316**: 2213–2219.
- Hoffmann, SC, Kampen, RL, Amur, S, Sharaf, MA, Kleiner, DE, Hunter, K, *et al.* (2002). Molecular and immunohistochemical characterization of the onset and resolution of human renal allograft ischemia-reperfusion injury. *Transplantation* **74**: 916–923.

- Honczarenko, M, Le, Y, Swierkowski, M, Ghiran, I, Glodek, AM, Silberstein, LE (2006). Human Bone Marrow Stromal Cells Express a Distinct Set of Biologically Functional Chemokine Receptors. *Stem Cells* **24**: 1030–1041.
- Honmou, O, Houkin, K, Matsunaga, T, Niitsu, Y, Ishiai, S, Onodera, R, *et al.* (2011). Intravenous administration of auto serum-expanded autologous mesenchymal stem cells in stroke. *Brain* **134**: 1790–1807.
- Hossain, MA, Kocan, M, Yao, ST, Royce, SG, Nair, VB, Siwek, C, *et al.* (2016). A single-chain derivative of the relaxin hormone is a functionally selective agonist of the G protein-coupled receptor, RXFP1. *Chem. Sci.* **7**: 3805–3819.
- Hossain, MA, Rosengren, KJ, Haugaard-Jönsson, LM, Zhang, S, Layfield, S, Ferraro, T, *et al.* (2008). The A-chain of human relaxin family peptides has distinct roles in the binding and activation of the different relaxin family peptide receptors. *J. Biol. Chem.* **283**: 17287–17297.
- Hossain, MA, Wade, J (2014). Synthetic relaxins. *Curr Opin Chem Biol* **22**: 47–55.
- Hrenák, J, Arendášová, K, Ová, RRČ, Aziriová, S, Repová, K, Ová, KKČÍČ, *et al.* (2013). Protective Effect of Captopril , Olmesartan , Melatonin and Compound 21 on Doxorubicin-Induced Nephrotoxicity in Rats. *Physiol. Res.* **62**: S181-189.
- Hsu, S, Nakabayashi, K, Nishi, S, Kumagai, J (2002). Activation of orphan receptors by the hormone relaxin. *Science (80-.).* **295**: 671–673.
- Huang, X, Gai, Y, Yang, N, Lu, B, Samuel, CS, Thannickal, VJ, *et al.* (2011). Relaxin Regulates Myofibroblast Contractility and Protects against Lung Fibrosis. *Am. J. Pathol.* **179**: 2751–2765.
- Huuskens, B, Ricardo, S, Samuel, C (2012). The combined effects of mesenchymal stem cells & relaxin in an experimental model of fibrotic kidney disease.
- Huuskens, BM, Wise, AF, Cox, AJ, Lim, EX, Payne, NL, Kelly, DJ, *et al.* (2015). Combination therapy of mesenchymal stem cells and serelaxin effectively attenuates renal fibrosis in obstructive nephropathy. *FASEBJ* **29**: 540–553.
- Jain, G, Campbell, RC, Warnock, DG (2009). Mineralocorticoid receptor blockers and chronic

kidney disease. *Clin. J. Am. Soc. Nephrol.* **4**: 1685–1691.

Jelinic, M, Marshall, SA, Stewart, D, Unemori, E, Parry, LJ, Leo, CH (2018). Peptide hormone relaxin: from bench to bedside. *Am. J. Physiol. Integr. Comp. Physiol.* **314**: R753–R760.

Jha, V, Garcia-Garcia, G, Iseki, K, Li, Z, Naicker, S, Plattner, B, *et al.* (2013). Chronic kidney disease: Global dimension and perspectives. *Lancet* **382**: 260–272.

Jones, ES, Borgo, MP Del, Kirsch, JF, Clayton, D, Bosnyak, S, Welungoda, I, *et al.* (2011). A single β -amino acid substitution to angiotensin II confers AT₂ receptor selectivity and vascular function. *Hypertension* **57**: 570–576.

Jones, ES, Vinh, A, McCarthy, CA, Gaspari, TA, Widdop, RE (2008). AT₂ receptors: Functional relevance in cardiovascular disease. *Pharmacol. Ther.* **120**: 292–316.

Kagami, S, Border, WA, Miller, DE, Noble, NA (1994). Angiotensin II stimulates extracellular matrix protein synthesis through induction of transforming growth factor- β expression in rat glomerular mesangial cells. *J. Clin. Invest.* **93**: 2431–2437.

Kakoki, M, McGarrah, RW, Kim, H-S, Smithies, O (2007). Bradykinin B₁ and B₂ receptors both have protective roles in renal ischemia/reperfusion injury. *Proc. Natl. Acad. Sci. U. S. A.* **104**: 7576–81.

Kang, D, Joly, A, Oh, S, Hugo, C, Kerjaschki, D, Gordon, K, *et al.* (2001). Impaired angiogenesis in the remnant kidney model: I. Potential role of vascular endothelial growth factor and thrombospondin-1. *J Am Soc Nephrol* **12**: 1434–1447.

Kang, Y, Lee, H, Moon, S, Kang, H, Choi, Y (2017). Relaxin Modulates the Expression of MMPs and TIMPs in Fibroblasts of Patients with Carpal Tunnel Syndrome. *Yonsei Med. J.* **58**: 415–422.

Kaschina, E, Grzesiak, A, Li, J, Foryst-Ludwig, A, Timm, M, Rompe, F, *et al.* (2008). Angiotensin II type 2 receptor stimulation: A novel option of therapeutic interference with the renin-angiotensin system in myocardial infarction? *Circulation* **118**: 2523–2532.

Keller, S, Rupp, C, Stoeck, A, Runz, S, Fogel, M, Lugert, S, *et al.* (2007). CD24 is a marker of exosomes secreted into urine and amniotic fluid. *Kidney Int.* **72**: 1095–1102.

Keller, SR (2004). Aminopeptidases in Health and Disease Role of the Insulin-Regulated Aminopeptidase IRAP in Insulin Action and Diabetes. *Biol. Pharm. Bull.* **27**: 761–764.

Keller, SR, Scott, HM, Mastick, CC, Aebersold, R, Lienhard GE (1995). Cloning and characterization of a novel insulin-regulated membrane aminopeptidase from GluT4 vesicles. *J Biol Chem.* **270**, 23612-23618.

Kikuchi, K, Rudolph, R, Murakami, C, Kowdley, K, GB, M (2002). Portal vein thrombosis after hematopoietic cell transplatation: frequency, treatment and outcome. *Bone Marrow Transplant.* **29**: 329–333.

King, A, Balaji, S, Keswani, SG, Crombleholme, TM (2014). The Role of Stem Cells in Wound Angiogenesis. *Adv. Wound Care* **3**: 614–625.

Klahr, S, Morrissey, J (2002). Obstructive nephropathy and renal fibrosis. *Am. J. Physiol. Physiol.* **283**: F861–F875.

Klinkhammer, BM, Goldschmeding, R, Floege, J, Boor, P (2017). Treatment of Renal Fibrosis—Turning Challenges into Opportunities. *Adv. Chronic Kidney Dis.* **24**: 117–129.

Kljajic, ST, Vinh, A, Welungoda, I, Bosnyak, S, Jones, ES, Gaspari, TA, *et al.* (2013). Direct AT2 receptor stimulation is athero-protective and stabilizes plaque in Apolipoprotein E-deficient mice. *Int. J. Cardiol.* **169**: 281–287.

Knight, D, Rossi, F, Hackett, T (2010). Mesenchymal stem cells for repair of the airway epithelium in asthma. *Expert Rev. Respir. Med.* **4**: 747–765.

Kolios, G, Moodley, Y (2013). Introduction to stem cells and regenerative medicine. *Respiration* **85**: 3–10.

Kong, P, Christia, P, Frangogiannis, N (2014). The Pathogenesis of Cardiac Fibrosis Ping. *Cell. Mol. Life Sci.* **71**: 549–574.

Kordelas, L, Rebmann, V, Ludwig, A-K, Radtke, S, Ruesing, J, Doeppner, TR, *et al.* (2014). MSC-derived exosomes: a novel tool to treat therapy-refractory graft-versus-host disease. *Leukemia* 970–973.

- Koulis, C, Chow, BSM, Mckelvey, M, Steckelings, UM, Unger, T, Thallas-Bonke, V, *et al.* (2015). AT2R agonist, compound 21, is Reno-protective against type 1 diabetic nephropathy. *Hypertension* **65**: 1073–1081.
- Kovacic, JC, Mercader, N, Torres, M, Boehm, M, Fuster, V (2012). Epithelial-to-mesenchymal and endothelial-to-mesenchymal transition from cardiovascular development to disease. *Circulation* **125**: 1795–1808.
- Kyriakou, C, Rabin, N, Pizzey, A, Nathwani, A, Yong, K (2008). Factors that influence short-term homing of human bone marrow-derived mesenchymal stem cells in a xenogeneic animal model. *Haematologica* **93**: 1457–1465.
- Lai, RC, Arslan, F, Lee, MM, Sze, NSK, Choo, A, Chen, TS, *et al.* (2010). Exosome secreted by MSC reduces myocardial ischemia/reperfusion injury. *Stem Cell Res.* **4**: 214–222.
- Lam, EYM, Funder, JW, Nikolic-Paterson, DJ, Fuller, PJ, Young, MJ (2006). Mineralocorticoid receptor blockade but not steroid withdrawal reverses renal fibrosis in deoxycorticosterone/salt rats. *Endocrinology* **147**: 3623–3629.
- Lauer, D, Slavic, S, Sommerfeld, M, Thone-Reineke, C, Sharkovska, Y, Hallberg, A, *et al.* (2013). AT2 receptor agonism regulates TIMP1/MMP9 axis in the heart preventing cardiac fibrosis and improving heart function after experimental myocardial infarction. *Hypertension*.
- Lauer, D, Slavic, S, Sommerfeld, M, Thöne-Reineke, C, Sharkovska, Y, Hallberg, A, *et al.* (2014). Angiotensin type 2 receptor stimulation ameliorates left ventricular fibrosis and dysfunction via regulation of tissue inhibitor of matrix metalloproteinase 1/Matrix metalloproteinase 9 axis and transforming growth factor β 1 in the rat heart. *Hypertension* **63**: 60–67.
- LeBleu, VS, Taduri, G, O’Connell, JO, Teng, Y, Cooke, VG, Woda, C, *et al.* (2013). Origin and function of myofibroblasts in kidney fibrosis. *Nat. Med.* **19**: 1047–54.
- Lee, WJ, Kim, YO, Choi, IK, Rah, DK, Yun, C (2011). Adenovirus-relaxin gene therapy for keloids : implication for reversing pathological fibrosis. *Br. J. Dermatol.* **165**: 673–677.
- Lekgabe, ED, Kiriazis, H, Zhao, C, Xu, Q, Moore, XL, Su, Y, *et al.* (2005). Relaxin reverses cardiac

and renal fibrosis in spontaneously hypertensive rats. *Hypertension* **46**: 412–418.

Lemley, K V, Kriz, W (1991). Anatomy of the renal interstitium. *Kidney Int.* **39**: 370–381.

Lener, T, Gimona, M, Aigner, L, Borger, V, Buzas, E, Camussi, G, *et al.* (2015). Applying extracellular vesicles based therapeutics in clinical trials - an ISEV position paper. *J Extracell Vesicles* **4**: 30087.

Leu, S, Lin, YC, Yuen, CM, Yen, CH, Kao, YH, Sun, CK, *et al.* (2010). Adipose-derived mesenchymal stem cells markedly attenuate brain infarct size and improve neurological function in rats. *J. Transl. Med.* **8**: 11–14.

Lew, RA, Mustafa, T, Ye, S, Mcdowall, SG, Chai, SY, Albiston, AL (2003). Angiotensin AT 4 ligands are potent , competitive inhibitors of insulin regulated aminopeptidase (IRAP). *J. Neu* **86**: 344–350.

Lewis, M, Deshpande, U, Guzman, L, Grove, B, Huang, X, Erikson, M, *et al.* (2001). Systemic relaxin administration stimulates angiogenic cytokine expression and vessel formation in a rat myocardial infarct model. In *Relaxin 2000*, pp 159–167.

Li, C, Wang, W, Summer, SN, Westfall, TD, Brooks, DP, Falk, S, *et al.* (2008). Molecular Mechanisms of Antidiuretic Effect of Oxytocin. *J. Am. Soc. Nephrol.* **19**: 225–232.

Li, N, Xie, C, Lu, N-H (2015). Transforming growth factor- β : an important mediator in Helicobacter pylori-associated pathogenesis. *Front. Cell. Infect. Microbiol.* **5**: 1–10.

Liu, C, Chen, J, Sutton, S, Roland, B, Kuei, C, Farmer, N, *et al.* (2003). Identification of Relaxin-3/INSL7 as a Ligand for GPCR142. *J. Biol. Chem.* **278**: 50765–50770.

Liu, Y (2006). Renal fibrosis: new insights into the pathogenesis and therapeutics. *Kidney Int* **69**: 213–217.

Lo, B, Parham, L (2009). Ethical issues in stem cell research. *Endocr. Rev.* **30**: 204–213.

Loffek, S, Schilling, O, Franzke, C-W (2010). Biological role of matrix metalloproteinases: a critical balance. *Eur. Respir. J.* **38**: 191–208.

Longo, DL, Rockey, DC, Bell, PD, Hill, J a (2015). Fibrosis — A Common Pathway to Organ Injury

and Failure. *N. Engl. J. Med.* **372**: 1138–1149.

Lozano, R, Naghavi, M, Foreman, K, Lim, S, Shibuya, K, Aboyans, V, *et al.* (2012). Global and regional mortality from 235 causes of death for 20 age groups in 1990 and 2010: A systematic analysis for the Global Burden of Disease Study 2010. *Lancet* **380**: 2095–2128.

Lukaszuk, A, Demaegdt, H, Feytens, D, Vanderheyden, P, Vauquelin, G, Tourw, D (2009). The Replacement of His (4) in Angiotensin IV by Conformationally Constrained Residues Provides Highly Potent and Selective Analogues. *J. Med. Chem.* **52**: 5612–5618.

Lukaszuk, A, Demaegdt, H, Szemenyei, E, Tóth, G, Tymecka, D, Misicka, A, *et al.* (2008). B-Homo-amino Acid Scan of Angiotensin IV. *J. Med. Chem.* **51**: 2291–2296.

Ma, Y, Xu, Y, Xiao, Z, Yang, W, Zhang, C, Song, E, *et al.* (2006). Reconstruction of Chemically Burned Rat Corneal Surface by Bone Marrow-Derived Human Mesenchymal Stem Cells. *Stem Cells* **24**: 315–321.

Marshall, SA, O’Sullivan, KO, Ng, HH, Bathgate, RAD, Parry, LJ, Hossain, MA, *et al.* (2017). B7-33 replicates the vasoprotective functions of human relaxin-2 (serelaxin). *Eur. J. Pharmacol.* **807**: 190–197.

Martin, B, Gabris-Weber, BA, Reddy, R, Romero, G, Chattopadhyay, A, Salama, G (2018). Relaxin reverses inflammatory and immune signals in aged hearts. *PLoS One* **13**: 1–17.

Martina, K, Mohsin, S, Sheng, YA, Xiao, J, Juan, JM, H, A, *et al.* (2017). ML290 is a biased allosteric agonist at the relaxin receptor RXFP1. *Sci. Rep.* **7**: 2968.

Masini, E, Bani, D, Bello, MG, Bigazzi, M, Mannaioni, PF, Sacchi, TB (1997). Relaxin Counteracts Myocardial Damage Induced by Ischemia-Reperfusion in Isolated Guinea Pig Hearts: Evidence for an Involvement of Nitric Oxide ¹. *Endocrinology* **138**: 4713–4720.

Masuda, S, Hattori, A, Matsumoto, H, Miyazawa, S, Natori, Y (2003). Involvement of the V 2 receptor in vasopressin-stimulated translocation of placental leucine aminopeptidase / oxytocinase in renal cells. *Eur. J. Biochem.* **270**: 1988–1994.

Matavelli, L, Huang, J, Siragy, H (2011). Angiotensin AT2 Receptor Stimulation Inhibits Early Renal

Inflammation in Renovascular Hypertension. *Hypertension* **57**: 308–313.

Mavrakanas, T a, Gariani, K, Martin, P-Y (2014). Mineralocorticoid receptor blockade in addition to angiotensin converting enzyme inhibitor or angiotensin II receptor blocker treatment: an emerging paradigm in diabetic nephropathy: a systematic review. *Eur. J. Intern. Med.* **25**: 173–6.

McDonald, G a, Sarkar, P, Rennke, H, Unemori, E, Kalluri, R, Sukhatme, VP (2003). Relaxin increases ubiquitin-dependent degradation of fibronectin in vitro and ameliorates renal fibrosis in vivo. *Am. J. Physiol. Renal Physiol.* **285**: F59–F67.

McGuane, JT, Debrah, JE, Sautina, L, Jarajapu, YPR, Novak, J, Rubin, JP, *et al.* (2011). Relaxin induces rapid dilation of rodent small renal and human subcutaneous arteries via PI3 kinase and nitric oxide. *Endocrinology* **152**: 2786–2796.

Mehanni, SS, Ibrahim, NF, Hassan, AR, Rashed, LA (2013). New Approach of Bone Marrow-Derived Mesenchymal Stem Cells and Human Amniotic Epithelial Cells Applications in Accelerating Wound Healing of Irradiated Albino Rats. *Int J Stem Cells* **6**: 45–54.

Mehta, PK, Griendling, KK (2007). Angiotensin II cell signaling: physiological and pathological effects in the cardiovascular system. *Am. J. Physiol. - Cell Physiol.* **292**: C82–C97.

Mezzano, S, Ruiz-Ortega, M, Egido, J (2001). Angiotensin II and renal fibrosis. *Hypertension* 635–638.

Moeller, I, Albiston, AL, Lew, RA, Mendelsohn, FAO, Chai, SY (1999). A globin fragment, LVV-hemorphin-7, induces [3H]thymidine incorporation in a neuronal cell line via the AT4 receptor. *J. Neurochem.* **73**: 301–308.

Moll, G, Alm, JJ, Davies, LC, Bahr, L Von, Heldring, N, Stenbeck-Funke, L, *et al.* (2014). Do cryopreserved mesenchymal stromal cells display impaired immunomodulatory and therapeutic properties? *Stem Cells* **32**: 2430–2442.

Moodley, Y, Ilancheran, S, Samuel, C, Vaghjiani, V, Atienza, D, Williams, ED, *et al.* (2010). Human amnion epithelial cell transplantation abrogates lung fibrosis and augments repair. *Am. J. Respir. Crit. Care Med.* **182**: 643–51.

- Mookerjee, I, Hewitson, TD, Halls, ML, Summers, RJ, Mathai, ML, Bathgate, R a D, *et al.* (2009). Relaxin inhibits renal myofibroblast differentiation via RXFP1, the nitric oxide pathway, and Smad2. *FASEB J.* **23**: 1219–29.
- Moore, KA, Lemischka, IR (2006). Stem Cells and Their Niches. *Science (80-.).* **331**: 1880–1885.
- Morigi, M, Imberti, B, Zoja, C, Corna, D, Tomasoni, S, Abbate, M, *et al.* (2004). Mesenchymal stem cells are renotropic, helping to repair the kidney and improve function in acute renal failure. *J. Am. Soc. Nephrol.* **15**: 1794–1804.
- Morrissey, JJ, Klahr, S (1999). Effect of AT2 receptor blockade on the pathogenesis of renal fibrosis. *Am. J. Physiol.* **276**: F39–F45.
- Motedayyen, H, Esmail, N, Tajik, N, Khadem, F, Ghotloo, S, Khani, B, *et al.* (2017). Method and key points for isolation of human amniotic epithelial cells with high yield, viability and purity. *BMC Res. Notes* **10**: 1–8.
- Mountford, SJ, Albiston, AL, Charman, WN, Ng, L, Holien, JK, Parker, MW, *et al.* (2014). Synthesis, Structure – Activity Relationships and Brain Uptake of a Novel Series of Benzopyran Inhibitors of Insulin-Regulated Amino-peptidase. *J. Med. Chem.* **57**: 1368–1377.
- Murphy, S, Atala, A (2013). Amniotic Fluid and Placental Membranes: Unexpected Sources of Highly Multipotent Cells. *Semin Reprod Med* **31**: 62–68.
- Nagase, H (1997). Activation mechanisms of matrix metalloproteinases. *Biol. Chem.* **378**: 151–160.
- Nagase, H, Visse, R, Murphy, G (2006). Structure and function of matrix metalloproteinases and TIMPs. *Cardiovasc. Res.* **69**: 562–573.
- Nakajima, M, Hutchinson, HG, Fujinaga, M, Hayashida, W, Morishita, R, Zhang, L, *et al.* (1995). The angiotensin II type 2 (AT2) receptor antagonizes the growth effects of the AT1 receptor : Gain-of-function study using gene transfer. *Proc. Natl. Acad. Sci. U. S. A.* **92**: 10663–10667.
- Namsolleck, P, Recarti, C, Foulquier, S, Steckelings, UM, Unger, T (2014). AT(2) receptor and tissue injury: therapeutic implications. *Curr. Hypertens. Rep.* **16**: 416.

Ng, KS, Kuncewicz, TM, Karp, JM (2015). Beyond hit-and-run: Stem cells leave a lasting memory. *Cell Metab.* **22**: 541–543.

Nikolaou, A, Eynde, I Van Den, Vauquelin, G, Tourwe, D, Mallareddy, JR, Poglitsch, M, *et al.* (2013). [³ H] IVDE77 , a novel radioligand with high affinity and selectivity for the insulin-regulated aminopeptidase. *Eur. J. Pharmacol.* **702**: 93–102.

Ninichuk, V, Gross, O, Segerer, S, Hoffmann, R, Radomska, E, Buchstaller, A, *et al.* (2006). Multipotent mesenchymal stem cells reduce interstitial fibrosis but do not delay progression of chronic kidney disease in collagen4A3-deficient mice. *Kidney Int.* **70**: 121–129.

Nistri, S, Chiappini, L, Sassoli, C, Bani, D, Medicine, F (2003). Relaxin inhibits lipopolysaccharide-induced adhesion of neutrophils to coronary endothelial cells by a nitric oxide- mediated mechanism. *FASEB J.*

Nistri, S, Cinci, L, Perna, AM, Masini, E, Bani, D (2008). Mast cell inhibition and reduced ventricular arrhythmias in a swine model of acute myocardial infarction upon therapeutic administration of relaxin. *Inflamm. Res.* **57**: 7–9.

Novak, J, Ramirez, RJJ, Gandley, RE, Sherwood, OD, Conrad, KP (2015). Myogenic reactivity is reduced in small renal arteries isolated from relaxin-treated rats. *Am. J. Physiol. Integr. Comp. Physiol.* **283**: R349–R355.

Ortiz, L a, Gambelli, F, McBride, C, Gaupp, D, Baddoo, M, Kaminski, N, *et al.* (2003). Mesenchymal stem cell engraftment in lung is enhanced in response to bleomycin exposure and ameliorates its fibrotic effects. *Proc. Natl. Acad. Sci. U. S. A.* **100**: 8407–11.

Padia, S, Howell, N, Siragy, H, Carey, R (2006). Renal angiotensin type 2 receptors mediate natriuresis via angiotensin III in the angiotensin II type 1 receptor-blocked rat. *Hypertension* **47**: 537–544.

Padia, S, Kemp, B, Howell, N, Fournie-Zaluski, M, Roques, B, Carey, R (2008). Conversion of renal angiotensin II to angiotensin III is critical for AT2 receptor mediated natriuresis in rats. *Hypertension* **51**: 460–465.

- Palmer, S, Craig, J, Nvaneethan, S, Tonelli, M, Strippoli, G (2012). Benefits and Harms of Statin Therapy for Persons With Chronic Kidney Disease A Systematic Review and Meta-analysis. *Ann Intern Med* **157**: 263–275.
- Panja, AB, Panja, P, Bhatt, R, Joseph, A (2017). Expression and regulation of chemokine receptor CXCR3 (CD183) on human gastrointestinal stem cells (hGISC) derived primary epithelial cells. *J Immunol* **198**: 55.47.
- Patel, JM, Martens, JR, Li, YD, Gelband, CH, Raizada, MK, Block, ER (1998). Angiotensin IV receptor-mediated activation of lung endothelial NOS is associated with vasorelaxation. *Am. J. Physiol.* **275**: L1061-8.
- Paulis, L, Becker, STR, Lucht, K, Schwengel, K, Slavic, S, Kaschina, E, *et al.* (2015). Direct Angiotensin II Type 2 Receptor Stimulation in N -Nitro- L -Arginine-Methyl Ester – Induced Hypertension The Effect on Pulse Wave Velocity and Aortic Remodeling. *Hypertension* **59**: 485–493.
- Pini, A, Boccalini, G, Lucarini, L, Catarinicchia, S, Guasti, D, Masini, E, *et al.* (2016). Protection from Cigarette Smoke – Induced Lung Dysfunction and Damage by H2 Relaxin (Serelaxin). **2**: 451–458.
- Plante, E, Menaouar, A, Danalache, BA, Yip, D, Broderick, TL, Chiasson, JL, *et al.* (2015). Oxytocin treatment prevents the cardiomyopathy observed in obese diabetic male db/db mice. *Endocrinology* **156**: 1416–1428.
- Polymeri, A, Giannobile, W V., Kaigler, D (2016). Bone Marrow Stromal Stem Cells in Tissue Engineering and Regenerative Medicine. *Horm. Metab. Res.* **48**: 700–713.
- Ponte, AL, Marais, E, Gallay, N, Langonné, A, Delorme, B, Hérault, O, *et al.* (2007). The In Vitro Migration Capacity of Human Bone Marrow Mesenchymal Stem Cells: Comparison of Chemokine and Growth Factor Chemotactic Activities. *Stem Cells* **25**: 1737–1745.
- Qi, S, Wu, D (2013). Bone marrow-derived mesenchymal stem cells protect against cisplatin-induced acute kidney injury in rats by inhibiting cell apoptosis. *Int J Mol Med* **32**: 1262–1272.
- Raleigh, JV, Mauro, AG, Devarakonda, T, Marchetti, C, He, J, Kim, E, *et al.* (2017). Reperfusion

therapy with recombinant human relaxin-2 (Serelaxin) attenuates myocardial infarct size and NLRP3 inflammasome following ischemia / reperfusion injury via eNOS-dependent mechanism. *Cardio* **113**: 609–619.

Rehman, A, Leibowitz, A, Yamamoto, N, Rautureau, Y, Paradis, P, Schiffrin, EL (2012). Angiotensin type 2 receptor agonist compound 21 reduces vascular injury and myocardial fibrosis in stroke-prone spontaneously hypertensive rats. *Hypertension* **59**: 291–299.

Ricard-Blum, S (2011). The Collagen Family. *Cold Spring Harb. Perspect. Biol.* **3**: 1–19.

Riet, L Te, Esch, J van, Roks, A, Meiracker, A van Den, Danser, A (2015). Hypertension: renin-angiotensin-aldosterone system alterations. *Circ. Res.* **116**: 960–975.

Ringe, J, Strassburg, S, Neumann, K, Endres, M, Notter, M, Burmester, GR, *et al.* (2007). Towards in situ tissue repair: Human mesenchymal stem cells express chemokine receptors CXCR1, CXCR2 and CCR2, and migrate upon stimulation with CXCL8 but not CCL2. *J. Cell. Biochem.* **101**: 135–146.

Rodrigues Díez, R, Rodrigues-Díez, R, Lavozy, C, Rayego-Mateos, S, Civantos, E, Rodríguez-Vita, J, *et al.* (2010). Statins inhibit angiotensin II/sm α d pathway and related vascular fibrosis, by a TGF- β -independent process. *PLoS One* **5**:.

Rompe, F, Artuc, M, Hallberg, A, Alterman, M, Str??der, K, Th??ne-Reineke, C, *et al.* (2010). Direct angiotensin II type 2 receptor stimulation acts anti-inflammatory through epoxyeicosatrienoic acid and inhibition of nuclear factor ??b. *Hypertension* **55**: 924–931.

Royce, SG, Sedjatera, A, Samuel, CS, Tang, MLK (2013). Combination therapy with relaxin and methylprednisolone augments the effects of either treatment alone in inhibiting subepithelial fibrosis in an experimental model of allergic airways disease. *Clincial Sci.* **124**: 41–51.

Royce, SG, Shen, M, Patel, KP, Huuskes, BM, Ricardo, SD, Samuel, CS (2015). Mesenchymal stem cells and serelaxin synergistically abrogate established airway fibrosis in an experimental model of chronic allergic airways disease. *Stem Cell Res.* **15**: 495–505.

Royce, SG, Tominaga, AM, Shen, M, Patel, KP, Huuskes, BM, Lim, R, *et al.* (2016). Serelaxin improves the therapeutic efficacy of RXFP1-expressing human amnion epithelial cells in

experimental allergic airway disease. *Clin. Sci.* **130**: 2151–2165.

Samuel, C, Hewitson, T (2007). Drugs of the future: the hormone relaxin. *Cell. Mol. Life Sci.* **64**: 1539–1557.

Samuel, CS, Bodaragama, H, Chew, JY, Widdop, RE, Royce, SG, Hewitson, TD (2014). Serelaxin is a more efficacious antifibrotic than enalapril in an experimental model of heart disease. *Hypertension* **64**: 315–322.

Samuel, CS, Cendrawan, S, Gao, X-M, Ming, Z, Zhao, C, Kiriazis, H, *et al.* (2011). Relaxin remodels fibrotic healing following myocardial infarction. *Lab. Invest.* **91**: 675–90.

Samuel, CS, Hewitson, TD (2009). Relaxin and the progression of kidney disease. *Curr. Opin. Nephrol. Hypertens.* **18**: 9–14.

Samuel, CS, Hewitson, TD, Unemori, EN, Tang, ML-K (2007). Drugs of the future: the hormone relaxin. *Cell. Mol. Life Sci.* **64**: 1539–57.

Samuel, CS, Mookerjee, I, Masterson, R, Tregear, GW, Hewitson, TD (2005). Relaxin regulates collagen overproduction associated with experimental progressive renal fibrosis. *Ann. N. Y. Acad. Sci.* **1041**: 182–184.

Samuel, CS, Royce, SG, Hewitson, TD, Denton, KM, Cooney, TE, Bennett, RG (2017). Anti-fibrotic actions of relaxin. *Br. J. Pharmacol.* **174**: 962–976.

Samuel, CS, Unemori, EN, Mookerjee, I, Bathgate, RAD, Layfield, SL, Mak, J, *et al.* (2004a). Relaxin modulates cardiac fibroblast proliferation, differentiation, and collagen production and reverses cardiac fibrosis in vivo. *Endocrinology* **145**: 4125–4133.

Samuel, CS, Zhao, C, Bond, CP, Hewitson, TIMD (2004b). Relaxin-I-deficient mice develop an age-related progression of renal fibrosis. *Kidney Int* **65**: 2054–2064.

Sardinia, MF, Hanesworth, JM, Krishnan, F, Harding, JW (1994). AT4 receptor structure-binding relationship: N-terminal-modified angiotensin IV analogues. *Peptides* **15**: 1399–1406.

Sarwar, M, Du, XJ, Dschietzig, TB, Summers, RJ (2017). The actions of relaxin on the human

cardiovascular system. *Br. J. Pharmacol.* **174**: 933–949.

Sarwar, M, Samuel, CS, Bathgate, RA, Stewart, DR, Summers, RJ (2015). Serelaxin-mediated signal transduction in human vascular cells: bell-shaped concentration – response curves reflect differential coupling to G proteins. *Br. J. Pharmacol.* **172**: 1005–1019.

Sasaki, M, Abe, R, Fujita, Y, Ando, S, Inokuma, D, Shimizu, H (2008). Mesenchymal Stem Cells Are Recruited into Wounded Skin and Contribute to Wound Repair by Transdifferentiation into Multiple Skin Cell Type. *J. Immunol.* **180**: 2581–2587.

Sasser, JM, Molnar, M, Baylis, C (2011). Relaxin ameliorates hypertension and increases nitric oxide metabolite excretion in angiotensin II but not Nw-Nitro-L-arginine methyl ester hypertensive rats. *Hypertension* **58**: 197–204.

Sassoli, C, Chellini, F, Pini, A, Tani, A, Nistri, S, Nosi, D, *et al.* (2013). Relaxin Prevents Cardiac Fibroblast-Myofibroblast Transition via Notch-1-Mediated Inhibition of TGF- β /Smad3 Signaling. *PLoS One* **8**: 1–8.

Saura, M, Zaragoza, C, Herranz, B, Grier, M, Diez-Marqués, L, Rodriguez-Puyol, D, *et al.* (2005). Nitric oxide regulates transforming growth factor- β signaling in endothelial cells. *Circ. Res.* **97**: 1115–1123.

Saveanu, L, Endert, P Van (2012). The role of insulin-regulated aminopeptidase in MHC class I antigen presentation. *Front. Immunol.* **3**: 1–13.

Sayeski, PP, Ali, MS, Semeniuk, DJ, Doan, TN, Bernstein, KE (1998). Angiotensin II signal transduction pathways. *Regul. Pept.* **78**: 19–29.

Sayeski, PP, Bernstein, KE (2001). Signal transduction mechanisms of the angiotensin II type AT(1)-receptor: looking beyond the heterotrimeric G protein paradigm. *J. Renin. Angiotensin. Aldosterone. Syst.* **2**: 4–10.

Schelbert, EB, Fonarow, GC, Bonow, RO, Butler, J, Gheorghiade, M (2014). Therapeutic targets in heart failure: Refocusing on the myocardial interstitium. *J. Am. Coll. Cardiol.* **63**: 2188–2198.

Sherwood, CD, O’Byrne, E (1974). Purification and Characterization of Porcine Relaxin. *Arch.*

Biochem. Biophys. **160**: 185–196.

Sherwood, L (2007). *Human Physiology: From Cells to System* (Thomson Brooks/Cole).

Sherwood, OD (2004). Relaxin's physiological roles and other diverse actions. *Endocr. Rev.* **25**: 205–234.

Silverthorn, D, Johnson, B, Ober, W, Garrison, C, Silverthorn, A (2013). *Human Physiology: An Integrated Approach* (Boston: Pearson Education).

Silvertown, J, Symes, J, Neschadim, A, Nonaka, T, Kao, JCH, Summerlee, AJS, *et al.* (2007). Analog of H2 relaxin exhibits antagonistic properties and impairs prostate tumor growth. *FASEBJ* **21**: 754–765.

Sinha, AD, Agarwal, R (2015). Thiazide Diuretics in Chronic Kidney Disease. *Curr. Hypertens. Rep.* **17**:

Strauer, B, Brehm, M, Zeus, T, Kosterling, M, Hernandez, A, Sory, R, *et al.* (2002). Repair of infarcted myocardium by autologous intracoronary mononuclear bone marrow cell transplantation in humans. *Circulation* **106**: 1913–1918.

Strippoli, GF, Perkovic, V, Craig, JC, Foote, C V, Lv, J, Craig, ME (2012). Antihypertensive agents for preventing diabetic kidney disease. *Cochrane Database Syst. Rev.*

Suzuki, Y, Ruiz-ortega, M, Lorenzo, O, Ruperez, M, Esteban, V, Egido, J (2003). Inflammation and angiotensin II. *Int. J. Biochem. Cell Biol.* **35**: 881–900.

Takahashi, K, Yamanaka, S (2006). Induction of pluripotent stem cells from mouse embryonic and adult fibroblast cultures by defined factors. *Cell* **126**: 663–76.

Teerlink, JR (2009). A novel approach to improve cardiac performance: Cardiac myosin activators. *Heart Fail. Rev.* **14**: 289–298.

Thomson, JA, ItsKovitz-Eldor, J, Shapiro, SS, Waknitz, MA, Swierhiel, JJ, Marshall, VS, *et al.* (1998). Embryonic Stem Cell Lines Derived from Human Blastocysts. *Science (80-.)*. **282**: 1145–1147.

Togel, F, Hu, Z, Weiss, K, Isaac, J, Lange, C, Westenfelder, C (2005). Administered mesenchymal

stem cells protect against ischemic acute renal failure through differentiation-independent mechanisms. *AJP Ren. Physiol.* **289**: F31–F42.

Tromp, TR, Jonge, N de, Joles, JA (2015). Left ventricular assist devices: a kidney's perspective. *Heart Fail. Rev.* 519–532.

Tugtepe, H, Sener, G, Biyikli, N, Yuksel, M, Cetinel, S, Gedik, N, *et al.* (2007). The protective effect of oxytocin on renal ischemia/reperfusion injury in rats. *Regul. Pept.* **140**: 101–108.

Unemori, EN, Amento, EP (1990). Relaxin Modulates Synthesis and Secretion of Procollagenase Collagen by Human Dermal Fibroblasts. *J. Biol. Chem.* **265**: 10661–10665.

Unemori, EN, Lewis, M, Constant, J, Arnold, G, Grove, BH, Normand, J, *et al.* (2000). Relaxin induces vascular endothelial growth factor expression and angiogenesis selectively at wound sites. *Wound Repair Regen.* **8**: 361–370.

Unemori, EN, Pickford, LB, Salles, AL, Piercy, CE, Grove, BH, Erikson, ME, *et al.* (1996). Relaxin Induces an Extracellular Matrix-degrading Phenotype in Human Lung Fibroblasts In Vitro and Inhibits Lung Fibrosis in a Murine Model In Vivo. *J. Clin. Invest.* **98**: 2739–2745.

Urbanelli, L, Buratta, S, Sagini, K, Ferrara, G, Lanni, M, Emiliani, C (2015). Exosome-based strategies for Diagnosis and Therapy. *Recent Pat CNS Drug Discov* **10**: 10–27.

Valadi, H, Ekstrom, K, Bossios, A, Sjostrand, M, Lee, JJ, Lotvall, JO (2007). Exosome-mediated transfer of mRNAs and microRNAs is a novel mechanism of genetic exchange between cells. *Nat. Cell Biol.* **9**: 654–659.

Vanderheyden, PML (2009). From angiotensin IV binding site to AT4 receptor. *Mol. Cell. Endocrinol.* **302**: 159–166.

Vasavada, N, Saha, C, Agarwal, R (2003). A double-blind randomized crossover trial of two loop diuretics in chronic kidney disease. *Kidney Int.* **64**: 632–640.

Vinh, A, Widdop, RE, Chai, SY, Gaspari, TA (2008). Angiotensin IV-evoked vasoprotection is conserved in advanced atheroma. *Atherosclerosis* **200**: 37–44.

Visse, R, Nagase, H (2003). Matrix metalloproteinases and tissue inhibitors of metalloproteinases: Structure, function, and biochemistry. *Circ. Res.* **92**: 827–839.

Volk, MJ, Bomback, AS, Klemmer, PJ (2011). Mineralocorticoid receptor blockade in chronic kidney disease. *Curr. Hypertens. Rep.* **13**: 282–8.

Wallis, MG, Lankford, MF, Keller, SR (2007). Vasopressin is a physiological substrate for the insulin-regulated aminopeptidase IRAP. *Am. J. Physiol. Metab.* **293**: E1092–E1102.

Walshe, TE, Leach, LL, D’Amore, PA (2011). TGF- β signaling is required for maintenance of retinal ganglion cell differentiation and survival. *Neuroscience* **189**: 123–131.

Wang, C, Kemp-Harper, BK, Kocan, M, Ang, SY, Hewitson, TD, Samuel, CS (2016). The anti-fibrotic actions of relaxin are mediated through a NO-sGC-cGMP-dependent pathway in renal myofibroblasts in vitro and enhanced by the NO donor, diethylamine NONOate. *Front. Pharmacol.* **7**: 1–12.

Wang, D, Luo, Y, Myakala, K, Orlicky, DJ, Dobrinskikh, E, Wang, X, *et al.* (2017a). Serelaxin improves cardiac and renal function in DOCA-salt hypertensive rats. *Sci. Rep.* **7**: 9793.

Wang, Y, Borgo, M Del, Lee, HW, Baraldi, D, Hirmiz, B, Gaspari, TA, *et al.* (2017b). Anti-fibrotic potential of AT₂ receptor agonists. *Front. Pharmacol.* **8**: 1–7.

Weber, KT (2000). Fibrosis and hypertensive heart disease. *Curr. Opin. Cardiol.* **15**: 264–272.

Weber, KT, Brilla, CG, Campbell, SE, Guarda, E, Zhou, G, Sriram, K (1993). Myocardial fibrosis: role of angiotensin II and aldosterone. *Basic Res. Cardiol.* **88**: 107–124.

Weiss, G, O’Byrne, E, Steinetz, B (1976). Relaxin: a product of the human corpus luteum of pregnancy. *Sci. (New York, NY)* **194**: 948–949.

Westhuizen, E Van Der, Summers, R, Halls, M, Bathgate, R, Sexton, P (2007). Relaxin receptors--new drug targets for multiple disease states. *Curr. Drug Targets* **8**: 91–104.

Widdop, RE, Jones, ES, Hannan, RE, Gaspari, TA (2003). Angiotensin AT₂ receptors: cardiovascular hope or hype? *Br. J. Pharmacol.* **140**: 809–824.

Widdop, RE, Matrougui, K, Levy, BI, Henrion, D (2002). AT₂ receptor-mediated relaxation is preserved after long-term AT₁ receptor blockade. *Hypertension* **40**: 516–520.

Wilkinson, TN, Speed, TP, Tregear, GW, Bathgate, R a D (2005). Evolution of the relaxin-like peptide family. *BMC Evol. Biol.* **5**: 14.

Williams, EJ, Benyon, RC, Trim, N, Hadwin, R, Grove, BH, Arthur, MJP, *et al.* (2001). Relaxin inhibits effective collagen deposition by cultured hepatic stellate cells and decreases rat liver fibrosis in vivo. Relaxin inhibits effective collagen deposition by cultured hepatic stellate cells and decreases rat liver fibrosis in vivo. *Gut* **49**: 577–583.

Wise, AF, Ricardo, SD (2012). Mesenchymal stem cells in kidney inflammation and repair. *Nephrology* **17**: 1–10.

Wright, JT, Bakris, G, Greene, T, Appel, LJ, Cheek, D, Douglas-baltimore, JG, *et al.* (2002). Effect of Blood Pressure Lowering and Antihypertensive Drug Class on Progression of Hypertensive Kidney Disease. *Jama* **288**: 2421–2432.

Wright, JW, Mizutani, S, Murray, C, Amir, H, Harding, JW (1990). Amino-peptidase-induced elevations and reductions in blood pressure in the spontaneously hypertensive rat. *J. Hypertens.* **8**: 969–974.

Wu, Y, Mao, N, Jiang, X-X, Liu, B, Zhang, Y, Yu, X-D, *et al.* (2005). Human mesenchymal stem cells inhibit differentiation and function of monocyte-derived dendritic cells. *Blood* **105**: 4120–4126.

Wynn, T, Ramalingam, T (2012). Mechanisms of fibrosis therapeutic translation for fibrotic disease. *Nat. Med.* **18**: 1028–40.

Wynn, TA, Ramalingam, TR (2013). Mechanisms of fibrosis: therapeutic translation for fibrotic disease. *Nat. Med.* **18**: 1028–1040.

Xin, H, Li, Y, Cui, Y, Yang, JJ, Zhang, ZG, Chopp, M (2013). Systemic administration of exosomes released from mesenchymal stromal cells promote functional recovery and neurovascular plasticity after stroke in rats. *J. Cereb. Blood Flow Metab.* **33**: 1711–1715.

Yang, J, Chen, C, Ren, H, Han, Y, He, D, Zhou, L, *et al.* (2012). Angiotensin II AT₂ receptor decreases

AT1 receptor expression and function via nitric oxide/cGMP/Sp1 in renal proximal tubule cells from Wistar–Kyoto rats. *J. Hypertens.* **30**: 1176–1184.

Yang, L, Humphreys, B, Bonventre, J (2011). Pathophysiology of acute kidney injury to chronic kidney disease: maladaptive repair. *Contrib Nephrol* **174**: 149–155.

Yang, P, Yuan, W, Liu, J, Li, J, Tan, B, Qiu, C, *et al.* (2018). Biological characterization of human amniotic epithelial cells in a serum-free system and their safety evaluation. *Acta Pharmacol. Sin.* **39**: 1305–1316.

Yoshida, T, Kumagai, H, Kohsaka, T, Ikegaya, N (2013). Relaxin protects against renal ischemia-reperfusion injury. *Am. J. Physiol. Physiol.* **305**: F1169–F1176.

Yoshida, T, Kumagai, H, Kohsaka, T, Ikegaya, N (2014). Protective Effects of Relaxin against Cisplatin-Induced Nephrotoxicity in Rats. *Nephron Exp. Nephrol.* **128**: 9–20.

Yoshida, T, Kumagai, H, Suzuki, A, Kobayashi, N, Ohkawa, S, Odamaki, M, *et al.* (2012). Relaxin ameliorates salt-sensitive hypertension and renal fibrosis. *Nephrol. Dial. Transplant* **27**: 2190–7.

Yu, C, Jeremy, RW (2018). Angiotensin, transforming growth factor β and aortic dilatation in Marfan syndrome: Of mice and humans. *IJC Hear. Vasc.* **18**: 71–80.

Zacharek, A, Shehadah, A, Chen, J, Cui, X, Roberts, C, Lu, M, *et al.* (2010). Comparison of Bone Marrow Stromal Cells Derived From Stroke and Normal Rats for Stroke Treatment. *Stroke* **41**: 524–530.

Zeisberg, EM, Tarnavski, O, Zeisberg, M, Dorfman, AL, McMullen, JR, Gustafsson, E, *et al.* (2007). Endothelial-to-mesenchymal transition contributes to cardiac fibrosis. *Nat. Med.* **13**: 952–961.

Zhang, YE (2009). Non-Smad pathways in TGF- β signaling. *Cell Res.* **19**: 128–139.

Zheng, G, Cai, J, Chen, X, Chen, L, Ge, W, Zhou, X, *et al.* (2017). Relaxin Ameliorates Renal Fibrosis and Expression of Endothelial Cell Transition Markers in Rats of Isoproterenol-Induced Heart Failure. *Biol. Pharm. Bull.* **40**: 960–966.

Zhou, X, Chen, X, Cai, JJ, Chen, LZ, Gong, YS, Wang, LX, *et al.* (2015). Relaxin inhibits cardiac fibrosis

and endothelial–mesenchymal transition via the Notch pathway. *Drug Des. Devel. Ther.* **9**: 4599–4611.

Zhu, H, Mitsuhashi, N, Klein, A, Barsky, LW, Weinberg, K, Barr, ML, *et al.* (2006). The Role of the Hyaluronan Receptor CD44 in Mesenchymal Stem Cell Migration in the Extracellular Matrix. *Stem Cells* **24**: 928–935.

Zini, S, Chauvelt, E, Roquest, BP, Corvol, P, Llorens-cortes, C (1996). Identification of metabolic pathways of brain angiotensin II and III using specific aminopeptidase inhibitors : Predominant role of angiotensin III in the control of vasopressin release Arg-Val-Tyr-Ile-His-Pro-Phe. *Proc. Natl. Acad. Sci.* **93**: 11968–11973.

Chapter 2

General Methods

2.0 Materials & Methods

General reagents and materials used in this thesis are detailed in this Chapter, unless otherwise specified. The methodologies described in this Chapter are methods which have been utilized in Chapters 3-5. More specific details of specialized methods are discussed in the appropriate individual Chapters.

2.1 Relaxin

Recombinant H2 relaxin (now known as serelaxin; RLX) was generously provided by Corthera Inc (San Carlos, CA, USA; a subsidiary of Novartis International AG, Basel, Switzerland). For all subsequent experiments, 0.5mg/kg/day of serelaxin was administered via osmotic mini-pump infusion (further described in section 1.4) based on previous studies showing that this concentration, at the rate infused (0.5-1 μ l/hour), produces ~20ng/ml of circulating hormone after 5-7 days of administration in mice (Samuel *et al.*, 2003); a level which is known to prevent and reduce tissue fibrosis in numerous diseased models regardless of etiology (Garber *et al.*, 2001; Hewitson *et al.*, 2010; Huuskes *et al.*, 2015; Royce *et al.*, 2015; Samuel *et al.*, 2017).

As RLX is used across all Chapters, other treatments used will be addressed independently in the appropriate Chapters.

2.2 Animals

All mice used in this thesis were obtained from Monash Animal Services (Monash University, Clayton, Victoria, Australia) and contained within a controlled environment, in the Department of Pharmacology's holding facility (Monash University, Clayton, Victoria, Australia). Animals were maintained at a temperature of 21 \pm 5°C, and on a fixed lighting (12 hours light and 12 hours dark) schedule with access to normal rodent or high salt (5% NaCl)-containing lab chow (Barastock Stockfeeds, Pakenham, Victoria, Australia) and water ad libitum dependent on the study detailed in Chapters 3-5. All mice were provided an acclimatization period of 4-5 days before commencement of experiments. All experiments and procedures were approved by the Monash

University Animal Ethics Committee, which adheres to the Australian Guidelines for Care and Use of Laboratory Animal for Scientific Purposes.

2.3 High salt model

Within Chapter 3 and 4, a high-salt diet (5% NaCl) model was implemented to replicate the clinically relevant increasing problem with western diet, a consistent high salt intake leads to changes within the kidneys and heart to induce organ remodelling and fibrosis. Populations with higher salt consumption have been linked with increased hypertension and the development of CKD (Ha, 2014). Thus, sub-groups of mice had their normal rodent chow replaced with high salt (5% NaCl)-containing lab chow (Barastock Stockfeeds, Pakenham, Victoria, Australia). The use of this model allowed for significant increase in fibrotic development in organs within 4 weeks inside the mice, therefore the treatments were administered thereafter and their ability to reverse renal fibrosis were compared.

2.4 Unilateral ureteric obstruction (UUO) model

In Chapter 5, UUO was chosen as a more severe model compared with high salt diet and for its reproducibility of primary tubulointerstitial disease-like the pathology of human progressive renal disease that leads to progressive interstitial fibrosis independently of species and strain (Chevalier *et al.*, 2010). UUO surgery was performed under anaesthesia of 3% isoflurane (Baxter Healthcare Pty Ltd; NSW, Australia) via inhalation and maintained by a nose cone. Subsequently mice were placed over a heat pad, shaved on their left flank and cleansed with 70% ethanol. The left ureter was located by a 2 cm wide flank incision and ligated using 5.0 surgical silk (Johnson & Johnson, NJ, USA). The right contralateral unobstructed kidney served as biological control. In sham-operated animals, the left ureter was isolated without ligation. After the flank incision and/or ligation, mice were sutured closed with suture silk and monitored until they were fully recovered within 10-15 minutes (Figure 2.1). By ligating the left ureter, within several days hydronephrosis accompanied with inflammatory infiltration, tubular cell death and fibrosis develops to mimic the pathology of CKD.

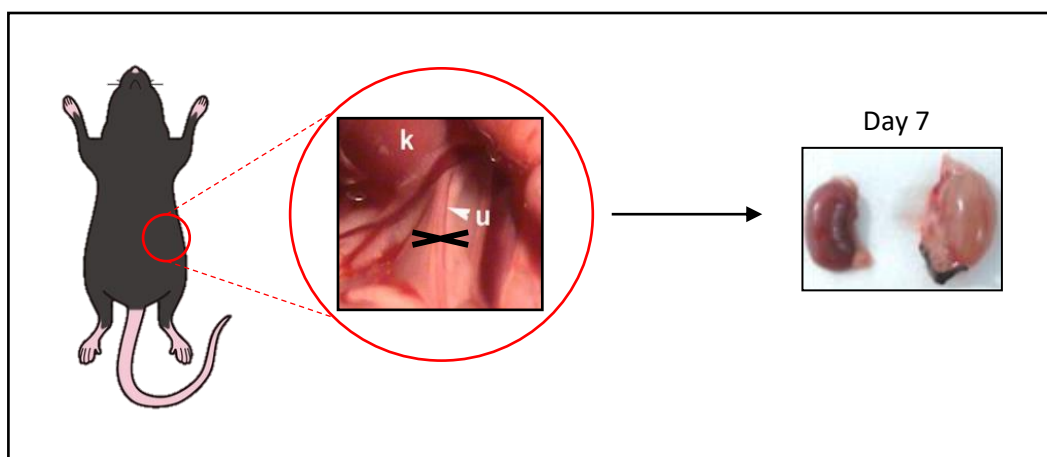


Figure 2.1 UUO surgery

Once the mouse is under anaesthesia, a 2 cm wide incision was made on the left flank. The left ureter is then located and ligated. Afterwards, mice were sutured closed and monitored once a day for 7-days. By day 7, the mouse was culled, and kidneys were dissected out. When compared to the right contralateral kidney, the obstructed kidney was significantly bigger due to build-up of fluids and paler. k: kidney; u: ureter.

2.5 Body weight & blood pressure measurements

The body weight of mice was recorded in grams fortnightly (for studies involving the high salt model) or weekly (for studies involving the obstructive nephropathy model); before the commencement of any experimentation and any blood pressure measurements; or prior to, and after drug treatment; or prior to animals being culled. Systolic blood pressure (SBP) was measured every 2 weeks (for studies involving the high salt model) using non-invasive tail-cuff plethysmography apparatus (MC400 Blood Pressure Analysis System, Hatteras Instrument Inc). At least 15 to 20 measurements per time point were pooled to obtain a mean for each animal.

2.6 Osmotic mini-pump implantation

Prior to mini-pump implantation, mice were administered 3% isoflurane (Baxter Healthcare Pty Ltd; NSW, Australia) via an anaesthetic induction chamber. Once anaesthetized, mice were shaved at the back of the neck and cleansed with 70% ethanol. A small incision was made between the scapulae on the dorsal surface of each mouse. A pocket was then created by spreading the

subcutaneous connective tissue apart by blunt dissection. A 7-day osmotic mini-pump (model 1007D; Alzet, Cupertino, CA, USA) was filled with the appropriate treatment, and subcutaneously inserted into the pocket and closed by Michel suture clips.

2.7 Animal cull and tissue collection

Once mice were weighed, they were culled by an overdose of isoflurane anaesthesia (5% in oxygen). An incision was rapidly made from the abdomen to the top of the thorax when the mice were placed in a supine position. The sternum was then lifted and both sides of the lower rib cage and diaphragm were removed to expose the heart. Blood was then drawn for plasma collection via cardiac puncture into the apex of the left ventricle with a 27 gauge (20mm) hypodermic needle (Terumo, Leuven, Belgium) and collected with a 1ml syringe (Terumo, Leuven, Belgium). The blood was then transferred to a heparinised-tube (0.5 ml; LH Lithium Heparin Minicollect® Tube, Greiner Bio-One GmbH, Austria) to prevent coagulation and spun with a centrifuge at 10,000 rpm, 4°C, 10min. Plasma was then extracted and transferred into 1.5ml Eppendorf tubes and stored at -80°C (until required for analysis). An incision was then made in the abdomen moving laterally towards the left and right flanks. Both kidneys were dissected from each mouse, decapsulated and weighed. The kidneys were cut and divided into equal portions containing the cortex, medulla and papilla or stored at -80°C as a whole organ depending on the experiment. The tissue portions were either fixed in 10% formalin or embedded in a cryomold containing optimum cutting temperature (OCT) compound (Tissue Tek, Tokyo, Japan) and frozen with methylbutane (Uvasol, Merk Millipore, Darmstadt, Germany) and then with liquid nitrogen, or snap frozen immediately in liquid nitrogen before being stored in -80°C (Figure 2.2).

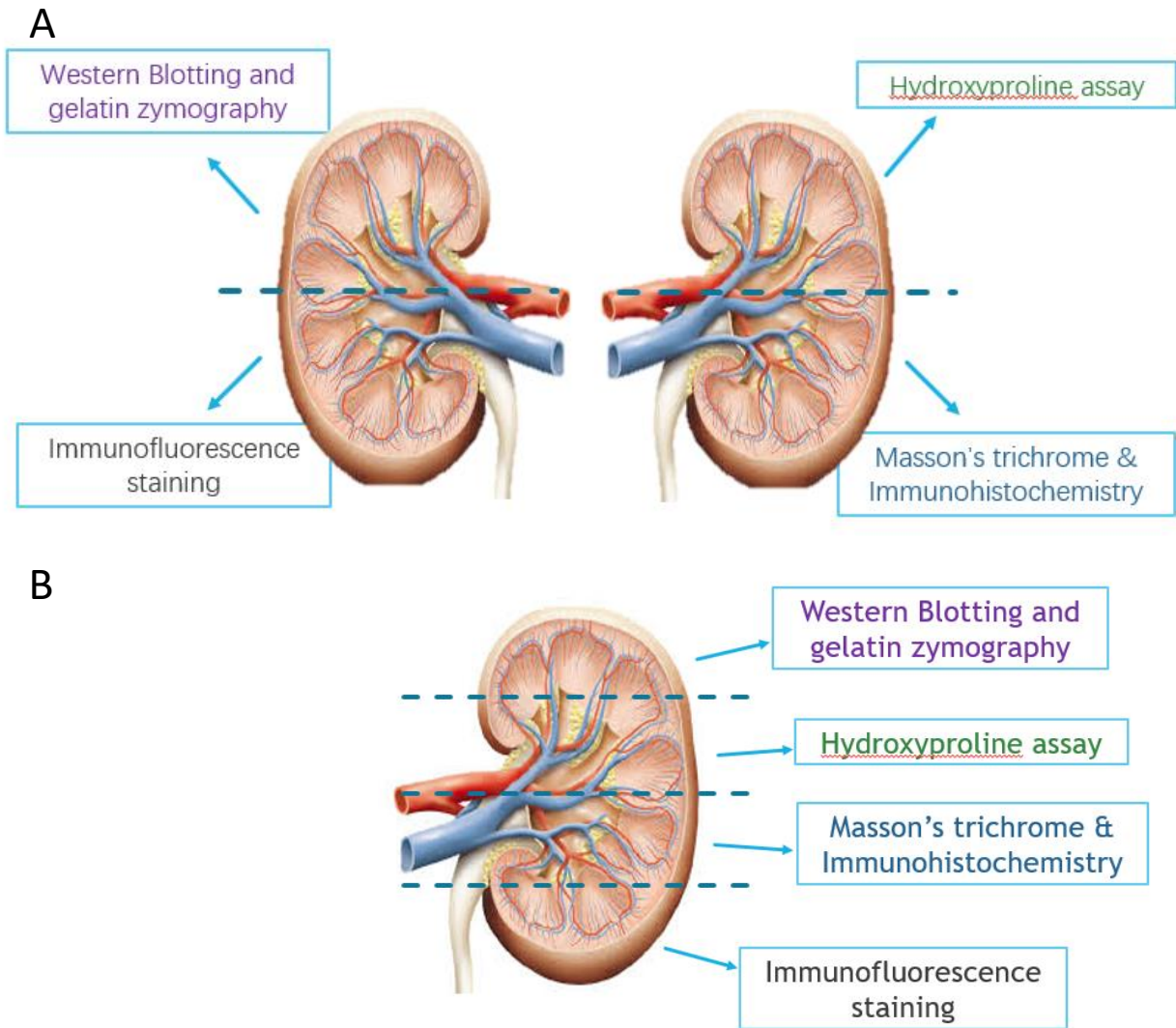


Figure 2.2 Kidney collection and allocation for analysis

Once kidneys were dissected out of each mouse, they were subsequently weighed and further divided into even sections for: protein analysis (by Western blotting and gelatin zymography), immunofluorescence staining, hydroxyproline analysis and immunohistochemistry. **A)** For the first two studies involving mice fed on a high salt diet, both kidneys were equally divided in half, whereas, **B)** for the third aim, only the UUO-obstructed left kidney was divided into quarters, for the respective analyses detailed above.

2.8 Tissue sectioning and morphometry

Kidney tissues fixed in 10% formalin were sent to Monash Histology Services (Monash University) for processing. Kidneys were then embedded using molten paraffin into a metal mould and solidified into blocks with a cold plate. The tissue blocks were then cut at 5µm using a microtome (Leica Microsystems Ltd, Wetzlar, Germany) to achieve 6-8 serial-sections, which were transferred into a 37°C water bath before being mounted on Superfrost® Plus slides (Thermo Scientific, Rockford, IL, USA) and dried overnight before use.

One set of these paraffin-embedded kidney sections from each treatment group was also given to Monash Histology Services to stain for extracellular matrix deposition (primarily collagen in blue) using Masson's Trichrome, where interstitial and glomerulosclerosis score was able to be imaged and analysed.

2.9 Immunohistochemistry

Immunohistochemistry was used to detect various markers of ECM remodelling, fibrosis and tissue injury, inclusive of transforming growth factor 1 (TGF-β1), alpha-smooth muscle actin (α-SMA; a marker of myofibroblast differentiation), and CD31 (a marker of endothelial cells used here to measure vascular rarefaction), amongst others (see Table 2.1 for full list of markers analysed). One serial section per slide from each animal/treatment group was used to evaluate each marker detailed above, while one additional slide from a high salt or UUO-injured mouse kidney was used as the negative control (for each antibody used). Serial sections on each slide were first dewaxed twice in xylene (15 minutes each), then twice in absolute ethanol (10 minutes each), rehydrated in 70% ethanol and washed in deionized water before the serial sections were transferred and submerged into 3% hydrogen peroxide for 10 minutes (Ajax Finechem, NSW, Australia) to inhibit endogenous peroxidase activity. The slides were then washed and placed in pre-heated citrate buffer (pH 6) for antigen retrieval by incubating for 5 minutes and then cooling to room temperature in a water bath for 25 minutes. Each section was then circled with a Dako hydrophobic pen and incubated in 50µl of Dako Diluent (Dako North America Inc., CA, USA) for 10 minutes to block non-specific protein binding. Diluent was then removed and 50µl of a selected primary antibody (see Table 2.1 with appropriate dilution), with/without biotinylation

(using Dako ARK™ biotinylating kit, K3964, CA, USA) if a primary mouse antibody was used, was then added to corresponding sections and left covered overnight at room temperature in a humidification box.

The following day, the sections were washed and placed in tris buffer for 14 minutes to remove excess primary antibody residue. Appropriate sections were then treated with a Dako enVision+ system-HRP labelled polymer anti-rabbit secondary antibody (for detection of markers that were stained with polyclonal antibodies) or Dako enVision+ streptavidin-HRP labelled polymer anti-mouse secondary antibody (for detection of markers that were stained with monoclonal antibodies) for 30 minutes. Subsequently, the slides were rinsed in tris buffer for 14 minutes and incubated in DAB chromagen (Dako liquid DAB+ substrate chromogen system, K3468, CA, USA) for 5 minutes before being soaked in distilled water to stop any further reaction. The slides were then counter-stained with haematoxylin for 1 minute, rinsed in distilled water and then washed with Scott's tap water for a further 1 minute. Following staining, the slides were dehydrated in 70% ethanol and absolute ethanol and were cleared with xylene prior to being mounted with a coverslip with DPX (VWR International, PA, USA). Positive DAB staining was visualized and scanned by Monash Histology Services for morphometric analysis.

Table 2.1. Primary antibody details of the various markers of ECM remodelling, fibrosis and tissue injury that were analysed by Western blotting (WB), immunohistochemistry (IHC) and/or immunofluorescence (IF).

Antibody	Species	Dilution	Company	Product number
α-SMA	Mouse monoclonal	IHC: 1:500	Dako	M0851
CD31	Rabbit polyclonal	IHC: 1:100	Abcam	Ab28364
F4/80	Rat monoclonal	IHC: 1:200 IMF: 1:100	Bio-Rad	MCA497R
IRAP (D7C5)	Rabbit monoclonal	IMF: 1:500	Cell signalling	#6918S
KIM-1 (TIM-1)	Mouse monoclonal	IHC: 1:100	R&D systems	MAB1817
p-IKβ	Rabbit polyclonal	IMF: 1:50	Cell Signalling	#28595S
TGF-β1	Rabbit polyclonal	IHC: 1:1000	Abcam	Ab92486

TIMP-1	Rabbit polyclonal	IHC: 1:1000 WB: 1:2500	Abcam	Ab38978
--------	-------------------	---------------------------	-------	---------

2.10 Immunofluorescence

Immunofluorescence was used to detect markers of renal inflammation. Frozen tissue blocks were sectioned at 5µm on a cryostat (Leica) and mounted on Superfrost® Plus slides (Thermo Scientific, Rockford, IL, USA). The frozen tissue slides were then air dried and fixed in cold acetone for 10 minutes at room temperature. Subsequently, the slides were washed in 0.01M PBS buffer containing: NaCl 5.84M, KCl 7.46M, Na₂HPO₄ 14.19M and KH₂PO₄ 13.61M for 10 minutes, 3 times. Sections were then incubated with 10% goat serum in 0.01M PBS for 30 minutes, which was used as a blocking solution to reduce non-specific binding. At the same time, primary antibodies were prepared using antibody diluent (DAKO) to reach optimized concentration (see Table 2.1). Following the 30 minutes of blocking, the goat serum was removed and 50µl of primary antibody was added onto each slide before being left to incubate overnight in a humidification slide box at room temperature.

The following day after >16 hours of incubation, sections were washed again with cold 0.01M PBS, 3 times per wash for 10 minutes each. The secondary antibody was prepared similarly to the primary except in the dark and applied on each slide for 2-3 hours at room temperature with goat anti-rat Alexa Fluor 488 IgG (A11006, Life technologies, CA, USA) diluted in diluent at a 1:500 ratio. Finally, sections were washed 3 times again with 0.01M PBS, mounted with mounting medium (VectaShield H-1000, Vector), and cover slipped for imaging.

2.11 Imaging and analysis

All kidney sections were scanned, captured and viewed under Monash Histology Service's Aperio Scanscope AT Turbo (Leica Microsystems Pty Ltd, VIC, Australia) or with a confocal microscope at x20-x40 magnification for morphometric analysis of immunohistochemically- or immunofluorescently-labelled tissue images. Images were blinded and quantified with ImageJ 1.48 software (Java, NIH) (Figure 2.3).

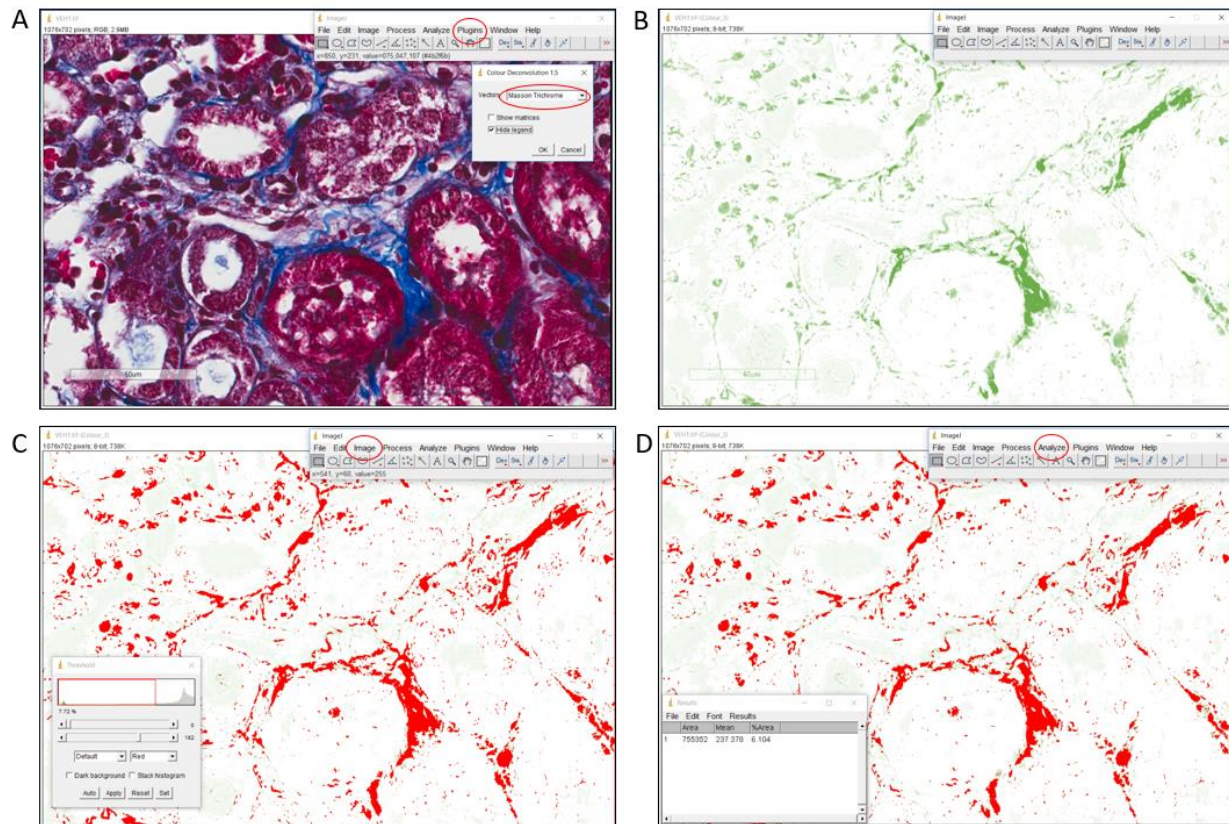


Figure 2.3 morphometric analysis using ImageJ

A) Once image is imported into ImageJ, select “Plugins” tab → Colour Deconvolution and a pop-up menu would appear. Select the appropriate vector filter for Masson’s Trichrome or DAB staining via a dropdown menu. For IMF, instead, select “Image” tab → “Type” → RGB stack. **B)** Subsequently 3 colour filters appear, select the filter which enhances the target staining. **C)** Under “Image” tab → “Adjust” → Threshold. A pop-up menu would appear for the selected staining to be overlayed by red pixels. All images are adjusted to the appropriate amount of target staining seen when compared to the original image via “Auto” threshold tab or by manual slider adjustment. **D)** To analyse % staining/field, select “Analyze” tab → Measure to display % area of red pixel count within the given field.

2.12 Protein analysis

2.12.1 Protein extraction

The portion of each collected kidney sample that was allocated for protein extraction, was homogenized in a buffer containing 0.25% (w/v) Triton X-100 and 10mM CaCl₂ (at a ratio of 20ml of homogenization buffer/gram of wet tissue weight); using a Ultra-Turrax T8 homogenizer (IKA Labortechnik, Germany). Once samples were homogenized, they were stored in ice until all samples had been homogenized, before all samples were centrifuged (Eppendorf Centrifuge 5810 R, Hamburg, Germany) at 3000g for 20 minutes at 4°C. The supernatant (containing 5-10% of total protein) from each centrifuged sample was then subsequently separated from the pellets and discarded. The remaining pellets (containing 90-95% of the total protein) was then re-suspended in 0.1M CaCl₂ (at a ratio of 20ml of solution/gram of wet weight tissue), before samples were vortexed and heated in a shaking water bath at 60°C for 4min. The heated samples were then cooled down and centrifuged again at 3000g for 20 minutes at 4°C. This time the separated supernatants were transferred into Millipore concentrators with a 10kDa cut-off (Merk Millipore, Darmstadt, Germany; which elute proteins smaller than 10kDa, but retain and concentrate proteins larger than 10kDa when centrifuged). The supernatants were concentrated to ~100-200µl in volume by centrifugation (at 3,000g) before 1ml of 0.5M Tris-HCl, pH 6.8 buffer was added to each sample (to equilibrate each sample in Tris-HCl buffer. Samples were then further centrifuged until they were concentrated down to approximately 100µl in volume, before being stored at -20°C.

2.12.2 Protein assay

To determine the protein content of each sample, a Bradford protein assay was completed by adding 2x5µl of each sample to 795µl of distilled water in duplicate Eppendorf tubes. Subsequently, a bovine serum albumin (BSA) standard curve was established (0µg, 5µg, 10µg, 15µg, 20µg and 25 µg) by diluting a 0.5mg/ml BSA stock in Tris-HCl, Ph 6.8 buffer in appropriate amounts of distilled water, totalling 800µl in separate Eppendorf tubes. 200µl of Protein Assay Dye Reagent (Bio-Rad Laboratories, Richmond, CA, USA) was then added into standard and duplicate sample tube. All samples were then incubated and vortexed at room temperature for

10 minutes before being decanted into disposable cuvettes. The absorbance values of each standard and sample was then measured at 595nm using the Beckman DU-64 spectrophotometer (Beckman Instruments, CA, USA) and levels of BSA-equivalent protein present in each sample were extrapolated from the BSA standard curve constructed from the respective absorbance values from each standard concentration (which was performed in Microsoft Excel).

2.13 Gelatin zymography

Gelatin zymography was performed to determine the effects of each treatment in each study on either or both gelatinase A (MMP-2) and/or gelatinase B (MMP-9) expression and activity. Depending on the study, a fixed (5-10µg) amount of BSA-equivalent protein from each sample was selected and made up to 6-9µl with distilled water. A sample loading buffer (which contained 62.5mM Tris-HCl, Ph 6.8, 2% sodium dodecyl sulphate (SDS), 10% glycerol and 0.001% bromophenol blue) was then added to each sample at a sample-to-loading buffer ratio of 3:1. Samples were then vortexed and incubated for an hour at room temperature to allow the SDS to block the gelatinases from undergoing proper folding (and hence, any proteolytic activity). 7.5% polyacrylamide gels contained 1mg/ml of gelatin were first made and solidified with 10% ammonium persulfate (APS) and tetramethylethylenediamine (TEMED) for 30 minutes on the gel caster. A 3.5% stacking gel with 15 well dividers was placed on top of the separating gel and solidified with 10% APS and TEMED for a further 20 minutes. Samples (8-12µl in volume) were then dry loaded into the gel wells before the sample wells were filled with running buffer and samples then electrophoresed at 120V until they reached the bottom of the gel cast. During electrophoresis, the samples migrated to fixed positions on the gel depending on their molecular weight (with MMP-9 and MMP-2 being approximately 92kDa and 72kDa in size, respectively). Once the dye front had reached the bottom of the gel casts, each gel was removed and washed twice in 0.25% Triton X-100 (15 min each wash) on a shaking incubator to remove excess SDS from the gel and allowed MMPs to refold. Gels were then incubated at 37°C in incubation buffer (containing 50mM Tris-HCl, Ph 7.5, 10mM CaCl₂, 1µM ZnCl₂ and 1% Triton X-100) overnight; as the presence of calcium and zinc promotes the activation of MMPs, allowing them to cleave the gelatin substrate on the positions of the gel to which that they migrate.

The following day, the incubation buffer was removed, and gels were stained with 0.1% (w/v) Coomassie blue containing 40% (v/v) isopropanol for an hour on a shaking incubator at room temperature. The gels were then destained with 7% (v/v) acetic acid to reveal clear bands, associated with MMP-2 and MMP-9 activity. Densitometry of the gel bands was performed using the Bio-Rad ChemiDoc MP imaging system and ImageLab software (Bio-Rad).

2.14 Western blotting

Equal amounts of each sample (containing 10-20µg of total protein) were mixed with sample loading buffer (containing 0.5M Tris-HCl pH 6.8, 10% (w/v) glycerol, 2% (w/v) SDS and 0.01% (w/v) bromophenol blue) in a volumetric ratio of 3:1 (sample:loading buffer), vortexed and heated for 3 minutes at 95°C before being stored in an ice box. Before samples were analysed, 10% acrylamide gels (containing 3.5% acrylamide stacking gels with 15 wells) were made up using a TGX Stain-Free FastCast Acrylamide starter kit (#161-0183, Bio-Rad, Hercules, CA, USA). The bottom (separating) gel required Resolver A, Resolver B (provided in kit), TEMED and 10% APS (diluted with DH₂O) to be mixed and solidified in 30 minutes, before the top (stacking) gel layer (consisting of Stacker A and Stacker B with TEMED and 10% APS) containing 15 wells required a further 30 minutes to be solidified. The gels were then loaded into a vertical gel electrophoresis cell (Bio-Rad, Hercules, CA, USA) filled with premade Bio-Rad 1X running buffer (diluted from 10x buffer, #161-0732). Protein samples were then transferred into the individual wells and gel electrophoresis was maintained at 200V for ~40-60 minutes. Once the desired protein bands were separated, the gel electrophoresis was stopped. Trans-Blot Turbo mini-size LF PVDF membranes (#170-4272, Bio-Rad) were soaked in methanol for 10 seconds and the gels were sandwiched accordingly between two transfer stacks saturated with Trans-Blot Turbo Transfer Buffer (#170-4272, Bio-Rad). The sandwich stacks were placed into a cassette box and proteins were transferred from the gel onto the membrane using the Trans-Turbo Transfer System, which took 7 minutes to complete. Upon completion, each membrane was washed in Tris-buffered saline-tween (TBS-T) (0.1% Tween-20 in 1x TBS) for 5 minutes. Ponceau S was then used for rapid reversible detection of protein bands on the membrane before membranes were washed again in TBS-T until the red stain was removed. Membranes were then exposed to a blocking buffer

(TBS-T/5% skim milk; 5g/100ml) for 1 hour at room temperature, on a mechanical shaker set at 70rpm (to block any non-specific binding from occurring). Primary antibodies were then appropriately diluted in the same blocking buffer (see Table 2.1) before being added to each respective membrane, before membranes were incubated in primary antibody at 4°C overnight on a mechanical shaker.

On the following day, membranes were washed 3 times (15 minutes per wash) using TBS-T. Subsequently, the membranes were then incubated with either conjugated anti-rabbit or anti-mouse secondary antibodies diluted in blocking buffer on the mechanical shaker at room temperature for 1 hour. After a series of another 3 washes (15 minutes per wash) in TBS-T, membranes were incubated with ECL reagent (Clarity™ Western ECL Blotting Substrate, Bio-Rad) for 5 minutes before transferred and imaged with the Bio-Rad ChemiDoc MP imaging system. Individual bands were quantified by measuring the optical density (OD) per unit area of each corresponding antibody-stained band and corrected for any differences in protein loaded by normalising with the OD of alpha-tubulin (a house-keeping protein) for each sample using ImageLab software. Depending on sample amount, the membranes were kept in TBS if needed to be stripped and reprobed using another primary antibody.

2.14.1 PVDF Membrane stripping for reprobing

If required, membranes stored in TBS were washed with TBS-T 3 times (15 minutes per wash) at room temperature on a mechanical shaker. During this washing period, 100ml of stripping buffer was prepared by mixing 6.25ml of 1M Tris-HCl pH 6.8, 10ml of 20% SDS and 700µl of β-mercaptoethanol and 83.05ml of distilled H₂O. Once membranes are washed, they were incubated in the stripping buffer at room temperature (on the mechanical shaker), at 20rpm for 30 minutes. Afterwards, membranes were washed with TBS-T 3 times (15 minutes per wash), before being subjected to the Western blotting protocol described in section 2.13) with the addition of a separate primary antibody.

2.15 Hydroxyproline assay

To assess changes in total kidney collagen concentration, hydroxyproline analysis was conducted on one half or one quarter of each kidney collected, as hydroxyproline is an amino acid that is almost unique to collagen and usually represents ~14.4% of the amino acid composition of collagen (Neuman and Logan, 1950). Appropriate kidney portions (which had been stored at -80°C) were first lyophilized to dry weight in a Labcono Free-Zone freeze-dryer (VWR International; Brisbane, QLD, Australia) overnight and measured. The samples were then rehydrated in a buffer containing sodium chloride (0.15M), Tris-HCl (0.05M, pH 7.5) and the protease inhibitors, N-ethylmaleimide (10mM), phenylmethylsulfonyl fluoride (0.1mM), benzamidinium hydrochloride (1mM) and EDTA (10mM) (for 2-3 hours at 4°C). Afterwards, the rehydrated samples were transferred to Kimax™ screw-capped glass tubes (Kimble/Kontes), submerged in 0.5ml of 6M HCl and hydrolysed for 18-24 hours at 110°C (during which time the collagen triple helix within kidney tissues is broken down into individual amino acids).

The following day, the hydrolysed samples were cooled at 4°C before being lyophilized overnight (to remove the HCl). The dried samples were then dissolved in 1ml of 0.1M HCl, before duplicate (10µl) aliquots assayed for their hydroxyproline content and compared against a standard curve of purified trans-4-hydroxy-L-proline (Sigma-Aldrich, MO, USA). Briefly, duplicate 10µl aliquots of each sample were added with 90µl distilled water, 200µl isopropanol and 100µl of oxidation buffer containing 7% chloramine-T immediately before they were vortexed and incubated at room temperature for 4min (±30sec). 1.3ml of Erlich's reagent was then added to each sample, vortexed and incubated at 60°C on a shaking water bath for 25min. The samples were then cooled for 2-3min at 4°C before 3.3ml of isopropanol was added (to make a final volume of 5.0ml), vortexed and then decanted into disposable cuvettes (Lake Charles Manufacturing, LA, USA). Purified hydroxyproline standards (0-5µg) were made up to 100µl with water and were treated in the same way as the samples, described above. The absorbance of each standard and sample was then measured at 558nm in a DU-64 spectrophotometer (Beckman Coulter Inc., CA, USA). The levels of hydroxyproline present in each sample were then extrapolated from the standard curve constructed from the absorbance values of each standard (in Microsoft Excel). Hydroxyproline

values from each sample were then multiplied by 6.94 to determine total collagen content and divided by the dry weight of each corresponding kidney section to yield collagen concentration (%).

2.16 Plasma urea

For Chapter 3 and 4, frozen plasma was collected during tissue collection (Section 2.7) and thawed. 100 µl of plasma was transferred into Chem8+ cartridges (Abbott Laboratories, Illinois, USA) and inserted into the i-STAT point-of-care handheld device (Abbott Laboratories, Illinois, USA). The device then produces plasma urea levels recorded as mmol/L.

2.17 Statistical analysis

All comparative data were analysed using a one-way analysis of variance (ANOVA), with Newman-Keuls *post hoc* testing used to make multiple comparisons between groups (GraphPad Prism 7; San Diego, CA, USA), unless otherwise stated. All graphs in this thesis were plotted via GraphPad Prism 7 and expressed as the mean ± standard error of the mean (SEM) unless otherwise specified, with $p < 0.05$ considered as statistically significant.

2.18 References

- Chevalier, R, Thornhill, B, Forbes, M, Kiley, S (2010). Mechanisms of renal injury and progression of renal disease in congenital obstructive nephropathy. *Pediatr Nephrol* **25**: 687–697.
- Garber, SL, Mirochnik, Y, Brecklin, CS, Unemori, EN, Singh, AK, Slobodskoy, L, *et al.* (2001). Relaxin decreases renal interstitial fibrosis and slows progression of renal disease. *Kidney Int.* **59**: 876–882.
- Ha, SK (2014). Dietary Salt Intake and Hypertension. *Electrolyte Blood Press* **12**: 7–18.
- Hewitson, TD, Ho, WY, Samuel, CS (2010). Antifibrotic Properties of Relaxin : In Vivo Mechanism of Action in Experimental Renal Tubulointerstitial. *Endocrinology* **151**: 4938–4948.
- Huuskes, BM, Wise, AF, Cox, AJ, Lim, EX, Payne, NL, Kelly, DJ, *et al.* (2015). Combination therapy of mesenchymal stem cells and serelaxin effectively attenuates renal fibrosis in obstructive nephropathy. *FASEBJ* **29**: 540–553.
- Neuman, RE, Logan, MA (1950). The determination of hydroxyproline. *J. Biol. Chem.* **184**: 299–306.
- Royce, SG, Shen, M, Patel, KP, Huuskes, BM, Ricardo, SD, Samuel, CS (2015). Mesenchymal stem cells and serelaxin synergistically abrogate established airway fibrosis in an experimental model of chronic allergic airways disease. *Stem Cell Res.* **15**: 495–505.
- Samuel, CS, Royce, SG, Hewitson, TD, Denton, KM, Cooney, TE, Bennett, RG (2017). Anti-fibrotic actions of relaxin. *Br. J. Pharmacol.* **174**: 962–976.
- Samuel, CS, Zhao, C, Bathgate, RAD, Bond, CP (2003). Relaxin deficiency in mice is associated with an age- related progression of pulmonary fibrosis. *FASEB J.* **17**: 121–123.

Chapter 3

**TO COMPARE AND COMBINE THE ANTI-FIBROTIC EFFECTS OF
SERELAXIN TO CANDESARTAN AND CGP42112 IN A HIGH SALT-
INDUCED MURINE MODEL OF KIDNEY DISEASE.**

3.1 Introduction

High dietary salt intake can lead to the risk of developing CVDs alongside CKDs. The National Health and Medical Research Council (NHMRC) of Australia advises the consumption of 5g of salt per day to avoid developing chronic diseases (National Health and Medical Research Council, 2017), whereas adults generally consume 9-12g of salt per day on average (Ha, 2014). Populations with higher average salt intake have been linked with increases in hypertension and the development of CKD. If left untreated, injury-induced renal dysfunction accompanied by fibrosis can lead to ESRD (Hill *et al.*, 2016). Current pharmacological treatments to combat CKD include ARBs, however, their primary effect alleviates CKD symptoms rather than eliminating the underlying fibrosis (Shihab, 2007). Furthermore, chronic administration of ARBs or their administration at high doses can result in a number of side-effects including the exacerbation of renal failure (Dézsi, 2014; Schelbert *et al.*, 2014). Henceforth, more direct and rapidly-acting anti-fibrotic therapies that can reduce and even reverse established fibrosis associated with CKD, is needed. In this study the effects of the ARB, candesartan cilexetil (CAND), were compared and combined against two pre-clinically established treatments that target the organ-protective effects of the AT₂ receptor (CGP42112/CGP) or RXFP1 receptor (serelaxin/RLX). The long-term (4 week) application of these treatments were investigated in a 8 week high salt (HS; 5% NaCl)-induced model of kidney disease.

It is widely known that ARBs inhibit the binding of Ang II to AT₁ receptors, thereby impeding the prolonged contribution of Ang II to the progression of tissue damage (Crowley *et al.*, 2006). However, ARBs are primarily known for their blood-pressure lowering and anti-inflammatory effects (Imig and Ryan, 2013), and have slow-acting anti-fibrotic efficacy (Nishiyama *et al.*, 2004; Ecelbarger *et al.*, 2010). On the other hand, AT₂ receptors have been shown to provide a counter-regulatory role on tissue remodelling, where the activation of these receptors oppose the actions of AT₁ receptor activation (Arima and Ito, 2000; De Gasparo *et al.*, 2000). Hence, an agonist to this receptor may provide anti-fibrotic efficacy outside blockade of AT₁ receptor activity. In normal adult kidneys, AT₂ receptors are detected in low abundance within glomerular mesangial cells, preglomerular arteries and the tubular interstitium. In disease states, however, these receptors become significantly upregulated and contribute towards their organ-protective

properties (De Gasparo *et al.*, 2000). This provides a potential opportunity to target AT₂ receptor with agonists, specifically during kidney injury to elicit renal protection. Thus, more recent attention has been turned to finding therapies that can specifically activate AT₂ receptors. Currently, there are two main AT₂ receptors agonists used as pharmacological tools in preclinical studies: the peptide-agonist, CGP (Whitebread, 1989) and its non-peptide counterpart, C21 (Wan *et al.*, 2004). Both compounds have been used in various rodent models of CVD and shown to have effective anti-inflammatory effects that are mediated by their ability to inhibit TNF α -induced IL-6, NF-kB activity and oxidative stress (Rompe *et al.*, 2010; Namsolleck *et al.*, 2014). Furthermore, C21 can also reduce collagen deposition leading to reduced myocardial and vascular fibrosis in stroke-prone spontaneously hypertensive rats (Rehman *et al.*, 2012). In rodent models of diabetic nephropathy and renovascular hypertension, similar anti-inflammatory and anti-fibrotic benefits were observed following C21-treatment (Matavelli *et al.*, 2011; Castoldi *et al.*, 2014). Hence, as the anti-fibrotic effects of CGP have been less investigated, an objective of this study was to compare the renal protective properties of CGP to CAND against HS-induced kidney disease.

Another experimental therapy that can consistently reduce established fibrosis is RLX, the recombinant form of the H2 relaxin hormone, which is the major stored and circulating form of human relaxin (Samuel and Hewitson, 2007). RLX's anti-fibrotic actions have been tested in various cell culture and animal models and within the heart, lungs, liver, skin and kidneys of these experimental models (Unemori and Amento, 1990; Heeg *et al.*, 2005; Hewitson *et al.*, 2007; Tang *et al.*, 2009; Bennett *et al.*, 2013; Fallowfield *et al.*, 2014; Samuel *et al.*, 2014). In various *in vitro* and *in vivo* models of disease, RLX consistently inhibits the pro-fibrotic actions of TGF- β 1 (Samuel *et al.*, 2007) and other pro-fibrotic cytokines, without affecting basal matrix turnover (i.e in the absence of any pro-fibrotic stimulation). At the signal transduction level, RLX has been shown to act through RXFP1 and an RXFP1-ERK1/2-nNOS-NO-sGC-cGMP-dependent pathway to inhibit the phosphorylation of intracellular Smad2, a regulatory protein that promotes TGF- β 1 signal transduction (Heeg *et al.*, 2005; Mookerjee *et al.*, 2009; Wang *et al.*, 2016). This in turn results in the inhibition of TGF- β 1-induced myofibroblast activation and myofibroblast-mediated ECM/collagen production (Heeg *et al.*, 2005; Mookerjee *et al.*, 2009), and reversal of the TGF- β 1-

induced suppression of matrix metalloproteinase (MMPs) activity and inhibition of TIMP-1 activity to induce the degradation of excessive collagen accumulation (Chow *et al.*, 2012). In addition, RLX also has other organ protective effects including anti-inflammatory, anti-apoptotic, vasodilatory, angiogenic which may aid in reducing kidney damage (reviewed in Samuel *et al.*, 2007). Thus, the reno-protective effects of serelaxin will be compared and combined with CGP or CAND against established HS-induced kidney disease.

3.2 Materials and methods

Materials

Recombinant H2 Relaxin (serelaxin; was kindly provided by Corthera Inc (San Carlos, CA, USA; a subsidiary of Novartis AG, Basel, Switzerland); candesartan cilexetil was purchased from AstraZeneca (Södertälje, Sweden); CGP42112 was purchased from GL Biochem (Shanghai) Ltd (Shanghai, China).

3.2.1 Animals

6 to 8-week-old male FVB/N mice were obtained from Monash Animal Services (Monash University, Clayton, Victoria, Australia) and housed under a controlled environment, on a 12 hour light/12 hour dark lighting cycle with tap water provided *ad libitum* throughout the experiment and diet initially maintained on normal lab chow (Barastock Stockfeeds, Pakenham, Victoria, Australia). All mice were provided an acclimatization period of at least 5 days before any experimentation and procedures were performed. All animal use and procedures were approved by a Monash University Animal Ethics Committee (Ethics number: MARP/2013/118), which complies with the Australian Guidelines for the Care and Use of Laboratory Animals for Scientific Purposes.

3.2.2 Experimental design

Mice were divided into 7 treatment groups with n=8 animals per group. These groups consisted of i) mice fed a normal salt (NS; 0.5% NaCl) diet (negative control) for 8 weeks; ii) high salt (HS; 5% NaCl) diet (positive control; Barastock Stockfeeds, Pakenham, Victoria, Australia) for 8 weeks; iii) HS+CAND-treated group; iv) HS+CGP-treated group; v) HS+RLX-treated group; vi)

HS+CAND+RLX-treated group; and vii) HS+ CGP+RLX-treated group. All HS-diet fed groups were provided with NaCl lab chow containing 5% NaCl after the acclimatization period ended; which was expected to induce renal injury in the absence of any overt changes in blood pressure. After the completion of 4 weeks on the HS diet one sub-group of mice were given candesartan cilexetil (2mg/kg/d), which was delivered to each mouse via drinking water and adjusted to daily body weight from weeks 5-8. This dose of the ARB was chosen based on previous study showing that CAND (at 1mg/kg/day) could inhibit renal fibrosis after 4 weeks of treatment, albeit in rats (Noda *et al.*, 1999). Separate sub-groups of HS-fed mice were administered CGP ((1.44 mg/kg/d; a dose that had demonstrated protective effects against atherosclerosis in mice; (Kljajic *et al.*, 2013)) or RLX ((0.5mg/kg/d; a dose that had consistently demonstrated anti-fibrotic effects in other murine models of renal fibrosis; (Hewitson *et al.*, 2010; Chow *et al.*, 2014; Wetzl *et al.*, 2016)). Both CGP or RLX were administered via subcutaneously implanted osmotic mini-pumps (model 2004, Alzet, Cupertino, CA, USA; which continuously infused each drug into the circulation of treated mice at a flow rate of 0.25µl/hour, from weeks 5-8) (see Figure 3.2.2.1). Two additional sub-groups of mice were administered CAND (2mg/kg/day; via drinking water) and RLX (0.5mg/kg/day; via osmotic mini-pumps); or CGP (1.44mg/kg/day) and RLX (0.5mg/kg/day; both via osmotic mini-pumps (see Figure 2.2.1). Systolic blood pressure (SBP) was measured via tail-cuff plethysmography every 2 weeks from week 0 until week 8.

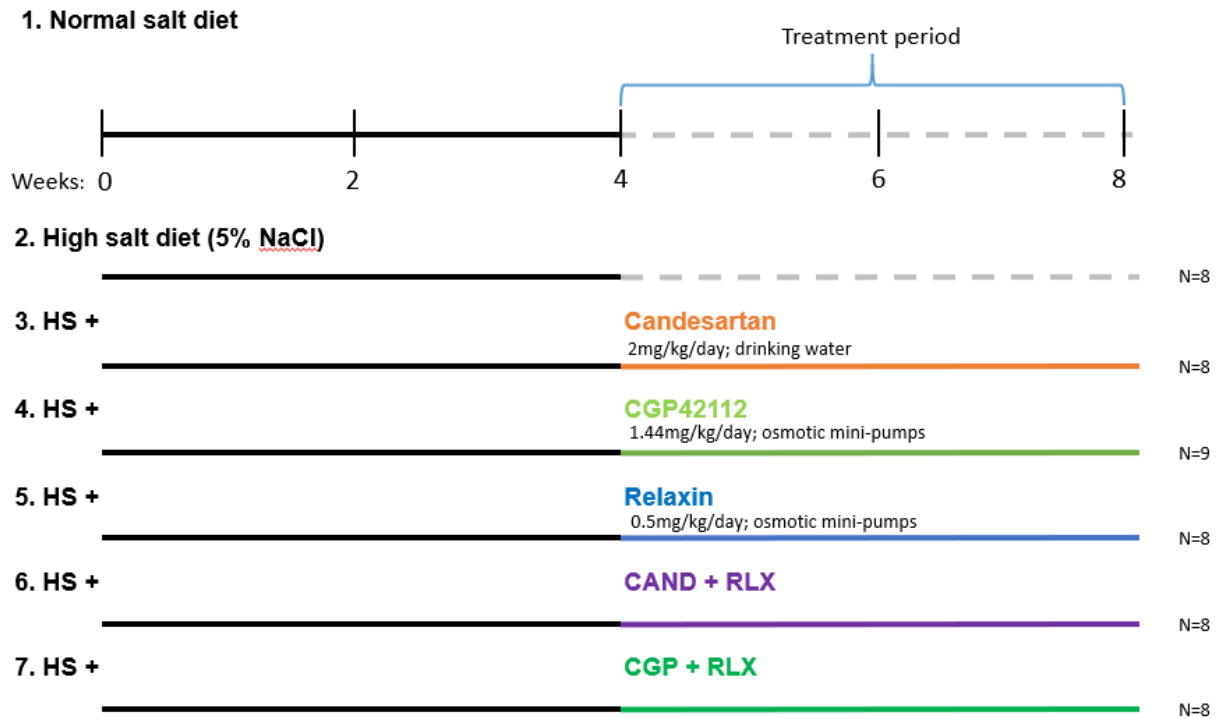


Figure 3.2.2.1. Experimental design for the 8-week high salt diet model

Mice were randomized into 7 treatment groups. Group 1 was fed normal lab chow containing 0.5% NaCl for the 8-week duration. The remaining groups received high salt lab chow containing 5% NaCl for the 8-week duration. Group 2 remained on a constant high salt diet for 8 weeks, while groups 3 to 7 were provided selected treatments from weeks 5-8. By week 8, mice were culled, and kidneys were taken for analysis.

3.2.3 Tissue collection

After 8 weeks of NS or HS feeding, all mice were killed by anaesthetic overdose, and blood was collected by cardiac puncture and spun down for plasma collection, which was subsequently stored at -80°C. Each kidney was then isolated and divided in half to obtain a total of 4 portions (2 from each kidney). One half was fixed in 10% neutral buffered formaldehyde overnight and processed by Monash Histology Services to be cut and embedded in paraffin wax. Another half was embedded in a cryomold filled with OCT, frozen in liquid nitrogen and stored at -80°C, until required. The other 2 portions were snap-frozen in liquid nitrogen and stored at -80°C for hydroxyproline analysis and extraction of proteins for gelatin zymography and Western blotting.

3.2.4 Kidney histopathology

Serial paraffin-embedded kidney sections (5µm thickness) from each mouse were placed on Superfrost® Plus slides (Thermo Scientific, Rockford, IL, USA) for histological and immunohistochemical staining. To assess glomerulosclerosis and interstitial collagen deposition, one section from each mouse was sent to Monash Histology Services and underwent Masson's trichrome staining.

3.2.5 Immunohistochemistry and Immunofluorescence

Immunohistochemistry (IHC) and immunofluorescence (IF) was used to detect markers of renal inflammation and fibrosis, inclusive of macrophage infiltration, NF-κB activity, α-smooth muscle actin (α-SMA; a marker of myofibroblast differentiation and vascular rarefaction), TGF-β1 and TIMP-1 levels. In each case, frozen serial sections from each mouse were subjected to either a monoclonal anti-rat F4/80 (1:200 dilution; MCA497R, Bio-Rad Laboratories, Richmond, CA, USA), biotinylated monoclonal anti-human SMA (1:200 dilution; M0851, DAKO Corp., Carpinteria, CA, USA), polyclonal anti-rabbit TGF-β1 (1:1000 dilution; Ab92486, Abcam, Cambridge, UK) or polyclonal anti-rabbit TIMP-1 (1:1000; Ab38978, Abcam, Cambridge, UK) primary antibody for IHC-staining of these markers and DAKO anti-mouse or anti-rabbit HRP kits containing appropriate secondary antibodies. IHC-stained sections were visualized with the avidin–biotin complex (ABC Elite; Vector, Burlingame, CA, USA) and 3,30-diaminobenzidine (DAB; Sigma-Aldrich). Frozen sections from each mouse were subjected to a polyclonal anti-rabbit p-IκB primary antibody (1:50; #28595S, Cell Signalling, Massachusetts, USA) and goat anti-rat Alexa Fluor 488 IgG secondary antibody (A11006, Life Technologies, CA, USA) for IF-staining of this marker.

3.2.6 Morphometric analysis

All kidney sections were scanned, captured and viewed under Monash Histology Service's Aperio Scanscope AT Turbo (Leica Microsystems Pty Ltd, VIC, Australia) or with a confocal microscope (Olympus, BX51, USA) at x20-x40 magnification for morphometric analysis of Masson's trichrome, IHC or IF-labelled tissue images. For each tissue section, 6-8 non-overlapping sections per mice were single-blinded and randomly selected. For each image, aside from glomerulosclerosis score, the percentage of positively-stained areas was quantified with ImageJ 1.48 software (Java, NIH).

3.2.7 Hydroxyproline assay

One half of the frozen kidney from each mouse was lyophilized to dry weight, hydrolysed in 6mmol/l hydrochloric acid as described previously (Mookerjee *et al.*, 2009; Samuel, 2009) for the measurement of hydroxyproline content, which was determined from a standard curve of purified trans-4-hydroxy-L-proline (Sigma-Aldrich). Hydroxyproline values were multiplied by a factor of 6.94 based on hydroxyproline representing ~14.4% of the amino acid composition of collagen in most mammalian tissues to extrapolate total collagen content (Gallop and Paz, 1975), which in turn was divided by the dry weight of each corresponding tissue to yield collagen concentration (expressed as a percentage).

3.2.8 Gelatin zymography

To determine if the treatment-induced effects on collagen expression were mediated via regulation by collagen-degrading gelatinases, gelatin zymography was performed on kidney protein extracts, which were isolated using the method of Woessner (Woessner Jr, 1995) and assessed for changes in expression and activity of MMP-2 (gelatinase-A). Equal aliquots of the protein extracts (containing 5µg of protein) were analysed on zymogram gels consisting of 7.5% acrylamide and 1 mg/ml gelatin. The gels were subsequently treated as previously detailed (Woessner, 1995). Gelatinolytic activity was identified by clear bands at the appropriate molecular weight, quantitated by densitometry and the relative optical density (OD) of MMP-2 in each group, and expressed as the respective ratio to that in the NS-fed mouse group, which was expressed as 1.

3.2.9 Plasma urea

Plasma samples from each mouse, obtained from the cardiac puncture of mice were thawed before 100µl of each sample was transferred onto Chem8+ cartridges to be inserted and rapidly measured by the i-STAT point-of-care handheld device (Abbott Laboratories, Illinois, USA). Plasma urea was then recorded as mmol/L.

3.2.10 Statistical analysis

All statistical analysis was performed using GraphPad Prism v7.0 (Graphpad Software Inc., CA, USA) and expressed as the mean ± SEM. Data were analysed via a one-way ANOVA with Neuman-

Keuls post-hoc test for multiple comparisons between groups. In each case, data were considered significant with a p-value less than 0.05.

3.3 Results

3.3.1 The effects of HS and the treatments investigated on systolic blood pressure.

SBP was measured fortnightly via tail-cuff plethysmography in each sub-group of mice, from weeks 0-8 (Figure 3.3.1). Mice fed a HS diet had similar SBP measurements (of around 107-115mmHg) throughout the 8 week experimental period, to that measured from mice fed a NS diet, confirming that mice fed a diet of 5% NaCl did not undergo hypertension in this strain. Mice that received CGP alone, RLX alone or the combined effects of CGP and RLX also maintained normotensive SBP levels, whereas CAND alone or in combination with RLX significantly lowered SBP ~98mmHg and ~104mmHg after 4 weeks of treatment (both $p < 0.05$ vs NS group; Figure 3.3.1). These findings suggested that CAND administration was inducing hypotension when administered to normotensive mice.

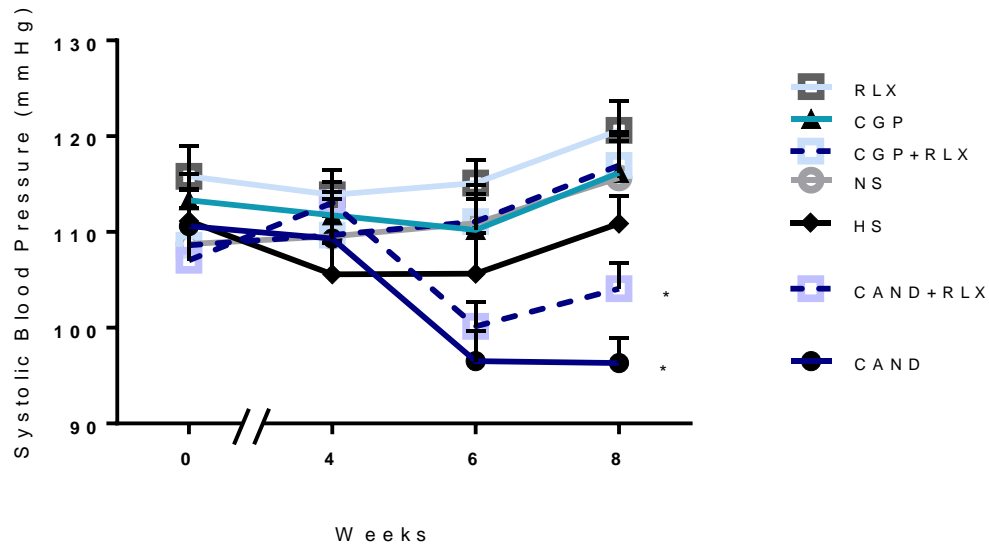


Figure 3.3.1. The effects of HS and the treatments investigated on systolic blood pressure (SBP).

Shown are fortnightly mean \pm SEM SBP measurements from mice fed a NS (0.5% NaCl) or HS (5% NaCl) diet over 8 weeks, and from HS-fed mice treated with CAND, CGP or RLX alone, CAND+RLX or CGP+RLX over the final 4 weeks of the 8 week model; as determined by tail cuff plethysmography. Neither HS alone or HS+CGP, HS+RLX or HS+CGP+RLX significantly altered SBP compared to that obtained from NS-fed mice. However, only mice treated with CAND or CAND+RLX significantly lowered SBP over 2-4 weeks of treatment; suggesting that the ARB was inducing hypotension when administered to a normotensive model. * $P < 0.05$ vs NS group at week 8.

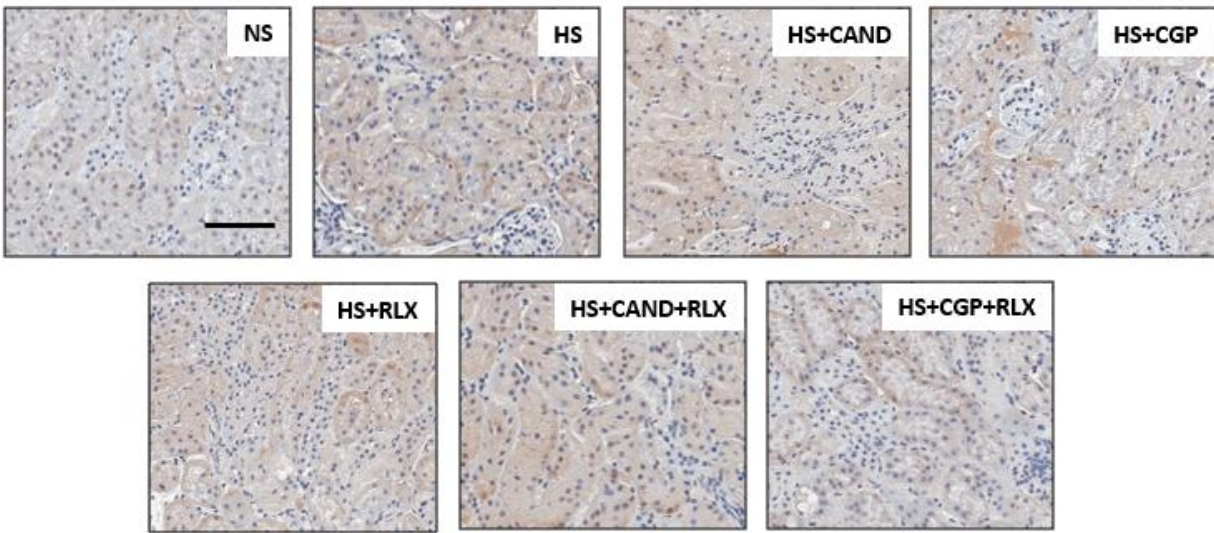
3.3.2 The effects of HS and the treatments investigated on measures of renal inflammation.

F4/80-stained macrophage infiltration (Figure 3.3.2) and P- $\text{I}\kappa\text{B}$ staining (used as a surrogate marker of NF- κB activity; Figure 3.3.3) were both significantly increased in HS-fed mice (by ~3-fold and ~4.8-fold, respectively; both $P < 0.001$ vs NS group) compared to respective measurements obtained from NS-fed controls. This indicated that HS (5% NaCl)-feeding led to renal inflammation after 8 weeks. Whereas neither CAND treatment alone, RLX treatment alone, or the combined effects of CAND+RLX affected the HS-increased macrophage infiltration (Figure 3.3.2), these treatments alone or in combination attenuated the HS-induced P- $\text{I}\kappa\text{B}$ staining after 4 weeks of treatment (all by ~16-58%; all $p < 0.05$ vs HS group; Figure 3.3.3).

In comparison, CGP alone or in combination with RLX significantly reduced the HS-induced increase in F4/80 staining (by ~60-70%; both $P < 0.001$ vs HS group; Figure 3.3.2), as well as P- $\text{I}\kappa\text{B}$ staining (by ~76-86%; both $P < 0.001$ vs HS group; Figure 3.3.3) after 4 weeks of treatment. CGP or CGP+RLX treatment also significantly reduced both measures of renal inflammation to a greater extent than CAND alone, RLX alone or the combined effects of CAND+RLX (both $p < 0.01$ vs CAND, RLX or CAND+RLX).

However, neither of the individual or combined treatments investigated fully reduced macrophage infiltration (Figure 3.3.2) or P- $\text{I}\kappa\text{B}$ staining (Figure 3.3.3) to levels that were measured from mice on the NS diet (all $p < 0.05$ vs respective measurements from NS group)

A



B

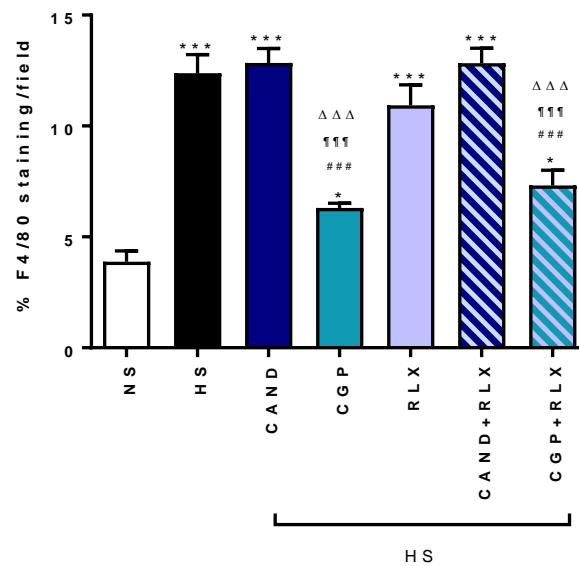
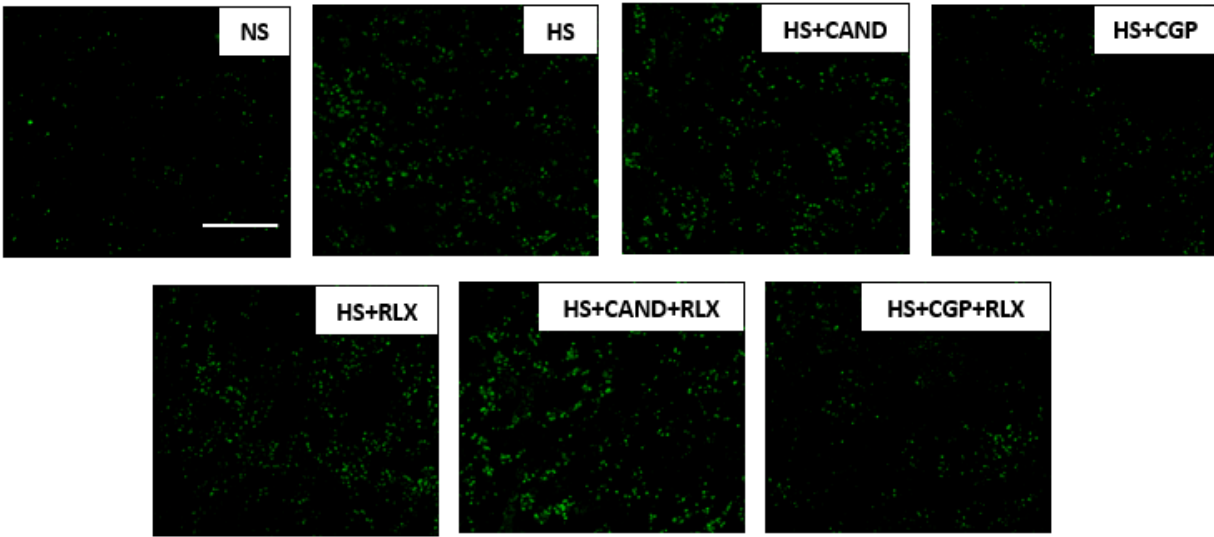


Figure 3.3.2. The effects of HS and the treatments investigated on F4/80 macrophage infiltration.

A) Representative images of IHC-stained kidney sections from each group studied for F4/80, a marker for macrophage infiltration. Scale bar = 50 μ m. B) Also shown is the mean \pm SEM % F4/80 stained per section (per total area stained), which was averaged from the measurements of 8 fields per section, $n=8$ mice/group. * $P<0.05$, *** $P<0.001$ vs NS group; ### $P<0.001$ vs HS group; 111 $P<0.001$ vs HS+CAND group; $\Delta\Delta\Delta P<0.001$ vs HS+CAND+RLX group (one-way ANOVA).

A



B

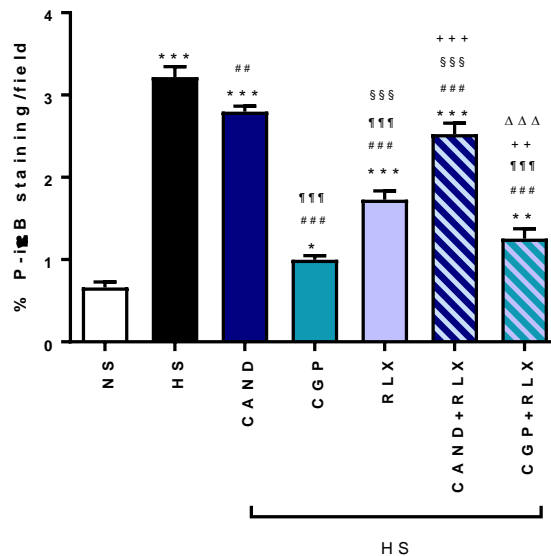


Figure 3.3.3. The effects of HS and the treatments investigated on P-ikB staining.

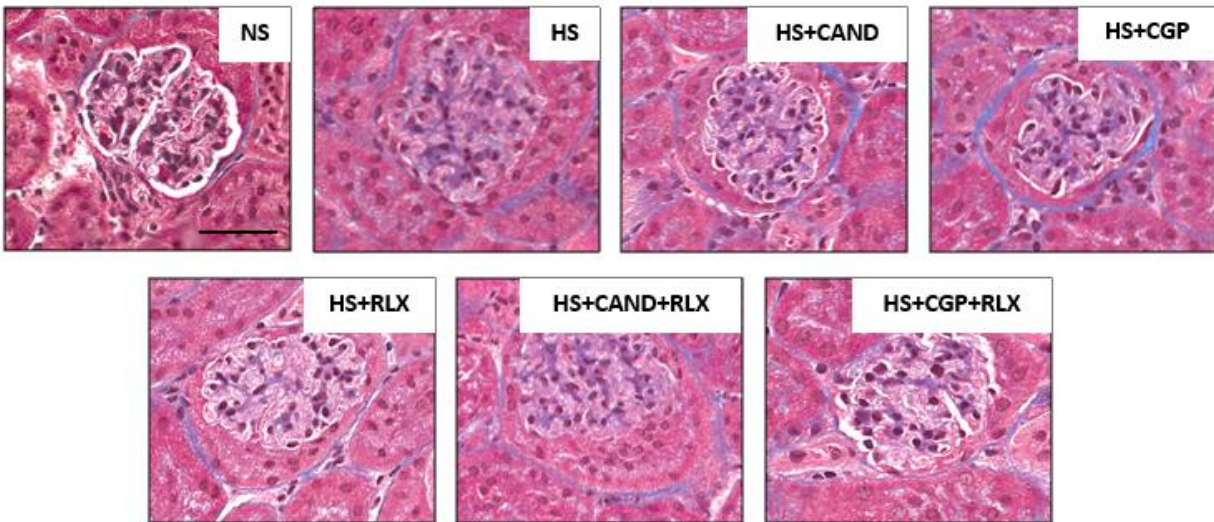
A) Representative images of IF-stained kidney sections from each group studied for P-ikB, a marker for NF- κ B activity. Scale bar = 50 μ m. B) Also shown is the mean \pm SEM % P-ikB stained per section (per total area stained), which was averaged from the measurements of 8 fields per section, $n=8$ mice/group. * $P<0.05$, ** $P<0.01$, *** $P<0.001$ vs NS group; ## $P<0.01$, ### $P<0.001$ vs HS group; ¶¶¶ $P<0.001$ vs HS+CAND group; §§§ $P<0.001$ vs HS+CGP group; ++ $P<0.01$, +++ $P<0.001$ vs HS+RLX group; ΔΔΔ $P<0.001$ vs HS+CAND+RLX group (one-way ANOVA).

3.3.3 The effects of HS and the treatments investigated on glomerulosclerosis.

Masson's trichrome-stained images were used to assess glomerulosclerosis score (Figure 3.3.4) from each mouse kidney (from 8 glomeruli per kidney section). This score was arbitrarily assigned where 0 represented no collagen staining inside the glomeruli, 1 represented mild (1-33%) collagen staining, 2 represented medium (33-67%) collagen staining and 3 represented severe (67-100%) collagen staining within the glomeruli which was adapted from the glomerulosclerotic index (Maric *et al.*, 2004) and scoring of respiratory inflammatory cell aggregates (Royce *et al.*, 2015). HS-fed mice had a greater glomerulosclerosis score (by ~1.5-fold increase, $P < 0.001$ vs NS group) compared to that measured from NS-fed controls. This HS-induced increase in glomerulosclerosis score was unaffected by CAND, CGP or CAND+RLX treatment (all $P < 0.001$ vs NS group; no different to HS alone) but was partially and equivalently reduced by RLX or CGP+RLX treatment (by ~40%; both $P < 0.01$ vs HS group; Figure 3.3.4).

However, RLX and CGP+RLX treatment did not reduce the HS-induced glomerulosclerosis score down to levels seen in NS-fed mice (both $p < 0.01$ vs NS group).

A



B

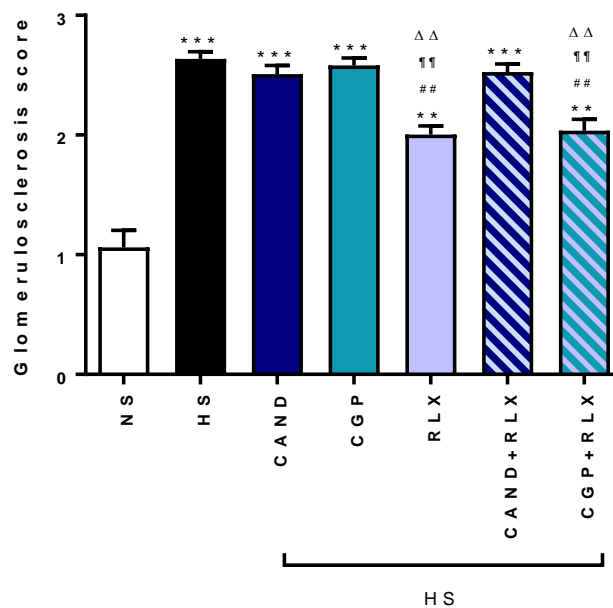


Figure 3.3.4. The effects of HS and the treatments investigated on glomerulosclerosis score.

A) Representative images of Masson's trichrome-stained kidney sections from each group studied of glomerulosclerosis. Scale bar = 100 μ m. B) Also shown is the mean \pm SEM glomerulosclerosis score, which was averaged from the measurements of 25 glomeruli per section, n=8 mice/group. Glomeruli were scored from a scale ranging from 0 to 3 for normal (0), 1 = mild (1-33%) collagen staining within glomeruli, 2 = medium (33-67%) collagen staining within glomeruli, and 3 = severe (67-100%) collagen staining within glomeruli. ***P<0.001 vs NS group; ##P<0.01 vs HS group; ¶¶P<0.01 vs HS+CAND group; ΔΔP<0.01 vs HS+CAND+RLX group (one-way ANOVA).

3.3.4 The effects of HS and the treatments investigated on interstitial and total renal collagen (fibrosis).

Six randomly selected fields per section from Masson's trichrome-stained images were also analysed for interstitial kidney collagen deposition (Figure 3.3.5). A significant increase in interstitial renal collagen staining was observed in HS-fed mice (by ~4.8-fold, $P < 0.001$ vs NS group) compared to that measured from NS-fed control. This HS-induced increase in interstitial fibrosis was unaffected by CAND, CGP or CAND+RLX treatment (all $p < 0.001$ vs NS group; no different to HS group; Figure 3.3.5) but was significantly reduced by RLX and CGP+RLX treatment (by ~27%; both $P < 0.01$ vs HS group). However, neither RLX or CGP-RLX treatment fully reduced the HS-induced interstitial renal collagen staining back to levels seen in NS-fed controls (both $p < 0.01$ vs measurements from NS group; Figure 3.3.5B).

Total kidney collagen concentration was also examined using the hydroxyproline assay (Figure 3.3.5C) and was found to be significantly increased in HS-fed mice (by ~30%; $p < 0.01$ vs NS group) compared to respective measurements from NS-fed counterparts. This increase in HS-induced collagen concentration was unaffected by CAND or CAND+RLX treatment but was significantly reduced by CGP treatment (by ~70%) and normalised by RLX or CGP+RLX treatment (all $p < 0.05$ vs HS alone; all no different to NS alone; Figure 3.3.5C).

In general, RLX and the combined effects of CGP+RLX demonstrated greater anti-fibrotic effects over that of CAND alone or CAND+RLX treatment (both $p < 0.01$ vs CAND or CAND+RLX for each measure of fibrosis determined)

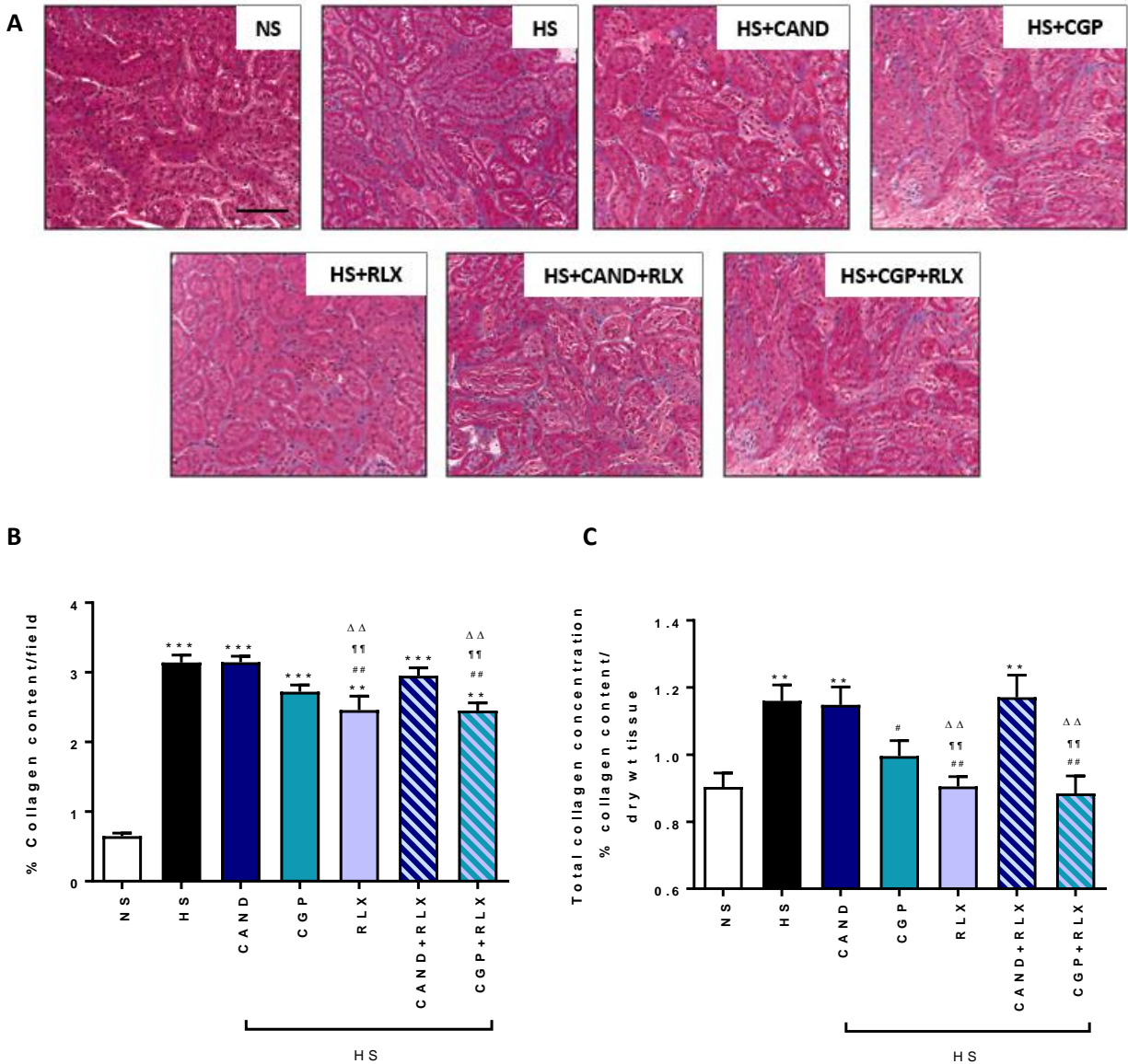


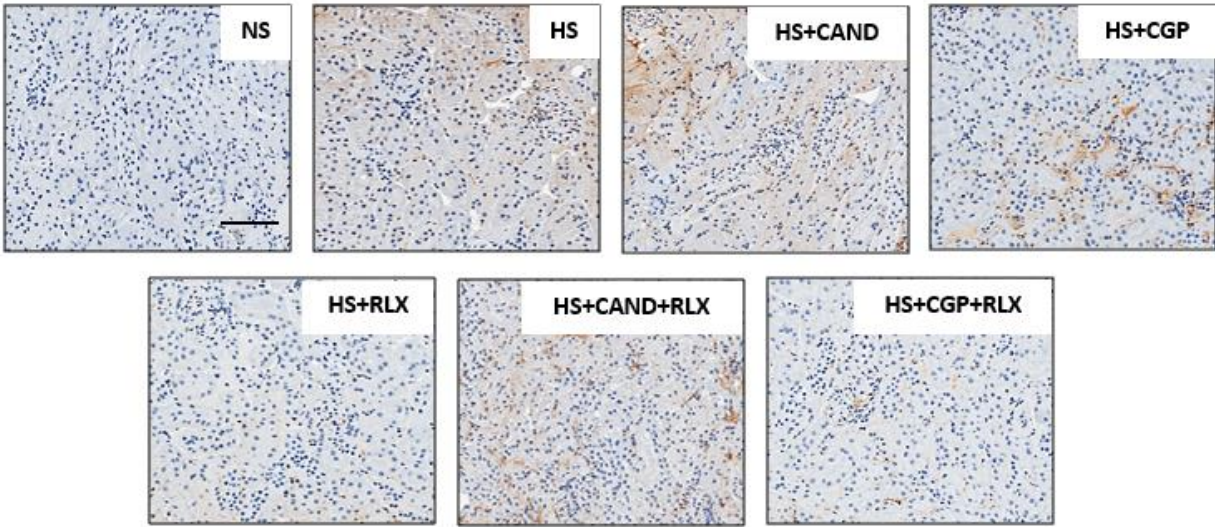
Figure 3.3.5. The effects of HS and the treatments investigated on interstitial collagen and total kidney collagen concentration.

A) Representative images of Masson's trichrome-stained kidney sections from each group studied of interstitial ECM/collagen deposition. Scale bar = 100 μ m. B) Also shown is the mean \pm SEM % interstitial ECM/collagen staining per section (per total area stained), which was averaged from the measurements of 8 fields per section, n=8 mice/group. C) Additionally shown is the mean \pm SEM % total kidney collagen concentration (which was extrapolated from dividing the collagen content of each kidney portion analysed by the dry weight of that portion); obtained from hydroxyproline analysis of n=6-8 mice/group. **P<0.01, ***P<0.001 vs NS group; #P<0.05, ##P<0.01 vs HS group; ††P<0.01 vs HS+CAND group; $\Delta\Delta$ P<0.01 vs HS+CAND+RLX group (one-way ANOVA).

3.3.5 The effects of HS and the treatments investigated on TGF- β 1 staining.

TGF- β 1 immunostaining was then carried out to determine the impact of the HS-fed diet and the treatments investigated on renal expression of the pro-fibrotic cytokine (Figure 3.3.6). As expected, the HS-fed mice had significant increased interstitial renal TGF- β 1 staining (by ~6-fold, $P < 0.001$ vs NS group) compared to that measured from NS-fed controls (Figure 3.3.6B). The HS-induced increase in kidney TGF- β 1 staining was unaffected by CAND or CAND+RLX treatment, but reduced by CGP (by ~50%; $P < 0.01$ vs HS group) and to a further extent by RLX or CGP+RLX treatment (by 70-77%; both $p < 0.01$ vs HS group; Figure 3.3.6B). However, neither CGP, RLX or CGP+RLX treatment fully reduced renal TGF- β 1 staining back to that measured from mice on the NS diet (all $p < 0.05$ vs measurements from NS group).

A



B

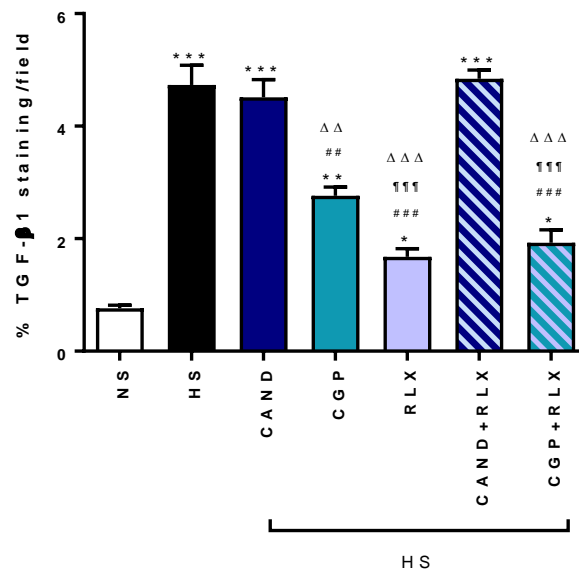


Figure 3.3.6. The effects of HS and the treatments investigated on renal TGF- β 1 expression levels.

A) Representative images of IHC-stained kidney sections from each group studied for interstitial expression of the pro-fibrotic cytokine, TGF- β 1. Scale bar = 100 μ m. B) Also shown is the mean \pm SEM % TGF- β 1 stained per section (per total area stained), which was averaged from the measurements of 8 fields per section, $n=8$ mice/group. * $P<0.05$, ** $P<0.01$, *** $P<0.001$ vs NS group; ## $P<0.01$, ### $P<0.001$ vs HS group; ¶¶¶ $P<0.001$ vs HS+CAND group; ΔΔΔ $P<0.001$ vs HS+CAND+RLX group (one-way ANOVA).

3.3.6 The effects of HS and the treatments investigated on myofibroblast differentiation and vascular rarefaction.

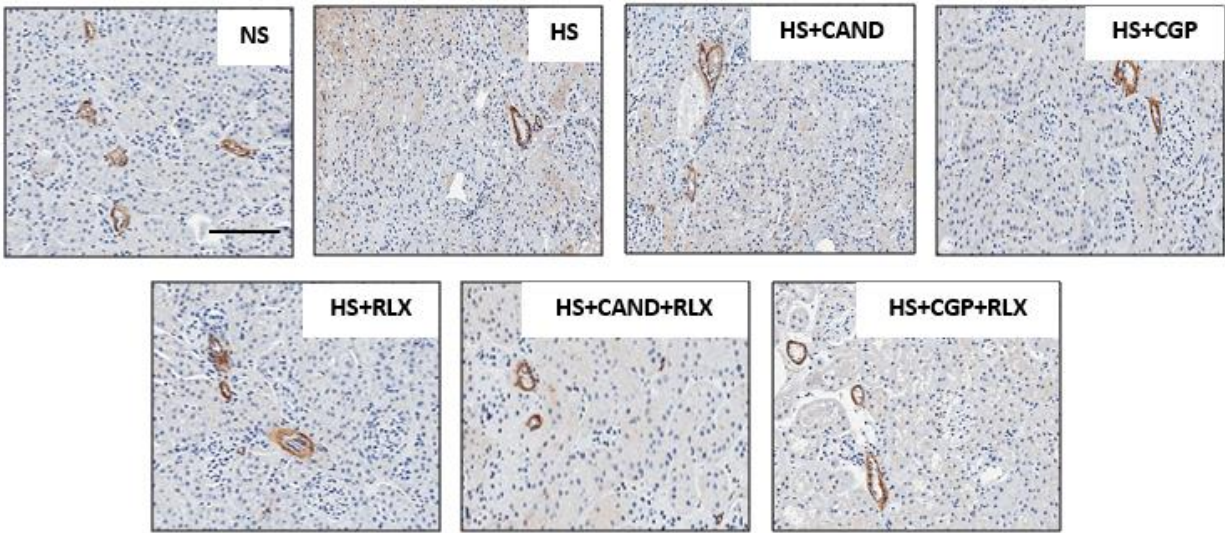
α -SMA-stained tissue sections (Figure 3.3.7) were used to detect the impact of the HS-fed diet and the treatments investigated on interstitial myofibroblast accumulation (Figure 3.3.7B) and vascular rarefaction (blood vessel loss; Figure 3.3.7C). Interstitial renal myofibroblast accumulation was significantly increased in HS-fed mice (by 3.2-fold; $P < 0.001$ vs NS group) compared to that measured from NS-fed controls. While this HS-induced increase in interstitial myofibroblast accumulation was unaffected by CAND, CGP or CAND+RLX treatment, it was significantly reduced by RLX or CGP+RLX treatment (by ~85% and ~65%, respectively; both $P < 0.01$ vs HS group). As a result, RLX treatment alone was found to reduce interstitial myofibroblast accumulation to a significantly greater extent compared to CAND (by ~65%; $P < 0.01$ vs CAND group), CGP (by ~43%; $P < 0.01$ vs CGP group) or CAND+RLX (by ~60%; $P < 0.001$ vs CAND+RLX group) treatment (Figure 3.3.7B). However, neither RLX or CGP+RLX treatment fully reduced interstitial myofibroblast accumulation back to that measured in NS-fed mice (both $p < 0.05$ vs measurements from NS-fed mice).

HS-fed mice were also found to be associated with increased vascular rarefaction (~50% loss of blood vessel density; $p < 0.001$ vs NS group; Figure 3.3.7C) compared to that measured from NS-fed counterparts. This HS-induced loss of blood vessel density was unaffected by CAND, CGP or CAND+RLX treatment, but was restored by RLX or CGP+RLX (by ~57% and ~41%, respectively; both $P < 0.01$ vs HS group). Furthermore, both RLX and CGP+RLX treatment restored vascular rarefaction to a greater extent than CAND (by ~58% and ~42%, respectively; both $P < 0.001$ vs CAND group) or CAND+RLX (~48% and ~32%, respectively; both $P < 0.05$ vs CAND+RLX group) treatment. However, neither RLX or CGP+RLX treatment fully restored the HS-induced loss of blood vessel density back to that measured in NS-fed mice (both $p < 0.01$ vs NS group; Figure 3.3.7C).

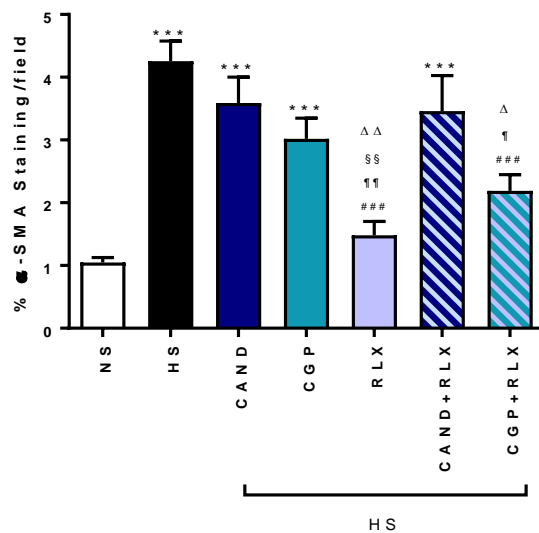
The findings presented in Figures 3.3.6-3.3.7 were consistent with those presented in Figure 3.3.5 in demonstrating that RLX or the combined effects of CGP+RLX demonstrated greater anti-fibrotic effects over that of CAND or CAND+RLX treatment; and also over CGP treatment in

reducing interstitial renal myofibroblast accumulation. RLX or its combined effects with CGP also restored vascular rarefaction to a greater extent than CAND, CGP or CAND+RLX treatment.

A



B



C

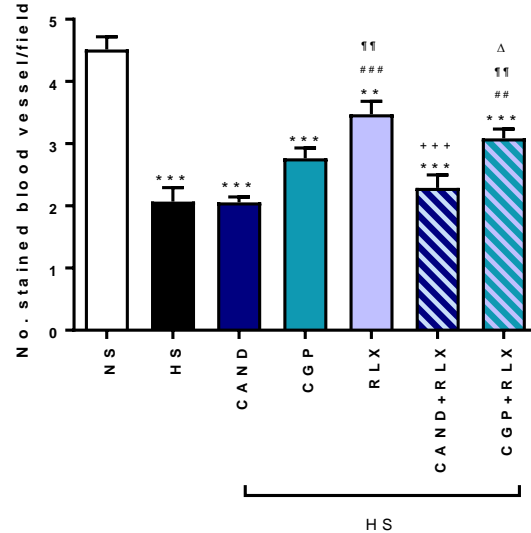


Figure 3.3.7. The effects of HS and the treatments investigated on renal myofibroblast accumulation and vascular rarefaction.

A) Representative images of IHC-stained kidney sections from each group studied for α -SMA-associated interstitial myofibroblast accumulation and vascular rarefaction. Scale bar= 100 μ m. Also shown is the mean \pm SEM B) % α -SMA-stained myofibroblast accumulation per section (per total area stained) or C) number of blood vessel counts per section stained; which in each case was averaged from the measurements of 8 fields per section, n=8 mice/group. **P<0.01, ***P<0.001 vs NS group; ##P<0.01, ###P<0.001 vs HS group. ¶P<0.05, ¶¶P<0.01 vs HS+CAND group; §§P<0.01 vs HS+CGP, +++P<0.001 vs HS+RLX group; ΔP<0.05, ΔΔP<0.01 vs HS+CAND+RLX group (one-way ANOVA).

3.3.7 The effects of HS and the treatments investigated on gelatinase expression.

Gelatin zymography was then completed to determine the impact of the HS-fed diet and the treatments investigated on mediators of ECM degradation, namely MMP-2 and MMP-9 expression and activity (Figure 3.3.8). Mice fed a HS-diet did not present with significantly altered MMP-9 (Figure 3.3.8B) or MMP-2 (Figure 3.3.8C) expression levels compared to that measured from NS-fed mice. Likewise, neither CAND or CAND+RLX-treatment of HS-fed mice affected the expression levels of these gelatinases compared to mice fed a NS-diet. CGP treatment of HS-fed mice did not affect MMP-9 levels, but modestly increased MMP-2 levels (by ~30%; $p < 0.05$ vs HS alone; Figure 3.3.8C). On the other hand, RLX or CGP+RLX treatment of HS-fed mice significantly increased MMP-9 expression levels (by ~2.2-fold and ~1.25-fold, respectively; both $P < 0.05$ vs NS group; $P < 0.05$ vs HS group; Figure 3.3.8B) and MMP-2 expression levels (by 76-88%; both $P < 0.001$ vs NS group; $P < 0.001$ vs HS group; Figure 3.3.8C). RLX alone or in combination with CGP was also able to promote MMP-9 levels to a greater extent than CAND or CGP treatment; and MMP-2 levels to a greater extent than CAND or CAND+RLX-treatment.

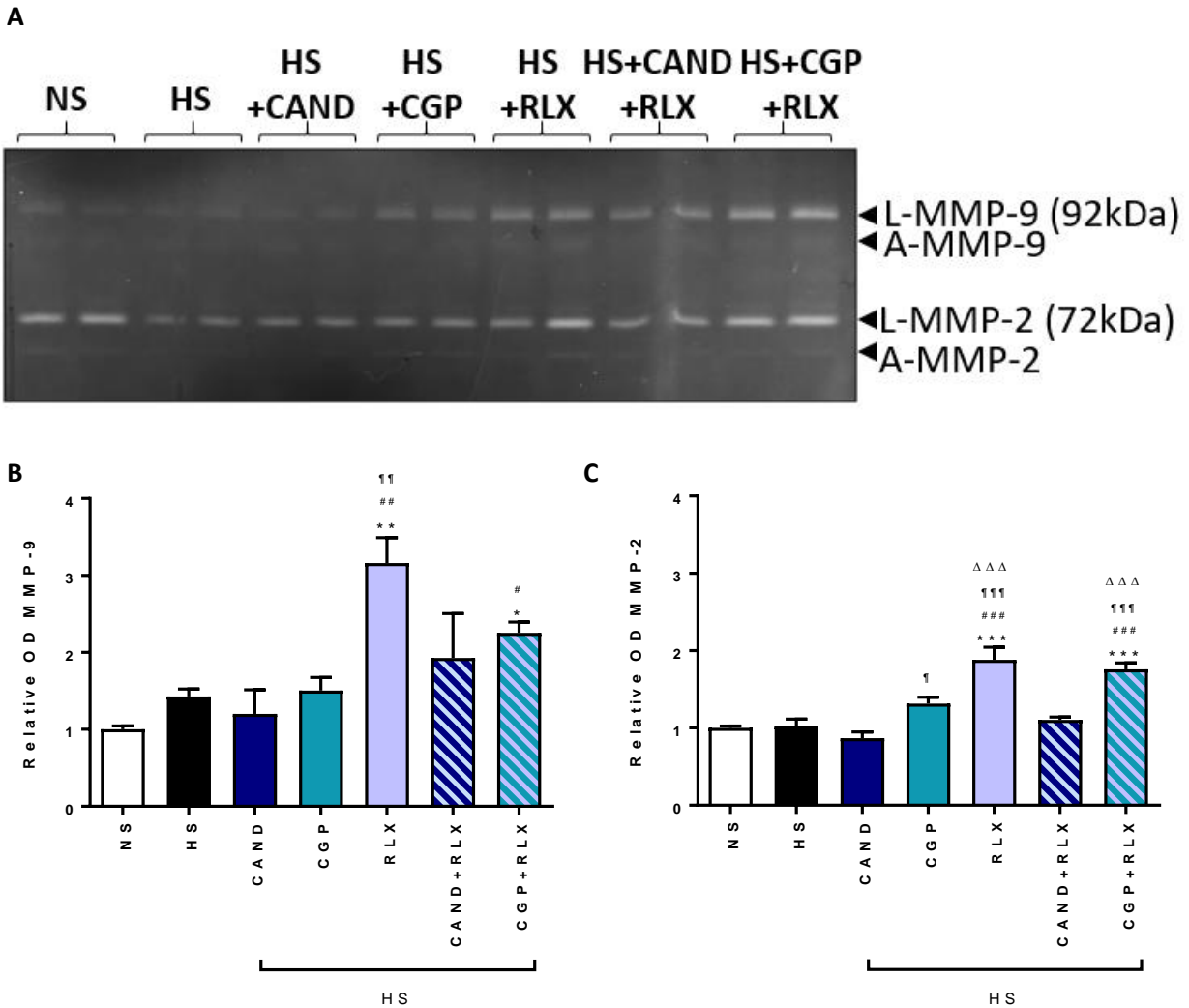


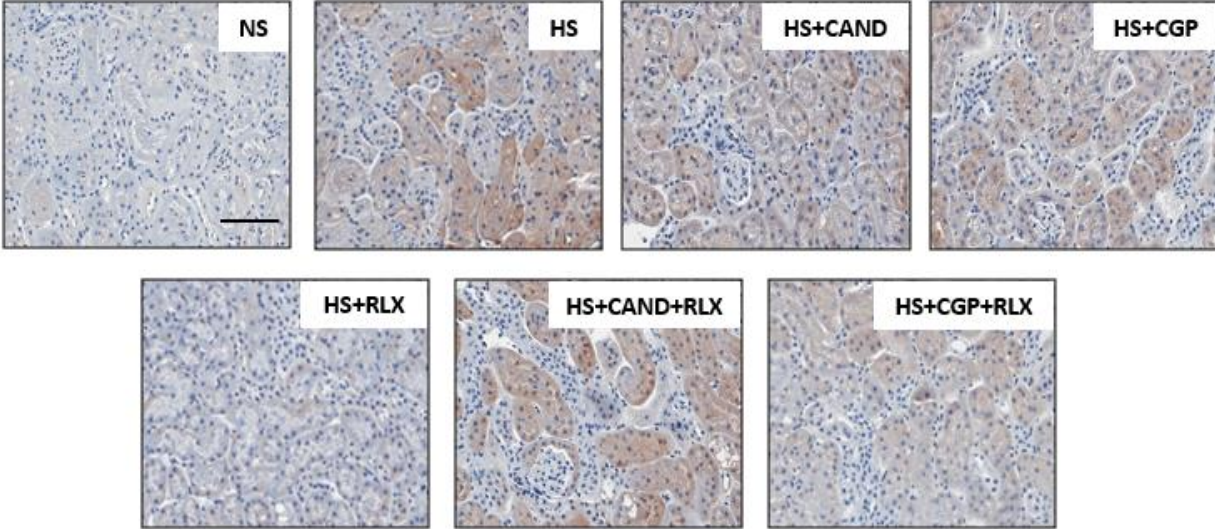
Figure 3.3.8. The effects of HS and the treatments investigated on renal gelatinase expression levels.

A) A representative gelatin zymography which shows latent MMP-9 (92kDa) and MMP-2 (72kDa) expression levels from the kidneys of the control and treatment groups studied. Also shown is mean \pm SEM relative OD B) MMP-9 expression and C) MMP-2 expression (as determined by densitometry of the bands shown), which in each case was expressed as the relative value to the value from NS control group, which was expressed as 1 in each case; from $n=6$ mice per group studied. The remaining four samples per group were analysed on separate gelatin zymographs. * $P<0.05$, ** $P<0.01$, *** $P<0.001$ vs NS group; † $P<0.05$, †† $P<0.01$, ††† $P<0.001$ vs HS group; †††† $P<0.001$, ††††† $P<0.001$ vs HS+CAND group; †††††† $P<0.001$ vs HS+CAND+RLX group (one-way ANOVA).

3.3.8 The effects of HS and the treatments investigated on TIMP-1 expression.

Subsequently, changes in the expression levels of the endogenous inhibitor of the above-detailed MMPs, TIMP-1, was examined by immunohistochemistry (Figure 3.3.9). HS-fed mice had an approximate doubling of renal TIMP-1 staining compared to that seen in the kidneys of NS-fed mice ($P < 0.001$ vs NS group). This increase in HS-induced TIMP-1 levels was unaffected by CAND, CGP or CAND+RLX treatment, fully reduced by RLX treatment alone ($p < 0.001$ vs HS group; no different to NS group), and partially reduced by CGP+RLX treatment (by ~55% $P < 0.001$ vs HS group; $P < 0.01$ vs NS group). Hence, RLX alone and its combined effects with CGP significantly reduced TIMP-1 levels to a greater extent than CAND, CGP or CAND+RLX treatment (Figure 3.3.9B).

A



B

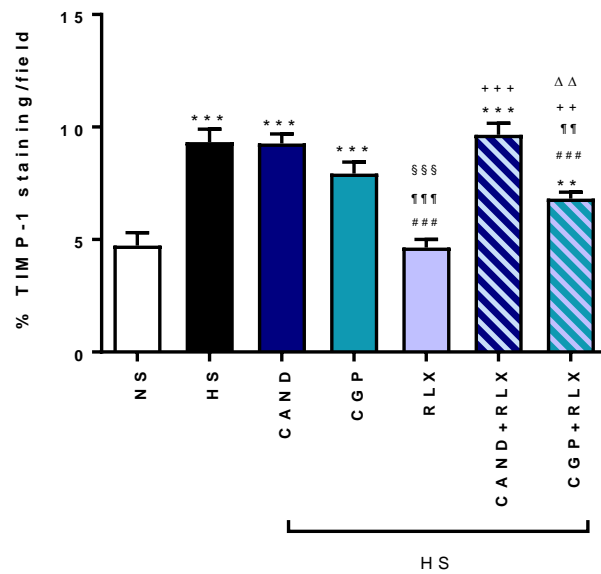


Figure 3.3.9. The effects of HS and the treatments investigated on renal TIMP-1 expression.

Representative images of IHC-stained kidney sections from each group studied for TIMP-1 expression. Scale bar = 100 μ m. B) Also shown is the mean \pm SEM % TIMP-1 stained per section (per total area stained), which was averaged from the measurements of 8 fields per section, n=8 mice/group. ** P <0.01, *** P <0.001 vs NS group; ### P <0.001 vs HS; ¶¶ P <0.01, ¶¶¶ P <0.001 vs HS+CAND group; §§§ P <0.001 vs HS+CGP group, +++ P <0.001 vs HS+RLX group; $\Delta\Delta$ P <0.01 vs HS+CAND+RLX group (one-way ANOVA).

3.3.9 The effects of HS and the treatments investigated on plasma urea levels.

Plasma urea levels were used as a surrogate marker of renal dysfunction (Figure 3.3.10). It was found that mice fed a HS (5% NaCl)-diet for 8 weeks had significantly increase plasma urea levels (9.2 ± 0.4 mmol/L) over that measured from mice fed a NS-diet (7.7 ± 0.3 mmol/L; $p < 0.05$ vs HS group), indicating that mice fed the HS diet had a significant lowering of renal function. This HS-induced increase in plasma urea levels was normalised by CGP, RLX or CGP+RLX treatment (all $p < 0.05$ vs HS group; all no different to NS group), but not by CAND or CAND+RLX treatment (both no different to HS group; both $p < 0.05$ vs NS group; Figure 3.3.10).

These findings suggested that only CGP alone, RLX alone or the combined effects of CGP+RLX could abrogate the HS-induced renal dysfunction that was associated with the model studied.

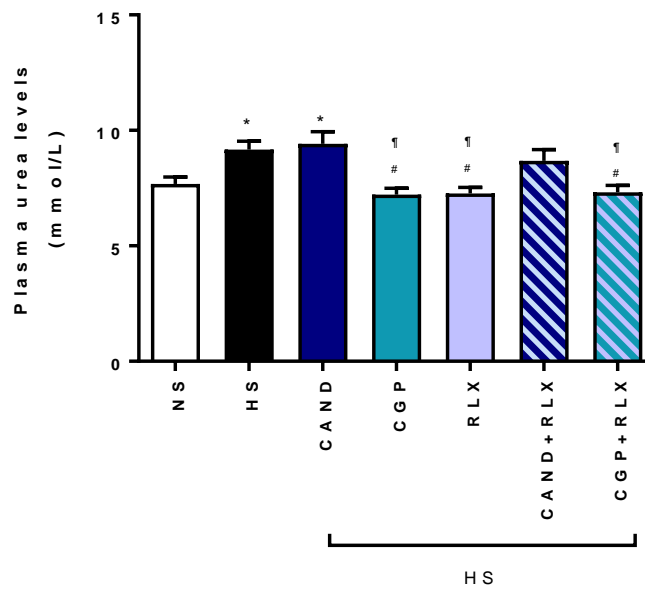


Figure 3.3.10. The effects of HS and the treatments investigated on plasma urea levels.

Shown is the mean \pm SEM plasma urea levels from each of the control and treatment groups studied, which was evaluated from the i-STAT device using 100 μ l of plasma from each animal; $n=6-8$ mice per group. * $P<0.05$ vs NS group; # $P<0.05$ vs HS group; ¶ $P<0.05$ vs HS+CAND group (one-way ANOVA).

3.4 Discussion

This study compared the anti-fibrotic effects of the current standard-of-care medication, candesartan cilexetil (CAND), to the RXFP1 agonist, serelaxin (RLX) and AT2 receptor agonist, CGP42112 (CGP). This was the first study to make a head-to-head comparison between these treatments in a high salt-induced model of kidney damage, using doses of each drug that had previously demonstrated anti-fibrotic efficacy in other models of disease. As the high-salt diet (5% NaCl) utilised, induced renal damage and related fibrosis in the absence of any overt changes in blood pressure, the model allowed for the evaluation of the direct anti-fibrotic efficacy of each drug studied in a normotensive setting, when administered over a 4-week period to established disease.

CAND (2mg/kg/day) was able to reduce SBP and induce some anti-inflammatory effects (on HS-induced P-iKB levels) when therapeutically administered over 4 weeks to the normotensive model, demonstrating that it was biologically active at the dose administered. However, at this same dose, it failed to affect renal macrophage infiltration, TGF- β 1 expression levels, myofibroblast accumulation, vascular rarefaction, interstitial and total collagen concentration (fibrosis), and gelatinase and TIMP-1 levels, which resulted in its inability to affect the HS-induced increase in plasma urea levels, despite being added at double the dose that was found to suppress 5/6 nephrectomy-induced renal fibrosis in rats (Noda *et al.*, 1999). Similarly, CAND (at 1 or 10mg/kg/day) also failed to affect glomerulosclerosis when therapeutically administered to Dahl-sensitive rats over a 4 week treatment period (Yao *et al.*, 2004). These findings are consistent with the slow-acting anti-fibrotic efficacy of ARBs in general (Noda *et al.*, 1999; De las Heras *et al.*, 2006), where CAND (when administered at 1-2mg/kg/day to rat models of renal injury) required 10-16 weeks of treatment to therapeutically attenuate renal inflammation and fibrosis. CAND (1mg/kg/day) was only effective at preventing renal fibrosis over 4 weeks of treatment, which suggested that the dose administered to the HS model, over the time-frame studied, may have been too low to induce any effects as an intervention. However, ARBs are known to induce various side-effects when administered at higher concentrations (Hou and Zhou, 2010; Ahmed *et al.*, 2016).

Contrary to the findings reported in this study, a recently published study found that 4 weeks of CAND administration (at 1mg/kg/day) to diabetic db/db mice did reduce the renal damage, glomerulosclerosis and albuminuria associated with the model (Callera *et al.*, 2016). However, the drug was administered to mice at 7 weeks of age, suggesting that it was only able to limit the early onset of renal damage and associated fibrosis over 4 weeks of treatment. Other studies have additionally shown that CAND (at 1 or 3mg/kg/day) and other ARBs can demonstrate modest anti-fibrotic effects in 8% HS-diet induced models of disease (Ina *et al.*, 2004; Liang and Leenen, 2008; Rafiq *et al.*, 2014). These combined studies suggest that while ARBs can demonstrate mild anti-fibrotic effects, there are many factors that can impact on these effects, including the degree of injury-induced fibrosis that is generated by the model studied; the efficacy of the drug at the dose administered; and the length of time the drug is administered for. These variables in the studies reported to date may account for the various discrepancies associated with the use of ARBs as anti-fibrotic; which are still better known for their anti-hypertensive and anti-inflammatory effects.

In comparison, CGP (1.44mg/kg/day) appeared to demonstrate marked anti-inflammatory effects in the model studied, being the only drug to be able to reduce both the HS-induced increase in macrophage infiltration and P-iKB levels by 70-86%. Of note, CGP was able to reduce macrophage infiltration to a greater extent than CAND or RLX treatment, suggesting that it was able to inhibit the infiltration of a major source of TGF- β 1 in the absence of any effects on SBP. Consistent with this, CGP treatment was able to partially reduce the HS-induced increase in renal TGF- β 1 expression levels and total kidney collagen concentration but did not markedly affect the HS-induced glomerulosclerosis, interstitial renal fibrosis or vascular rarefaction. These findings suggested then that CGP was more likely inhibiting basement membrane collagen IV, which is the major collagenous constituent of the kidney (Yu *et al.*, 1998; Hewitson *et al.*, 2010), without affecting collagen I and/or III-induced interstitial renal fibrosis; and through its ability to suppress TGF- β 1-induced fibrosis progression while promoting MMP-2 collagen degradation. Although the effects of CGP42112 have not been investigated in other models of kidney disease, a study by Gelosa and colleagues (Gelosa *et al.*, 2009) demonstrated that C21 needed to be administered at 10mg/kg/day over 6 weeks, to SHR fed a HS diet, to be able to reduce inflammatory cell

infiltration, glomerulosclerosis and renal collagen accumulation in general. These findings suggest that the therapeutic effects of AT₂ receptor agonists, like ARBs, are dose- and time-dependent (Sumners *et al.*, 2019).

RLX (0.5mg/kg/day) did not demonstrate any marked effects on SBP or macrophage infiltration but was able to partially reduce the HS-induced increase in P-ikB levels. A previous study had shown that RLX could inhibit M2 macrophage accumulation in a DOCA salt-induced model of hypertensive kidney (Wang *et al.*, 2017), although at 16mg/kg/day (which was a 32-fold higher dose than that administered in this study); and had also been shown to inhibit M1 to M2 macrophage polarisation (Chen *et al.*, 2017). RLX is also known to inhibit neutrophil (Masini *et al.*, 2004) and mast cell infiltration (Nistri *et al.*, 2008), which was not investigated in this study. Noteworthy was the finding that RLX demonstrated greater anti-fibrotic efficacy compared to the effects of CAND (2mg/kg/day) or CGP (1.44mg/kg/day), and was the only drug evaluated to be able to effectively reduce the HS-induced glomerulosclerosis, interstitial/total renal collagen deposition, TGF- β 1 expression and myofibroblast accumulation. These findings are consistent with its known anti-fibrotic properties in other models of kidney disease at the 0.5mg/kg/day dose administered in this study (Samuel *et al.*, 2016, 2017; Ng *et al.*, 2019). Furthermore, RLX had a greater effect in promoting MMP-9 and MMP-2 levels and reducing TIMP-1 levels compared to the other two other drugs studied, which would have likely contributed to its ability to stimulate MMP-induced collagen degradation.

In disease states, vascular rarefaction coupled with fibrosis, leads to reduced oxygen and nutrients being delivered to the kidney, resulting in a loss of function due to the kidney's inability to facilitate repair via angiogenesis (Afsar *et al.*, 2018). When vascular rarefaction was examined, only RLX alone restored the number of blood vessels back to that measured in NS-fed mice. This coincides with the ability of RLX to promote angiogenesis via its ability to promote factors such as vascular endothelial growth factor (VEGF) and basic fibroblast growth factor (bFGF) (Uneimori *et al.*, 2000; Samuel *et al.*, 2011). Despite CAND not affecting the HS-induced vascular rarefaction and CGP only demonstrating mild angiogenic effects, ARBs and AT₂ receptor agonists have previously been shown to possess pro-angiogenic properties that are mediated via their ability to stimulate bradykinin and VEGF-driven vascular responses (Battegay *et al.*, 2007). Blocking AT₁

receptors with losartan (30mg/kg/day) attenuated peritubular capillary rarefaction in a rat model of tubulointerstitial injury (Kitayama *et al.*, 2006), but again at a 15-fold higher dose than that used in the current study. It has been speculated that ARB administration leads to an increase in circulating Ang II, which can act on unopposed AT₂ receptors (which are up-regulated following injury) to release kinins and promote NO bioavailability, which contribute to the promotion of angiogenesis and restoration of blood vessel density (Seyedi *et al.*, 1995).

Finally, changes in plasma urea were determined as a measure of renal function, as urea is the principal nitrogenous metabolic waste product cleared by the kidneys. An increase in urea content within the plasma indicates that kidney function has been compromised as it is unable to eliminate waste products. Interestingly, the potent anti-inflammatory effects of CGP and potent anti-fibrotic effects of RLX were able to normalise the modest HS-induced increase in plasma urea levels measured. Although CGP and RLX appeared to be working through different modes of action to reduce renal fibrosis, it could be proposed that the ability of each drug to reduce total kidney collagen concentration (although not fully) resulted in their ability to abrogate the renal dysfunction associated with the HS model studied. This is based on findings from a chronic allergic airways disease model, where it was found that the ability of various treatments to reduce airway reactivity (airway dysfunction induced by chronic allergic airways disease) correlated with how effectively they reduced total lung collagen concentration (Patel *et al.*, 2016; Royce *et al.*, 2016, 2019). In line with this theory, CAND did not affect the HS-induced increase in renal dysfunction measured, as it was not able to affect the HS-induced increase in total kidney collagen concentration.

Regarding the effectiveness of the combination treatments investigated, the combined effects of CGP and RLX appeared to retain the anti-inflammatory effects of CGP alone which had greater effects compared to RLX alone and retained the anti-fibrotic effects to that of RLX which have greater effects compared to CGP alone. However, it did not offer any further additive synergistic effects over either therapy alone. Certainly though, CGP+RLX treatment reduced the HS-induced increase in renal inflammation (specifically macrophage infiltration) to a greater extent than RLX alone, and renal fibrosis to a greater extent than CGP alone, demonstrating the feasibility and efficacy of combining both drugs. By being able to effectively reduce the HS-induced increase in

renal collagen concentration, CGP+RLX treatment also effectively promoted angiogenesis and normalised the HS-induced renal dysfunction. As this is the first time both drugs have been combined together, there is no other literature to which the findings from this study (combining CGP and RLX) can be compared.

Of interest, however, when CAND was combined with RLX, CAND appeared to consistently block the renoprotective effects of RLX on all endpoints measured. Whereas RLX alone demonstrated marked anti-fibrotic effects and modest anti-inflammatory effects when administered alone, its co-administration with CAND resulted in all end-points measured resembling respective measurements obtained from HS-injured mice. Similar unpublished findings from our Lab also found that co-administration of CAND+RLX inhibited the anti-fibrotic effects of RLX in isoproterenol-and ureteric obstruction-induced models of interstitial heart and kidney disease *in vivo*, respectively. One possible theory as to how this could possibly occur has emerged from unpublished findings from our lab showing that AT₁ receptors can form heterodimers with RXFP1 receptors. As it was also previously shown that RXFP1 could form heterodimer with AT₂ receptors, which RLX could signal through to abrogate renal fibrosis (Chow *et al.*, 2014); and heterodimerization can also occur between AT₁ receptors and AT₂ receptors (AbdAlla *et al.*, 2001; Miura *et al.*, 2010), it may be possible then that all three receptors interact in some way, either directly or through crosstalk. Whether these receptors interact through heterodimer crosstalk or through direct heterodimer interactions (Figure 3.4.1) it is proposed that this would allow AT₁ receptor antagonists such as CAND to allosterically inhibit the actions of agonists acting at the RXFP1 (RLX) or AT₂ (CGP) receptors. Although the combined effects of CAND and CGP were not detailed in this study, unreported studies from our Lab have found that the cGMP-promoting effects of C21 in human cardiac myofibroblasts, and the ability of C21 to inhibit renal myofibroblast differentiation and collagen-I deposition in rat renal myofibroblasts *in vitro*, was abrogated by CAND treatment, which fits with the above-detailed theory.

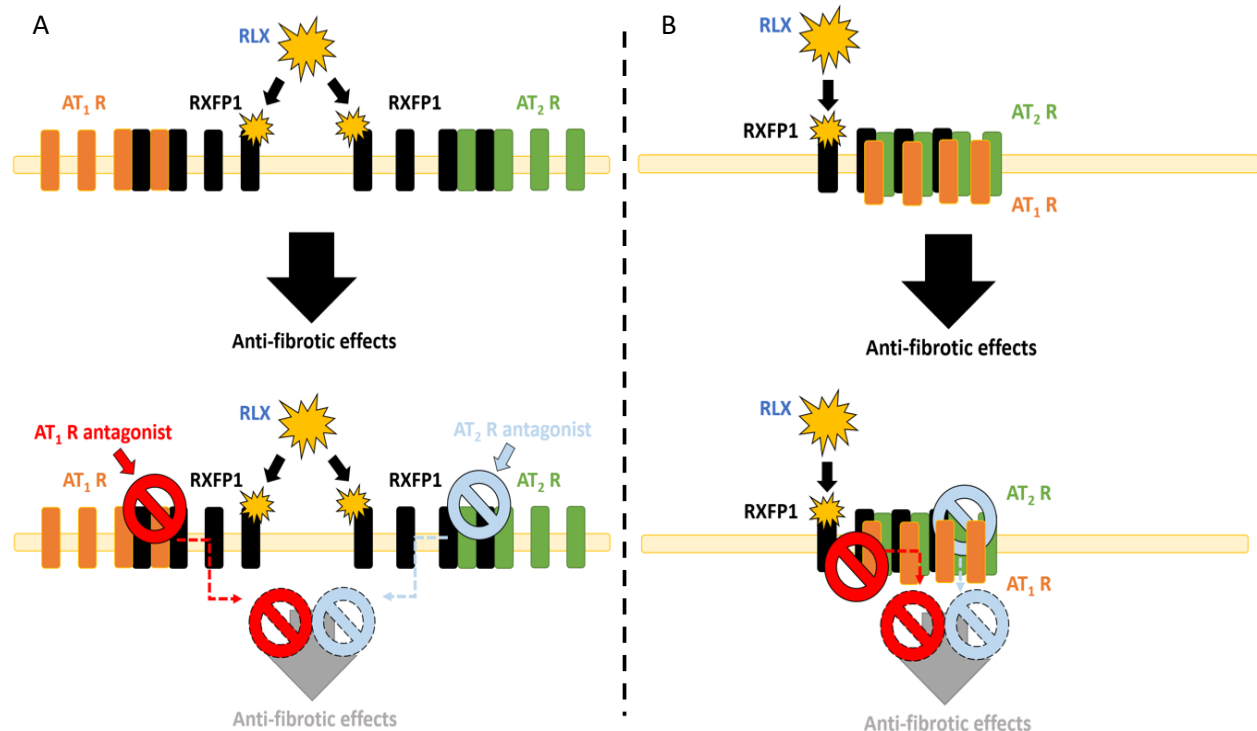


Figure 4.1. Possible interactions between RXFP1, AT1 and AT2 receptors.

The crosstalk between RXFP1-AT₁, RXFP1-AT₂ and AT₁-AT₂ receptors (A) or the direct interaction of these three receptors via heterodimerisation (B) is likely to allow for ARBs (such as CAND) to allosterically block the actions of agonists acting at the RXFP1 (RLX) or AT₂ (CGP) receptors. Hence, combining RLX with ARBs has been found to abrogate the anti-fibrotic actions of RLX alone, suggesting that it would not be clinically be useful to combine RLX with ARBs as treatments for fibrotic diseases.

In conclusion, this study compared and combined the effects of the currently-used ARB, CAND, to emerging therapies such as CGP and RLX. The results obtained demonstrated that both CGP and RLX offered greater renoprotective properties compared to that of CAND alone (at each drug dose administered) in the absence of any effects on blood pressure, with CGP demonstrating marked anti-inflammatory effects and more modest anti-remodelling effects, while RLX demonstrated weak anti-inflammatory effects but strong anti-fibrotic effects. Either way, the ability of either CGP or RLX to reduce total kidney collagen concentration appeared to correlate with their effective ability to normalise HS-induced renal dysfunction. Combining CGP and RLX appeared to feasibly maintain the anti-inflammatory effects of CGP and anti-fibrotic effects of

RLX when added together, and offered greater anti-inflammatory effects to that of RLX alone and greater anti-fibrotic efficacy to that of CGP alone, and also normalised the HS-induced increase in renal dysfunction. However, combining RLX with CAND (or other ARBs for that matter) may not be ideally suited to treating fibrotic disease due to the ability of CAND to allosterically antagonise the anti-fibrotic effects of RLX alone (as outlined in Figure 3.4.1) suggesting no clinical feasibility in combining RLX with ARBs. These studies have provided further insights into the therapeutic potential of CGP and RLX as treatments for kidney disorders and suggest that agonists targeting AT2 or RXFP receptors may offer greater renoprotection and direct anti-fibrotic efficacy compared to drugs that block AT1 receptor activity.

3.5 References

- AbdAlla, S, Lothar, H, Abdel-tawab, AM, Quitterer, U (2001). The angiotensin II AT2 receptor is an AT1 receptor antagonist. *J Biol Chem* **276**: 39721–39726.
- Afsar, B, Afsar, RE, Dagel, T, Kaya, E, Erus, S, Ortiz, A, *et al.* (2018). Capillary rarefaction from the kidney point of view. *Clin. Kidney J.* **11**: 295–301.
- Ahmed, A, Jorna, T, Bhandari, S (2016). Should We STOP Angiotensin Converting Enzyme Inhibitors/Angiotensin Receptor Blockers in Advanced Kidney Disease? *Nephron* **133**: 147–158.
- Arima, S, Ito, S (2000). Angiotensin II type 2 receptors in the kidney : evidence for endothelial-cell-mediated renal vasodilatation. 448–451.
- Battegay, EJ, Miguel, LS de, Petrimpol, M, Humar, R (2007). Effects of anti-hypertensive drugs on vessel rarefaction. *Curr. Opin. Pharmacol.* **7**: 151–157.
- Bennett, RG, Heimann, DG, Singh, S, Simpson, RL, Tuma, DJ (2013). Relaxin decreases the severity of established hepatic fibrosis in mice. *Liver Int.* 416–426.
- Callera, GE, Antunes, TT, Correa, JW, Moorman, D, Gutsol, A, He, Y, *et al.* (2016). Differential renal effects of candesartan at high and ultra-high doses in diabetic mice-potential role of the ACE2/AT2R/Mas axis. *Biosci. Rep.* **36**: e00398–e00398.
- Castoldi, G, Gioia, CRT di, Bombardi, C, Maestroni, S, Carletti, R, Steckelings, UM, *et al.* (2014). Prevention of diabetic nephropathy by compound 21, selective agonist of angiotensin type 2 receptors, in Zucker diabetic fatty rats. *AJP Ren. Physiol.* **307**: F1123–F1131.
- Chen, L, Sha, M, Li, D, Zhu, Y, Wang, X (2017). Relaxin abrogates renal interstitial fibrosis by regulating macrophage polarization via inhibition of Toll-like receptor 4 signaling. *Oncotarget* **8**: 21044–21053.
- Chow, BSM, Chew, EGY, Zhao, C, Bathgate, RAD, Hewitson, TD, Samuel, CS (2012). Relaxin signals through a RXFP1-pERK-nNOS-NO-cGMP-dependent pathway to up-regulate matrix metalloproteinases: The additional involvement of iNOS. *PLoS One* **7**..

Chow, BSM, Kocan, M, Bosnyak, S, Sarwar, M, Wigg, B, Jones, ES, *et al.* (2014). Relaxin requires the angiotensin II type 2 receptor to abrogate renal interstitial fibrosis. *Kidney Int.* **86**: 75–85.

Crowley, SD, Gurley, SB, Herrera, MJ, Ruiz, P, Griffiths, R, Kumar, AP, *et al.* (2006). Angiotensin II causes hypertension and cardiac hypertrophy through its receptors in the kidney. *Proc. Natl. Acad. Sci. U. S. A.* **103**: 17985–17990.

Dézsai, CA (2014). Differences in the clinical effects of angiotensin-converting enzyme inhibitors and angiotensin receptor blockers: A critical review of the evidence. *Am. J. Cardiovasc. Drugs* **14**: 167–173.

Ecelbarger, CM, Rash, A, Sinha, RK, Tiwari, S (2010). The effect of chronic candesartan therapy on the metabolic profile and renal tissue cytokine levels in the obese Zucker rat. *Mediators Inflamm.* **2010**: 841343.

Fallowfield, JA, Hayden, AL, Snowdon, VK, Aucott, RL, Stutchfield, BM, Mole, DJ, *et al.* (2014). Relaxin Modulates Human and Rat Hepatic Myofibroblast Function and Ameliorates Portal Hypertension InVivo. *Hepatology* **59**: 1492–1504.

Gallop, PM, Paz, MA (1975). Posttranslational protein modifications, with special attention to collagen and elastin. *Physiol. Rev.* **55**: 418–487.

Gasparo, M De, Catt, K, Inagami, T, Wright, J, Unger, T (2000). International Union of Pharmacology . XIII . The Angiotensin II Receptors. *Pharmacol. Rev.* **52**: 415–472.

Gelosa, P, Pignieri, A, Fändriks, L, Gasparo, M de, Hallberg, A, Banfi, C, *et al.* (2009). Stimulation of AT2 receptor exerts beneficial effects in stroke-prone rats: focus on renal damage. *J. Hypertens.* **27**: 2444–2451.

Ha, SK (2014). Dietary Salt Intake and Hypertension. *Electrolyte Blood Press* **12**: 7–18.

Heeg, MHJ, Koziolk, MJ, Vasko, R, Schaefer, L, Sharma, K, Müller, GA, *et al.* (2005). The antifibrotic effects of relaxin in human renal fibroblasts are mediated in part by inhibition of the Smad2 pathway. *Kidney Int.* **68**: 96–109.

Hewitson, TD, Ho, WY, Samuel, CS (2010). Antifibrotic Properties of Relaxin : In Vivo Mechanism

of Action in Experimental Renal Tubulointerstitial. *Endocrinology* **151**: 4938–4948.

Hewitson, TD, Mookerjee, I, Masterson, R, Zhao, C, Tregear, GW, Becker, GJ, *et al.* (2007). Endogenous relaxin is a naturally occurring modulator of experimental renal tubulointerstitial fibrosis. *Endocrinology* **148**: 660–669.

Hill, NR, Fatoba, ST, Oke, JL, Hirst, JA, O’Callaghan, CA, Lasserson, DS, *et al.* (2016). Global Prevalence of Chronic Kidney Disease – A Systematic Review and Meta-Analysis. *PLoS One* **11**: e0158765.

Hou, FF, Zhou, QG (2010). Optimal dose of angiotensin-converting enzyme inhibitor or angiotensin II receptor blocker for renoprotection. *Nephrology* **15**: 57–60.

Imig, JD, Ryan, MJ (2013). Immune and inflammatory role in renal disease. *Compr. Physiol.* **3**: 957–976.

Ina, Y, Yao, K, Ohno, T, Suzuki, K, Sonoka, R, Sato, H (2004). Effects of Benidipine and Candesartan on Kidney and Vascular Function in Hypertensive Dahl Rats. *Hypertens. Res.* **26**: 569–576.

Kitayama, H, Maeshima, Y, Takazawa, Y, Yamamoto, Y, Wu, Y, Ichinose, K, *et al.* (2006). Regulation of Angiogenic Factors in Angiotensin II Infusion Model in Association With Tubulointerstitial Injuries. *Am. J. Hypertens.* **19**: 718–727.

Kljajic, ST, Vinh, A, Welungoda, I, Bosnyak, S, Jones, ES, Gaspari, TA, *et al.* (2013). Direct AT2 receptor stimulation is athero-protective and stabilizes plaque in Apolipoprotein E-deficient mice. *Int. J. Cardiol.* **169**: 281–287.

las Heras, N De, Ruiz-Ortega, M, Ruperez, M, Sanz-Rosa, D, Miana, M, Aragoncillo, P, *et al.* (2006). Role of connective tissue growth factor in vascular and renal damage associated with hypertension in rats. Interactions with angiotensin II. *J. Renin Angiotensin Aldosterone Syst.* **7**: 192–200.

Liang, B, Leenen, FHH (2008). Prevention of salt-induced hypertension and fibrosis by AT 1-receptor blockers in Dahl S rats. *J. Cardiovasc. Pharmacol.* **51**: 457–466.

Maric, C, Sandberg, K, Hinojosa-Laborde, C (2004). Glomerulosclerosis and tubulointerstitial fibrosis are attenuated with 17 β -estradiol in the aging Dahl salt sensitive rat. *J. Am. Soc. Nephrol.* **15**: 1546–1556.

Masini, E, Nistri, S, Vannacci, A, Bani Sacchi, T, Novelli, A, Bani, D (2004). Relaxin inhibits the activation of human neutrophils: involvement of the nitric oxide pathway. *Endocrinology* **145**: 1106–12.

Matavelli, L, Huang, J, Siragy, H (2011). Angiotensin AT₂ Receptor Stimulation Inhibits Early Renal Inflammation in Renovascular Hypertension. *Hypertension* **57**: 308–313.

Miura, S, Matsuo, Y, Kiya, Y, Karnik, SS, Saku, K (2010). Molecular mechanisms of the antagonistic action between AT₁ and AT₂ receptors. *Biochem. Biophys. Res. Commun.* **391**: 85–90.

Mookerjee, I, Hewitson, TD, Halls, ML, Summers, RJ, Mathai, ML, Bathgate, R a D, *et al.* (2009). Relaxin inhibits renal myofibroblast differentiation via RXFP1, the nitric oxide pathway, and Smad2. *FASEB J.* **23**: 1219–29.

Namsolleck, P, Recarti, C, Foulquier, S, Steckelings, UM, Unger, T (2014). AT₂ receptor and tissue injury: therapeutic implications. *Curr. Hypertens. Rep.* **16**: 416.

National Health and Medical Research Council (2017). Sodium. *Nutr. Ref. Values Aust. New Zeal. Incl. Recomm. Diet. Intakes* 210–216.

Ng, HH, Shen, M, Samuel, CS, Schlossmann, J, Bennett, RG (2019). Relaxin and extracellular matrix remodeling: Mechanisms and signaling pathways. *Mol. Cell. Endocrinol.* **487**: 59–65.

Nishiyama, A, Yoshizumi, M, Rahman, M, Kobori, H, Seth, DM, Miyatake, A, *et al.* (2004). Effects of AT₁ receptor blockade on renal injury and mitogen-activated protein activity in Dahl salt-sensitive rats. *Kidney Int.* **65**: 972–981.

Nistri, S, Cinci, L, Perna, AM, Masini, E, Mastroianni, R, Bani, D (2008). Relaxin induces mast cell inhibition and reduces ventricular arrhythmias in a swine model of acute myocardial infarction. *Pharmacol. Res.* **57**: 43–48.

Noda, M, Matsuo, T, Fukuda, R, Ohta, M, Nagano, H, Shibouta, Y, *et al.* (1999). Effect of candesartan cilexetil (TCV-116) in rats with chronic renal failure. *Kidney Int.* **56**: 898–909.

Patel, KP, Giraud, AS, Samuel, CS, Royce, SG (2016). Combining an epithelial repair factor and anti-fibrotic with a corticosteroid offers optimal treatment for allergic airways disease. *Br. J. Pharmacol.* **173**: 2016–2029.

Rafiq, K, Nishiyama, A, Konishi, Y, Morikawa, T, Kitabayashi, C, Kohno, M, *et al.* (2014). Regression of glomerular and tubulointerstitial injuries by dietary salt reduction with combination therapy of angiotensin II receptor blocker and calcium channel blocker in Dahl salt-sensitive rats. *PLoS One* **9**:

Rehman, A, Leibowitz, A, Yamamoto, N, Rautureau, Y, Paradis, P, Schiffrin, E (2012). Angiotensin type 2 receptor agonist compound 21 reduces vascular injury and myocardial fibrosis in stroke-prone spontaneously hypertensive rats. *Hypertension* **59**: 291–299.

Rompe, F, Artuc, M, Hallberg, A, Alterman, M, Str??der, K, Th??ne-Reineke, C, *et al.* (2010). Direct angiotensin II type 2 receptor stimulation acts anti-inflammatory through epoxyeicosatrienoic acid and inhibition of nuclear factor ??b. *Hypertension* **55**: 924–931.

Royce, SG, Patel, KP, Mao, W, Zhu, D, Lim, R, Samuel, CS (2019). *Serelaxin enhances the therapeutic effects of human amnion epithelial cell-derived exosomes in experimental models of lung disease.*

Royce, SG, Shen, M, Patel, KP, Huuskes, BM, Ricardo, SD, Samuel, CS (2015). Mesenchymal stem cells and serelaxin synergistically abrogate established airway fibrosis in an experimental model of chronic allergic airways disease. *Stem Cell Res.* **15**: 495–505.

Royce, SG, Tominaga, AM, Shen, M, Patel, KP, Huuskes, BM, Lim, R, *et al.* (2016). Serelaxin improves the therapeutic efficacy of RXFP1-expressing human amnion epithelial cells in experimental allergic airway disease. *Clin. Sci.* **130**: 2151–2165.

Samuel, C, Hewitson, T (2007). Drugs of the future: the hormone relaxin. *Cell. Mol. Life Sci.* **64**: 1539–1557.

Samuel, CS (2009). Determination of Collagen Content, Concentration, and Sub-types in Kidney Tissue. In Kidney Research. Methods in Molecular Biology (Methods and Protocols), G. Becker, and T.D. Hewitson, eds. (Humana Press), p.

Samuel, CS, Bodaragama, H, Chew, JY, Widdop, RE, Royce, SG, Hewitson, TD (2014). Serelaxin is a more efficacious antifibrotic than enalapril in an experimental model of heart disease. *Hypertension* **64**: 315–322.

Samuel, CS, Cendrawan, S, Gao, X-M, Ming, Z, Zhao, C, Kiriazis, H, *et al.* (2011). Relaxin remodels fibrotic healing following myocardial infarction. *Lab. Invest.* **91**: 675–90.

Samuel, CS, Hewitson, TD, Unemori, EN, Tang, ML-K (2007). Drugs of the future: the hormone relaxin. *Cell. Mol. Life Sci.* **64**: 1539–57.

Samuel, CS, Royce, SG, Hewitson, TD, Denton, KM, Cooney, TE, Bennett, RG (2017). Anti-fibrotic actions of relaxin. *Br. J. Pharmacol.* **174**: 962–976.

Samuel, CS, Summers, RJ, Hewitson, TD (2016). Antifibrotic Actions of Serelaxin - New Roles for an Old Player. *Trends Pharmacol. Sci.* **37**: 485–497.

Schelbert, EB, Fonarow, GC, Bonow, RO, Butler, J, Gheorghiade, M (2014). Therapeutic targets in heart failure: Refocusing on the myocardial interstitium. *J. Am. Coll. Cardiol.* **63**: 2188–2198.

Seyedi, N, Xu, X, Nasjletti, A, Hintze, T (1995). Coronary kinin generation mediates nitric oxide release after angiotensin receptor stimulation. *Hypertension* **26**: 164.

Shihab, FS (2007). Do we have a pill for renal fibrosis? *Clin. J. Am. Soc. Nephrol.* **2**: 876–878.

Sumners, C, Augusto Peluso, A, Houe Hausgaard, A, Bertelsen, J, Steckelings, U (2019). Anti-fibrotic mechanisms of angiotensin AT2-receptor stimulation. *Acta Physiol.* e13280.

Tang, MLK, Samuel, CS, Royce, SG (2009). Role of relaxin in regulation of fibrosis in the lung. *Ann. N. Y. Acad. Sci.* **1160**: 342–7.

Uneimori, E, Lewis, M, Constant, J, Arnold, G, Grove, G, Normand, J, *et al.* (2000). Relaxin induces vascular endothelial growth factor expression and angiogenesis selectively at wound

sites. *Wound Repair Regen.* **8**: 367–370.

Unemori, EN, Amento, EP (1990). Relaxin Modulates Synthesis and Secretion of Procollagenase Collagen by Human Dermal Fibroblasts. *J. Biol. Chem.* **265**: 10661–10665.

Wan, Y, Wallinder, C, Plouffe, B, Pettersson, A, Nyberg, F (2004). Design , Synthesis , and Biological Evaluation of the First Selective Nonpeptide AT 2 Receptor Agonist. *J. Med. Chem.* **47**: 5995–6008.

Wang, C, Kemp-Harper, BK, Kocan, M, Ang, SY, Hewitson, TD, Samuel, CS (2016). The anti-fibrotic actions of relaxin are mediated through a NO-sGC-cGMP-dependent pathway in renal myofibroblasts in vitro and enhanced by the NO donor, diethylamine NONOate. *Front. Pharmacol.* **7**: 1–12.

Wang, D, Luo, Y, Myakala, K, Orlicky, DJ, Dobrinskikh, E, Wang, X, *et al.* (2017). Serelaxin improves cardiac and renal function in DOCA-salt hypertensive rats. *Sci. Rep.* **7**: 9793.

Wetzel, V, Schinner, E, Kees, F, Hofmann, F, Faerber, L, Schlossmann, J (2016). Involvement of cyclic guanosine monophosphate-dependent protein kinase I in renal antifibrotic effects of serelaxin. *Front. Pharmacol.* **7**: 1–13.

Whitebread, S (1989). Preliminary biochemical characterization of two angiotensin II receptor subtypes. *Biochem. Biophys. Res. Commun.* **163**: 284–291.

Woessner Jr, J (1995). Quantification of matrix metalloproteinases in tissue samples. *Methods Enzym.* **248**: 510–52.

Yao, K, Sato, H, Ina, Y, Suzuki, K, Ohno, T, Shirakura, S (2004). Renoprotective Effects of Benidipine in Combination with Angiotensin II Type 1 Receptor Blocker in Hypertensive Dahl Rats. *Hypertens. Res.* **26**: 635–641.

Yu, H, Burrell, L, Black, MJ, Wu, LL, Dilley, RJ, Cooper, ME, *et al.* (1998). Salt Induces Myocardial and Renal Fibrosis in Normotensive and Hypertensive Rats. *Circulation* **98**: 2621–2628.

Chapter 4

**TO COMPARE AND COMBINE THE ANTI-FIBROTIC EFFECTS OF RELAXIN
TO AN ACEI (PERINDOPRIL) AND AN IRAP INHIBITOR (HFI-419) IN THE
HIGH SALT-INDUCED MURINE MODEL OF KIDNEY DISEASE.**

4.1. Introduction

Chronic kidney disease (CKD) is a widespread clinical problem which encompasses various aetiologies that can progress to end-stage renal failure (ESRF). Globally, CKD has had an 82% increase in incident rates within the past two decades and is primarily attributed to the rise in our population that are affected by diabetes and hypertension (Lozano *et al.*, 2012). Aside from the aforementioned risk factors, dietary factors especially involving the increase in sodium chloride consumption within the Western diet has also contributed to the significant rise in CKD (Weir and Fink, 2005). Often CKD results from the establishment of fibrosis with accompanied cardiovascular complications leading to renal dysfunction and eventually, ESRF if left untreated (Hill *et al.*, 2016). Histologically, CKD exhibits as glomerulosclerosis, vascular sclerosis, and tubulointerstitial fibrosis caused by an excessive accumulation of extracellular matrix (ECM) components, mainly consisting of collagen (Anders *et al.*, 2003). This increase in ECM deposition followed by inhibited breakdown ultimately leads to glomerular loss, tubular atrophy, capillary reduction and podocyte depletion; subsequently resulting in reduced renal function and eventual renal failure (Bohle *et al.*, 1987; Edwards *et al.*, 2015; Longo *et al.*, 2015). Despite CKD being prevalent, therapeutic options for the treatment of the fibrosis that contributes to disease progression are limited. As discussed in Chapter 3, currently-available treatments target the symptoms associated with CKD rather than ECM accumulation itself. For example, angiotensin-converting enzyme inhibitors (ACEi) and angiotensin receptor blockers (ARBs) mainly act to lower hypertension and the impact of hypertension on aberrant ECM accumulation, while growth factor inhibitors such as pirfenidone, act to block the actions of specific factors that promote ECM-producing cells to secrete ECM molecules (Shihab, 2007). However, due to the indirect nature of these therapies, their chronic use or administration at high doses often results in reduced efficacy and several side-effects (Dézsi, 2014; Schelbert *et al.*, 2014). Therefore, novel treatments that more directly target ECM/collagen accumulation or stimulate the rapid degradation of existing ECM components contributing to fibrosis are urgently required.

One novel treatment that meets the above-mentioned criteria is serelaxin (RLX), the drug-based form of the major stored and circulating form of the peptide hormone, H2 relaxin (as investigated in Chapter 3). RLX mediates rapidly-occurring anti-fibrotic actions through its cognate G protein-

coupled receptor, RXFP1, to inhibit TGF- β 1-, IL-1 β - and/or angiotensin (Ang) II-induced fibroblast proliferation and differentiation into myofibroblasts which results in the reduction of myofibroblast-induced collagen production (reviewed in (Samuel *et al.*, 2017)). RLX limits fibrosis in two ways: 1) it reduces myofibroblast-induced ECM synthesis via RXFP1-ERK1/2 phosphorylation-nNOS-NO-sGC-cGMP-dependent pathway to inhibit TGF- β 1 signal transduction at the level of intracellular Smad2 phosphorylation (Mookerjee *et al.*, 2009; Chow *et al.*, 2012, 2014; Wang *et al.*, 2016). 2) The ability of RLX to inhibit the TGF- β 1/Smad2 axis also results in its ability to up-regulate various collagen-degrading MMPs (such as MMP-1/-13, MMP-2 and MMP-9) to facilitate the breakdown of existing ECM components (Chow *et al.*, 2012). Given that RLX demonstrated greater anti-fibrotic efficacy to the ARB, Candesartan and broader anti-fibrotic efficacy to the AT2R agonist, CGP42112, against HS-induced renal pathology, its anti-fibrotic effects were further evaluated against a recently-developed inhibitor of insulin-regulated aminopeptidase (IRAP) activity in this Chapter.

IRAP is a single transmembrane integral protein comprising of 916 amino acids, and contains an extracellular aminopeptidase catalytic site (Albiston *et al.*, 2001). IRAP is expressed on inflammatory cells and in organs including kidneys, adrenal glands, cardiac muscle and the placenta (Chai *et al.*, 2004; Saveanu and Van Endert, 2012). More recently, unpublished findings have determined that IRAP is also expressed on myofibroblasts and up-regulated in the ageing and diseased murine heart and kidney (personal communication; Huey Wen Lee, Tracey Gaspari and Robert Widdop, Monash Pharmacology); suggesting that IRAP may be a previously unrecognised contributor to disease-induced fibrosis and end-organ damage. IRAP is known to break down several substrates including lys-bradykinin, vasopressin, oxytocin, and Ang III, all of which have some form of organ-protective and anti-fibrotic properties (Kakoki *et al.*, 2007; Albiston *et al.*, 2010; Plante *et al.*, 2015). The endogenous inhibitor of IRAP is Ang IV, which prevents the degradation of these substrates. However, due to its low specificity and stability, Ang IV is limited in its therapeutic use. Thus, the synthetic small molecule non-peptide IRAP inhibitor, HFI-419 was developed (Albiston *et al.*, 2008). Unsurprisingly, HFI-419 showed similar results to those following Ang IV treatment, and demonstrated significant effects in reducing cardiac, renal and hepatic fibrosis (Chai *et al.*, 2017). Specifically, the patent highlights the

reduction in fibrosis in ageing- and Ang II-induced mouse models of kidney damage (Chai *et al.*, 2017). Hence, these findings highlight the therapeutic potential of using HFI-419 to treat CKD.

In this Chapter, the anti-fibrotic effects of RLX were compared to that of HFI-419 (HFI), candesartan cilexetil (CAND), and the clinically-used ACE-inhibitor, perindopril (PERIN), in the HS-induced model of renal disease; but using a different strain of mice. To further evaluate the therapeutic potential of HFI, its anti-fibrotic and reno-protective effects were also combined with RLX, CAND and PERIN in the model studied.

4.2. Materials and methods

Materials

Recombinant H2 Relaxin (serelaxin; was kindly provided by Corthera Inc (San Carlos, CA, USA; a subsidiary of Novartis AG, Basel, Switzerland); candesartan cilexetil was a gift from AstraZeneca (Södertälje, Sweden); Perindopril was purchased from LabChem Express (Zelienople, Pam USA); while HFI-419 was kindly provided by A/Prof. Siew Yeen Chai (Department of Physiology, Monash University).

4.2.1 Animals

6 to 8-week-old male C57BL/6J mice were obtained from Monash Animal Services (Monash University, Clayton, Victoria, Australia) and housed under a controlled environment, on a 12 hour light/12 hour dark lighting cycle with tap water provided *ad libitum* throughout the experiment and diet initially maintained on normal lab chow (Barastock Stockfeeds, Pakenham, Victoria, Australia). FVB/N mice were used in Chapter 3, as they are the background that AT2R knockout mice were established on (to further validate the effects of CGP42112 if required). However, as AT2R agonists were not studied in this Chapter, C57B6J mice were used instead. All mice were provided an acclimatisation period of at least 5 days before any experimentation and procedures were performed. All animal use and procedures were approved by a Monash University Animal Ethics Committee (Ethics number: MARP/2013/118), which complies with the Australian Guidelines for the Care and Use of Laboratory Animals for Scientific Purposes.

4.2.2 Experimental design

Mice were divided into 9 treatment groups with n=6 animals per group. These groups consisted of i) mice fed a normal salt (NS; 0.5% NaCl) diet (negative control) for 8 weeks; ii) mice fed a high salt (HS; 5% NaCl) diet (positive control; Barastock Stockfeeds, Pakenham, Victoria, Australia) for 8 weeks; iii) HS+CAND-treated group; iv) HS+PERIN-treated group; v) HS+RLX-treated group; vi) HS+HFI-treated group; vii) HS+ HFI+CAND-treated group; viii) HS+HFI+PERIN-treated group; and ix) HS+HFI+RLX-treated group. All HS-diet fed groups were provided with NaCl lab chow containing 5% NaCl after the acclimatisation period ended; which was expected to induce renal injury in the absence of any overt changes in blood pressure. After the completion of 4 weeks on

the HS diet, two sub-group of mice were given either candesartan cilexetil (2mg/kg/d) or perindopril (4mg/kg/d), which was delivered to each mouse via drinking water and adjusted to daily body weight from weeks 5-8. This dose of the ARB was chosen based on results obtained on Chapter 3, also noting that a previous study showed that CAND (at 1mg/kg/day) could inhibit renal fibrosis after 4 weeks of treatment, in rats (Noda *et al.*, 1999). The dose of the ACEi used was chosen based on previous study showing 4mg/kg/d demonstrated protective effects in the brain and kidneys of stroke-prone spontaneously hypertensive rats (Wang *et al.*, 1997). Separate sub-group of mice were administered RLX as per Chapter 3 ((0.5mg/kg/d; a dose that had consistently demonstrated anti-fibrotic effects in other murine models of renal fibrosis; (Hewitson *et al.*, 2010; Chow *et al.*, 2014; Wetzl *et al.*, 2016)) or HFI (0.72 mg/kg/d; a dose that demonstrated reduced heart fibrosis in aged mice (Chai *et al.*, 2017)). RLX or HFI were administered via subcutaneously implanted osmotic mini-pumps (model 2004, Alzet, Cupertino, CA, USA; which continuously infused each drug into the circulation of treated mice at a flow rate of 0.25µl/hour, from weeks 5-8) (see Figure 4.2.2.1). Three additional sub-groups of mice were administered HFI (0.72mg/kg/day; via osmotic mini-pumps) with CAND (2mg/kg/day; via drinking water), HFI with PERIN (4mg/kg/day; via drinking water); or HFI with RLX (0.5mg/kg/day; both via osmotic mini-pumps (see Figure 4.2.2.1). Systolic blood pressure (SBP) was measured via tail-cuff plethysmography every 2 weeks from week 0 until week 8.

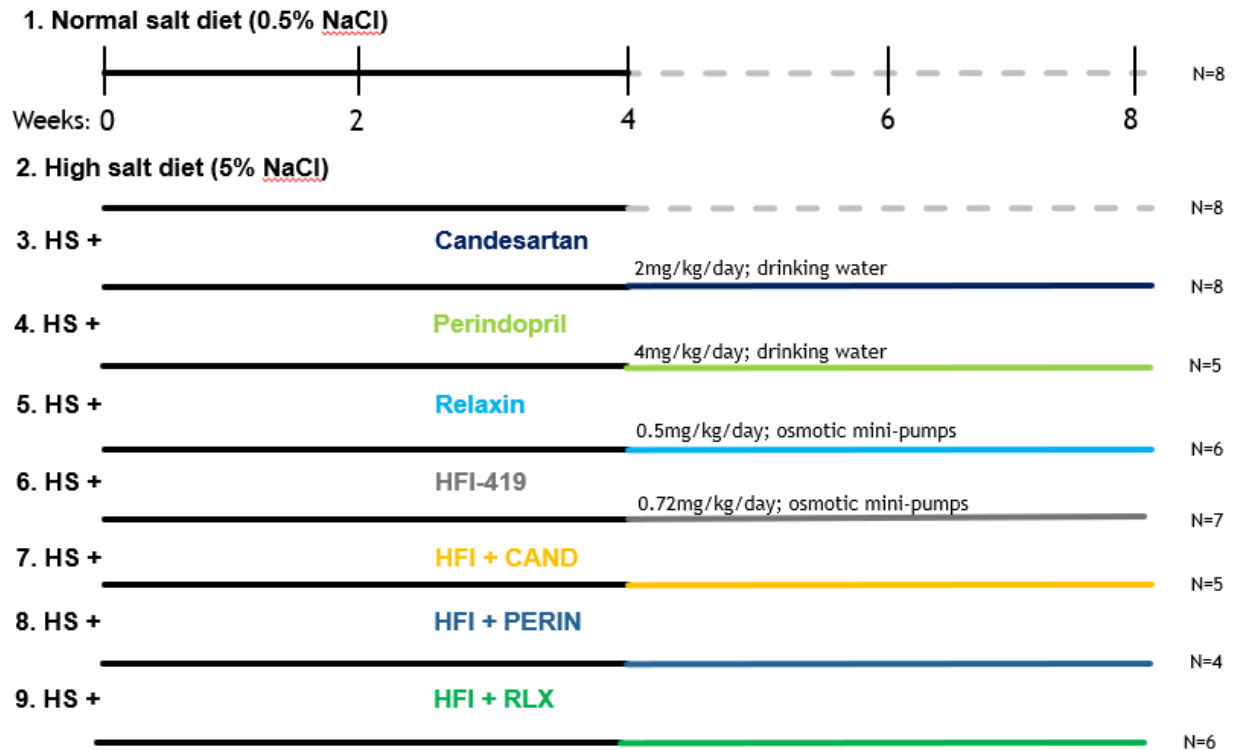


Figure 4.2.2.1. Experimental design for the 8-week high salt diet model

Mice were randomised into 9 treatment groups. Group 1 was fed 0.5% NaCl normal lab chow for the 8-week duration. The remaining groups received 5% NaCl high salt lab chow for the 8-week duration. Group 2 remained on a constant high salt diet for 8 weeks. While groups 3 to 9 were provided with the selected treatments at the end of week 4. By week 8, mice were culled, and kidneys were taken for analysis.

4.2.3 Tissue collection

After 8 weeks of NS or HS feeding, all mice were killed by anaesthetic overdose, and blood was collected by cardiac puncture and spun down for plasma collection, which was subsequently stored at -80°C. Each kidney was then isolated and divided in half to obtain a total of 4 portions (2 from each kidney). One half was fixed in 10% neutral buffered formaldehyde overnight and processed by Monash Histology Services to be cut and embedded in paraffin wax. Another half was embedded in a cryomold filled with OCT, frozen in liquid nitrogen and stored at -80°C, until required. The other 2 portions were snap-frozen in liquid nitrogen and stored at -80°C for hydroxyproline analysis and extraction of proteins for gelatin zymography and Western blotting.

4.2.4 Kidney histopathology

Serial paraffin-embedded kidney sections (5µm thickness) from each mouse were placed on Superfrost® Plus slides (Thermo Scientific, Rockford, IL, USA) for histological and immunohistochemical staining. To assess glomerulosclerosis and interstitial collagen deposition, one section from each mouse was sent to Monash Histology Services and underwent Masson's trichrome staining.

4.2.5 Immunohistochemistry and Immunofluorescence

Immunohistochemistry (IHC) and immunofluorescence (IF) were used to detect markers of renal inflammation and fibrosis, inclusive of macrophage infiltration, NF-κB activity, α-smooth muscle actin (α-SMA; a marker of myofibroblast differentiation) CD31 (a marker for vascular rarefaction of the peritubular capillaries), and TIMP-1 levels. In each case, serial sections from each mouse were subjected to either a biotinylated monoclonal anti-human SMA (1:200 dilution; M0851, DAKO Corp., Carpinteria, CA, USA), polyclonal anti-rabbit CD31 (1:100 dilution; ab28364, Abcam, Cambridge, UK) or polyclonal anti-rabbit TIMP-1 (1:1000; Ab38978, Abcam, Cambridge, UK) primary antibody for IHC-staining of these markers and DAKO anti-mouse or anti-rabbit HRP kits containing appropriate secondary antibodies. IHC-stained sections were visualised with the avidin-biotin complex (ABC Elite; Vector, Burlingame, CA, USA) and 3,30-diaminobenzidine (DAB; Sigma-Aldrich). Frozen sections from each mouse were subjected to either a monoclonal anti-rat F4/80 (1:200 dilution; MCA497R, Bio-Rad Laboratories, Richmond, CA, USA), or a polyclonal anti-rabbit p-IκB primary antibody (1:50; #28595S, Cell Signalling, Massachusetts, USA) and goat anti-rat Alexa Fluor 488 IgG secondary antibody (A11006, Life Technologies, CA, USA) for IF-staining of the two markers.

4.2.6 Morphometric analysis

All kidney sections were scanned, captured and viewed under Monash Histology Service's Aperio Scanscope AT Turbo (Leica Microsystems Pty Ltd, VIC, Australia) or with a confocal microscope (Olympus, BX51, USA) at x20-x40 magnification for morphometric analysis of Masson's trichrome, IHC or IF-labelled tissue images. For each tissue section, 6-8 non-overlapping sections per mice were single-blinded and randomly selected. For each image, aside from glomerulosclerosis score,

the percentage of positively-stained areas was quantified with ImageJ 1.48 software (Java, NIH); and expressed as the % staining per field analysed.

4.2.7 Hydroxyproline assay

One half of the frozen kidney from each mouse was lyophilized to dry weight, hydrolysed in 6mmol/l hydrochloric acid as described previously (Mookerjee *et al.*, 2009; Samuel, 2009) for the measurement of hydroxyproline content, which was determined from a standard curve of purified trans-4-hydroxy-L-proline (Sigma-Aldrich). Hydroxyproline values were multiplied by a factor of 6.94 based on hydroxyproline representing ~14.4% of the amino acid composition of collagen in most mammalian tissues to extrapolate total collagen content (Gallop and Paz, 1975), which in turn was divided by the dry weight of each corresponding tissue to yield collagen concentration (expressed as a percentage).

4.2.8 Gelatin zymography

To determine if the treatment-induced effects on collagen deposition were mediated via their ability to regulate MMPs/gelatinases that are known to induce collagen degradation, gelatin zymography was performed on kidney protein extracts, which were isolated using the method of Woessner (Woessner Jr, 1995) and assessed for changes in expression and activity of MMP-2 (gelatinase-A). Equal aliquots of the protein extracts were analysed on zymogram gels consisting of 7.5% acrylamide and 1 mg/ml gelatin. The gels were subsequently treated as previously detailed (Woessner, 1995). Gelatinolytic activity was identified by clear bands at the appropriate molecular weight, quantitated by densitometry and the relative optical density (OD) of MMP-2 in each group expressed as the respective ratio to that in the NS-fed control group, which was expressed as 1.

4.2.9 Western blotting

Using the protein extracts obtained for gelatin zymography, equivalent sample proteins (10µg) were separated on pre-cast 10% SDS-polyacrylamide separating gels (Bio-Rad, Philadelphia, PA, USA) and transferred to PVDF membranes using the Bio-Rad Trans-Blot Turbo transfer system (Bio-Rad, Philadelphia, PA, USA). Membranes were then blocked for 1 hour with 5% (w/v) skim milk powder and then probed with primary rabbit TIMP-1 (1:1000 dilution; ab38978, Abcam) or

TGF- β 1 (1:1000 dilution; ab92486, Abcam) for at least 16 hours at 4°C. Subsequently, the membranes were then probed with a conjugated anti-rabbit secondary antibody (1:2500 dilution; DAKO). Membranes were then developed with the Bio-Rad Clarity Western ECL substrate kit (Bio-Rad) for 5 min according to the manufacturer's protocol followed by visualisation and imaging using the Bio-rad ChemicDoc MP. The optical density (OD) of the appropriate bands were then quantified and analysed using Image Lab software (Bio-Rad). The measured density of TIMP-1 and TGF- β 1 bands were then corrected to the density of alpha-tubulin in each sample and was then expressed as the relative ratio from the NS-fed control group, which was expressed as 1.

4.2.10 Plasma urea

Plasma samples from each mouse, obtained from the cardiac puncture of mice were thawed before 100 μ l of each sample was transferred onto Chem8+ cartridges to be inserted and rapidly measured by the i-STAT point-of-care handheld device (Abbott Laboratories, Illinois, USA). Plasma urea was then recorded as mmol/L.

4.2.11 Statistical analysis

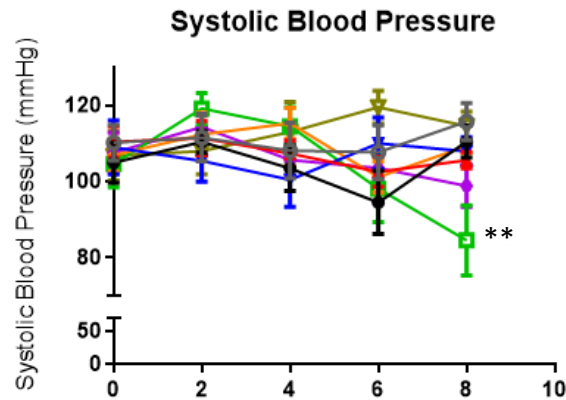
All statistical analysis was performed using GraphPad Prism v7.0 (Graphpad Software Inc., CA, USA) and expressed as mean \pm SEM. Data were analysed via one-way ANOVA with Neuman-Kuels post-hoc test for multiple comparisons between groups. In each case, data were considered significant with a p-value less than 0.05.

4.3. Results

4.3.1 The effects of HS and the treatments investigated on systolic blood pressure and body weight.

Blood pressure was measured fortnightly via tail-cuff plethysmography in each sub-group of mice, from weeks 0-8 (Figure 4.3.1). Mice fed a HS diet had similar SBP measurements (of around 100-120mmHg) throughout the 8 week experimental period, to that measured from mice fed a NS diet, confirming that mice fed a diet of 5% NaCl did not undergo hypertension in this strain. Mice that received CAND alone, RLX alone, HFI alone or the three combination therapies also maintained normotensive SBP levels. In contrast, PERIN treatment alone significantly lowered SBP to around 85mmHg after 4 weeks of treatment ($P<0.01$ vs NS group; Figure 4.3.1A). Body weight was measured before the introduction of diet at week 0, pre-treatment at week 4 and at the end of treatment at week 8. Mice fed a NS or HS diet maintained similar body weights of 32-35g throughout the 8 week experimental period (Figure 4.3.1B). Although some treatments such as CAND alone or the combined effects of HFI+PERIN induced a trend towards mice having lower body weights after 4 weeks of treatment (at week 8), in general there were no significant differences in the body weights of NS- and HS-fed mice and HS-fed mice treated with CAND alone, RLX alone, HFI alone, HFI+CAND, HFI+PERIN and HFI+RLX; which maintained body weight of 29-35g from weeks 5-8. Once again, only PERIN-treatment alone significantly lowered the body weight of treated mice to around 22g after 4 weeks of treatment, which was significantly lower than mice receiving the HS diet alone ($P<0.01$ vs HS group; Figure 4.3.1B). These findings suggested that PERIN administration was inducing hypotension and weight loss at the dose studied, when administered to normotensive mice. Interestingly though, the data presented suggested that combining PERIN with HFI ameliorated the PERIN-induced reduction of SBP and loss of body weight; indicating that HFI could counteract the detrimental effects of PERIN administration alone.

A



B

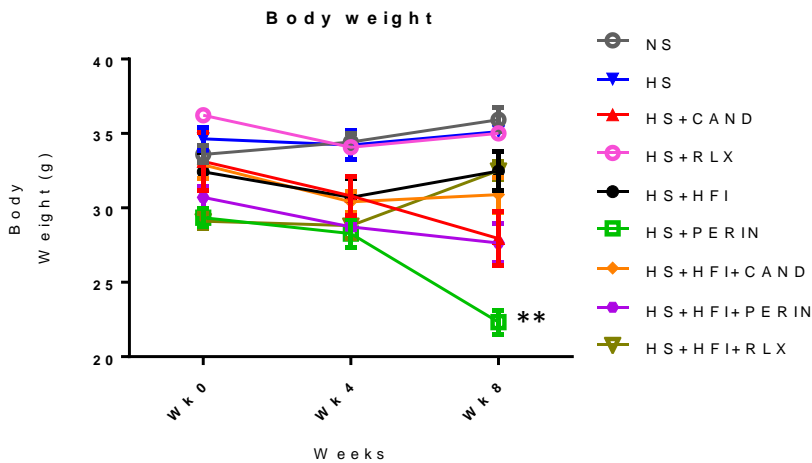


Figure 4.3.1. The effects of HS and the treatments investigated on systolic blood pressure (SBP) and body weight.

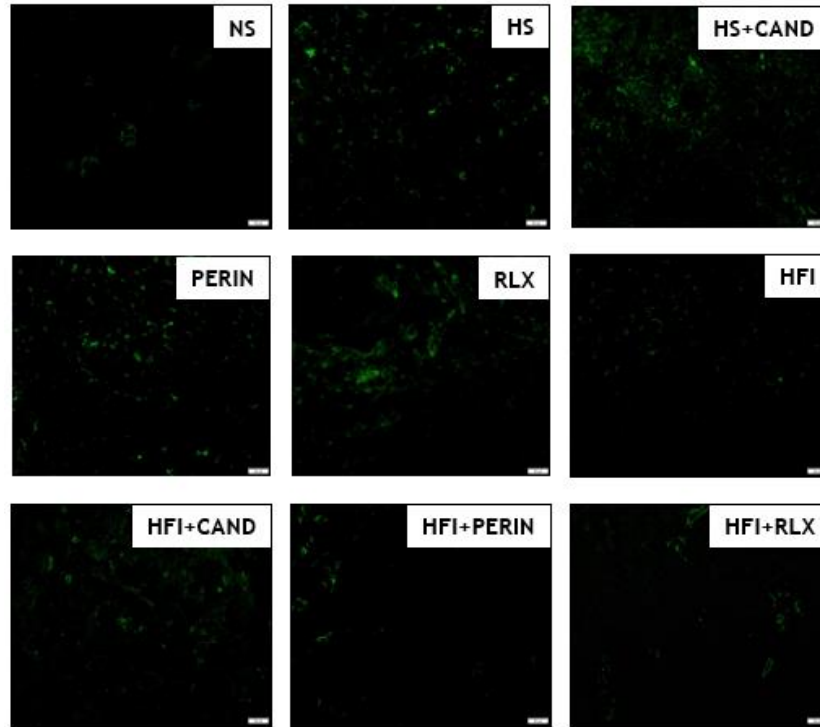
A) Fortnightly mean \pm SEM SBP measurements from mice fed a NS (0.5% NaCl) or HS (5% NaCl) fed diet over 8 weeks, and from HS-fed mice treated with CAND, PERIN, RLX or HFI alone, HFI+CAND, HFI+PERIN or HFI+RLX over the final 4 weeks of the 8-week model; as determined by tail cuff plethysmography. Only mice treated with PERIN alone significantly lowered SBP over the 4 weeks of treatment; suggesting that the ACEi was inducing hypotension when administered to a normotensive model. **B)** Mean \pm SEM body weight (g) measurements from each group measured before diet at week 0, before treatment at week 4, and after treatment at week 8. Only mice treated with PERIN alone significantly lowered body weight by the end of treatment period. ** $P < 0.01$ vs NS group.

4.3.2 The effects of HS and the treatments investigated on measures of renal inflammation.

F4/80-stained macrophage infiltration (Figure 4.3.2) and P- $\text{i}\kappa\text{B}$ staining (used as a surrogate marker of NF- κB activity; Figure 4.3.3) were both significantly increased in HS-fed mice (by ~ 3.9 -fold and ~ 3.6 -fold, respectively; both $P < 0.001$ vs NS group) compared to respective measurements obtained from NS-fed controls. This indicated that HS (5% NaCl)-feeding led to renal inflammation after 8 weeks. Whereas neither CAND, PERIN nor RLX treatment alone affected the HS-increased macrophage infiltration (Figure 4.3.2), CAND was able to partially reduce P- $\text{i}\kappa\text{B}$ expression levels (by $\sim 54\%$; $p < 0.01$ vs HS group, $p < 0.01$ vs NS group), while PERIN and RLX were able to almost fully reduce the HS-increase in P- $\text{i}\kappa\text{B}$ levels (by 80-85%; both $p < 0.001$ vs HS group, no different to NS group; Figure 4.3.3) after 4 weeks of treatment.

In comparison, HFI alone or in combination with all other treatments (HFI+CAND, HFI+PERIN, HFI+RLX) significantly reduced both F4/80 staining (by ~ 56 -88%; all $P < 0.001$ vs HS group; only HFI+CAND was $p < 0.05$ vs NS group; Figure 4.3.2), as well as P- $\text{i}\kappa\text{B}$ staining (by ~ 73 -92%; all $P < 0.001$ vs HS group; both HFI+CAND and HFI+PERIN $p < 0.05$ vs NS group; Figure 4.3.3) after 4 weeks of treatment. HFI or HFI+RLX treatment also significantly reduced macrophage infiltration to a greater extent than HFI+CAND (by an additional 20-30%; both $P < 0.05$ vs HFI+CAND group) to measurements that were seen from mice fed a NS-diet. In addition, PERIN, RLX, HFI, and HFI+RLX treatment of HS-fed mice fully reduced P- $\text{i}\kappa\text{B}$ staining levels back to that measured from mice on the NS diet. These findings suggested that HFI alone or its combined effects with RLX offered optimal protection against HS-induced macrophage infiltration and $\text{i}\kappa\text{B}$ expression.

A



B

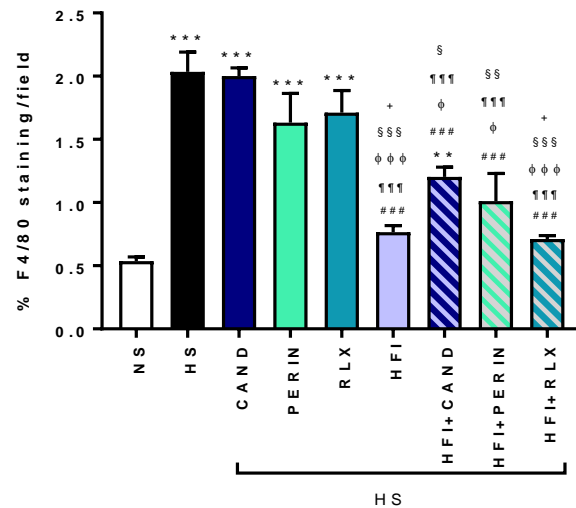


Figure 4.3.2. The effects of HS and the treatments investigated on F4/80 macrophage infiltration.

A) Representative images of IHC-stained kidney sections from each group studied for F4/80, a marker for macrophage infiltration. Scale bar = 50 μ m. **B)** Also shown is the mean \pm SEM % F4/80 stained per section (per total area stained), which was averaged from the measurements of 8 fields per section, $n=4-8$ mice/group. ** $P<0.01$, *** $P<0.001$ vs NS; ### $P<0.001$ vs HS; ¶¶¶ $P<0.001$ vs CAND; ¶ $P<0.05$, ¶¶¶ $P<0.001$ vs PERIN; § $P<0.05$, §§ $P<0.01$, §§§ $P<0.001$ vs RLX; + $P<0.05$ vs HFI+CAND (one-way ANOVA).

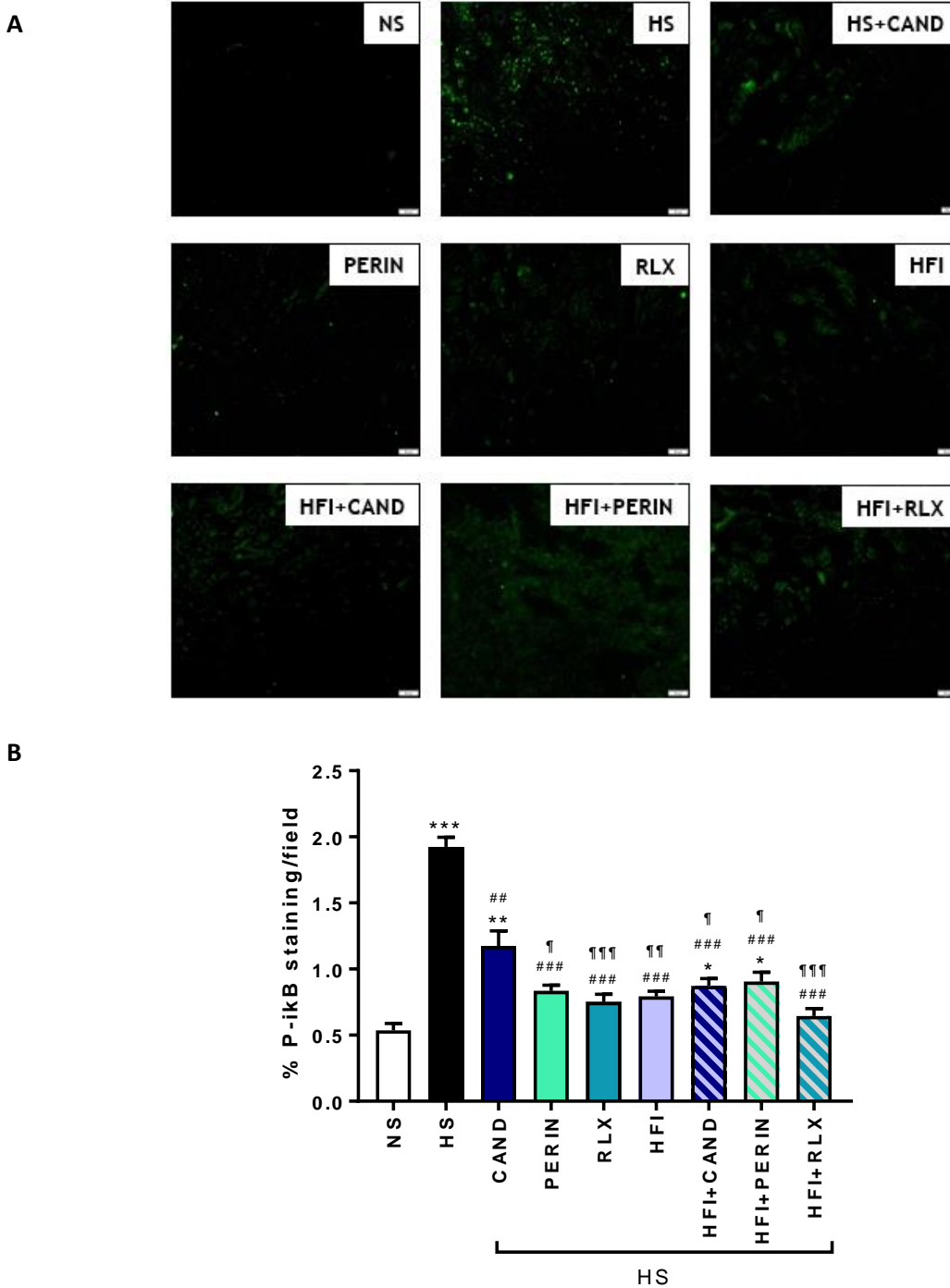


Figure 4.3.3. The effects of HS and the treatments investigated on P-ikB staining.

A) Representative images of IF-stained kidney sections from each group studied for P-ikB, a marker for NF- κ B activity. Scale bar = 50 μ m. **B)** Also shown is the mean \pm SEM % P-ikB stained per section (per total area stained), which was averaged from the measurements of 8 fields per section, $n=4-8$ mice/group. * $P<0.05$, *** $P<0.001$ vs NS; ### $P<0.001$ vs HS; ¶ $P<0.05$, ¶¶ $P<0.01$, ¶¶¶ $P<0.001$ vs CAND (one-way ANOVA).

4.3.3 The effects of HS and the treatments investigated on glomerulosclerosis.

Masson's trichrome-stained images were used to assess glomerulosclerosis score (Figure 4.3.4) from each mouse kidney. Eight glomeruli per kidney section at 40x magnification was assigned a score from 0-3 where 0 represented no collagen staining inside the glomeruli, 1 represented mild (1-33%) collagen staining, 2 represented medium (33-67%) collagen staining and 3 represented severe (67-100%) collagen staining within the glomeruli which was adapted from the glomerulosclerotic index (Maric *et al.*, 2004) and scoring of respiratory inflammatory cell aggregates (Royce *et al.*, 2015). As expected, NS-fed mice had minimal collagen within the glomeruli, whereas the HS-fed mice had an increased glomerulosclerosis score (by ~2.7-fold; $P<0.001$ vs NS group). This HS-induced increase in glomerulosclerosis score was unaffected by CAND, PERIN, HFI+CAND or HFI+PERIN treatment over 4 weeks. However, the HS-induced increase in glomerulosclerosis score was restored to similar levels measured from NS-fed mice by RLX, HFI or HFI+RLX treatment after 4 weeks (by ~81-100%; all $P<0.01$ vs HS group; no different to NS group; Figure 4.3.4).

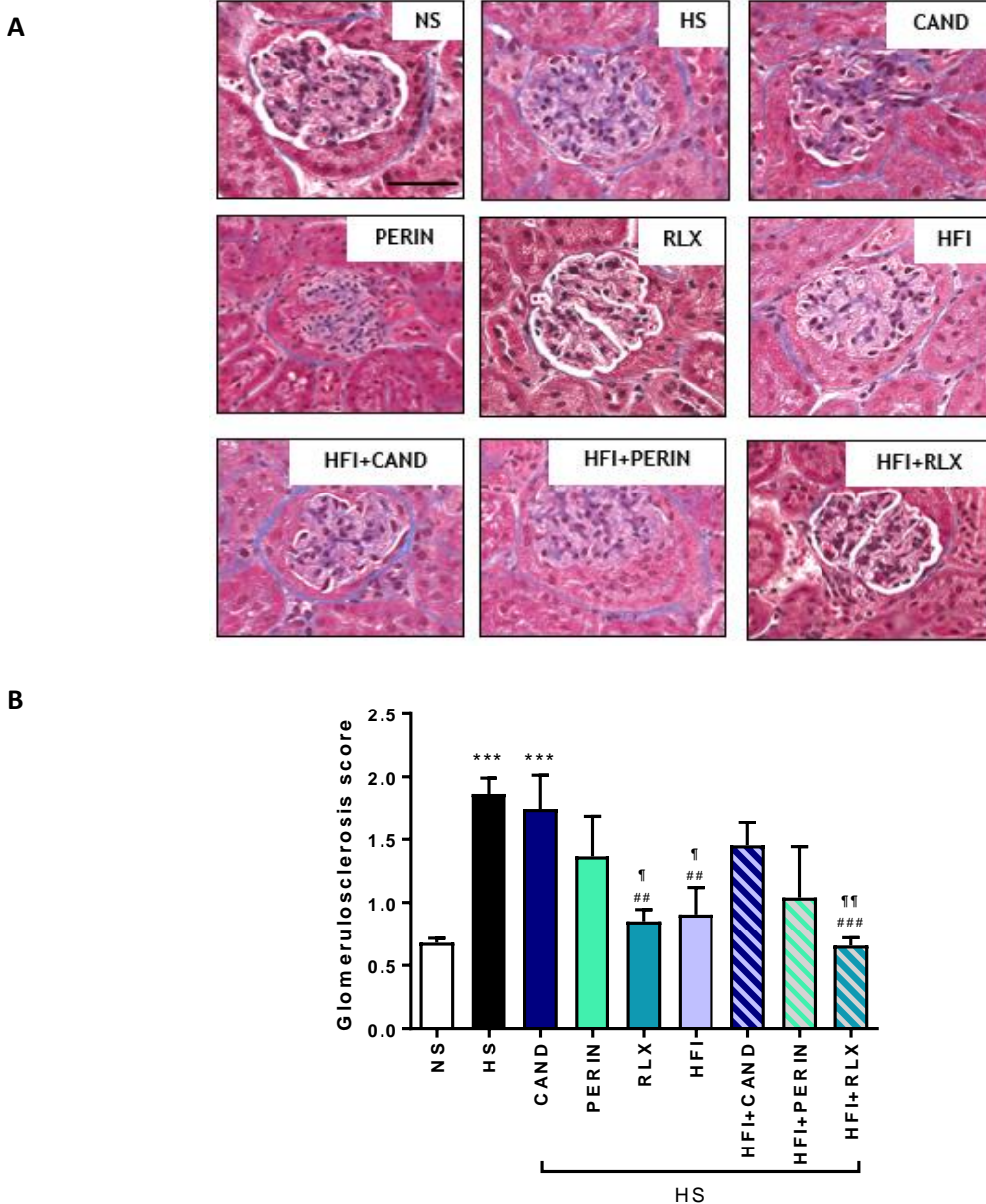


Figure 4.3.4. The effects of HS and the treatments investigated on glomerulosclerosis score.

A) Representative images of Masson's trichrome-stained kidney sections from each group studied of glomerulosclerosis. Scale bar = 100 μ m. **B)** Also shown is the mean \pm SEM glomerulosclerosis score, which was averaged from the measurements of 6-8 glomeruli per section, $n=4-8$ mice/group. Glomeruli were scored from a scale ranging from 0 to 3 for normal (0), 1 = mild (1-33%) collagen staining within glomeruli, 2 = medium (33-67%) collagen staining within glomeruli, and 3 = severe (67-100%) collagen staining within glomeruli. *** $P<0.001$ vs NS; ## $P<0.01$ vs HS; ¶ $P<0.5$, ¶¶ $P<0.01$ vs CAND (one-way ANOVA).

4.3.4 The effects of HS and the treatments investigated on interstitial and total renal collagen (fibrosis).

Another six randomly selected fields per section from Masson's trichrome-stained images were also analysed for interstitial kidney collagen deposition (Figure 4.3.5A). HS-fed mice were observed to have a significant increase in interstitial collagen staining (by ~3.2-fold, $P < 0.001$ vs NS group; Figure 4.3.5B) compared to that measured from NS-fed control mice. This increase was unaffected by CAND treatment alone but was abrogated by PERIN, RLX, HFI, HFI+PERIN and HFI+RLX treatment after 4 weeks (all $P < 0.001$ vs HS group; no different to NS group; Figure 4.3.5B). On the other hand, while HFI+CAND treatment partially lowered the HS-induced interstitial collagen deposition (by ~48%, $p < 0.01$ vs HS group; $p < 0.01$ vs NS group), it did not fully restore interstitial fibrosis back to levels measured in NS-fed mice.

Using hydroxyproline analysis as another measure of fibrosis (Figure 4.3.5C), total kidney collagen concentration was examined and expressed as % collagen content/dry weight of the kidney tissue. Expectedly, HS-fed mice had significantly increased kidney collagen concentration (by ~1.4-fold; $P < 0.05$ vs NS group) compared to that measured from their NS-fed counterparts. This HS-induced increase in collagen concentration was unaffected by CAND, PERIN, HFI, HFI+CAND or HFI+PERIN treatment. However, PERIN, HFI or HFI+CAND treatment induced a trend towards reduced hydroxyproline levels such that these levels were no longer different to that measured from the NS group. Only RLX treatment alone or its combination with HFI significantly reduced total collagen (both by ~73%; both $P < 0.05$ vs HS group). Additionally, RLX or HFI+RLX treatment were able to reduce total kidney collagen concentration levels to that which was not statistically different to measurements obtained from mice on a NS diet (Figure 4.3.5C).

These findings suggested that RLX, HFI and the combined effects of HFI+RLX demonstrated greater and broader anti-fibrotic efficacy over that of CAND, PERIN. CAND did not demonstrate any anti-fibrotic efficacy at the dose studied, while PERIN or HFI were only able to significantly reduce interstitial renal collagen but not total collagen (likely collagen IV in the kidney) at the doses studied. Curiously, it was found that combining HFI with RLX or PERIN was able to maintain the effects of HFI alone, whereas the therapeutic effects of HFI alone on glomerulosclerosis score (Figure 4.3.4B), interstitial renal collagen deposition (Figure 4.3.5B) and total kidney collagen

concentration (Figure 4.3.5C) were lost when it was combined with CAND (as per what was seen with RLX in Chapter 3).

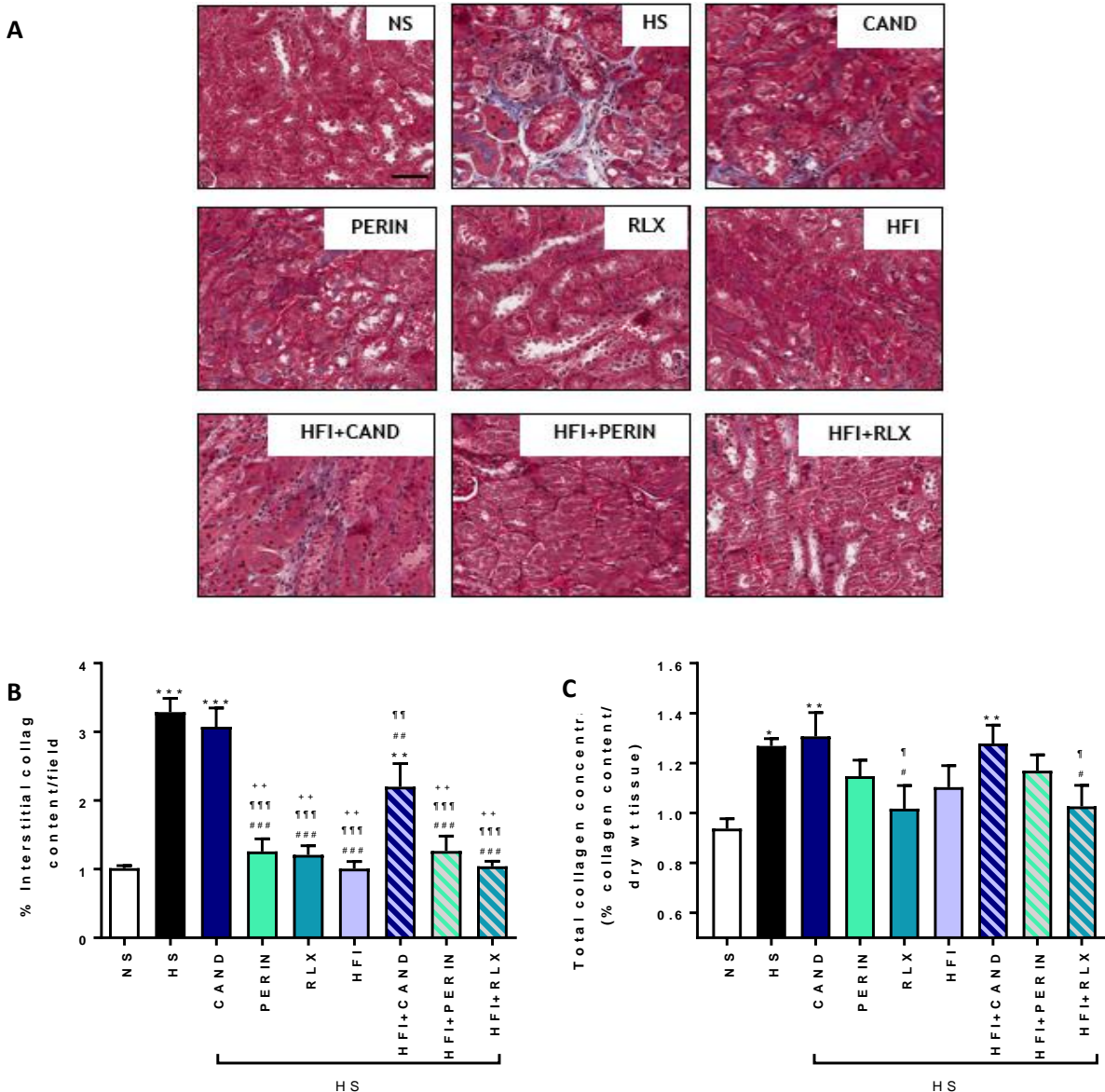


Figure 4.3.5. The effects of HS and the treatments investigated on interstitial collagen and total kidney collagen concentration.

A) Representative images of Masson's trichrome-stained kidney sections from each group studied of interstitial ECM/collagen deposition. Scale bar = 100 μ m. **B)** Also shown is the mean \pm SEM % interstitial ECM/collagen staining per section (per total area stained), which was averaged from the measurements of 8 fields per section, $n=4-8$ mice/group. **C)** Additionally, shown is the mean \pm SEM % total kidney collagen concentration (which was extrapolated from dividing the collagen content of each kidney portion analysed by the dry weight of that portion); obtained from hydroxyproline analysis of $n=4-6$ mice/group. ** $P<0.01$, *** $P<0.001$ vs NS; # $P<0.05$, ### $P<0.01$, ### $P<0.001$ vs HS; ¶ $P<0.05$, ¶¶ $P<0.01$, ¶¶¶ $P<0.001$ vs CAND; ++ $P<0.01$ vs HFI+CAND (one-way ANOVA).

4.3.5 The effects of HS and the treatments investigated on vascular rarefaction of peritubular capillaries.

Changes in CD31-stained peritubular capillary (Figure 4.3.6) density was evaluated as a measure of vascular rarefaction. Randomly selected images per kidney section were overlaid with a fixed grid (highlighted in blue with 10,000pixel² point intersections). Individual peritubular capillaries beneath grid intersections were counted using the grid method modified from (Yamaguchi *et al.*, 2012). As expected, mice fed the HS diet were associated with a loss of renal capillary density (by ~1.8-fold; $P<0.01$ vs NS group) compared to measurements obtained from mice fed the NS diet. This HS-induced vascular rarefaction within the kidney was unaffected by CAND, PERIN, HFI+CAND or HFI+PERIN treatment. While HFI treatment induced a trend towards restoring peritubular capillary density (by ~45%), only RLX treatment alone or the combination of HFI+RLX significantly restored peritubular capillary density over that measured in HS-fed mice (by ~80% and ~60% respectively; $P<0.01$ and $P<0.05$ vs HS group, respectively), and to levels that were no longer different to that measured from NS-fed mice (Figure 4.3.6).

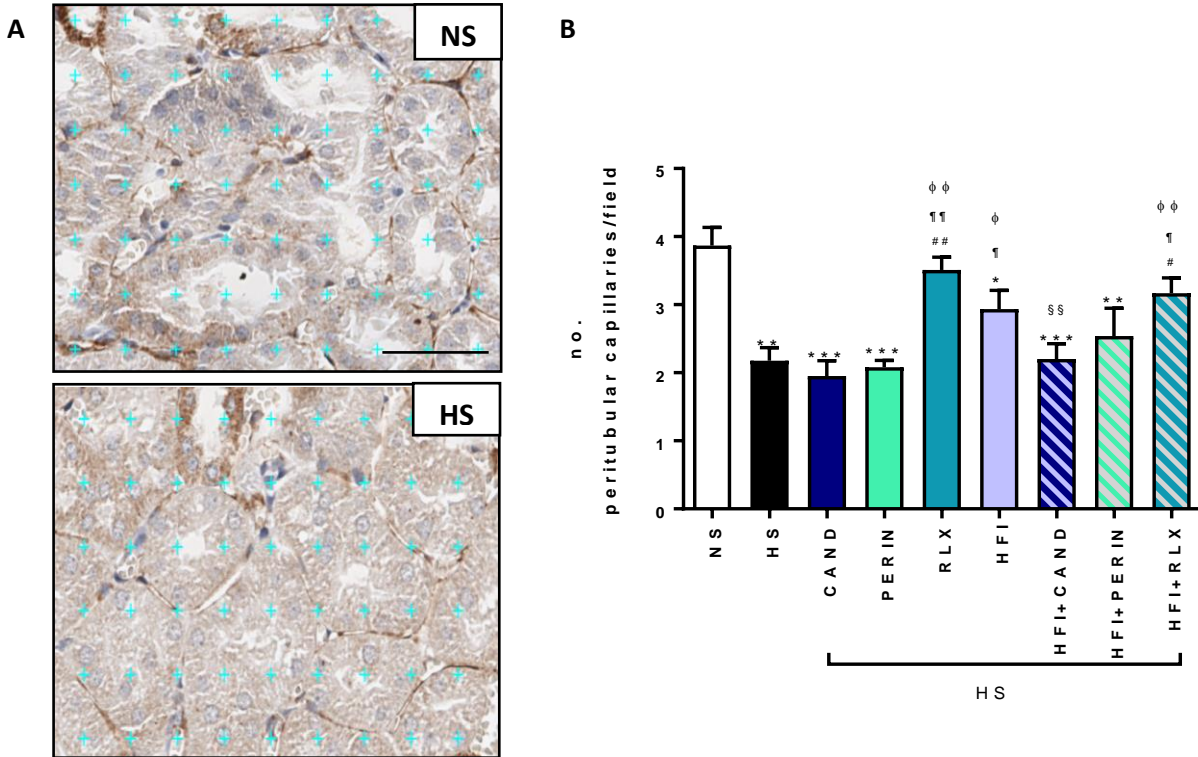


Figure 4.3.6. The effects of HS and the treatments investigated on vascular rarefaction of peritubular capillaries.

A) Representative photomicrographs of CD31-stained IHC kidney sections of NS and HS overlaid by a blue grid. Scale bar= 100 μ m. **B)** Also shown is the mean \pm SEM of the number of peritubular capillaries counted per field which was laying under each blue point below the grid of $n=4-8$ mice/group. * $P<0.05$, ** $P<0.01$, *** $P<0.001$ vs NS; # $P<0.05$, ## $P<0.01$ vs HS; † $P<0.05$, †† $P<0.01$ vs CAND, φ $P<0.05$, φφ $P<0.01$ vs PERIN; §§ $P<0.01$ vs RLX (one-way ANOVA).

4.3.6 The effects of HS and the treatments investigated on TGF- β 1 staining.

Renal TGF- β 1 (expressed as a dimer sized at 25kDa) levels were examined via Western blotting to determine the impact of HS and the treatments investigated on expression of the profibrotic cytokine (Figure 4.3.7). Compared to mice fed the NS-diet, HS-fed mice had significantly increased TGF- β 1 expression (by ~1-fold; $P < 0.01$ vs NS group). This HS-induced increase was unaffected by CAND treatment alone, partially but significantly reduced by PERIN treatment alone (by ~70%), and further reduced by RLX alone, HFI alone and the combination treatments (all $P < 0.05$ vs HS group) to levels that were similar to that measured from NS-fed mice (all no different to NS group; Figure 4.3.7B). Additionally, RLX treatment alone, HFI treatment alone and HFI+RLX treatment more effectively reduced renal TGF- β 1 expression levels compared to the effects of CAND treatment alone (all $P < 0.01$ vs CAND group).

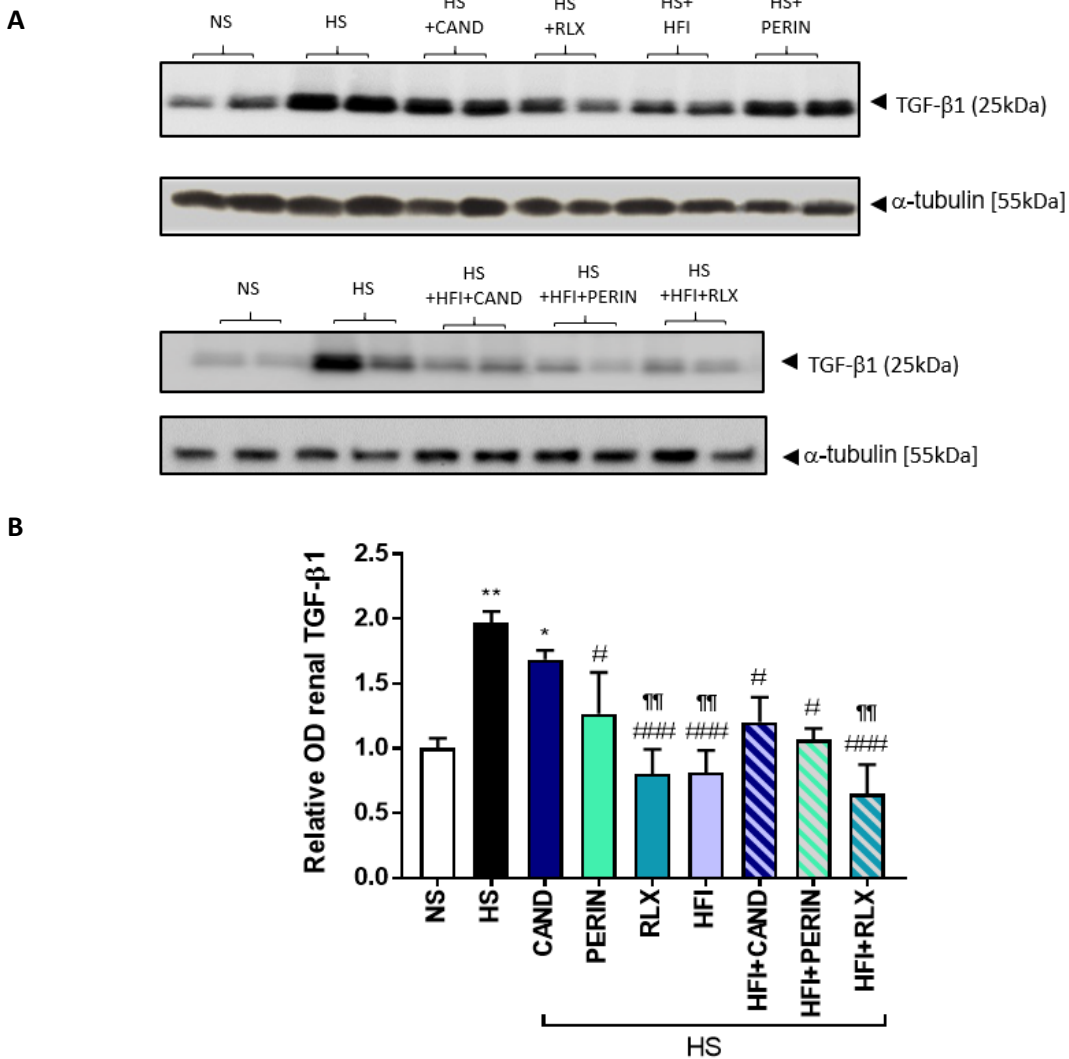


Figure 4.3.7. The effects of HS and the treatments investigated on renal TGF- β 1 expression levels.

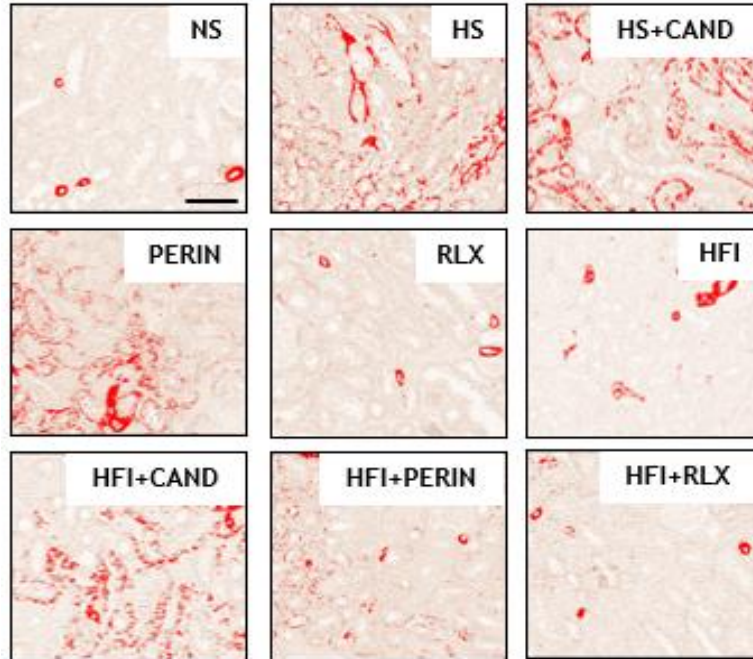
A) Representative Western blot images showing renal TGF- β 1 (25kDa) expression from duplicate samples from each treatment group studied. Corresponding representative Western blots for α -tubulin are included to demonstrate the quality and equivalent loading of protein samples. **B)** Also shown is the mean \pm SEM levels of TGF- β 1 (corrected for α -tubulin expression) which was determined by densitometry, from $n=4-6$ mice per group; and expressed as the relative ratio to the mean value of the NS group, which was expressed as 1. The four remaining samples per group were analysed in duplicates on separate membranes. * $P<0.05$, ** $P<0.01$ vs NS; # $P<0.05$, ### $P<0.001$ vs HS; ¶ $P<0.01$ vs CAND (one-way ANOVA).

4.3.7 The effects of HS and the treatments investigated on renal myofibroblast accumulation.

α -SMA-stained tissue sections were used to distinguish the impact of HS and the treatments investigated on interstitial myofibroblast accumulation (Figure 4.3.8). HS-fed mice had significantly increased interstitial renal myofibroblast accumulation (by ~2.5-fold; $P < 0.001$ vs NS group) compared to that measured in NS-fed mice. This HS-induced increase in renal myofibroblast accumulation was unaffected by CAND, PERIN or HFI+CAND treatment; while it was significantly reduced by RLX, HFI, HFI+PERIN or HFI+RLX (by ~56-90%; all $P < 0.01$ vs HS group) with levels returned to those seen in NS-fed mice. RLX, HFI and HFI+RLX treatment also significantly reduced renal myofibroblast accumulation compared to the effects of CAND alone (all $P < 0.001$ vs CAND group), PERIN alone (all $P < 0.01$ vs PERIN group) or HFI+CAND treatment (all $P < 0.01$ vs HFI+CAND group).

The findings presented in Figures 4.3.6-4.3.8 were consistent with those shown in Figure 4.3.5 in demonstrating that RLX or the combination of HFI+RLX demonstrated more rapid-occurring anti-fibrotic efficacy over that of CAND or in some cases over both CAND or PERIN treatment. Furthermore, RLX alone, HFI alone or the combination of HFI+RLX, also restored vascular rarefaction to a greater extent than the current treatments, CAND or PERIN.

A



B

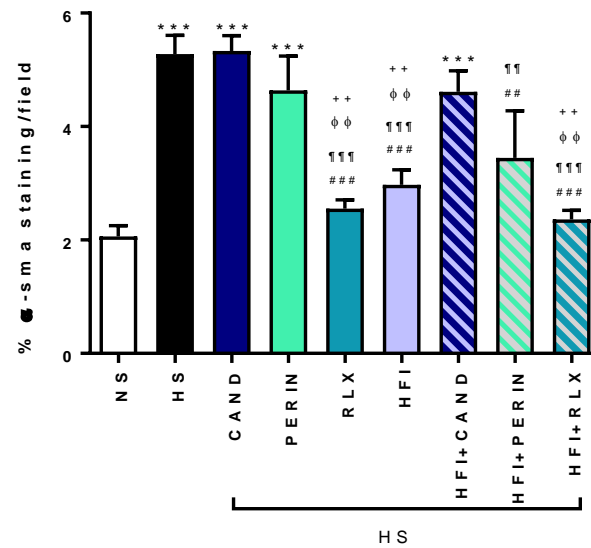


Figure 4.3.8. The effects of HS and the treatments investigated on renal myofibroblast accumulation.

A) Representative images of IHC-stained kidney sections from each group studied for α -SMA-associated interstitial myofibroblast accumulation enhanced with red colour threshold. Scale bar= 100 μ m. **B)** Also shown is the % α -SMA-stained myofibroblast accumulation per section (per total area stained), from n=4-8mice/group. ***P<0.001 vs NS; ##P<0.01, ###P<0.001 vs HS. ¶¶P<0.01, ¶¶¶P<0.001 vs CAND; ϕϕP<0.01 vs PERIN; ++P<0.01 vs HFI+CAND (one-way ANOVA).

4.3.8. The effects of HS and the treatments investigated on renal gelatinase expression levels.

Gelatin zymography was then completed to determine the impact of the HS-fed diet and the treatments investigated on MMP-2 expression and activity, a known inducer of ECM/collagen degradation (Figure 4.3.9). Mice fed a HS-diet did not present with significantly altered MMP-2 expression levels compared to that measured from NS-fed mice (Figure 4.3.9B). Furthermore, MMP-2 expression and activity were not altered by CAND, PERIN, HFI+CAND or HFI+PERIN treatment of HS-fed mice. Only the novel treatments, RLX alone, HFI alone and the combination of HFI+RLX significantly increased MMP-2 expression and activity (by ~0.8-1.5-fold; all $P < 0.05$ vs NS group; all $p < 0.05$ vs HS group) compared to that measured from mice fed a NS or HS diet.

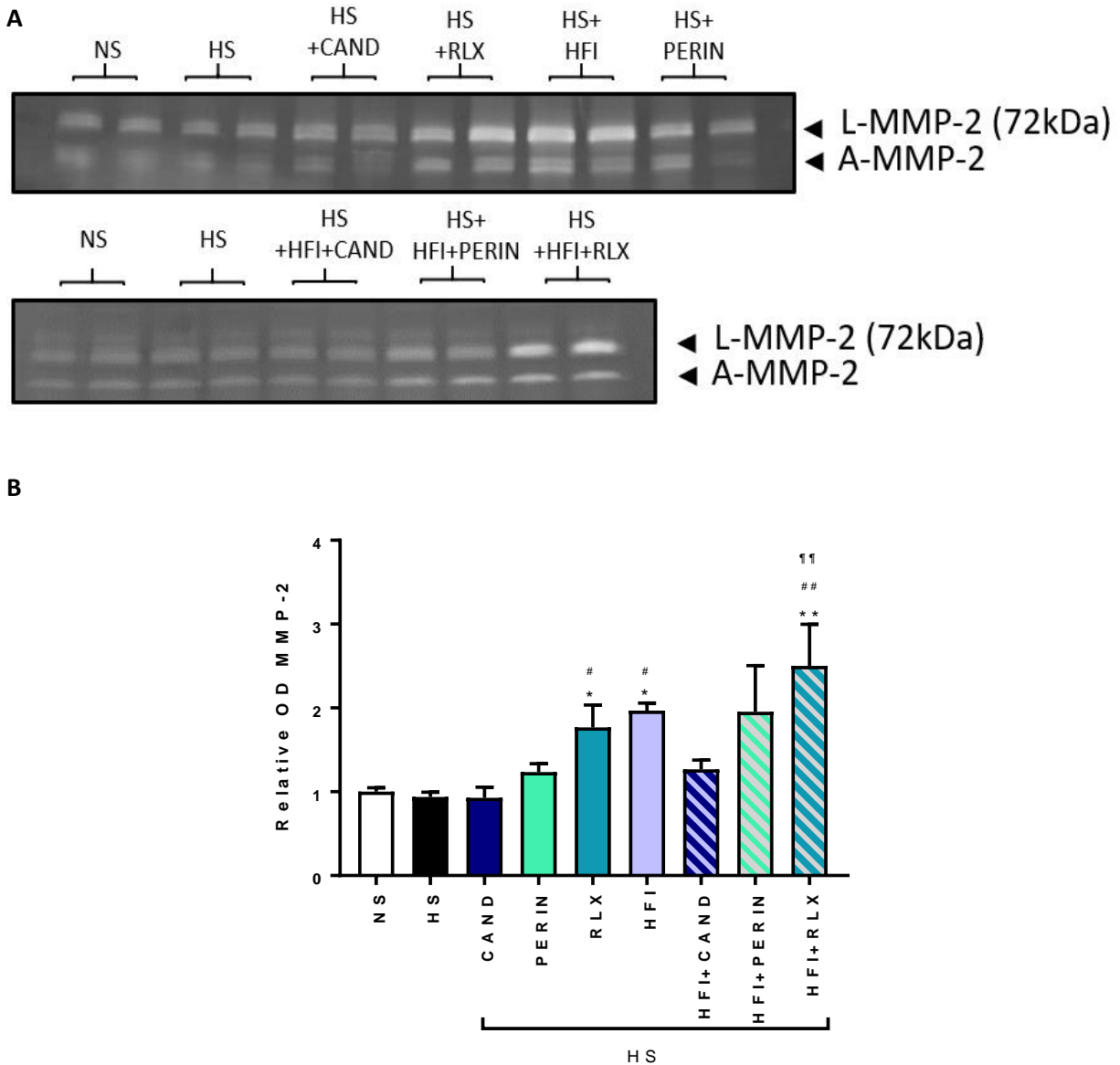


Figure 4.3.9. The effects of HS and the treatments investigated on renal gelatinase expression levels.

A) A representative gelatin zymography shows renal latent (L) and active (A) MMP-2 levels from duplicate samples from each of the treatment groups studied. **B)** Also shown is mean \pm SEM relative OD of MMP-2 expression (as determined by densitometry of the bands shown), which was expressed relative to the value from NS control group, which was expressed as 1 in each case; from $n=4-6$ mice per group studied. The four remaining samples per group were analysed in duplicates on separate gelatin zymographs. * $P<0.05$, ** $P<0.01$ vs NS; # $P<0.05$, ## $P<0.01$ vs HS, §§ $P<0.01$ vs CAND (one-way ANOVA).

4.3.9 The effects of HS and the treatments investigated on TIMP-1 expression.

Changes in the expression levels of the endogenous inhibitor of MMPs (collagenases and gelatinases), TIMP-1, was examined via Western blotting (Figure 4.3.10). Renal TIMP-1 levels were significantly increased (by ~2.4-fold; $P < 0.001$ vs NS group) in HS-fed mice compared to measurements seen in NS-fed mice. These increased TIMP-1 levels were unaffected by CAND, PERIN, HFI+CAND and HFI+PERIN, but significantly reduced by RLX treatment alone, HFI treatment alone or HFI+RLX treatment (by ~70-80%; all $P < 0.01$ vs HS group); to levels that were no longer different to that measured in NS-fed mice (all no different to NS-fed mice). Additionally, RLX, HFI and HFI+RLX treatment more effectively reduced the HS-induced increase in renal TIMP-1 expression levels compared to the effects of CAND or PERIN treatment (all $P < 0.01$ vs CAND group; all $P < 0.01$ vs PERIN group), further demonstrating how effective these novel therapies were in regulating mediators involved in ECM/collagen degradation, compared to the two current standard of care treatments.

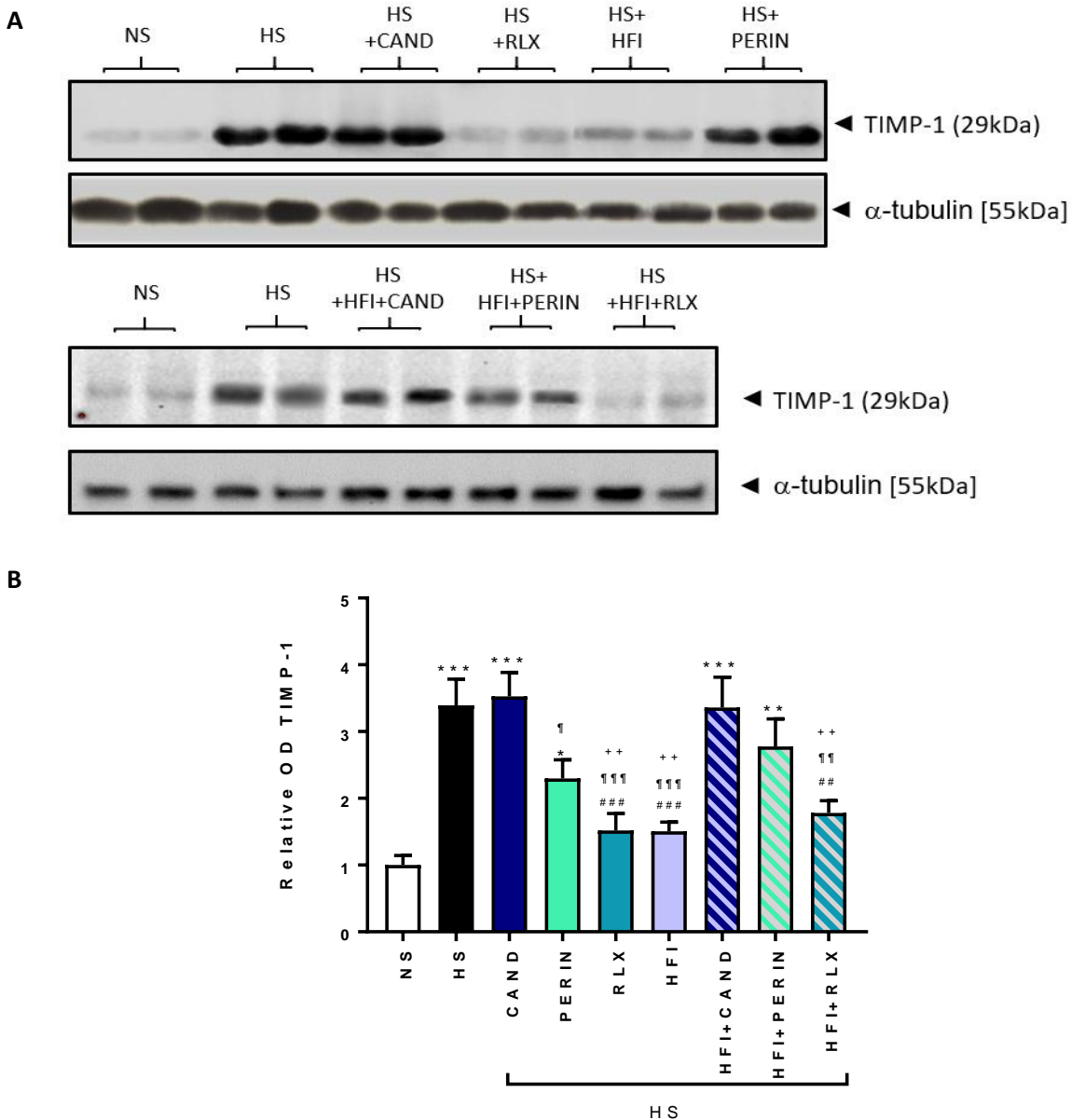


Figure 4.3.10. All treatments aside from candesartan reduce TIMP-1 expression.

A) Representative Western blot images showing renal TIMP-1 (29kDa) expression levels from duplicate samples from each treatment group studied. Corresponding representative Western blots for α-tubulin are included to demonstrate the quality and equivalent loading of protein samples. The four remaining samples per group were analysed in duplicates on separate western blots. **B)** Also shown are the mean ± SEM levels of TIMP-1 (corrected for α-tubulin expression) which were determined by densitometry, from n=4-6 mice per group; and expressed as the relative ratio to the mean value of the NS group, which was expressed as 1. *P<0.05, **P<0.01, ***P<0.001 vs NS; ##P<0.01, ###P<0.001 vs HS; ¶¶P<0.01, ¶¶¶P<0.001 vs CAND; ++P<0.01 vs HFI+CAND (one-way ANOVA).

4.3.10 The effects of HS and the treatments investigated on plasma urea levels.

Plasma urea levels were used as a surrogate marker of renal dysfunction (Figure 4.3.11). HS-fed mice had significantly increased plasma urea levels (by ~1.6-fold; $P < 0.05$ vs NS group) over that measured from mice fed a NS-diet, indicating that mice fed the HS diet had significantly reduced renal function. This HS-induced increase in plasma urea levels was unaffected by CAND treatment; attenuated to an extent by HFI, HFI+CAND and HFI+PERIN treatment (as plasma urea levels in these three groups were no longer significantly different to that measured from HS or NS-fed mice); but significantly reduced by RLX treatment alone and HFI+RLX treatment (all $p < 0.05$ vs HS group; Figure 4.3.11). Interestingly, PERIN treatment significantly exacerbated plasma urea levels, by ~1.9-fold over that measured in HS-fed mice ($P < 0.001$ vs HS group and all other groups studied).

These findings suggested 1) that the consistent and superior anti-fibrotic efficacy offered by RLX alone or the combined effects of HFI+RLX correlated with these treatments significantly reducing a measure of renal dysfunction. However, 2) although the dose of PERIN (4mg/kg/day) administered offered some ECM remodelling, it was found to exacerbate renal failure (compounded by its ability to significantly lower SBP and animal body weight).

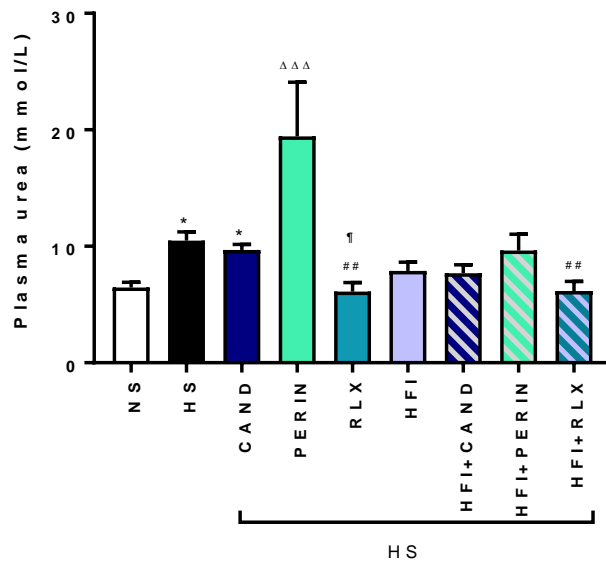


Figure 4.3.11. The effects of HS and the treatments investigated on plasma urea levels.

Shown are the mean \pm SEM plasma urea levels from each of the control and treatment groups studied, which were evaluated from the i-STAT device using 100 μ l of plasma from each animal; $n=4-8$ mice per group. ** $P<0.01$ vs NS; # $P<0.05$, ## $P<0.01$ vs HS; † $P<0.05$ vs PERIN; ΔΔΔ $P<0.001$ vs all treatment groups (one-way ANOVA).

4.4. Discussion

This study aimed to compare current standard-of-care medication such as the ARB, candesartan cilexetil (CAND) and ACE inhibitor, perindopril (PERIN), to experimentally-investigated therapies, serelaxin (RLX), HFI-419 (HFI) and their combination in reversing established salt-induced kidney fibrosis. This was the first study to make a direct comparison between HFI and its combinations with CAND, PERIN or RLX, as treatments for HS-induced kidney disease, using doses of each drug that had previously demonstrated anti-fibrotic efficacy in other models of disease. Consistent with the data demonstrated in Chapter 3 (utilizing mice on an FVB/N background), the HS (5% NaCl) fed mice on the C57B6J background used in this study underwent significant renal damage, inflammation, remodelling, fibrosis and dysfunction after 8 weeks, in the absence of any marked BP changes. Using this model thus, allowed for the evaluation of the direct renoprotective effects of each treatment/combination administered in the absence of elevated BP as a confounding variable.

4.4.1 Renoprotective effects of the current standard of care treatments against HS-induced pathology.

At the dose administered, CAND (2mg/kg/day) was only found to partially reduce the HS-induced increase in P-IKB levels when administered over 4 weeks to C57B6J mice with established disease, demonstrating that it was biologically active and able to induce modest anti-inflammatory effects, as seen in Chapter 3 and in previous *in vivo* and *in vitro* models of kidney disease (Chen *et al.*, 2008; Ma *et al.*, 2011). However, similar to what was reported in Chapter 3, CAND failed to reduce HS-induced increases in renal macrophage infiltration, glomerulosclerosis, collagen concentration, vascular rarefaction, myofibroblast differentiation, TGF- β 1 expression levels, MMP-2 and TIMP-1 levels, which led to its inability to improve renal dysfunction (as measured by elevated plasma urea levels). These findings again were contrary to previously published findings which showed that CAND, when administered at 1mg/kg/day (half the dose of that used in the current study) to diabetic db/db mice (Callera *et al.*, 2016) or at 1 or 3mg/kg/day to 8% HS-diet-fed mice (Ina *et al.*, 2004; Liang and Leenen, 2008; Rafiq *et al.*, 2014), reduced renal damage and related dysfunction. Additionally, previous findings from our lab showed that 2mg/kg/day of CAND significantly reduced aberrant collagen deposition (fibrosis) in the heart of hypertensive

rats (Jones *et al.*, 2012). As db/db mice (Senador *et al.*, 2009) and mice fed an 8% HS diet (Huang *et al.*, 2019) are known to undergo hypertension, the discrepancy between the current study and those previously reported findings may be explained by the fact that CAND (at 1-3mg/kg/day) can exert therapeutic effects in hypertensive models (owing to its BP-lowering effects), but cannot maintain these effects in normotensive models that are not associated with an up-regulation of BP. This in turn perhaps confirms that CAND mainly acts to reduce the impact of BP on kidney remodelling and fibrosis, rather than having any direct anti-remodelling effects.

On the other hand, PERIN (4mg/kg/day) significantly decreased the HS-induced P-I κ B levels, TGF- β 1 expression levels, interstitial collagen content and TIMP-1 levels, at the cost of inducing hypotension when administered to a normotensive model, significantly reducing animal body weight, and significantly exacerbating renal dysfunction when administered to HS-fed mice. These findings highlight that although ACEi can induce anti-inflammatory and anti-fibrotic effects, they also promote unwanted side-effects (on SBP, BW and renal function) at doses that are capable of inducing collagen remodelling. In terms of body weight changes, ACEi have been known to decrease body weight as a side effect over long-term use, in a similar fashion to that of ARBs when administered to patients with hypertension (Santos *et al.*, 2009). The findings of this study though, suggested that perindopril was able to inhibit the pro-fibrotic influence of TGF- β 1 on interstitial collagen deposition, although not necessarily through regulation of myofibroblast differentiation since α -SMA was unchanged. This may be consistent with the findings that ACEi may inhibit the contribution of the RAS in promoting epithelial to mesenchymal cell transition (EMT) (Wontanawatot *et al.*, 2011; Chen *et al.*, 2018). Furthermore, although not having a direct effect on MMP-2 activity, the finding that perindopril was able to reduce renal TIMP-1 levels suggests that it was able to increase the MMP-2/TIMP-1 ratio, which could facilitate a moderate level of collagen degradation. These findings are consistent with that of others in showing that compared to ARBs, ACEi are believed to have better anti-fibrotic efficacy owing to their ability to reduce Ang II production and promote the increase of prostaglandins, bradykinin and the bioavailability of nitric oxide; all of which have been shown to mediate some form of organ protection (Chen *et al.*, 2002). However, the findings that perindopril did not significantly affect glomerulosclerosis or total collagen concentration suggests that it was only able to reduce

interstitial types I and III collagen without affecting basement membrane collagen IV, the predominant collagen isotype in the kidney (as inferred from the hydroxyproline analysis).

4.4.2 Effects of novel treatments.

In comparison to the current treatments evaluated, RLX (0.5mg/kg/day) alone significantly improved all endpoints measured except for SBP, body weight or macrophage infiltration. When observing markers of collagen synthesis, relaxin decreased both TGF- β 1 and α -SMA-stained myofibroblast differentiation. RLX also promoted collagen breakdown by stimulating an increase in MMP-2 activity and decreasing TIMP-1 levels, that would favour collagen degradation. These renoprotective effects of RLX were somewhat expected as they are consistent with the findings presented in Chapter 3 and upon RLX administration to other models of kidney damage where it was administered at the same dose (0.5mg/kg/day) (Garber *et al.*, 2001; Lekgabe *et al.*, 2005; Samuel and Hewitson, 2009; Hewitson *et al.*, 2010; Chow *et al.*, 2014).

In terms of the anti-inflammatory properties of RLX, it is known to reduce the recruitment and migration of inflammatory cells into the site of injury (Nistri *et al.*, 2003; Hewitson *et al.*, 2007; Martin *et al.*, 2018), as well as the pro-inflammatory and pro-fibrotic factors that are secreted by inflammatory cells (Bani *et al.*, 1997; Masini *et al.*, 1997, 2004; Nistri *et al.*, 2003). The ability of RLX to reduce P-I κ B levels is consistent with its ability to inhibit NF- κ B signalling, a crucial transcription factor for regulating many inflammatory genes (Martin *et al.*, 2018). Although RLX did not directly affect macrophage infiltration, a previous study suggested that RLX was more likely to promote M1 to M2 macrophage polarisation to inhibit renal fibrosis via a TLR4-NF- κ B pathway (Chen *et al.*, 2017), rather than inhibit macrophage numbers per se. Hence, the evaluation of specific M1 and M2 macrophage markers should be evaluated in future studies to address this more specifically.

Furthermore, RLX restored peritubular capillary density, which was ablated by HS-induced kidney damage. This is consistent with the angiogenic properties of RLX, where studies to date have demonstrated that its continuous infusion promotes the formation of new blood vessels and the reversal of vascular rarefaction (Bani *et al.*, 1997; Cai *et al.*, 2017; Sanchez-Mas *et al.*, 2017). This recovery in peritubular capillary density is likely due to its ability to up-regulate factors such as

basic fibroblast growth factor (Lewis *et al.*, 2001) and vascular endothelial growth factor (VEGF) (Unemori *et al.*, 2000), which contribute to its angiogenic actions.

These combined anti-inflammatory, angiogenic and anti-fibrotic properties of RLX were found to provide close to optimal protection against HS-induced renal damage (compared to the other individual and combination treatments evaluated), which resulted in a significant improvement of HS-induced renal dysfunction (as measured by plasma urea levels). This decrease in HS-induced plasma urea levels indicated that the kidneys were able to more efficiently eliminate waste products after RLX treatment, which is consistent with the ability of RLX to improve effective renal plasma flow (ERPF) and glomerular filtration rate (GFR) when administered to conscious rats (Danielson *et al.*, 1999) and age-induced kidney disease (Danielson, 2006) in rats.

Although the expression of IRAP in the ageing/injured kidney and the renoprotective effects of IRAP inhibition have only been recently examined, and there are very limited published reports on the therapeutic effects of HFI and other IRAP inhibitors, our results showed significant benefits of using HFI (0.72mg/kg/day) in the kidneys of HS-fed mice. Consistent with data presented in a published patent on the effects of HFI in models of ageing, cardiovascular and hepatic disease (Chai *et al.*, 2017), HFI (0.72mg/kg/day) significantly reduced renal p-IkB and macrophage infiltration (F4/80) in the kidneys of HS-fed mice, confirming that it offered effective anti-inflammatory properties. The current theory in regard to its mechanisms of action, suggests that HFI prevents the breakdown of IRAP substrates such as oxytocin and vasopressin, which have been known to reduce renal injury through the reduction of inflammatory cell recruitment and protection against oxidative damage (Biyikli *et al.*, 2006; Tugtepe *et al.*, 2007). Not only was HFI treatment alone able to decrease the HS-induced macrophage infiltration, it also maintained similar anti-fibrotic effects to that of RLX in inhibiting TGF- β 1 and myofibroblast-induced collagen synthesis while increasing collagen-degrading MMP-2 activity/decreasing TIMP-1 levels. However, while HFI also significantly reduced the HS-induced increase in glomerulosclerosis and interstitial renal fibrosis to the same extent as RLX, it did not quite reduce total renal collagen concentration to the same extent as the RXFP1-agonist, suggesting that it may not have been able to affect collagen IV to the same extent as its ability to affect interstitial collagens. Furthermore, despite its potent anti-inflammatory actions, the reduced efficacy of HFI in

reducing both the HS-induced increase in renal collagen concentration and vascular rarefaction may provide a reason as to why the IRAP inhibitor did not significantly effect HS-induced renal dysfunction. These findings may suggest that additional dose-ranging studies should be conducted to find an optimal dose of HFI that can maintain the renoprotective effects of RLX. However, it is important to note that these were only subtle differences in the ability of either HFI or RLX to inhibit the pathological effects of HS, since there was generally no significant difference between either therapy alone for any analysis. Additional functional assays or increased number of animals tested, could possibly further distinguish any significant differences.

Overall, when compared to the current standard of care treatments evaluated, CAND and PERIN (which act to suppress the Ang II/AT₁R axis), RLX alone (acting at the RXFP1 receptor) and HFI alone (acting at the AT₄R/IRAP) were found to provide enhanced renoprotective and anti-fibrotic efficacy against HS-induced kidney damage; owing to the ability of these drugs to inhibit TGF- β 1 and myofibroblast-induced collagen synthesis while promoting MMP-induced collagen degradation. Furthermore, targeting RXFP1 or IRAP appeared to provide safer protection against HS-induced kidney damage, as the drugs that targeted these receptors did not affect SBP nor BW, and ameliorated the renal dysfunction associated with the model studied.

4.4.3 Effects of combination treatments.

When examining the combination therapies administered (involving HFI with CAND, PERIN or RLX), neither of these combination treatments significantly affected SBP or body weight, demonstrating the feasibility and safety of combining such drugs. Interestingly though, for the most part, adding CAND with HFI appeared to inhibit the renoprotective effects of HFI alone on macrophage infiltration, glomerulosclerosis, interstitial and total renal collagen concentration (fibrosis), angiogenesis, TGF- β 1 expression levels, myofibroblast differentiation, MMP-2 levels and TIMP-1 levels; to a similar extent as what CAND did to RLX when added in combination (as reported in Chapter 3). The explanation for this inhibitory effect of CAND is unknown as there are no other publications that have combined ARBs with IRAP inhibitors previously. It is unlikely that AT₁ receptors form dimers to interact with AT₄ receptors, as the AT₄R is an enzyme. Although the initial screening of HFI-419 and related IRAP inhibitors (Mountford *et al.*, 2014) revealed that they do not bind to AT₁ receptors (unpublished findings from Prof. Siew Yeen Chai, Dept. of

Physiology, Monash University), studies have shown that high doses of Ang IV can promote AT₁R activity (De Bundel *et al.*, 2010); and in a model of abdominal aortic aneurysm, the anti-fibrotic effects of a moderate dose of Ang IV (1.44mg/kg/day) which provided anti-fibrotic effects, were subsequently abolished by co-administration of losartan, another AT₁ receptor antagonist (Kong *et al.*, 2015). These findings may suggest then that high enough concentrations IRAP inhibitors such as HFI-419 may activate the AT₁R, allowing ARBs such as CAND to inhibit the protective effects of these IRAP inhibitors. Clearly though, further studies are warranted to determine the concentrations at which HFI-419 binds to AT₁ receptors, if at all; and in the setting of kidney disease as opposed to the brain where most of the initial studies on these IRAP inhibitors were conducted (Albiston *et al.*, 2001, 2008, 2010; Mountford *et al.*, 2014). Nevertheless, the findings of this study suggested that combining IRAP inhibitors with ARBs would not ideally provide renoprotection in a clinical setting.

When comparing the combined effects of HFI and PERIN to the individual treatments alone, the addition of PERIN to HFI did not demonstrate any additive effects over HFI alone, but reduced the HS-induced macrophage infiltration to a greater extent than PERIN alone. This may have reflected the superior and broader anti-inflammatory effects of HFI, when added in combination with PERIN. Most importantly, the combined effects of HFI+PERIN did not exacerbate renal dysfunction to the same extent as PERIN alone. Despite this beneficial effect of the combination therapy (of HFI and PERIN) on renal dysfunction, the overall findings that this combination therapy did not offer any improved renoprotection over the effects of HFI alone nor affect the HS-induced renal dysfunction in the model studied suggested that it did not offer any added value over the use of HFI alone.

Finally, when comparing the renoprotective effects of HFI+RLX to the individual treatments administered, it was determined that the combined effects of HFI+RLX maintained the anti-inflammatory and anti-remodelling effects of HFI and the anti-remodelling and anti-fibrotic effects of RLX; which contributed to the significant abrogation of HS-induced renal dysfunction. Thus, although the combined effects of HFI+RLX did not offer any added efficacy over the individual treatments investigated, it provided broader anti-inflammatory effects compared to RLX alone and broader anti-fibrotic effects compared to HFI alone; thus, providing maximal

protection against HS-induced kidney disease pathogenesis. This study showed for the first time the feasibility of combining an IRAP inhibitor with an RXFP1 agonist, as the combination of HFI+RLX did not inhibit or compromise the therapeutic effects of each drug administered. Further validation of this combination therapy in other experimental models of fibrosis-induced disease may eventually lead to the clinical evaluation of this combination therapy approach.

4.4.4 Conclusion

In summary, this study compared and combined the effects of a currently-used ARB (CAND) and ACEi (PERIN) to emerging therapies that activate the RXFP1 receptor (RLX) or inhibit IRAP (HFI). The results obtained demonstrated the greater and broader renoprotection offered by these emerging therapies alone or in combination in the setting of HS-induced kidney disease; where the anti-inflammatory and anti-remodelling effects of HFI, when combined with the anti-remodelling and anti-fibrotic effects of RLX, offered optimal protection against the various end-points measured. As targeting the RXFP1 receptor and/or IRAP appeared to offer improved renoprotection over blockade of the Ang II/AT₁R axis, these findings may lead to additional dose-response studies of HFI and RLX, and/or the development of new RXFP1 agonists and IRAP inhibitors (with improved affinity and selectivity for these receptors) that can be evaluated as new treatments for CKDs characterised by fibrosis. Of note, this study also demonstrated that ARBs such as CAND do not appear to have direct anti-fibrotic effects, hence, are less effective as therapies when applied to normotensive models. On the other hand, ACEi such as PERIN offer some anti-inflammatory effects, but are likely to induce adverse side-effects at doses that promote collagen remodelling.

4.5. References

- Albiston, AL, Fernando, RN, Yeatman, HR, Burns, P, Ng, L, Daswani, D, *et al.* (2010). Gene knockout of insulin-regulated aminopeptidase: Loss of the specific binding site for angiotensin IV and age-related deficit in spatial memory. *Neurobiol. Learn. Mem.* **93**: 19–30.
- Albiston, AL, McDowall, SG, Matsacos, D, Sim, P, Clune, E, Mustafa, T, *et al.* (2001). Evidence That the Angiotensin IV (AT4) Receptor Is the Enzyme Insulin-regulated Aminopeptidase. *J. Biol. Chem.* **276**: 48623–48626.
- Albiston, AL, Morton, CJ, Ng, HL, Pham, V, Yeatman, HR, Ye, S, *et al.* (2008). Identification and characterization of a new cognitive enhancer based on inhibition of insulin-regulated aminopeptidase. *FASEB J.* **22**: 4209–17.
- Anders, HJ, Vielhauer, V, Schlöndorff, D (2003). Chemokines and chemokine receptors are involved in the resolution or progression of renal disease. *Kidney Int.* **63**: 401–415.
- Bani, D, Ballati, L, Masini, E, Bigazzi, M, Sacchi, TB (1997). Relaxin counteracts asthma-like reaction induced by inhaled antigen in sensitized guinea pigs. *Endocrinology* **138**: 1909–1915.
- Biyikli, N, Tugtepe, H, Sener, G, Velioglu-Ogunc, A, Cetinel, S, Midillioglu, S, *et al.* (2006). Oxytocin alleviates oxidative renal injury in pyelonephritic rats via a neutrophil-dependent mechanism. *Peptides* **27**: 2249–2257.
- Bohle, A, Mackensen-Haen, S, Gise, H von (1987). Significance of Tubulointerstitial Changes in the Renal Cortex for the Excretory Function and Concentration Ability of the Kidney: A Morphometric Contribution. *Am J Nephrol* **7**: 421–433.
- Bundel, D De, Demaegdt, H, Lahoutte, T, Caveliers, V, Kersemans, K, Ceulemans, AG, *et al.* (2010). Involvement of the AT 1 receptor subtype in the effects of angiotensin IV and LVV-haemorphin 7 on hippocampal neurotransmitter levels and spatial working memory. *J. Neurochem.* **112**: 1223–1234.
- Cai, J, Chen, X, Chen, X, Chen, L, Zheng, G, Zhou, H, *et al.* (2017). Anti-Fibrosis Effect of Relaxin and Spironolactone Combined on Isoprenaline-Induced Myocardial Fibrosis in Rats via Inhibition

of Endothelial-Mesenchymal Transition. *Cell. Physiol. Biochem.* **41**: 1167–1178.

Callera, GE, Antunes, TT, Correa, JW, Moorman, D, Gutsol, A, He, Y, *et al.* (2016). Differential renal effects of candesartan at high and ultra-high doses in diabetic mice-potential role of the ACE2/AT2R/Mas axis. *Biosci. Rep.* **36**: e00398–e00398.

Chai, SY, Fernando, R, Peck, G, Ye, SY, Mendelsohn, FAO, Jenkins, TA, *et al.* (2004). The angiotensin IV/AT4 receptor. *Cell. Mol. Life Sci.* **61**: 2728–2737.

Chai, SY, Widdop, RE, Gaspari, TA, Lee, HW (2017). *WO2017015720A1 Fibrotic Treatment* (Australia: FPA PATENT ATTORNEYS PTY LTD).

Chen, H, Yang, T, Wang, MC, Chen, DQ, Yang, Y, Zhao, YY (2018). Novel RAS inhibitor 25-O-methylalisol F attenuates epithelial-to-mesenchymal transition and tubulo-Interstitial fibrosis by selectively inhibiting TGF- β -mediated Smad3 phosphorylation. *Phytomedicine* **42**: 207–218.

Chen, J-W, Hsu, N-W, Wu, T-C, Lin, S-J, Chang, M-S (2002). Asymmetric Dimethylarginine and Improves Endothelial Nitric Oxide Bioavailability and Coronary Microvascular Function in Patients With Syndrome X. *Am. J. Cardiol.* **90**: 974–982.

Chen, L, Sha, M, Li, D, Zhu, Y, Wang, X (2017). Relaxin abrogates renal interstitial fibrosis by regulating macrophage polarization via inhibition of Toll-like receptor 4 signaling. *Oncotarget* **8**: 21044–21053.

Chen, S, Ge, Y, Si, J, Rifai, A, Dworkin, LD, Gong, R (2008). Candesartan suppresses chronic renal inflammation by a novel antioxidant action independent of AT1R blockade. *Kidney Int.* **74**: 1128–1138.

Chow, BSM, Chew, EGY, Zhao, C, Bathgate, RAD, Hewitson, TD, Samuel, CS (2012). Relaxin signals through a RXFP1-pERK-nNOS-NO-cGMP-dependent pathway to up-regulate matrix metalloproteinases: The additional involvement of iNOS. *PLoS One* **7**:

Chow, BSM, Kocan, M, Bosnyak, S, Sarwar, M, Wigg, B, Jones, ES, *et al.* (2014). Relaxin requires the angiotensin II type 2 receptor to abrogate renal interstitial fibrosis. *Kidney Int.* **86**: 75–85.

Danielson, LA (2006). Relaxin Improves Renal Function and Histology in Aging Munich Wistar

Rats. *J. Am. Soc. Nephrol.* **17**: 1325–1333.

Danielson, LA, Sherwood, OD, Conrad, KP (1999). Relaxin is a potent renal vasodilator in conscious rats. *J. Clin. Invest.* **103**: 525–533.

Dézsi, CA (2014). Differences in the clinical effects of angiotensin-converting enzyme inhibitors and angiotensin receptor blockers: A critical review of the evidence. *Am. J. Cardiovasc. Drugs* **14**: 167–173.

Edwards, NC, Moody, WE, Yuan, M, Hayer, MK, Ferro, CJ, Townend, JN, *et al.* (2015). Diffuse interstitial fibrosis and myocardial dysfunction in early chronic kidney disease. *Am. J. Cardiol.* **115**: 1311–1317.

Gallop, PM, Paz, MA (1975). Posttranslational protein modifications, with special attention to collagen and elastin. *Physiol. Rev.* **55**: 418–487.

Garber, SL, Mirochnik, Y, Brecklin, CS, Unemori, EN, Singh, AK, Slobodskoy, L, *et al.* (2001). Relaxin decreases renal interstitial fibrosis and slows progression of renal disease. *Kidney Int.* **59**: 876–882.

Hewitson, TD, Ho, WY, Samuel, CS (2010). Antifibrotic Properties of Relaxin : In Vivo Mechanism of Action in Experimental Renal Tubulointerstitial. *Endocrinology* **151**: 4938–4948.

Hewitson, TD, Mookerjee, I, Masterson, R, Zhao, C, Tregear, GW, Becker, GJ, *et al.* (2007). Endogenous relaxin is a naturally occurring modulator of experimental renal tubulointerstitial fibrosis. *Endocrinology* **148**: 660–669.

Hill, NR, Fatoba, ST, Oke, JL, Hirst, JA, O’Callaghan, CA, Lasserson, DS, *et al.* (2016). Global Prevalence of Chronic Kidney Disease – A Systematic Review and Meta-Analysis. *PLoS One* **11**: e0158765.

Huang, G, Cheng, P, Ding, L, Wang, L, Hu, J, Zhang, Y, *et al.* (2019). Protective effect of Xin-Ji-Er-Kang on cardiovascular remodeling in high salt-induced hypertensive mice. *Exp. Ther. Med.* **17**: 1551–1562.

Ina, Y, Yao, K, Ohno, T, Suzuki, K, Sonoka, R, Sato, H (2004). Effects of Benidipine and

Candesartan on Kidney and Vascular Function in Hypertensive Dahl Rats. *Hypertens. Res.* **26**: 569–576.

Jones, ES, Black, MJ, Widdop, RE (2012). Influence of angiotensin II subtype 2 receptor (AT 2R) antagonist, PD123319, on cardiovascular remodelling of aged spontaneously hypertensive rats during chronic angiotensin II subtype 1 receptor (AT 1R) blockade. *Int. J. Hypertens.* **2012**..

Kakoki, M, McGarrah, RW, Kim, H-S, Smithies, O (2007). Bradykinin B1 and B2 receptors both have protective roles in renal ischemia/reperfusion injury. *Proc. Natl. Acad. Sci. U. S. A.* **104**: 7576–81.

Kong, J, Zhang, K, Meng, X, Zhang, Y, Zhang, C (2015). Dose-Dependent Bidirectional Effect of Angiotensin IV on Abdominal Aortic Aneurysm via Variable Angiotensin Receptor Stimulation. *Hypertension* **66**: 617–626.

Lekgabe, ED, Kiriazis, H, Zhao, C, Xu, Q, Moore, XL, Su, Y, *et al.* (2005). Relaxin reverses cardiac and renal fibrosis in spontaneously hypertensive rats. *Hypertension* **46**: 412–418.

Lewis, M, Deshpande, U, Guzman, L, Grove, B, Huang, X, Erikson, M, *et al.* (2001). Systemic relaxin administration stimulates angiogenic cytokine expression and vessel formation in a rat myocardial infarct model. In *Relaxin 2000*, pp 159–167.

Liang, B, Leenen, FHH (2008). Prevention of salt-induced hypertension and fibrosis by AT 1-receptor blockers in Dahl S rats. *J. Cardiovasc. Pharmacol.* **51**: 457–466.

Longo, DL, Rockey, DC, Bell, PD, Hill, J a (2015). Fibrosis — A Common Pathway to Organ Injury and Failure. *N. Engl. J. Med.* **372**: 1138–1149.

Lozano, R, Naghavi, M, Foreman, K, Lim, S, Shibuya, K, Aboyans, V, *et al.* (2012). Global and regional mortality from 235 causes of death for 20 age groups in 1990 and 2010: A systematic analysis for the Global Burden of Disease Study 2010. *Lancet* **380**: 2095–2128.

Ma, L-J, Corsa, BA, Zhou, J, Yang, H, Li, H, Tang, Y-W, *et al.* (2011). Angiotensin type 1 receptor modulates macrophage polarization and renal injury in obesity. *Am J Physiol Ren. Physiol* **300**: F1203–F1213.

Maric, C, Sandberg, K, Hinojosa-Laborde, C (2004). Glomerulosclerosis and tubulointerstitial fibrosis are attenuated with 17 β -estradiol in the aging Dahl salt sensitive rat. *J. Am. Soc. Nephrol.* **15**: 1546–1556.

Martin, B, Gabris-Weber, BA, Reddy, R, Romero, G, Chattopadhyay, A, Salama, G (2018). Relaxin reverses inflammatory and immune signals in aged hearts. *PLoS One* **13**: 1–17.

Masini, E, Bani, D, Bello, MG, Bigazzi, M, Mannaioni, PF, Sacchi, TB (1997). Relaxin Counteracts Myocardial Damage Induced by Ischemia-Reperfusion in Isolated Guinea Pig Hearts: Evidence for an Involvement of Nitric Oxide ¹. *Endocrinology* **138**: 4713–4720.

Masini, E, Nistri, S, Vannacci, A, Bani Sacchi, T, Novelli, A, Bani, D (2004). Relaxin inhibits the activation of human neutrophils: involvement of the nitric oxide pathway. *Endocrinology* **145**: 1106–12.

Mookerjee, I, Hewitson, TD, Halls, ML, Summers, RJ, Mathai, ML, Bathgate, R a D, *et al.* (2009). Relaxin inhibits renal myofibroblast differentiation via RXFP1, the nitric oxide pathway, and Smad2. *FASEB J.* **23**: 1219–29.

Mountford, SJ, Albiston, AL, Charman, WN, Ng, L, Holien, JK, Parker, MW, *et al.* (2014). Synthesis, Structure – Activity Relationships and Brain Uptake of a Novel Series of Benzopyran Inhibitors of Insulin-Regulated Aminoamidase. *J. Med. Chem.* **57**: 1368–1377.

Nistri, S, Chiappini, L, Sassoli, C, Bani, D, Medicine, F (2003). Relaxin inhibits lipopolysaccharide-induced adhesion of neutrophils to coronary endothelial cells by a nitric oxide- mediated mechanism. *FASEB J.*

Noda, M, Matsuo, T, Fukuda, R, Ohta, M, Nagano, H, Shibouta, Y, *et al.* (1999). Effect of candesartan cilexetil (TCV-116) in rats with chronic renal failure. *Kidney Int.* **56**: 898–909.

Plante, E, Menaouar, A, Danalache, BA, Yip, D, Broderick, TL, Chiasson, JL, *et al.* (2015). Oxytocin treatment prevents the cardiomyopathy observed in obese diabetic male db/db mice. *Endocrinology* **156**: 1416–1428.

Rafiq, K, Nishiyama, A, Konishi, Y, Morikawa, T, Kitabayashi, C, Kohno, M, *et al.* (2014).

Regression of glomerular and tubulointerstitial injuries by dietary salt reduction with combination therapy of angiotensin II receptor blocker and calcium channel blocker in Dahl salt-sensitive rats. *PLoS One* **9**:

Royce, SG, Shen, M, Patel, KP, Huuskes, BM, Ricardo, SD, Samuel, CS (2015). Mesenchymal stem cells and serelaxin synergistically abrogate established airway fibrosis in an experimental model of chronic allergic airways disease. *Stem Cell Res.* **15**: 495–505.

Samuel, CS (2009). Determination of Collagen Content, Concentration, and Sub-types in Kidney Tissue. In *Kidney Research. Methods in Molecular Biology (Methods and Protocols)*, G. Becker, and T.D. Hewitson, eds. (Humana Press), p.

Samuel, CS, Hewitson, TD (2009). Relaxin and the progression of kidney disease. *Curr. Opin. Nephrol. Hypertens.* **18**: 9–14.

Samuel, CS, Royce, SG, Hewitson, TD, Denton, KM, Cooney, TE, Bennett, RG (2017). Anti-fibrotic actions of relaxin. *Br. J. Pharmacol.* **174**: 962–976.

Sanchez-Mas, J, Lax, A, Asensio-Lopez, MC, Lencina, M, Fernandez-del Palacio, MJ, Soriano-Filiu, A, *et al.* (2017). Early Anti-inflammatory and Pro-angiogenic Myocardial Effects of Intravenous Serelaxin Infusion for 72 H in an Experimental Rat Model of Acute Myocardial Infarction. *J. Cardiovasc. Transl. Res.* **10**: 460–469.

Santos, E, Picoli Souza, K de, Silva, E da, Batista, E, Martins, P, D'Almeida, V, *et al.* (2009). Long term treatment with ACE inhibitor enalapril decreases body weight gain and increases life span in rats. *Biochem. Pharmacol.* **78**: 951–958.

Saveanu, L, Endert, P Van (2012). The role of insulin-regulated aminopeptidase in MHC class I antigen presentation. *Front. Immunol.* **3**: 1–13.

Schelbert, EB, Fonarow, GC, Bonow, RO, Butler, J, Gheorghiade, M (2014). Therapeutic targets in heart failure: Refocusing on the myocardial interstitium. *J. Am. Coll. Cardiol.* **63**: 2188–2198.

Senador, D, Kanakamedala, K, Irigoyen, MC, Morris, M, Elased, KM (2009). Cardiovascular and autonomic phenotype of db/db diabetic mice. *Exp. Physiol.* **94**: 648–658.

Shihab, FS (2007). Do we have a pill for renal fibrosis? *Clin. J. Am. Soc. Nephrol.* **2**: 876–878.

Tugtepe, H, Sener, G, Biyikli, N, Yuksel, M, Cetinel, S, Gedik, N, *et al.* (2007). The protective effect of oxytocin on renal ischemia/reperfusion injury in rats. *Regul. Pept.* **140**: 101–108.

Unemori, EN, Lewis, M, Constant, J, Arnold, G, Grove, BH, Normand, J, *et al.* (2000). Relaxin induces vascular endothelial growth factor expression and angiogenesis selectively at wound sites. *Wound Repair Regen.* **8**: 361–370.

Wang, C, Kemp-Harper, BK, Kocan, M, Ang, SY, Hewitson, TD, Samuel, CS (2016). The anti-fibrotic actions of relaxin are mediated through a NO-sGC-cGMP-dependent pathway in renal myofibroblasts in vitro and enhanced by the NO donor, diethylamine NONOate. *Front. Pharmacol.* **7**: 1–12.

Wang, H, Delaney, K, Kwiecien, J, Smeda, J, Lee, R (1997). Prevention of stroke with perindopril treatment in stroke-prone spontaneously hypertensive rats. *Clin Invest Med* **20**: 327–338.

Weir, MR, Fink, JC (2005). Salt intake and progression of chronic kidney disease: An overlooked modifiable exposure? A commentary. *Am. J. Kidney Dis.* **45**: 176–188.

Wetzel, V, Schinner, E, Kees, F, Hofmann, F, Faerber, L, Schlossmann, J (2016). Involvement of cyclic guanosine monophosphate-dependent protein kinase I in renal antifibrotic effects of serelaxin. *Front. Pharmacol.* **7**: 1–13.

Woessner Jr, J (1995). Quantification of matrix metalloproteinases in tissue samples. *Methods Enzym.* **248**: 510–52.

Wontanawatot, W, Eiam-Ong, S, Leelahavanichkul, A, Kanjanabuch, T (2011). An update on RAAS blockade and peritoneal membrane preservation: the ace of art. *J Med Assoc Thai* **94**: S175-183.

Yamaguchi, I, Tchao, BN, Burger, ML, Yamada, M, Hyodo, T, Giampietro, C, *et al.* (2012). Vascular endothelial cadherin modulates renal interstitial fibrosis. *Nephron - Exp. Nephrol.* **120**: e20–e31.

Chapter 5

**TO COMPARE AND COMBINE THE ANTI-FIBROTIC ACTIONS OF
SERELAXIN TO VARIOUS PEPTIDE- AND CELL-BASED TREATMENTS IN
AN UUO-INDUCED MOUSE MODEL OF TUBULOINTERSTITIAL FIBROSIS.**

5.1 Introduction

Renal fibrosis is a hallmark of CKD and can present itself as glomerulosclerosis, vascular sclerosis and/or interstitial fibrosis surrounding the kidney tubules (Hewitson, 2009). While high salt consumption is a clinically relevant problem, can have detrimental effects on glomerular hemodynamics, and can induce renal inflammation, hypertrophy, glomerular damage/sclerosis and interstitial fibrosis independently of blood pressure changes (Boero *et al.*, 2002), both experimentally (Weir and Fink, 2005) and clinically, it can take several weeks-to-months to induce CKD. Furthermore, the degree of experimental renal damage, hyperfiltration and dysfunction associated with salt-induced diets that do not induce hypertension is more moderate compared to hypertension-inducing salt-fed diets (Yoshida *et al.*, 2012). This moderate degree of renal damage and fibrosis associated with the 5% NaCl salt diet-induced murine model utilised in Chapters 3 and 4 may have contributed to the striking and similar anti-fibrotic effects of RLX and HFI. Hence, to further validate the anti-fibrotic efficacy of these therapies, their effects in a more severe model of kidney injury needed to be investigated.

Unilateral ureteric obstruction (UUO) of mice is well-established model of primary tubulointerstitial disease that is rapidly-occurring, reproducible and occurs independently of species, strain and sex (Chevalier *et al.*, 2010). It is a surgically-induced injury model that results in hydronephrosis, inflammation and severe scarring (fibrosis) of the kidney. Importantly, the pathogenesis of UUO is comparable to the cascade of events seen in human progressive kidney disease associated with a range of genitourinary tract obstruction disorders (Chevalier *et al.*, 2010), albeit at an accelerated rate. Similar to what occurs following HS diet-induced kidney disease, post-UUO there is a significant influx of inflammatory cell infiltration into the renal parenchyma (as part of the wound healing response to injury), which eventually contributes to pro-fibrotic cytokine release, and fibroblast proliferation and differentiation leading to a progressive increase in interstitial ECM/collagen deposition (fibrosis) (Cochrane, 2005). In turn, this leads to tubular atrophy, podocyte depletion and capillary reduction which are all factors that decrease the ability of the obstructed kidney to eliminate waste products, and regulate blood pressure and fluid balance (Huuskes *et al.*, 2015). For this reason the FDA considers this

model the 'gold-standard' to evaluate the anti-fibrotic and renoprotective efficacy of new therapies (Sasaki *et al.*, 2014).

The anti-fibrotic efficacy of RLX had already been evaluated in the UUO model (Hewitson *et al.*, 2010; Huuskes *et al.*, 2015). However, as this thesis focused on comparing its anti-fibrotic efficacy to that of several other currently-used and emerging/newly-developed compounds, this Chapter aimed to compare the effects of RLX to various other peptide and cell-based therapies, as well as combination therapies involving RLX, in the UUO model. Of these other compounds that were investigated, B7-33, the single B-chain mimetic of RLX that contained residues 7-29 of the original B-chain of RLX in addition to the residues lysine-arginine-serine-leucine (KRSL) at the C-terminus (Hossain *et al.*, 2016), was one of them. B7-33 retained the binding motif of the two-chained hormone, binds exclusively to RXFP1 and mimicked the anti-fibrotic efficacy of RLX in experimental mouse models of myocardial infarction-induced heart failure, isoproterenol-induced cardiomyopathy and ovalbumin-induced chronic allergic airways disease (Hossain *et al.*, 2016). Like RLX, B7-33 promoted ERK1/2 and MMP activity to induce its anti-fibrotic effects (Hossain *et al.*, 2016). Additionally, this Chapter aimed to compare the effects of RLX to compounds that targeted the RAS, including the IRAP inhibitor, HFI and a newly-developed compound, β -pro⁷-Ang III (BPRO), that more selectively targeted the AT₂R over the AT₁R (Del Borgo *et al.*, 2015). BPRO was developed by substituting the individual native amino acids of the angiotensin III (Ang III) sequence with β -amino acids. This resulted in a compound that had >20,000-fold selectivity for the AT₂R over the AT₁R, when a β -amino acid substitution was made at the proline amino acid, at position 7 of the Ang III sequence (Del Borgo *et al.*, 2015). Not only was BPRO more selective for the AT₂R compared to CGP, it evoked similar vasorelaxation to CGP in a concentration-dependent manner. However, neither the renoprotective and anti-fibrotic efficacy of B7-33, HFI or BPRO had been evaluated in the UUO model.

Additionally, as the anti-fibrotic effects of RLX were shown to either prevent (Huuskes *et al.*, 2015) or reduce (Royce *et al.*, 2015) fibrosis progression in the kidney and lung, respectively, to create an improved environment and enhance the therapeutic effects of stem cell-based therapies, the combined effects of RLX and human amnion epithelial cells (hAECs) were compared to the effects of RLX and the other drugs evaluated. hAECs can be easily isolated via non-invasive procedures

from the amniotic sac of the mature placenta (Miki *et al.*, 2005), are non-immunogenic (Akle *et al.*, 1981), and possess several therapeutic (anti-inflammatory and reparative) properties that have resulted in these cells inhibiting immune cell activation of pro-inflammatory cytokines and microRNAs in patients with acute kidney injury (Liu *et al.*, 2017). However, the fibrosis associated with chronic disease settings was shown to hinder hAEC viability and function, resulting in these cells only having a partial ability to inhibit chronic allergic airways disease-induced airway/lung remodelling, fibrosis and function (Royce *et al.*, 2016). As co-treatment of hAECs with RLX increased hAEC proliferation and normalisation of airway/lung fibrosis in the setting of chronic allergic airways disease (Royce *et al.*, 2016), the combined effects of this combination therapy was compared to the other treatments evaluated in the setting of UUO-induced kidney disease.

Furthermore, as there are other limitations to using stem cell-based therapies, attention has turned to determining if the vesicles (exosomes) that are secreted by stem cells such as hAECs, may offer advantages to mediating cell-induced therapeutic efficacy. Exosomes are ~40-100nm in diameter and contain the reparative components of their parental cells (such as proteins, lipids and microRNAs) (Valadi *et al.*, 2007; Urbanelli *et al.*, 2015). It has been postulated that owing to their smaller size (compared to their parental cells), exosomes avoid recognition by the immune system and maintain the integrity of cell membrane to avoid degradation (Vader *et al.*, 2016); and do not replicate as they lack a nucleus. Once isolated and purified, exosomes can be freeze-thawed for immediate use, overcoming the need for cell culture-induced expansion of hAECs for therapeutic administration, which can lead to culture-induced loss of function. hAECs can also aggregate and become entrapped in the lungs (when administered at >2 million cells), increasing the risk of an embolism and prevention of their migration to sites of damage (Kikuchi *et al.*, 2002; Kyriakou *et al.*, 2008; Moodley *et al.*, 2010; Moll *et al.*, 2014). Exosomes on the other hand are less likely to clog pulmonary microvessels and hence, can offer the therapeutic impact of several million hAECs, which can more effectively migrate to sites of damage. However, a recent study showed that the fibrosis associated with established/chronic lung diseases also impaired the therapeutic efficacy of hAEC-derived exosomes (EXO) (like their parental cells)(Royce *et al.*, 2016), which was effectively resolved by co-administration of RLX (Royce *et al.*, 2019). Hence, this Chapter also aimed to evaluate the effects of EXO alone and in combination with RLX to the other

therapies evaluated against UUO-induced nephropathy, which included an ACE inhibitor (PERIN) as a current standard of care medication.

5.2 Methods

Materials

Recombinant H2 Relaxin (RLX; was provided by Corthera Inc., San Carlos, CA, USA; a subsidiary of Novartis AG, Basel, Switzerland); and Perindopril was purchased from LabChem Express (Zelienople, Pa USA). HFI-419 was provided by A/Prof. Siew Yeen Chai (Department of Physiology, Monash University); B7-33 was provided by A/Prof. Akhter Hossain (Florey Institute of Neuroscience and Mental Health, University of Melbourne, Melbourne, Victoria, Australia); β -Pro⁷Ang III was provided by Dr. Mark Del Borgo (Department of Biochemistry, Monash University, Clayton, Victoria, Australia); hAECs and hAEC-derived exosomes were provided by A/Prof. Rebecca Lim (Hudson Institute of Medical Research, Clayton, Victoria, Australia).

5.2.1 Animals

7 to 8-week-old male C57BL/6J mice weighing between 20-25g were obtained from Monash Animal Research Platform (Monash University, Clayton, Victoria, Australia) and housed under a controlled environment, on a 12 hour light/12 hour dark lighting cycle with access to standard rodent lab chow (Barastock Stockfeeds, Pakenham, Victoria, Australia) and tap water *ad libitum* throughout the experimental period. All mice were provided an acclimatisation period of at least 5 days before any experimentation and procedures were performed. All animal use and procedures were approved by a Monash University Animal Ethics Committee (Ethics number: MARP/2017/034), which complies with the Australian Guidelines for the Care and Use of Laboratory Animals for Scientific Purposes.

5.2.2 Experimental model and treatments

The UUO model was utilised in this Chapter, as it recapitulates many of the primary mechanisms involved in human progressive renal disease within a short period (Chevalier *et al.*, 2010). UUO surgery was performed on sub-groups of mice (n=6 per group) under inhalation anaesthesia (2-3% isoflurane; Baxter Healthcare Pty Ltd; NSW, Australia). A 2 cm wide flank incision was made

to access the left ureter. Ligation of the ureter was completed with 5.0 surgical silk (Johnson & Johnson, NJ, USA). Once ligated, the ureter and corresponding kidney were placed back into their original positions within the body, before warm saline was applied to the wound site (to wash any blood associated with creating the 2cm flank incision).

As hAECs and hAEC-derived exosomes were administered via intra-renal (i.r) injection (which had allowed for direct delivery of mesenchymal stem cells into the damaged kidney post-UUO) (Huuskens *et al.*, 2015), it was recommended by the Monash Animal Ethics Committee, that this be completed while mice were anaesthetised for ligation of their left ureters (rather than undergo a separate period of anaesthesia post-surgery). Hence, for consistency, all treatments were administered at the time of UUO-induction. Over a period of 3 days, 22 mice (2 mice per group x 11 groups) were subjected to SHAM or UUO surgery and the various treatments administered. This was performed over a 3-week period so that n=6 mice per group could be achieved. Sub-groups of mice received 1) RLX (0.5 mg/kg/day; the same dose as that used in Chapters 3 and 4); 2) B7-33 (0.25mg/kg/day; an equivalent dose to that of RLX when corrected for molecular weight); 3) the vehicle (VEH) for HFI (which contained a 1:3 ratio of DMSO:30% 2-hydroxypropyl- β -cyclodextrin solution); 4) HFI (0.72 mg/kg/day; the same dose as that used in Chapter 4); 5) BPRO (0.1 mg/kg/day; a dose that had demonstrated vasorelaxation (Del Borgo *et al.*, 2015) and anti-fibrotic efficacy in experimental models of cardiovascular disease); 6) hAECs (1×10^6 cells/mouse) in combination with RLX (0.5mg/kg/day; based on this amount of cells in combination with this dose of RLX being able to effectively normalise airway/lung fibrosis in an experimental model of chronic allergic airways disease) (Royce *et al.*, 2016); 7) hAEC-derived exosomes (EXO; 25 μ g/mouse; based on this amount of EXO demonstrating partial therapeutic efficacy in experimental models of lung disease) (Royce *et al.*, 2019); 8) EXO (25 μ g/mouse) in combination with RLX (0.5mg/kg/day); or 9) PERIN (1mg/kg/day; a dose that had demonstrated anti-fibrotic and anti-hypertensive efficacy in renovascular hypertensive rats (Nagai *et al.*, 2004); and which was not expected to induce the adverse effects induced by 4mg/kg/day of the drug that was observed in Chapter 4). With the exception of hAECs or hAEC-EXO, all other treatments were delivered by subcutaneously administered 1007D osmotic mini-pumps (Alzet, CA, USA),

which continuously infused each drug into the circulation of treatment mice over a 7-day period, at a flow rate of 0.5µl/hour.

For mice receiving mini-pumps, the intraperitoneal muscle and skin overlaying the wound site was sutured (with 5.0 silk) prior to pump implantation. Pumps were administered on the dorsal surface of the mouse, via a 1cm incision that was undertaken to create a skin pocket for the pump to be placed into, which was closed with michelle clips (Becton & Dickinson, Sparks, MD, USA). For mice receiving i.r injections of hEACs or EXO, this was done into the renal vein immediately following UUO surgery using a 0.5mL syringe and 30-gauge needle (BD Ultra-Fine™ Insulin Syringe, BD Bioscience, Sparks, MD, USA) and before the intraperitoneal muscle and skin overlaying the wound site was sutured. Following i.r injection of cells, they were located within the kidneys and lungs of mice within 1 hour of injection, but were fully localised within the kidneys by 24-48 hours post-injection, as detected by bioluminescence scanning (Huuskes *et al.*, 2015). Immediately after UUO surgery was completed, all mice were provided buprenorphine analgesia (Rickett Benckiser, NSW, Australia) as pain relief while being sutured and allowed to recover from anaesthesia. Mice were then monitored until recovery was made. Sham-operated mice (n=6) underwent similar procedures except for ligation of the ureter and were thereby used as the healthy control group.

9 sub-groups of UUO-injured mice were randomly selected to receive the following treatments:

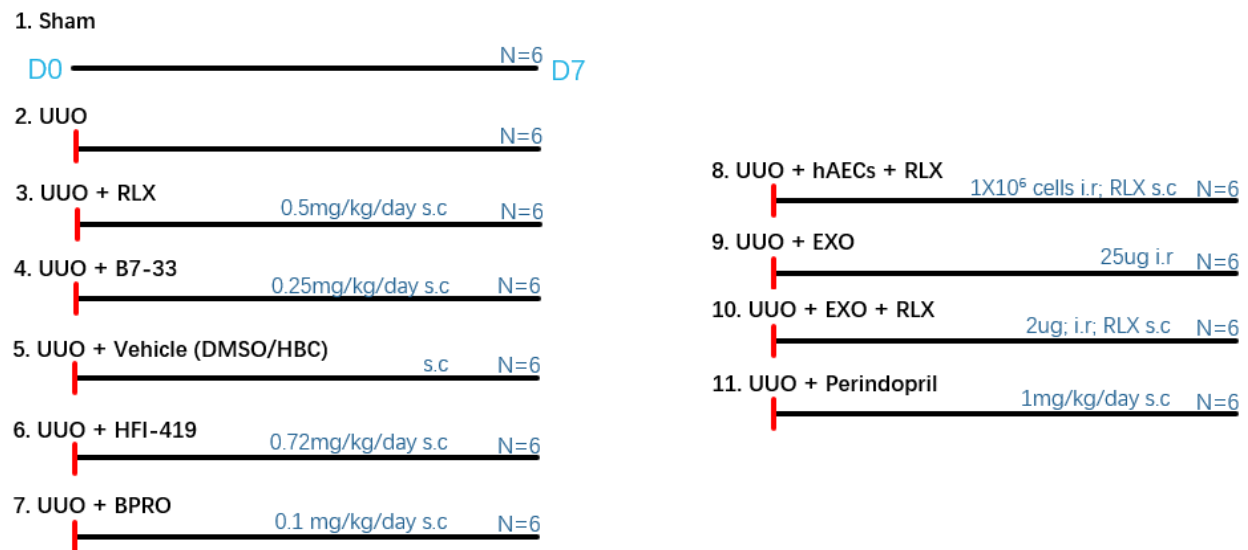


Figure 5.2.2.1. Experimental design for the UUO model

Mice were randomized into 11 treatment groups. Group 1 mice underwent sham surgery and no treatment. The remaining groups underwent UUO surgery for tubulointerstitial fibrosis to develop by 7 days. Group 2 received no treatment to act as the injury alone group. All other groups received the various treatments described above, which were administered s.c via osmotic minipump and/or by i.r injection into the renal vein on the same day as UUO surgery. On day 7 post-UUO, all mice were culled for kidney isolation and analysis.

5.2.3 Tissue collection

On day 7 post-UUO, all mice were killed for isolation of their obstructed and unobstructed kidneys, which were separately weighed. The unobstructed (right) kidney was snap frozen in liquid nitrogen and stored at -80°C. No further analysis was conducted on this kidney, as previous studies had demonstrated that although overworked, the pathology associated with the unobstructed kidney was similar to that observed in sham-operated control mice (Hewitson *et al.*, 2007). The obstructed (left) kidney was divided into four portions, two poles and two mid-portions. One mid-portion was fixed in 10% neutral buffered formaldehyde overnight, processed and embedded in paraffin wax. One pole was embedded in a cryomold filled with OCT, frozen in liquid nitrogen and stored at -80°C. The remaining mid-portion and pole were snap-frozen in

liquid nitrogen and stored at -80°C for hydroxyproline content analysis and protein extraction and analysis, respectively.

5.2.4 Kidney histopathology

Paraffin-embedded kidney sections from each mouse were serially sectioned (at 5µm thickness) and placed on Superfrost® Plus slides (Thermo Scientific, Rockford, IL, USA) for histological and immunohistochemical staining. To assess interstitial collagen deposition, one section from each mouse was sent to Monash Histology Services and underwent Masson's trichrome staining.

5.2.5 Immunohistochemistry and immunofluorescence

Immunohistochemistry (IHC) was used to detect markers of collagen turnover, inclusive of the pro-fibrotic cytokine, TGF-β1; α-smooth muscle actin (α-SMA; a marker of myofibroblast differentiation) and CD31 (a marker for vascular rarefaction of the peritubular capillaries). In each case, de-waxed slides from each mouse were subjected to either a polyclonal anti-rabbit TGF-β1 (Ab92486, 1:1000 dilution; Abcam, Cambridge, UK), monoclonal anti-human α-SMA (M0851; 1:200 dilution; DAKO Corp., Carpinteria, CA, USA) or polyclonal anti-rabbit CD31 (ab28364; 1:100 dilution; Abcam, Cambridge, UK) primary antibody and DAKO anti-mouse or anti-rabbit HRP kits containing appropriate secondary antibodies. IHC-stained sections were visualised with the avidin-biotin complex (ABC Elite; Vector, Burlingame, CA, USA) and 3,30-diaminobenzidine (DAB; Sigma-Aldrich). Immunofluorescence (IF) was used to detect markers of inflammation, inclusive of F4/80 staining for macrophage infiltration and p-IκB staining for NF-κB activity. In each case, slides from each mouse were subjected to either a monoclonal anti-rat F4/80 (MCA497R; 1:200 dilution; Bio-Rad Laboratories, Richmond, CA, USA) or polyclonal anti-rabbit p-IκB (#28595S; 1:50; Cell Signalling, Massachusetts, USA) primary antibody and a goat anti-rat Alexa Fluor 488 IgG secondary antibody (A11006, Life Technologies, CA, USA).

5.2.6 Morphometric analysis

All kidney sections were scanned, captured and viewed under Monash Histology Service's Aperio Scanscope AT Turbo (Leica Microsystems Pty Ltd, VIC, Australia) or with a confocal microscope (Olympus, BX51, USA) at x20-x40 magnification for morphometric analysis of Masson's trichrome, IHC or IF-labelled tissue images. For each tissue section, 6-8 non-overlapping sections per mouse

were single-blinded and randomly selected. For each image, aside from glomerulosclerosis score, the percentage of positively-stained areas was quantified with ImageJ 1.48 software (Java, NIH).

5.2.7 Hydroxyproline assay

One mid-portion (containing cortex and medulla) of the obstructed kidney from each mouse was lyophilised to dry weight and hydrolysed in 6mmol/l hydrochloric acid as described previously (Mookerjee *et al.*, 2009; Samuel, 2009) for the measurement of hydroxyproline content, which was determined from a standard curve of purified trans-4-hydroxy-L-proline (Sigma-Aldrich). Hydroxyproline values were multiplied by a factor of 6.94, based on hydroxyproline representing ~14.4% of the amino acid composition of collagen in most mammalian tissues (Gallop and Paz, 1975), to extrapolate total collagen content. The extrapolated collagen content in turn was divided by the dry weight of each corresponding tissue to yield collagen concentration (expressed as a percentage).

5.2.8 Gelatin zymography

To determine if the treatment-induced effects on collagen were associated with changes in the expression and activity of collagen-degrading gelatinases, gelatin zymography was performed on kidney protein extracts, which were isolated using the method of Woessner (Woessner Jr, 1995) and assessed for changes in the expression and activity of MMP-2 (gelatinase-A). Equal aliquots (5µg) of the protein extracts were analysed on gelatin zymographs consisting of 7.5% acrylamide and 1 mg/ml gelatin. The gels were subsequently treated as previously detailed (Woessner, 1995). Gelatinolytic activity was identified by clear bands at the appropriate molecular weight, quantitated by densitometry and the relative optical density (OD) of MMP-2 in each group expressed as the respective value to that of the saline-treated mouse group, which was expressed as 1. Due to the number of treatment groups incorporated into this study, not all treatment groups could be compared in the same zymograph when two samples per group were loaded. Hence, all zymographs contained duplicate samples from the sham and UUO groups, so that duplicate samples from the various treatments could be compared between zymographs. Separate zymographs were also run so that n=6 samples per group could be analysed for MMP-2 expression and activity.

5.2.9 Western blotting

Using the same protein extracts obtained for gelatin zymography, equivalent aliquots (10 μ g) of protein extracts were run on pre-cast 10% SDS-polyacrylamide separating gels (Bio-Rad, Philadelphia, PA, USA), as described before (Chow *et al.*, 2012) and transferred to PVDF membranes using the Bio-Rad Trans-Blot Turbo transfer system (Bio-Rad, Philadelphia, PA, USA). Membranes were then blocked for 1 hour with 5% (w/v) skim milk powder, and then probed with either a polyclonal antibody to TIMP-1 (ab38978; 1:1000 dilution; Abcam) or a monoclonal antibody for α -tubulin (house-keeping protein; ab52866; 1:2500 dilution; Abcam) for at least 16 hours at 4°C. Subsequently, the membranes were then probed with appropriate secondary anti-rabbit or anti-mouse antibodies (1:2500 dilution in each case) using the DAKO anti-rabbit or anti-mouse HRP kits, respectively. Membranes were then developed with the Bio-Rad Clarity Western ECL substrate kit (Bio-Rad) for 5 min according to the manufacturer's protocol followed by visualisation and imaging using the Bio-rad ChemicDoc MP. The optical density (OD) of the appropriate bands were then quantified and analysed using Image Lab software (Bio-Rad). The measured density of TIMP-1 bands was then corrected to the density of corresponding α -tubulin in each sample and was then expressed as the relative ratio to that from the sham-control group, which was expressed as 1. As per the analysis of samples by gelatin zymography, due to the number of treatment groups incorporated into this study, not all treatment groups could be compared in the same Western blot when two samples per group were loaded. Hence, all blots contained duplicate samples from the sham and UUO groups, so that duplicate samples from the various treatments could be compared between blots. Separate Westerns were also run so that n=6 samples per group could be analysed for changes in TIMP-1 expression levels. Based on densitometry measurements of MMP-2 (from gelatin zymography) and TIMP-1 (from Western blotting) for each sample analysed, the MMP-2/TIMP-1 ratio for each sample, and mean \pm SEM MMP-2/TIMP-1 ratio from each treatment group, was determined.

5.2.10 Statistical analysis

All data were expressed as the mean \pm SEM and statistically analysed using GraphPad Prism v7.0 (Graphpad Software Inc., CA, USA). Data were analysed via a one-way ANOVA with Neuman-Kuels

post-hoc test for multiple comparisons between groups. In each case, data were considered significant with a p-value less than 0.05.

5.3 Results

5.3.1 The effects of UUO and the treatments investigated on measures of renal inflammation.

F4/80-stained macrophage infiltration (Figure 5.3.1) and P- κ B staining (used as a surrogate marker of NF- κ B activity; Figure 5.3.2) were used as markers of renal inflammation post-UUO and were both significantly increased in UUO-injured mice (by ~4.5-fold and ~4.8-fold, respectively; both $P < 0.001$ vs SHAM group) compared to respective measurements obtained from sham-operated (SHAM) controls. This indicated that renal inflammation was clearly evident 7 days after UUO injury. Whereas neither RLX nor B7-33 treatment alone affected the UUO-induced increase in macrophage infiltration (Figure 5.3.1), both RXP1 agonists were able to equivalently prevent the UUO-induced increase in P- κ B staining levels (by ~60-70%; both $P < 0.001$ vs UUO alone; both $P < 0.01$ vs SHAM group; Figure 5.3.2). In comparison, the IRAP inhibitor, HFI (but not the vehicle it was reconstituted in), and AT₂R agonist, BPRO, both significantly prevented macrophage infiltration (by ~40-60%) and P- κ B staining (by ~60-67%) (both $P < 0.001$ vs UUO; $P < 0.01$ vs SHAM group); suggesting that targeting the RAS offered broader protection against UUO-induced renal inflammation compared to the targeting of RXFP1. EXO alone also partially prevented the UUO-induced macrophage and P- κ B infiltration (by ~57-63%; both $P < 0.001$ vs UUO; $P < 0.01$ vs SHAM group); while the combined effects of RLX and hAECs similarly inhibited both measures of renal inflammation by ~64-70% (both $P < 0.001$ vs UUO; $P < 0.01$ vs SHAM group). Of the treatment groups evaluated, the combined effects of RLX and EXO provided the greatest protection against UUO-induced macrophage and P- κ B infiltration (both by ~80%; both $P < 0.001$ vs UUO; $P < 0.05$ vs SHAM group); however neither treatment or combination strategy evaluated fully abrogated renal inflammation after 7 days of administration. In comparison, the ACEi, PERIN, only partially prevented UUO-induced macrophage infiltration (by ~38%) and P- κ B staining (by ~62%) (both $P < 0.001$ vs UUO; $P < 0.01$ vs SHAM group), suggesting that it demonstrated similar anti-inflammatory efficacy to that of HFI alone, BPRO alone or EXO alone (Figure 5.3.1, Figure 5.3.2).

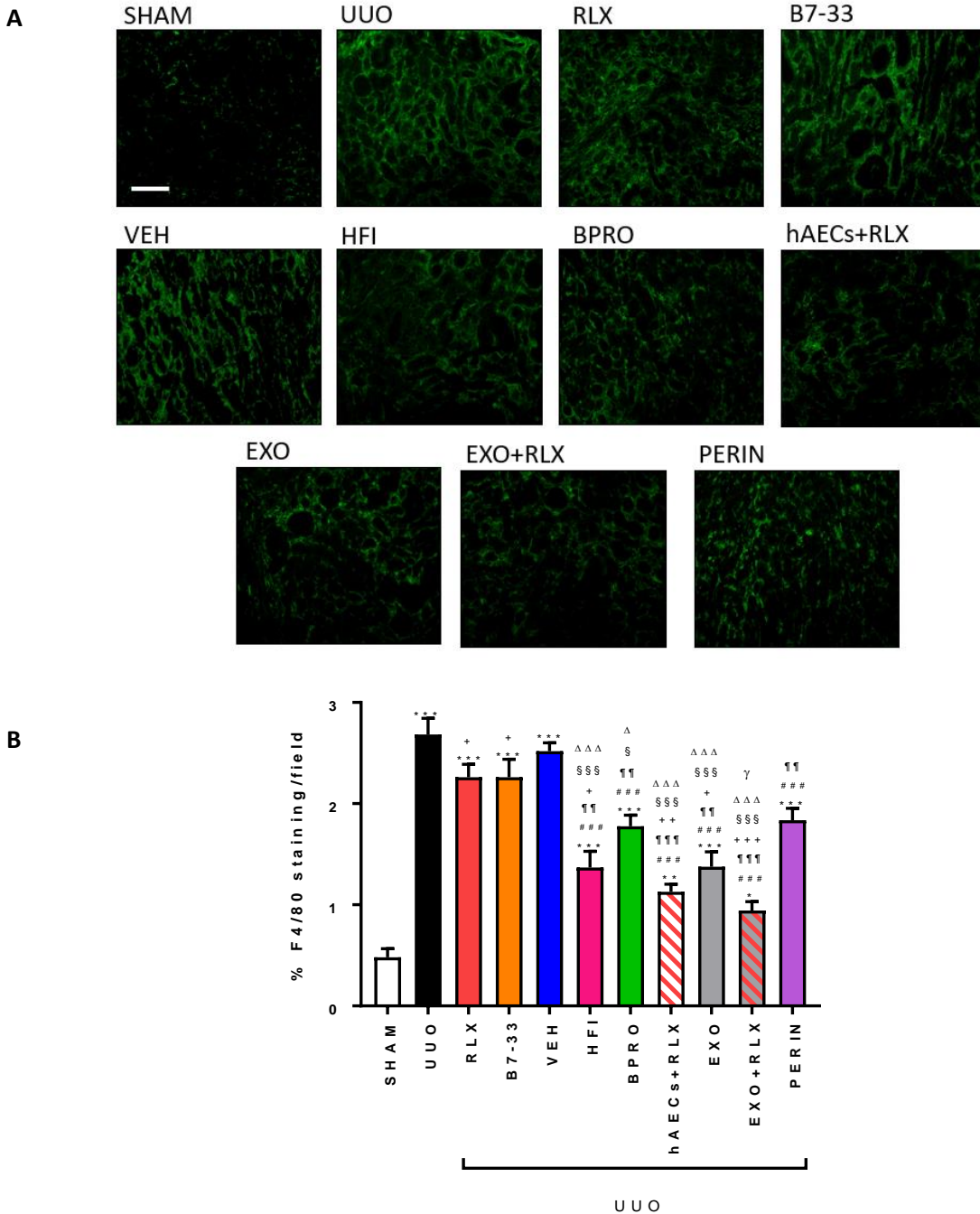


Figure 5.3.1. The effects of UUO and the treatments investigated on F4/80 staining.

A) Representative images of IF-stained kidney sections from each group studied showing F4/80 staining (macrophage infiltration). Scale bar= 50 μ m. B) also mean \pm SEM % F4/80 stained kidney sections for macrophage infiltration of n=6 mice/group. * P <0.05, ** P <0.01, *** P <0.001 vs SHAM; # P <0.05, ### P <0.001 vs UUO; ¶¶ P <0.01, ¶¶¶ P <0.001 vs VEH; § P <0.05, §§ P <0.01, §§§ P <0.001 vs RLX, Δ P <0.05, ΔΔΔ P <0.001 vs B7-33; ¶ P <0.05 vs EXO; * P <0.05, ** P <0.01, *** P <0.001 vs PERIN (one-way ANOVA).

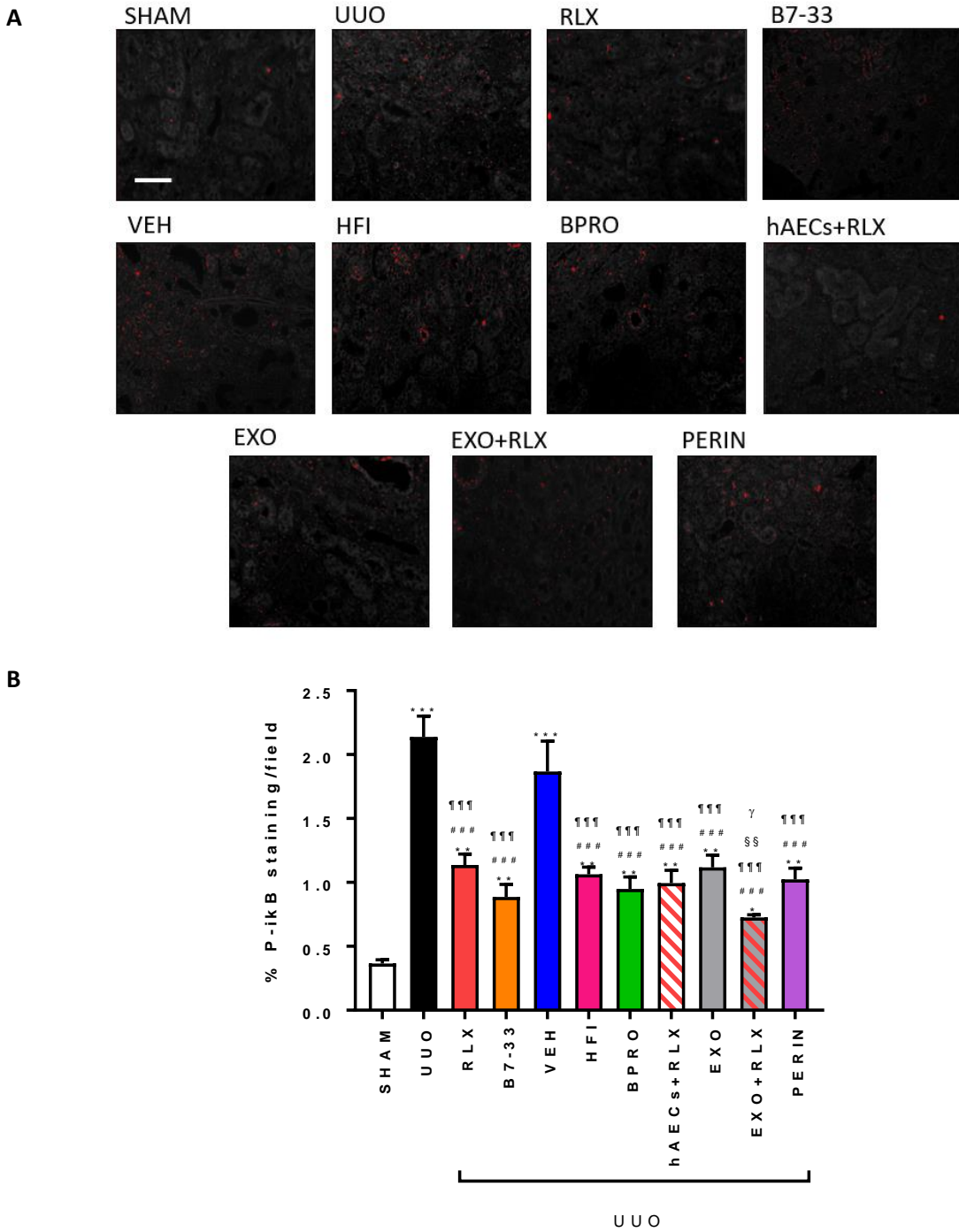


Figure 5.3.2. The effects of UUO and the treatments investigated on p-ikB staining.

A) Representative images of IF-stained kidney sections from each group studied for P-ikB, a marker for NF-kB activity. Scale bar = 50 μ m. B) Also shown is the mean \pm SEM % P-ikB stained per section (per total area stained), which was averaged from the measurements of 8 fields per section, n=6 mice/group. *P<0.05, **P<0.01, ***P<0.001 vs SHAM; ###P<0.001 vs UUO; §§P<0.01 vs RLX; ¶¶¶P<0.001 vs VEH; ¶P<0.05 vs EXO (one-way ANOVA).

5.3.2 The effects of UUO and the treatments investigated on interstitial and total renal collagen deposition (fibrosis).

Masson's trichrome-stained images were used to assess the effects of UUO and the treatments investigated on interstitial renal collagen deposition (as a measure of fibrosis). 6 randomly selected fields excluding glomeruli were analysed for interstitial collagen deposition in the cortical regions of the kidneys (Figure 5.3.3). Expectedly, UUO-injured mice had significantly increased interstitial renal collagen deposition (by ~4.2-fold; $P < 0.001$ vs SHAM group) compared to that measured in SHAM control mice (Figure 5.3.3B). This UUO-induced increase in interstitial renal fibrosis was similarly and most effectively prevented by RLX or B7-33 alone, HFI alone or by the combined effects of EXO and RLX (by ~70-80%; all $P < 0.001$ vs UUO alone; all no different to the SHAM group). In comparison, BPRO alone, EXO alone and the combined effects of hAECs and RLX only partially prevented the UUO-induced interstitial fibrosis (by ~48-57%; all $P < 0.01$ vs UUO alone; all $P < 0.01$ vs the SHAM group). However, neither the VEH for HFI or PERIN affected the UUO-induced increase in interstitial renal collagen deposition (both no different to UUO alone; Figure 5.3.3B).

Total kidney collagen concentration was also evaluated as another measure of fibrosis (Figure 5.3.3C) and was also found to be significantly increased in UUO-injured mice (by ~1-fold; $p < 0.001$ vs SHAM group) compared to respective measurements from their SHAM counterparts. This UUO-induced increase in renal collagen concentration was unaffected by VEH or PERIN treatment, but partially although significantly prevented by all other mono- and combination treatments evaluated (by ~20-38%; all $P < 0.05$ vs UUO; all $P < 0.001$ vs SHAM group) compared to UUO-injured mice alone (Figure 5.3.3C). These findings suggested that all the treatments evaluated were more effective at preventing interstitial collagen deposition compared to their ability to inhibit basement membrane collagen IV, which is the major collagenous constituent of the kidney.

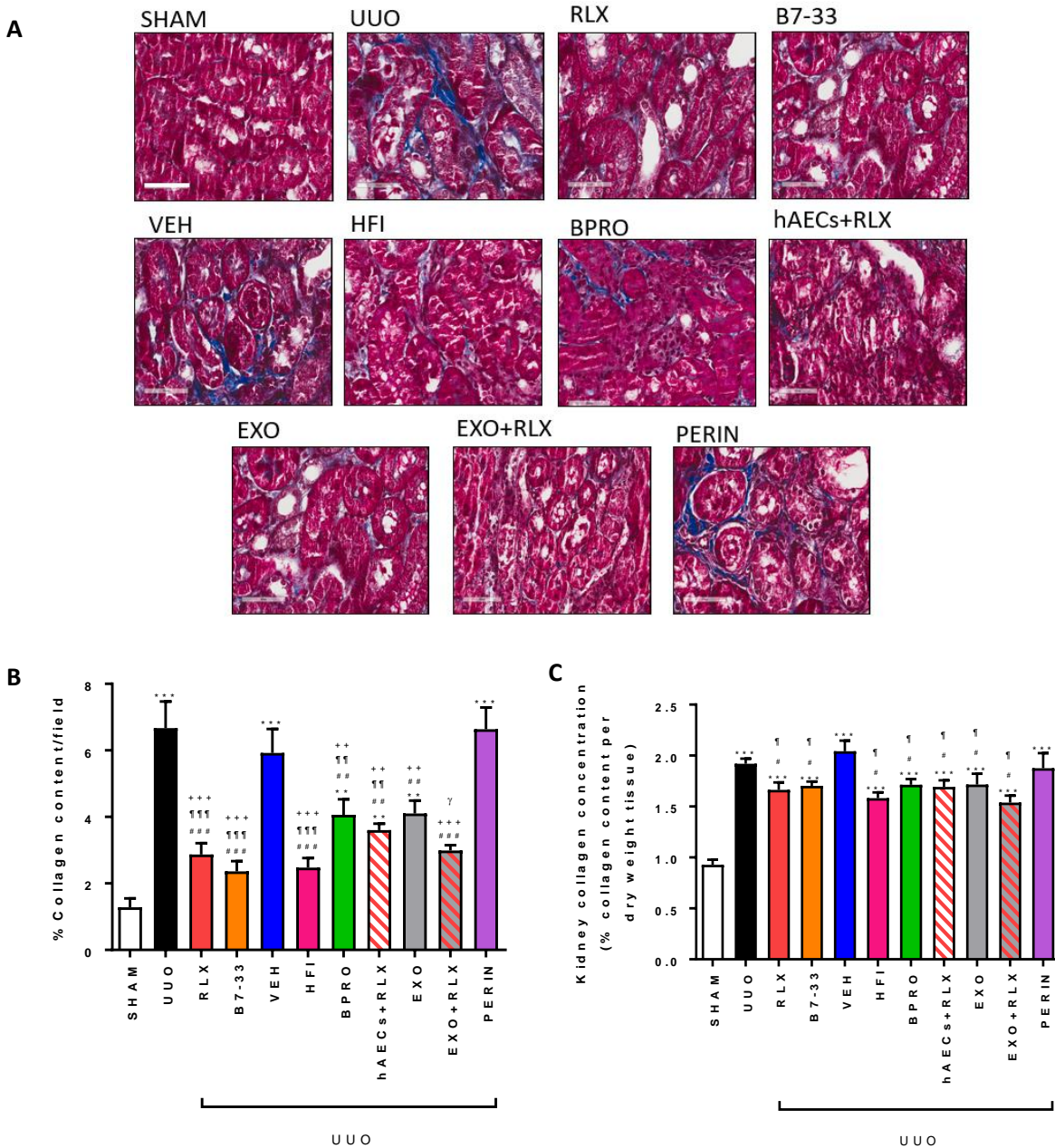


Figure 5.3.3. The effects of UUO and the treatments investigated on interstitial collagen and total kidney collagen concentration.

A) Representative photomicrographs of Masson's Trichrome stained kidney sections from each group studied showing interstitial space. Scale bar= 100 μ m. B) mean \pm SEM % interstitial collagen per 8 fields of each kidney per mice per group (n=6mice/group). C) mean \pm SEM of total kidney collagen concentration (% collagen content/dry weight tissue) obtained from hydroxyproline assay of n=6 mice/group. ** $P < 0.01$, *** $P < 0.001$ vs SHAM; # $P < 0.05$, ## $P < 0.01$, ### $P < 0.001$ vs UUO; ¶ $P < 0.05$, ¶¶ $P < 0.01$, ¶¶¶ $P < 0.001$ vs VEH; ¶ $P < 0.05$ vs EXO; ** $P < 0.01$, *** $P < 0.001$ vs PERIN (one-way ANOVA).

5.3.3 The effects of UUO and the treatments investigated on KIM-1 staining.

KIM-1-stained tissue sections (Figure 5.3.4) were used to detect the impact of the UUO injury and the treatments investigated on kidney damage. Consistent with the increased renal inflammation (Figures 5.3.1 and 5.3.2) and fibrosis (Figure 5.3.3) associated with UUO-injured mice, these mice had significantly increased KIM-1 stained renal damage (by ~4.6-fold; $P < 0.001$ vs SHAM group; Figure 5.3.4) compared to that measured in SHAM operated control mice. This UUO-induced increase in KIM-1 staining was again unaffected by VEH or PERIN treatment, partially prevented by HFI or BPRO treatment (by ~36-48%; both $P < 0.05$ vs UUO alone; both $P < 0.05$ vs SHAM alone), and further prevented by all other mono- and combination therapies evaluated (by ~70-97%; all $P < 0.01$ vs UUO alone; no different to SHAM alone) to levels that were no longer different to that measured from the SHAM control group (Figure 5.3.4B).

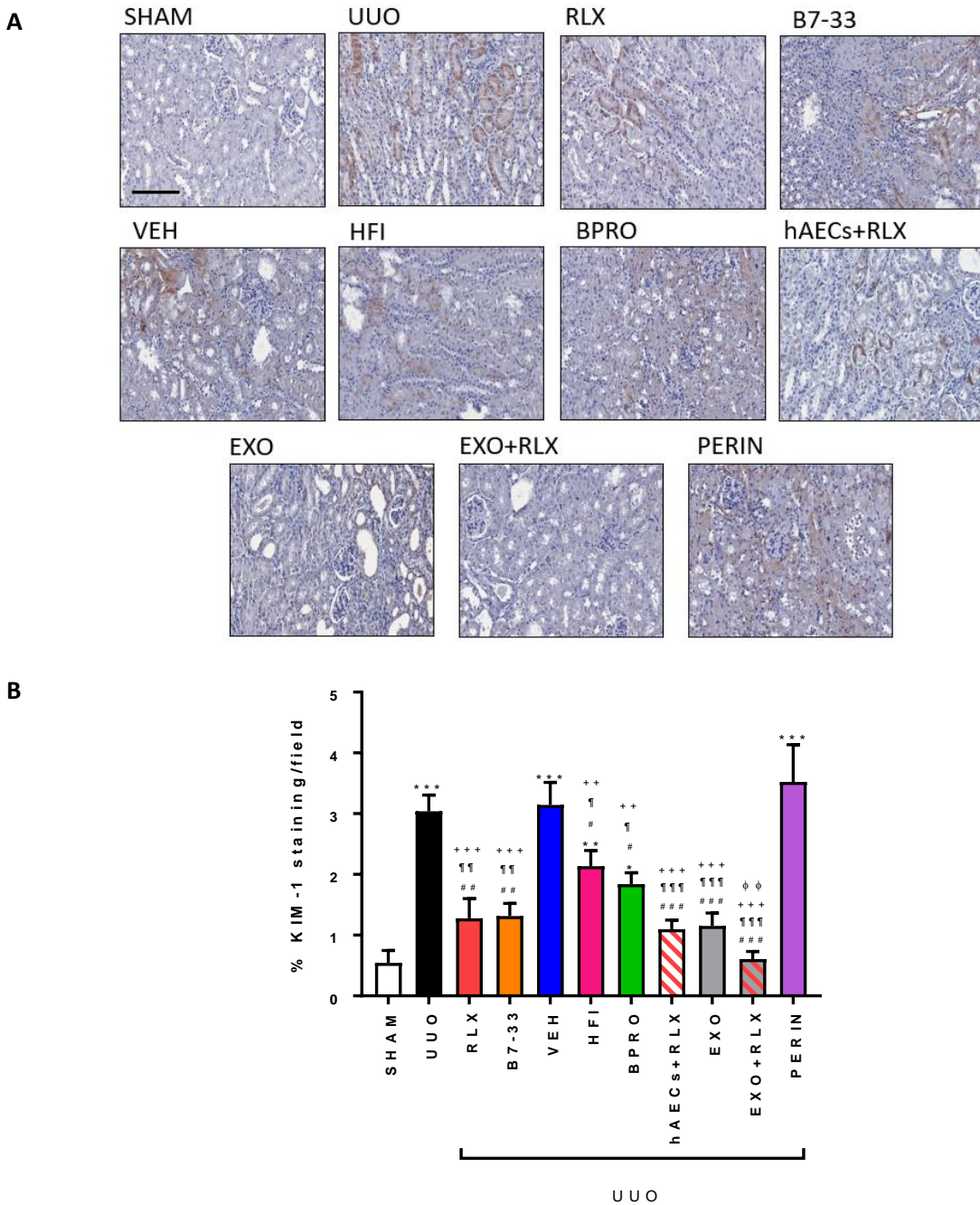


Figure 5.3.4. The effects of UUO and the treatments investigated on KIM-1 staining.

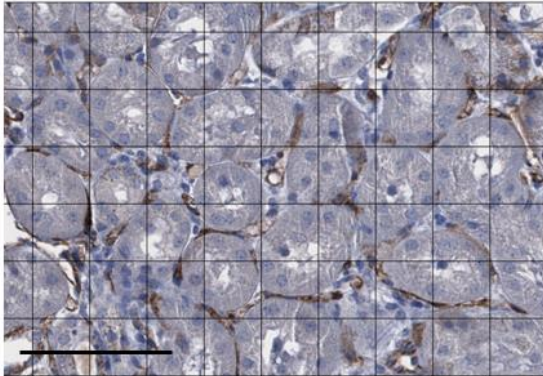
A) Representative images of IHC-stained kidney sections for KIM-1 from each group studied showing the extent of renal damage. Scale bar= 100 μ m. B) Also shown is the mean \pm SEM % KIM-1 staining per field, which was averaged from the measurements of 8 fields per section, n=6 mice/group. * P <0.05, ** P <0.01, *** P <0.001 vs SHAM; # P <0.05, ## P <0.01, ### P <0.001 vs UUO; ¶ P <0.05, ¶¶ P <0.01, ¶¶¶ P <0.001 vs VEH; ++ P <0.01, +++ P <0.001 vs PERIN; ϕϕ P <0.01 vs HFI (one-way ANOVA).

5.3.4 The effects of UUO and the treatments investigated on renal peritubular capillary density.

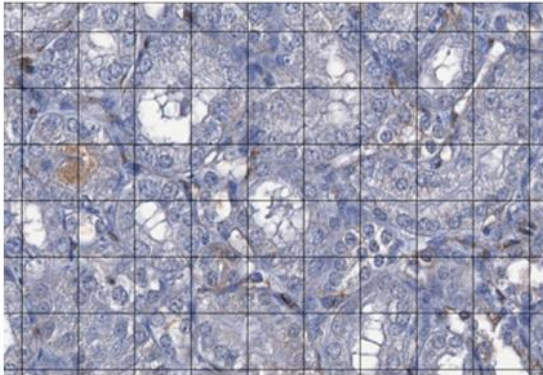
CD31-stained peritubular capillary density (Figure 5.3.5) was measured as a marker of vascular rarefaction, from randomly selected images per kidney section that were overlaid with a fixed grid (with 10,000pixel² point intersections). Individual peritubular capillaries beneath grid intersections were counted using the grid method modified by Yamaguchi and colleagues (Yamaguchi *et al.*, 2012). Consistent with the renal damage associated with UUO-injured mice (Figure 5.3.4), these mice had a ~50% reduction in renal peritubular capillary density ($P<0.001$ vs SHAM group) compared to that measured from SHAM operated control mice. This UUO-induced loss of renal peritubular capillary density was unaffected by VEH or PERIN treatment; partially restored by HFI or EXO alone treatment (by ~67%; both $P<0.05$ vs UUO alone; both $P<0.05$ vs SHAM alone), and further restored by all other mono- and combination therapies evaluated (by ~75-90%; all $P<0.01$ vs UUO alone; no different to SHAM alone) to levels that were no longer different to those measured from the SHAM control group (Figure 5.3.5B).

A

SHAM



UUO



B

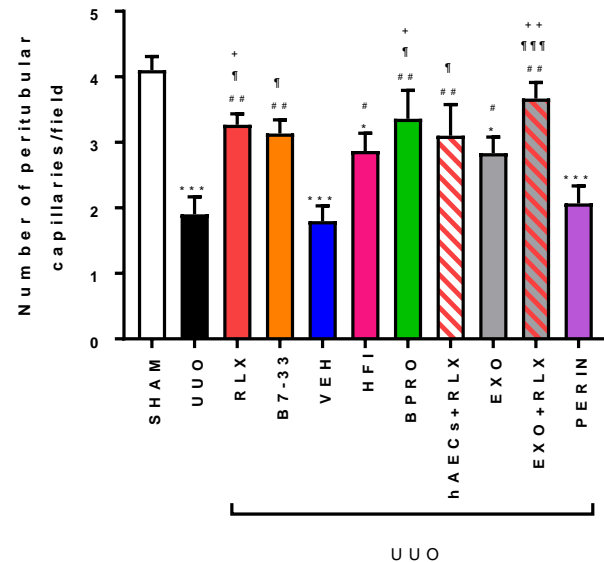


Figure 5.3.5. The effects of UUO and the treatments investigated on peritubular capillaries

A) Representative photomicrographs of CD31-stained IHC kidney sections of SHAM and UUO overlaid by a grid. Scale bar= 100 μ m. B) Also shown is the mean \pm SEM of the number of peritubular capillaries counted per field which was laying under each intersection below the grid of n=6 mice/group. * P <0.05, *** P <0.001 vs SHAM; # P <0.05, ## P <0.01 vs UUO; † P <0.05, ††† P <0.001 vs VEH; + P <0.05, ++ P <0.01 vs PERIN (one-way ANOVA).

5.3.5 The effects of UUO and the treatments investigated on renal TGF- β 1 staining.

TGF- β 1-stained kidney sections (Figure 5.3.6) were used to examine the impact of UUO-induced injury and the treatments investigated on the expression levels of this pro-fibrotic cytokine. Consistent with the increased renal inflammation (Figures 5.3.1 and 5.3.2), fibrosis (Figure 5.3.3) and damage (Figure 5.3.4) associated with UUO-injured mice, these animals had significantly increased renal cortical TGF- β 1-staining levels (by ~2-fold; $P < 0.001$ vs SHAM) compared to that measured from SHAM control mice. This UUO-induced renal cortical TGF- β 1 staining was unaffected by the VEH treatment, partially but significantly prevented by PERIN treatment (by ~35%; $P < 0.05$ vs UUO alone; $P < 0.01$ vs SHAM group), and further prevented by all other mono- and combination therapies evaluated (all $P < 0.001$ vs UUO alone; no different to SHAM alone) to levels that were no longer different to that measured from the SHAM control group (Figure 5.3.6B). Of further note, the combined effects of RLX and hAECs or EXO were able to prevent the UUO-induced increase in renal cortical TGF- β 1 staining to a greater extent than PERIN treatment alone (by ~52% and ~56%, respectively; both $P < 0.05$ vs UUO+PERIN group; Figure 5.3.6B).

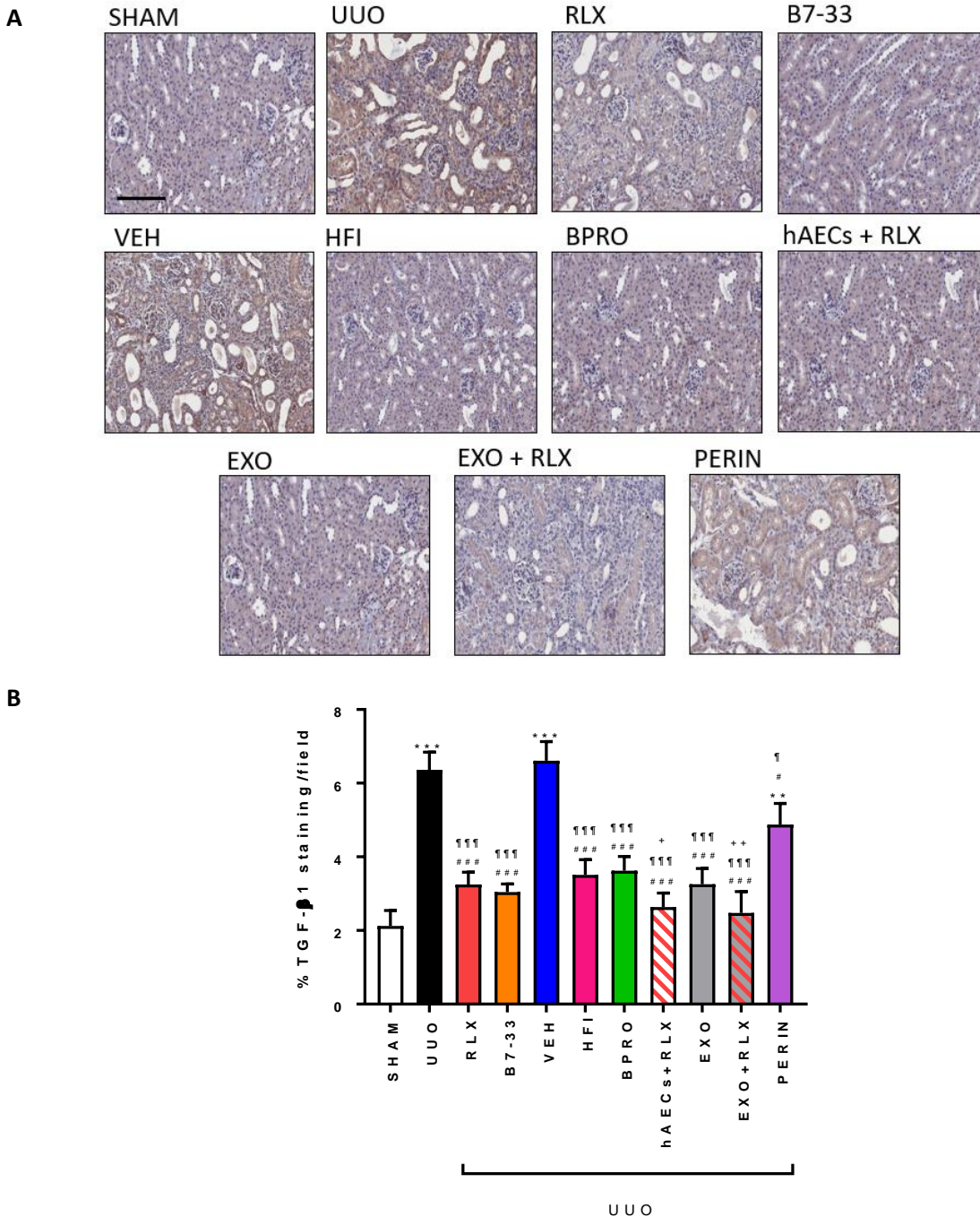


Figure 5.3.6. The effects of UUO and the treatments investigated on TGF-β1 staining.

A) Representative images of kidney sections for renal TGF-β1 expression from each group studied showing interstitial expression of the pro-fibrotic cytokine. Scale bar = 100 μm. B) Also shown is the mean ± SEM % TGF-β1 stained per field analysed, which was averaged from the measurements of 8 fields per section, n=6 mice/group. **P<0.01, ***P<0.001 vs SHAM; #P<0.05, ###P<0.001 vs UUO; ¶P<0.05, ¶¶¶P<0.001 vs VEH; +P<0.05, ++P<0.01 vs PERIN (one-way ANOVA).

5.3.6 The effects of UUO and the treatments investigated on renal myofibroblast differentiation.

α -SMA-stained tissue sections (Figure 5.3.7) were used to detect the impact of UUO injury and the treatments studied on interstitial myofibroblast accumulation. Consistent with the increased renal fibrosis (Figure 5.3.3) and renal cortical TGF- β 1 expression levels (Figure 5.3.6) that were measured in UUO-injured mice, these mice also had significant interstitial renal myofibroblast accumulation (by ~19-fold; $P < 0.001$ vs SHAM group) compared to that measured in SHAM control mice. This UUO-induced increase in renal myofibroblast accumulation was unaffected by VEH or PERIN treatment, partially and equivalent prevented by RLX, B7-33, HFI or BPRO alone treatment (by ~48-55%; all $P < 0.001$ vs UUO alone; all $P < 0.001$ vs SHAM alone), and to a slightly greater extent by EXO alone, hAECs+RLX or EXO+RLX (by ~70-80%; all $P < 0.001$ vs UUO alone; all $P < 0.001$ vs SHAM alone). In addition, EXO+RLX had a greater effect ($p < 0.01$ vs RLX alone) at reducing α -SMA-staining of tissues compared to RLX treatment alone, suggesting an additive effect of EXO and RLX. However, none of these treatments fully prevented the UUO-induced increase in interstitial renal myofibroblast accumulation (Figure 5.3.7).

In general, all individual and combination therapies evaluated demonstrated greater renoprotection compared to the effects of PERIN, which induced some anti-inflammatory but limited anti-fibrotic efficacy in the model studied. The findings that PERIN, however, was able to prevent measures of UUO-induced inflammation indicated that it was bioactive at the dose (1mg/kg/day) administered.

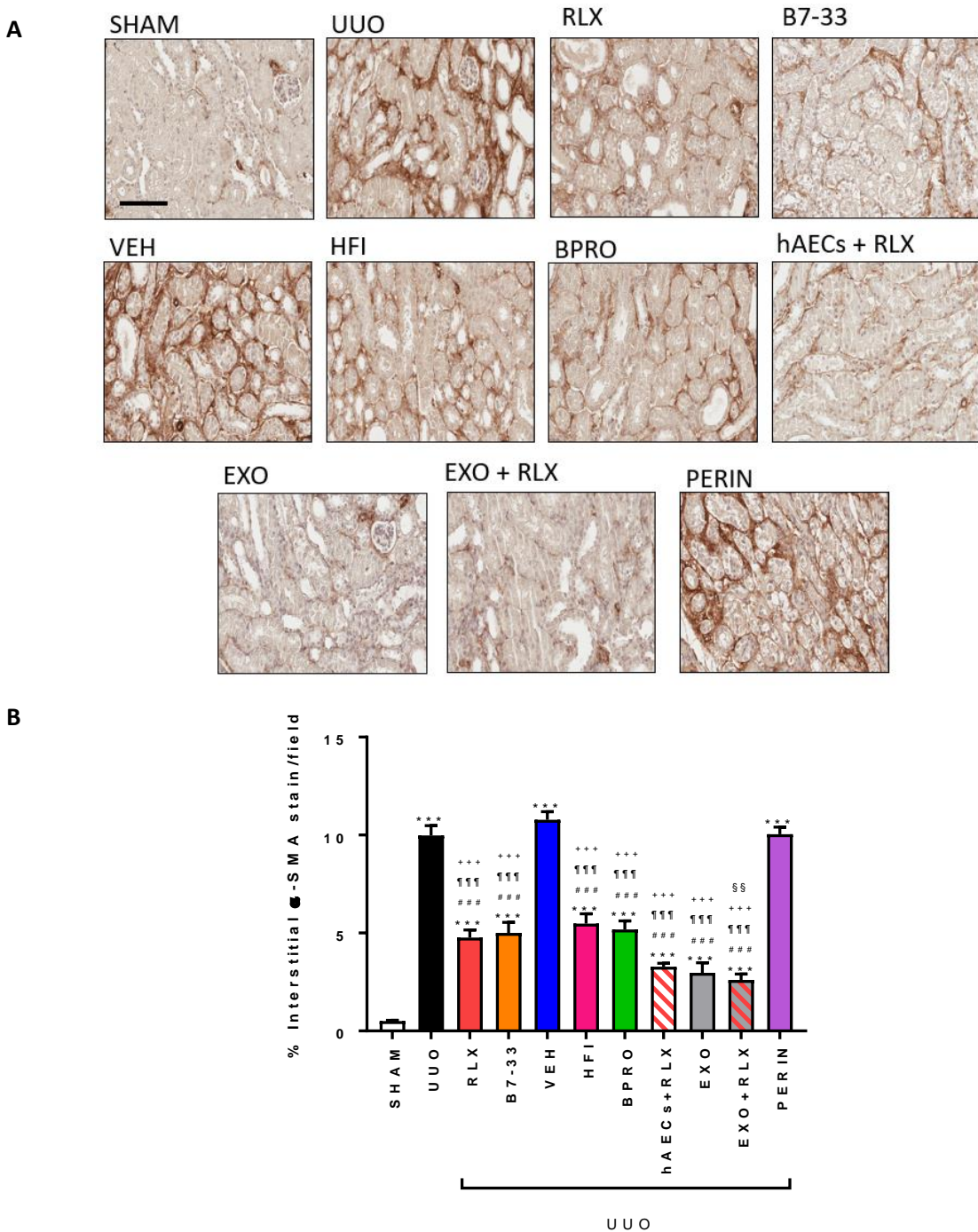


Figure 5.3.7. The effects of UUO and the treatments investigated on renal myofibroblast accumulation.

A) Representative photomicrographs of IHC stained α -SMA kidney sections from each group. Scale bar= 100 μ m. B) mean \pm SEM % α -SMA staining/field of 8 fields each kidney per mice per group (n= 6mice/group). *** P <0.001 vs SHAM; ### P <0.001 vs UUO; \$\$\$ P <0.01 vs RLX; \$\$\$ P <0.001 vs VEH; *** P <0.001 vs PERIN (one-way ANOVA).

5.3.7 The effects of UUO and the treatments investigated on MMP-2 expression.

Gelatin zymography was then used to determine the impact of UUO injury and the treatments investigated on MMP-2 expression and activity (Figure 5.3.8), which facilitates ECM/collagen degradation when activated. UUO-injured mice had significantly increased renal MMP-2 expression and activity levels compared to that measured in SHAM control mice (by ~4-5-fold; $P < 0.001$ vs SHAM group; Figures 5.3.8B, D and F); consistent with what was previously reported in this model (Hewitson *et al.*, 2010; Huuskes *et al.*, 2015). Renal MMP-2 expression/activity levels were further promoted by RLX alone, EXO alone, hAECs+RLX or EXO+RLX treatment (all by ~45-65%; all $P < 0.05$ vs UUO alone), but were not significantly altered by the other treatments evaluated over the effects of UUO alone (Figure 5.3.8).

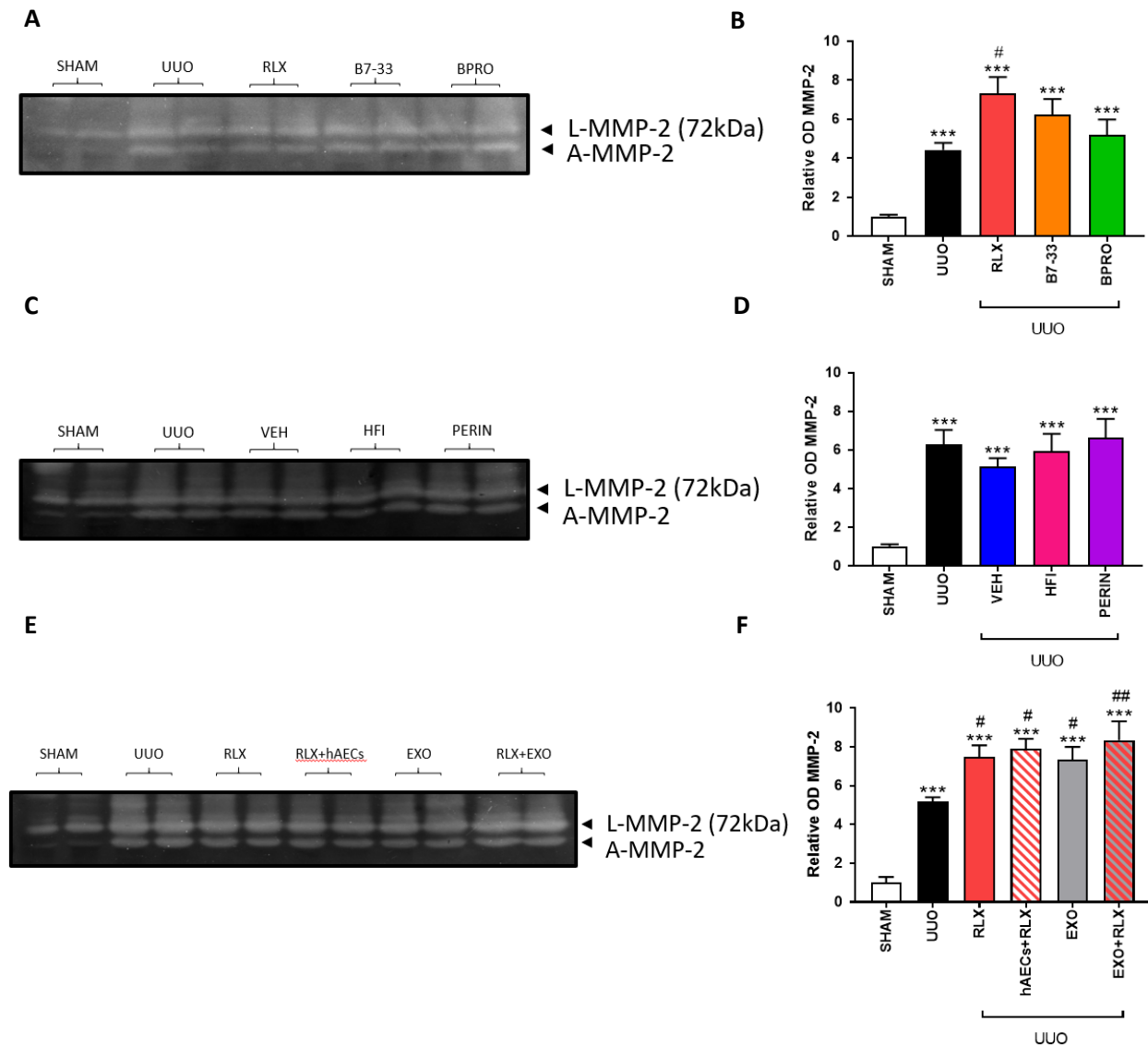


Figure 5.3.8. The effects of UUO and the treatments investigated on MMP-2 expression levels.

A, C, E) Representative gelatin zymographs from each group studied showing renal latent (L; 72kDa) and active (A) MMP-2 levels. B, D, F) Also shown is the mean \pm SEM levels of MMP-2 expression and activity as determined by densitometry, from $n=6$ mice per group and expressed as the relative ratio to the mean value of the SHAM group, which was expressed as 1 in each case. * $P<0.05$, ** $P<0.01$, *** $P<0.001$ vs SHAM; # $P<0.05$, ## $P<0.01$, ### $P<0.001$ vs UUO (one-way ANOVA).

5.3.8 The effects of UUO and the treatments investigated on TIMP-1 expression.

Subsequently, changes in the expression levels of the endogenous inhibitor of several MMPs, TIMP-1, was examined by Western blotting (Figure 5.3.9). Renal TIMP-1 levels were significantly increased in UUO-injured mice (by ~1.6-2.5-fold; all $P < 0.001$ vs SHAM group) compared to that measured in SHAM control mice. This UUO-induced increase in renal TIMP-1 levels was unaffected by VEH or PERIN treatment, but was normalised by all other treatments and combination strategies evaluated (all $P < 0.001$ vs UUO; all no different to values from SHAM control mice; Figure 5.3.9C).

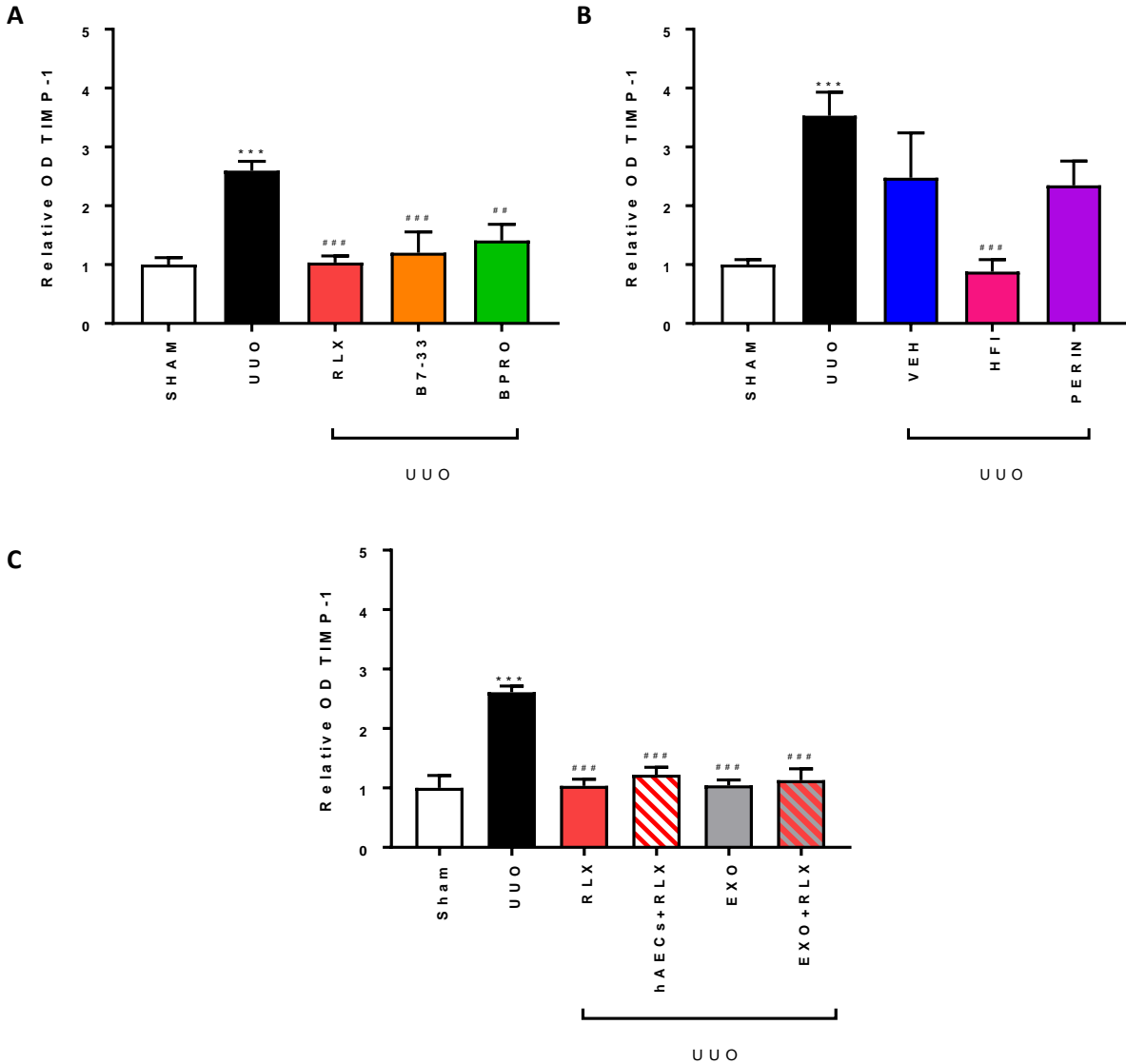


Figure 5.3.9. The effects of UUO and the treatments investigated on renal TIMP-1 expression.

Shown is the mean \pm SEM levels of TIMP-1 expression, which was determined by densitometry of Western blot bands (29kDa), from $n=6$ mice per group and expressed as the relative ratio to the mean value of the SHAM group, which was expressed as 1 in each case. * $P<0.05$, ** $P<0.01$ vs SHAM; # $P<0.05$, ## $P<0.01$, ### $P<0.001$ vs UUO (one-way ANOVA).

5.3.9 The effects of UUO and the treatments investigated on MMP-2/TIMP-1 ratio.

From the results shown in Figure 5.3.8 and Figure 5.3.9, the MMP-2/TIMP-1 ratio from each sample was derived from the relative OD MMP-2 over the corresponding relative OD TIMP-1, respectively. The mean \pm SEM of MMP-2/TIMP-1 ratio from each group was then obtained from the n=4-6 MMP-2/TIMP-1 ratios per group. All groups with the exception of the UUO alone and UUO+VEH-treated groups demonstrated significantly higher MMP-2/TIMP-1 ratios compared to that measured from the SHAM control group (all $P < 0.001$ vs SHAM group). Furthermore, all treatment groups aside from VEH-treated group had significantly higher MMP-2/TIMP-1 ratios compared to the UUO alone group (all $P < 0.05$ vs UUO group) (Table 5.3.1)

Table 5.3.1: MMP-2/TIMP-1 ratio from each of the groups studied

Groups	Mean \pm SEM	N
SHAM	1.1 \pm 0.1	6
UUO	1.8 \pm 0.2	6
RLX	7.2 \pm 0.6***, ##	6
B7-33	5.9 \pm 1.1***, ##	6
VEH	2.0 \pm 0.4	6
HFI	8.0 \pm 1.3***, ###, ¶¶¶, +++	6
BPRO	4.8 \pm 1.2***, #	6
hAEC+RLX	6.8 \pm 0.8***, ###	6
EXO	7.3 \pm 0.8***, ###	6
EXO+RLX	8.3 \pm 0.7***, ###	6
PERIN	3.4 \pm 0.5*, #	6

*In each case, statistical comparisons were made between the sub-groups evaluated in Figs 5.3.8B and 5.3.9A; 5.3.8D and 5.3.9B; and 5.3.8F and 5.3.9C, respectively. *P<0.05, *** P<0.001 vs SHAM; #P<0.05, ##P<0.01, ###P< 0.001 vs UUO; ¶¶¶P<0.001 vs VEH; +++P<0.001 vs PERIN (one-way ANOVA).*

5.4. Discussion

This study compared the renoprotective effects of the clinically-used anti-hypertensive drug, perindopril (PERIN), to the RXFP1 agonists, serelaxin (RLX) and B7-33, the IRAP inhibitor, HFI and the AT₂R agonist, BPRO in a murine model of UUO-induced tubulointerstitial renal disease. The combined effects of RLX with hAECs or hAEC-derived EXO were also compared to the effects of EXO alone and to the above-mentioned therapies in the model utilised. This was the first study to compare the head-to-head renoprotective effects of these various treatments in a model of obstructive nephropathy. The anti-inflammatory, anti-fibrotic and tissue-reparative efficacy of each treatment was assessed for its ability to prevent disease progression (due to Monash Animal Ethics Committee recommendations of avoiding animals having to undergo multiple anaesthesia following UUO-induced injury); which allowed investigation of how effectively each treatment inhibited established disease progression after 7 days of injury. Like the HS-induced model of renal injury used in Chapters 3 and 4, UUO-injured mice were normotensive; which allowed for the direct evaluation of the renoprotective effects of the various therapies/combination strategies investigated in the absence of alterations in blood pressure as a confounding variable.

5.4.1 Therapies targeting the RAS in the setting of obstructive nephropathy.

At the dose administered, PERIN (1mg/kg/day) partially prevented the UUO-induced macrophage infiltration (by ~38%), P-ikB infiltration (by ~62%) and renal cortical TGF- β 1 expression levels (by ~35%) after 7 days of treatment, confirming that the ACEi was bioactive and demonstrated rapid-occurring anti-inflammatory effects. However, at this same concentration, PERIN failed to prevent the UUO-induced loss of peritubular capillaries, nor UUO-induced increase in myofibroblast accumulation, interstitial and total kidney collagen deposition or MMP-2/TIMP-1 ratio (Table 5.3.1). These findings demonstrating that PERIN failed to induce rapid-occurring anti-fibrotic efficacy post-UUO are consistent with the slow-acting and perhaps indirect anti-fibrotic actions of ACEi such as PERIN, which are unlikely to regulate collagen turnover in such a short period of 7 days at doses that are safe. In line with this, daily oral administration of PERIN (1mg/kg/day) over 8 weeks was required for systolic blood pressure, glomerulosclerosis, renal hypertrophy and proteinuria to be reduced in obese Zucker rats that were hypertensive (Šebeková *et al.*, 2009). Similarly, PERIN (1mg/kg/day) treatment over 5 weeks was required for

blood pressure, cardiac hypertrophy and fibrosis to be reduced in hypertensive Goldblatt rats (Nagai *et al.*, 2004). Even at 2mg/kg/day, 14 weeks of PERIN treatment were required for renal inflammation, fibrosis and albuminuria to be reduced in STZ-induced diabetic mice (Barutta *et al.*, 2018). Although the effects of PERIN do not appear to have previously been investigated in the UUO model, another ACEi, captopril, had to be administered at a much higher dose (30mg/kg/day) for myofibroblast differentiation and collagen I/III mRNA to be prevented after 7 days of UUO (Chan *et al.*, 2015). Collectively, the findings from these studies suggest that 1) the dose and 2) treatment period of PERIN used was not sufficient enough for its anti-remodelling effects to be demonstrated post-UUO or 3) that it was unable to directly induce any anti-remodelling and anti-fibrotic effects in the absence of being able to regulate blood pressure in the normotensive model studied. However, as seen in Chapter 4, when administered at a higher dose (4mg/kg/day), PERIN affected animal body weight and induced hypotension and renal dysfunction in mice, while being able to reduce renal fibrosis after 4 weeks of treatment. These findings highlight the limited and slow-acting therapeutic efficacy that ACEi offer when administered at doses that do not induce any major side-effects.

In comparison, the AT₄R/IRAP inhibitor, HFI (0.72mg/kg/day), not only prevented the UUO-induced increase in renal inflammation and vascular rarefaction, but also significantly prevented the UUO-induced increase in renal fibrosis. Noteworthy was the finding that HFI almost fully prevented the UUO-induced increase in interstitial renal collagen deposition, renal cortical TGF- β 1 expression and renal TIMP-1 expression (to levels that were not different to that measured in SHAM control mice), while also being to significantly promote MMP-2 activity over the effects of UUO alone. These findings suggested that HFI was able to inhibit the UUO-induced increase in TGF- β 1-induced myofibroblast differentiation and ECM/collagen production, while also increasing the MMP-2/TIMP-1 ratio which would facilitate MMP-2-induced collagen degradation. Similar therapeutic effects of HFI (0.72mg/kg/day) were observed when it was administered to established HS-induced kidney disease in mice (which are presented in Chapter 4). Additionally, in a patent filed by Chai and colleagues (Chai *et al.*, 2017), HFI (0.72mg/kg/day) was shown to significantly reduce established F4/80-stained macrophage infiltration (F4/80), p-I κ B expression and collagen deposition in aged mice and mice with CVD. This suggests that HFI can mediate its

protective effects independently of etiology by targeting elevated levels of IRAP in aged and injured organs. Although not investigated in this study, as detailed in Chapter 4, it has been suggested that HFI mediates its therapeutic effects by preventing the breakdown of IRAP substrates such as oxytocin and vasopressin. As these substrates mediate tissue-protection, the prevention of their breakdown is likely to contribute to reduced renal injury via the inhibition of inflammatory cell infiltration and oxidative stress-induced kidney damage (Biyikli *et al.*, 2006; Tugtepe *et al.*, 2007). Although the UUO-induced vascular rarefaction, which has also been reported by others (Ohashi *et al.*, 2002), was significantly prevented by HFI treatment, it is unclear whether HFI was simply suppressing the contribution of IRAP to tissue damage-induced blood vessel and capillary loss, or whether it actually had angiogenic properties. As IRAP is highly expressed in damaged blood vessels (Zulli *et al.*, 2008), this may suggest that HFI was simply suppressing IRAP activity when administered as a preventative therapy. However, as endogenous inhibition of IRAP by Ang IV has been shown to increase eNOS-dependent NO bioavailability (Vinh *et al.*, 2008b), this may suggest that targeting IRAP can elicit angiogenic and vasoprotective effects to facilitate tissue repair. This requires further investigation by evaluating the therapeutic effects of HFI.

Promoting AT₂ receptor activity with BPRO (0.1 mg/kg/day) appeared to demonstrate similar anti-inflammatory efficacy to that of PERIN and HFI in the model studied, and similar anti-fibrotic efficacy to that of HFI but improved anti-fibrotic efficacy over the effects of PERIN after 7 days of treatment. BPRO also prevented the UUO-induced loss of peritubular capillary density and increased the MMP-2/TIMP-1 ratio, suggesting that it was also able to prevent TGF- β 1-induced myofibroblast differentiation and ECM/collagen production while augmenting MMP-2-induced collagen degradation. Taken together with the acute vasoprotection offered by BPRO in hypertensive rats (Del Borgo *et al.*, 2015), these collective findings suggest that enhancing AT₂R activity offers similar renoprotection to that mediated by inhibition of AT₄R/IRAP activity and more rapid-occurring anti-fibrotic efficacy over the targeting of the ACE/AT₁R axis. Although there are no published *in vivo* studies evaluating the effects of BPRO in other fibrosis-induced models of disease, other AT₂R agonists such as Compound 21 (C21) have exerted similar tissue-protective properties within the kidneys of various models of kidney disease (Gelosa *et al.*, 2009;

Castoldi *et al.*, 2014; Koulis *et al.*, 2015). C21 (0.3mg/kg/day) significantly reduced pro-inflammatory (TNF- α , IL-6) and pro-fibrotic (TGF- β 1) cytokine levels, and promoted NO bioavailability, in the kidneys of hypertensive rats subjected to a clipped kidney of 2-kidney, 1-clip (2K1C) (Matavelli *et al.*, 2011) over a 4 day-treatment period. C21 (1mg/kg/day) also reduced vascular injury and fibrosis when administered over longer periods (Rehman *et al.*, 2012). These findings further support the rapid-occurring renoprotection offered by agonists that promote AT₂R activity. Although no head-to-head comparisons have been conducted between AT₂R agonists (such as BPRO vs C21), the findings from this study suggest that lower doses of BPRO (0.1 mg/kg/day) may induce similar effects to that of higher doses of C21 (0.3-1mg/kg/day), due to the higher selectivity of BPRO for the AT₂R receptor. Again though, further studies are warranted to evaluate the dose-dependent effects of BPRO as an intervention therapy, to further validate its therapeutic efficacy as a treatment for fibrosis-induced kidney diseases.

In general, it was found that inhibiting AT₄R/IRAP activity or promoting AT₂R activity was able to exert rapid and equivalent renoprotection in a normotensive model; suggesting that the IRAP inhibitor (HFI) or AT₂R agonist (BPRO) evaluated exerted direct anti-inflammatory, anti-remodelling and anti-fibrotic effects without having to regulate blood pressure to protect the injured kidney from injury-induced fibrosis. Additionally noteworthy, is that both HFI (Patel *et al.*, 1998; Vinh *et al.*, 2008a) and C21 at least (acting as an AT₂R agonist; Matavelli *et al.*, 2011) increased NO bioavailability, which along with cGMP are known suppressors of pro-fibrotic TGF- β 1 signal transduction and activity (Saura *et al.*, 2005). On the other hand, ACE blockade (by PERIN) demonstrated similar anti-inflammatory but not anti-remodelling nor anti-fibrotic efficacy, to that induced by inhibition of IRAP activity or augmentation of AT₂R activity. This lack of an anti-fibrotic effect by PERIN administration was likely attributed to the fact that PERIN (at the dose administered) did not induce any direct collagen remodelling effects over the short time-period of treatment studied, particular when administered to a normotensive model. As discussed in Chapters 3 and 4, ACEi and ARBs appear to predominantly regulate collagen remodelling in hypertensive disease settings, where they ameliorate the impact of elevated blood pressure on tissue remodelling and dysfunction.

5.4.2 Therapies targeting RXFP1 in the setting of obstructive nephropathy.

Compared to the broader anti-inflammatory effects offered by HFI and BPRO post-UUO, the RXFP1 agonists, RLX (0.5mg/kg/day) and B7-33 (0.25mg/kg/day), were able to only suppress P-iKB expression levels without affecting macrophage infiltration. These findings are inconsistent with a previous study which showed that RLX (2mg/kg/day) was able to inhibit ED-1-associated macrophage infiltration in rats subjected to bromoethylamine-induced interstitial renal fibrosis after 4 weeks of treatment (Garber *et al.*, 2001). However, they are consistent with a separate report showed that macrophage infiltration was unaltered in relaxin-deficient mice (compared to that measured in wild-type animals) up to 10 days post-UUO (Hewitson *et al.*, 2007). Thus, it may be suggested that RLX (and B7-33) may indirectly inhibit macrophage infiltration when administered over longer periods of time, while being able to directly promote M1 to M2 macrophage infiltration as part of their anti-fibrotic actions in the kidney (Chen *et al.*, 2017). Consistent with this, the RLX- and B7-33-induced prevention of P-iKB (and NF- κ B) activity may eventually result in the inhibition of monocyte/macrophage infiltration into the kidney, as NF- κ B promotes macrophage relocation (Baker *et al.*, 2011). Furthermore, a previous report showed that the RLX-induced prevention of NF- κ B activity was associated with its ability to reduce TGF- β , MCP-1, IL-1, IL-6, ICAM-1 and VCAM-1 in the kidney to suppress renal inflammation (Wang *et al.*, 2017). This suggests that RLX and B7-33 may have a greater ability to suppress pro-inflammatory cytokine activity over their ability to inhibit inflammatory cell infiltration into damaged organs. As RXFP1 can form heterodimers with AT₂ receptors (Chow *et al.*, 2014), and antagonism of AT₂ receptors has also been found to partially reduce NF- κ B activity, monocyte recruitment/ infiltration and renal inflammation post-UUO (Esteban *et al.*, 2004), future studies could investigate the whether the combined effects of RLX or B7-33 with BPRO will more broadly suppress renal inflammation following injury or insult.

Expectedly, RLX and B7-33 demonstrated marked anti-fibrotic effects in the obstructed kidney of UUO-injured mice, which were found to be equivalent to that of HFI or EXO treatment alone, and more rapid-occurring compared to the effects of PERIN. This data extend previous findings (Hossain *et al.*, 2016), which showed that B7-33 could mimic the anti-fibrotic efficacy of RLX in experimental models of heart and lung disease, to now showing for the first time that it also

retained the anti-fibrotic effects of RLX in the injured kidney. This in turn confirmed that the targeting of RXFP1 also offered more rapid-occurring anti-fibrotic efficacy over the targeting of ACE/AT₁R axis. Consistent with previous reports on the renoprotective effects of RLX (Hewitson *et al.*, 2010; Chow *et al.*, 2014; Chen *et al.*, 2017), this study confirmed that both RLX and B7-33 mediated their anti-fibrotic effects in the obstructed kidney by suppressing the effects of TGF- β 1 on myofibroblast differentiation and ECM/collagen deposition, while also being able to promote MMP-2-induced collagen degradation. RLX at least, was shown to mediate its anti-fibrotic effects via an RXFP1-pERK1/2-nNOS-NO-soluble guanylate cyclase (sGC)-cGMP-dependent pathway on renal myofibroblasts to inhibit TGF- β 1 signal transduction at the level of intracellular Smad2 phosphorylation (activation) (Mookerjee *et al.*, 2009; Chow *et al.*, 2014; Wang *et al.*, 2016b), and also signalled through this pathway to promote MMP-2 activity by renal myofibroblasts isolated from UUO-injured rat kidneys (Chow *et al.*, 2012). Although B7-33 was shown to retain the pERK1/2-promoting effects of RLX (Hossain *et al.*, 2016), its ability to act through a nNOS-NO-sGC-cGMP-dependent pathway on myofibroblasts to inhibit TGF- β 1 signal transduction still needs to be confirmed.

Of note, RLX and B7-33 were also able to inhibit KIM-1-associated kidney damage post-UUO to a greater extent than, HFI, BPRO or PERIN. Together with their ability to protect the kidney from vascular rarefaction, this suggested that both RLX and B7-33 were able to induce concomitant anti-fibrotic and tissue-reparative effects. Consistent with this, RLX is known to have angiogenic properties, which have been shown to be mediated via its ability to promote the production of angiogenic factors such as VEGF and bFGF (Uneimori *et al.*, 2000; Samuel *et al.*, 2011). Similarly, RLX at least was shown to prevent tubular epithelial cell injury by suppressing UUO-induced KIM-1 expression (Huuskes *et al.*, 2015). Collectively, these findings suggested that the targeting of RXFP1 offered improved tissue-reparative effects, similar anti-fibrotic effects, and perhaps less broader anti-inflammatory effects to that of targeting IRAP or the AT₂R; but clearly offered more rapid-occurring and broader renoprotection over the targeting of ACE in a normotensive setting.

5.4.3 The therapeutic effects of exosomes and combination treatments in the setting of obstructive nephropathy.

The combined effects of RLX and hAECs reduced established chronic allergic airways disease (AAD)-induced airway fibrosis and airway reactivity to a greater extent than either therapy alone (Royce *et al.*, 2016). RLX also enhanced the therapeutic effects of EXO in experimental models of chronic AAD and pulmonary fibrosis (over the effects of EXO alone) (Royce *et al.*, 2019). In this study, the combined effects of hAECs (1×10^6 /mouse) or EXO (25 μ g/mouse; equivalent to 12.5×10^6 AECs/mouse) together with RLX were evaluated in the UUO model, and compared to the effects of RLX or EXO alone. Strikingly, the combined effects of EXO+RLX provided the optimal protection against UUO-induced pathology compared to the other mono- and combination treatments evaluated. This was evidenced by the combined effects of EXO+RLX being able to prevent UUO-induced renal inflammation (macrophage infiltration and P-I κ B expression levels) by ~80%, almost completely prevent the UUO-induced increase in renal damage, interstitial collagen deposition and TGF- β 1 expression levels, fully restore the UUO-induced vascular rarefaction and have the greatest impact in promoting the MMP-2/TIMP-1 ratio. Furthermore, the combined effects of EXO+RLX offered enhanced anti-inflammatory and to a lesser extent, anti-fibrotic efficacy (interstitial myofibroblast accumulation and collagen deposition) over the effects of EXO or RLX alone, and similar or slightly improved therapeutic efficacy over the combined effects of hAECs+RLX. As the administration of EXO alone, hAECs+RLX or EXO+RLX promoted the MMP-2/TIMP-1 ratio to a similar extent, this suggested that the combined effects of EXO+RLX offered greater synergistic effects (over the individual treatments) in preventing measures of renal inflammation leading to ECM/collagen synthesis and deposition, rather than on MMP-facilitated collagen degradation. However, as only one MMP was investigated, further studies need to be carried out on additional facilitators of collagen breakdown before any further conclusions can be drawn.

RLX can prevent the contribution of renal inflammation to fibrosis progression by inhibiting the infiltration of neutrophils (Masini *et al.*, 2004) and mast cells (Bani *et al.*, 1998) to the injured kidney, and suppressing the pro-inflammatory and pro-fibrotic actions of factors such as TGF- β 1 (Heeg *et al.*, 2005; Mookerjee *et al.*, 2009; Yoshida *et al.*, 2012), TNF- α (Brecht *et al.*, 2011;

Yoshida *et al.*, 2013, 2014), NF- κ B (Halls *et al.*, 2006; Wang *et al.*, 2017), IL-1/IL-6 (Wang *et al.*, 2017; Giam *et al.*, 2018), ICAM-1 and VCAM-1 (Brecht *et al.*, 2011; Wang *et al.*, 2017). As discussed above, RLX can also promote M1 to M2 macrophage polarisation which is anti-inflammatory and eventually inhibit the influence of NF- κ B on macrophage infiltration (Chen *et al.*, 2017). These RLX-induced events likely lead to its ability to inhibit fibroblast proliferation and differentiation into myofibroblasts, and hence, myofibroblast-induced ECM/collagen deposition (Hewitson *et al.*, 2010). On the other hand, in addition to being able to directly inhibit renal macrophage infiltration, studies conducted in experimental models of lung disease have shown that EXO are more involved in regulating cytokine signalling associated with the innate immune system, toll-like receptor (TLR) signalling and cell junction signalling (Tan *et al.*, 2018). EXO can also inhibit fibroblast migration, proliferation and differentiation, and the ability of myofibroblasts to deposit increased ECM components (Zhao *et al.*, 2017). Additionally, EXO contain microRNAs (such as miR-23a and miR-150) that can negatively impact on fibrosis (Tan *et al.*, 2018). For example, studies conducted in mice have shown that over-expression of miR-23a in conjunction with miR-27a inhibited diabetes-induced TGF- β 1 signal transduction, myofibroblast differentiation and related renal fibrosis (Zhang *et al.*, 2018). These synergistic actions of RLX and EXO may explain why the combined effects of both together had a greater impact on preventing renal damage, inflammation and fibrosis post-UUO, compared to the effects of either therapy alone.

It was estimated that the therapeutic impact of ~12.5 million hAECs were administered in the form of 25 μ g of EXO. Hence, the improved renoprotection offered by the combined effects EXO+RLX over that of hAECs+RLX post-UUO may simply be explained by the greater amount of hAECs that were delivered in the form of EXO in comparison to the 1 million hAECs that were used for comparison, and then combined with RLX. Nevertheless, the findings of this study confirmed recently published work from experimental models of lung disease (Royce *et al.*, 2019) in showing that 1) EXO retain the therapeutic efficacy of hAECs and can offer the impact and safety of a greater amount of cells (than what can physically be administered to mice); and 2) the anti-fibrotic effects of RLX can create an improved environment for the renoprotective effects of EXO. Given the manufacturing and regulatory advantages of EXO over their parental stem cells,

and the reduced likelihood of EXO inducing respiratory problems from aggregating within microvessels of the lungs, the findings of this study demonstrated the feasibility and advantages to combining EXO with RLX for treating kidney disorders associated with fibrosis. Furthermore, as EXO are likely to induce tissue regeneration and can be engineered to over-express factors that can aid in reducing fibrosis and augmenting tissue repair (Wang *et al.*, 2016a; Aghajani Nargesi *et al.*, 2017), there may be additional benefits to employing this combination therapy, which offered far superior and rapid-occurring renoprotection to that of the ACEi, PERIN. Further studies investigating the therapeutic efficacy of this combination therapy in different models of kidney disease may contribute to its eventual clinical evaluation as a treatment for patients with CKD.

4.4 Limitations and conclusion.

This was the first study to demonstrate the renoprotective impact of B7-33, HFI, BPRO, EXO and the combined effects of hAECs or EXO with RLX in a model of UUO-induced nephropathy, in comparison to the effects of the ACEi, PERIN. However, there were some limitations to this study in that each of these treatments investigated were administered at the time of injury onset and hence, only their preventative effects were examined post-UUO. Furthermore, only one dose of each drug or cell/combination-based therapy was evaluated based on previous studies, which had demonstrated the efficacy of each therapy investigated (at the doses administered) in other models of organ disease. The significance between the renoprotective effects of the therapies evaluated may have been better differentiated if fewer groups were compared in this head-to-head study, which may have increased the power to identify clearer differences between the efficacy of each treatment studied. The safety of each drug or cell/combination-based therapy alone was also not investigated following their administration to uninjured mice. Having said that, it appeared that most of these therapies induced their anti-fibrotic effects by inhibiting renal inflammation and the impact of pro-inflammatory cytokines on myofibroblast-differentiation and myofibroblast-induced ECM/collagen deposition; while also being able to promote MMP-2-induced collagen degradation rather than directly affecting collagen *per se*. In other words, these therapies are unlikely to alter normal collagen levels which are not stimulated by factors such as TGF- β 1 or Ang II, and hence, are likely to be safe therapies that would not induce any side-effects

when administered to uninjured mice. Finally, the impact of each treatment evaluated on renal function could not be measured, as the contralateral (unobstructed) kidney is known to compensate for the loss of renal function associated with the obstructed kidney.

Although working through different mechanisms of action, the findings from this study validated the anti-fibrotic and broader renoprotective efficacy offered by both RLX and HFI in a rapidly-occurring and more severe model of UUO-induced kidney injury. Combined with the data presented in Chapters 3 and 4 and previous studies investigating the renoprotective effects of RLX (Garber *et al.*, 2001; Lekgabe *et al.*, 2005; Hewitson *et al.*, 2010; Huuskes *et al.*, 2015), it is suggested that the anti-fibrotic efficacy of these therapies can be maintained independently of etiology. This study also highlighted that compounds that targeted RXFP1 (RXL, B7-33), IRAP (HFI) or the AT₂R (BPRO) demonstrated more direct and rapid-occurring renoprotective efficacy compared to a clinically-used ACEi, which did not induce any marked effects when applied to a normotensive model. Of greater note, this study also demonstrated that combining RLX with hAECs or EXO offered even greater protection compared to the effects of RLX or EXO alone, suggesting that combining the synergistic impact of two therapies would result in even greater renoprotection compared to that offered by either therapy alone.

In addition to the various future directions detailed above, additional studies are required to validate the optimal dose and delivery route of each therapy studied for treating various renal disorders, and whether they are best delivered as stand-alone or adjunct therapies. However, it should be noted that several studies have already shown that B7-33 (Hossain *et al.*, 2016), EXO (Royce *et al.*, 2019) and the combined effects of hAECs+RLX (Royce *et al.*, 2016) or EXO+RLX (Royce *et al.*, 2019) can reduce established fibrosis albeit in other disease settings. Thus, it is likely that these therapies would also reduce established renal fibrosis when administered as intervention therapies. As hAEC-derived EXO (ClinicalTrials.gov Identifier NCT02138331; NCT03384433) and RLX (Teerlink *et al.*, 2013) have separately been evaluated in clinical trials, novel strategies incorporating this combination therapy can be fast-tracked for human trials. Additional work is also being conducted to identifying clinical targets for the therapeutic administration of B7-33, HFI and AT₂R agonists such as BPRO, which should also be combined with EXO as possible future therapies for CKD patients.

5.5 References

- Aghajani Nargesi, A, Lerman, LO, Eirin, A (2017). Mesenchymal stem cell-derived extracellular vesicles for kidney repair: Current status and looming challenges. *Stem Cell Res. Ther.* **8**: 1–12.
- Akle, CA, Welsh, KI, Adinolfi, M, Leibowitz, S, Mccoll, I (1981). Immunogenicity of Human Amniotic Epithelial Cells After Transplantation Into Volunteers. *Lancet* **318**: 1003–1005.
- Baker, RG, Hayden, MS, Ghosh, S (2011). NF- κ B, inflammation, and metabolic disease. *Cell Metab.* **13**: 11–22.
- Bani, D, Masini, E, Bello, MG, Bigazzi, M, Sacchi, TB (1998). Relaxin protects against myocardial injury caused by ischemia and reperfusion in rat heart. *Am. J. Pathol.* **152**: 1367–76.
- Barutta, F, Bellini, S, Mastrocola, R, Gambino, R, Piscitelli, F, Marzo, V di, *et al.* (2018). Reversal of albuminuria by combined AM6545 and perindopril therapy in experimental diabetic nephropathy. *Br. J. Pharmacol.* **175**: 4371–4385.
- Biyikli, N, Tugtepe, H, Sener, G, Velioglu-Ogunc, A, Cetinel, S, Midillioglu, S, *et al.* (2006). Oxytocin alleviates oxidative renal injury in pyelonephritic rats via a neutrophil-dependent mechanism. *Peptides* **27**: 2249–2257.
- Boero, R, Pignataro, A, Quarello, F (2002). Salt intake and kidney disease. *J. Nephrol.* **15**: 225–229.
- Borgo, M Del, Wang, Y, Bosnyak, S, Khan, M, Walters, P, Spizzo, I, *et al.* (2015). β -Pro7Ang III is a novel highly selective angiotensin II type 2 receptor (AT2R) agonist, which acts as a vasodepressor agent via the AT2R in conscious spontaneously hypertensive rats. *Clin. Sci.* **129**: 505–513.
- Brecht, A, Bartsch, C, Baumann, G, Stangl, K, Dschietzig, T (2011). Relaxin inhibits early steps in vascular inflammation. *Regul. Pept.* **166**: 76–82.
- Castoldi, G, Gioia, CRT di, Bombardi, C, Maestroni, S, Carletti, R, Steckelings, UM, *et al.* (2014). Prevention of diabetic nephropathy by compound 21, selective agonist of angiotensin type 2 receptors, in Zucker diabetic fatty rats. *AJP Ren. Physiol.* **307**: F1123–F1131.

Chai, SY, Widdop, RE, Gaspari, TA, Lee, HW (2017). *WO2017015720A1 Fibrotic Treatment* (Australia: FPA PATENT ATTORNEYS PTY LTD).

Chan, GCW, Yiu, WH, Wu, HJ, Wong, DWL, Lin, M, Huang, XR, *et al.* (2015). N-Acetyl-seryl-aspartyl-lysyl-proline Alleviates Renal Fibrosis Induced by Unilateral Ureteric Obstruction in BALB / C Mice. *Mediators Inflamm.* **2015**: 283123.

Chen, L, Sha, M, Li, D, Zhu, Y, Wang, X (2017). Relaxin abrogates renal interstitial fibrosis by regulating macrophage polarization via inhibition of Toll-like receptor 4 signaling. *Oncotarget* **8**: 21044–21053.

Chevalier, R, Thornhill, B, Forbes, M, Kiley, S (2010). Mechanisms of renal injury and progression of renal disease in congenital obstructive nephropathy. *Pediatr Nephrol* **25**: 687–697.

Chow, BS, Kocan, M, Bosnyak, S, Sarwar, M, Wigg, B, Jones, ES, *et al.* (2014). Relaxin requires the angiotensin II type 2 receptor to abrogate renal interstitial fibrosis. *Kidney Int* **86**: 75–85.

Chow, BSM, Chew, EGY, Zhao, C, Bathgate, RAD, Hewitson, TD, Samuel, CS (2012). Relaxin signals through a RXFP1-pERK-nNOS-NO-cGMP-dependent pathway to up-regulate matrix metalloproteinases: The additional involvement of iNOS. *PLoS One* **7**..

Cochrane, AL (2005). Renal Structural and Functional Repair in a Mouse Model of Reversal of Ureteral Obstruction. *J. Am. Soc. Nephrol.* **16**: 3623–3630.

Esteban, V, Lorenzo, O, Rupérez, M, Suzuki, Y, Mezzano, S, Blanco, J, *et al.* (2004). Angiotensin II, via AT1 and AT2 receptors and NF-κB pathway, regulates the inflammatory response in unilateral ureteral obstruction. *J. Am. Soc. Nephrol.* **15**: 1514–1529.

Gallop, PM, Paz, MA (1975). Posttranslational protein modifications, with special attention to collagen and elastin. *Physiol. Rev.* **55**: 418–487.

Garber, S, Mirochnik, Y, Brecklin, C, Unemori, E, Singh, A, Slobodskoy, L, *et al.* (2001). Relaxin decreases renal interstitial fibrosis and slows progression of renal disease. *Kidney Int* **59**: 804–809.

Gelosa, P, Pignieri, A, Fändriks, L, Gasparo, M de, Hallberg, A, Banfi, C, *et al.* (2009). Stimulation

of AT2 receptor exerts beneficial effects in stroke-prone rats: focus on renal damage. *J. Hypertens.* **27**: 2444–2451.

Giam, B, Chu, PY, Kuruppu, S, Smith, AI, Horlock, D, Murali, A, *et al.* (2018). Serelaxin attenuates renal inflammation and fibrosis in a mouse model of dilated cardiomyopathy. *Exp. Physiol.* **103**: 1593–1602.

Halls, ML, Bathgate, RAD, Summers, RJ (2006). Comparison of Signaling Pathways Activated by the Relaxin Family Peptide Receptors, RXFP1 and RXFP2, Using Reporter Genes. *J. Pharmacol. Exp. Ther.* **320**: 281–290.

Heeg, MHJ, Koziolk, MJ, Vasko, R, Schaefer, L, Sharma, K, Müller, GA, *et al.* (2005). The antifibrotic effects of relaxin in human renal fibroblasts are mediated in part by inhibition of the Smad2 pathway. *Kidney Int.* **68**: 96–109.

Hewitson, TD (2009). Renal tubulointerstitial fibrosis: common but never simple. *Am. J. Physiol. Physiol.* **296**: F1239–F1244.

Hewitson, TD, Ho, WY, Samuel, CS (2010). Antifibrotic Properties of Relaxin : In Vivo Mechanism of Action in Experimental Renal Tubulointerstitial. *Endocrinology* **151**: 4938–4948.

Hewitson, TD, Mookerjee, I, Masterson, R, Zhao, C, Tregear, GW, Becker, GJ, *et al.* (2007). Endogenous relaxin is a naturally occurring modulator of experimental renal tubulointerstitial fibrosis. *Endocrinology* **148**: 660–669.

Hossain, MA, Kocan, M, Yao, ST, Royce, SG, Nair, VB, Siwek, C, *et al.* (2016). A single-chain derivative of the relaxin hormone is a functionally selective agonist of the G protein-coupled receptor, RXFP1. *Chem. Sci.* **7**: 3805–3819.

Huuskens, BM, Wise, AF, Cox, AJ, Lim, EX, Payne, NL, Kelly, DJ, *et al.* (2015). Combination therapy of mesenchymal stem cells and serelaxin effectively attenuates renal fibrosis in obstructive nephropathy. *FASEBJ* **29**: 540–553.

Kikuchi, K, Rudolph, R, Murakami, C, Kowdley, K, GB, M (2002). Portal vein thrombosis after hematopoietic cell transplantation: frequency, treatment and outcome. *Bone Marrow*

Transplant. **29**: 329–333.

Koulis, C, Chow, BSM, Mckelvey, M, Steckelings, UM, Unger, T, Thallas-Bonke, V, *et al.* (2015). AT2R agonist, compound 21, is Reno-protective against type 1 diabetic nephropathy.

Hypertension **65**: 1073–1081.

Kyriakou, C, Rabin, N, Pizzey, A, Nathwani, A, Yong, K (2008). Factors that influence short-term homing of human bone marrow-derived mesenchymal stem cells in a xenogeneic animal model.

Haematologica **93**: 1457–1465.

Lekgabe, ED, Kiriazis, H, Zhao, C, Xu, Q, Moore, XL, Su, Y, *et al.* (2005). Relaxin reverses cardiac and renal fibrosis in spontaneously hypertensive rats. *Hypertension* **46**: 412–418.

Liu, J, Hua, R, Gong, Z, Shang, B, Huang, Y, Guo, L, *et al.* (2017). Human amniotic epithelial cells inhibit CD4 + T cell activation in acute kidney injury patients by influencing the miR-101-c-Rel-IL-2 pathway. *Mol. Immunol.* **81**: 76–84.

Masini, E, Nistri, S, Vannacci, A, Bani Sacchi, T, Novelli, A, Bani, D (2004). Relaxin inhibits the activation of human neutrophils: involvement of the nitric oxide pathway. *Endocrinology* **145**: 1106–12.

Matavelli, L, Huang, J, Siragy, H (2011). Angiotensin AT2 Receptor Stimulation Inhibits Early Renal Inflammation in Renovascular Hypertension. *Hypertension* **57**: 308–313.

Miki, T, Lehmann, T, Cai, H, Stolz, DB, Strom, SC (2005). Stem Cell Characteristics of Amniotic Epithelial Cells. *Stem Cells* **23**: 1549–1559.

Moll, G, Alm, JJ, Davies, LC, Bahr, L Von, Heldring, N, Stenbeck-Funke, L, *et al.* (2014). Do cryopreserved mesenchymal stromal cells display impaired immunomodulatory and therapeutic properties? *Stem Cells* **32**: 2430–2442.

Moodley, Y, Ilancheran, S, Samuel, C, Vaghjiani, V, Atienza, D, Williams, ED, *et al.* (2010). Human amnion epithelial cell transplantation abrogates lung fibrosis and augments repair. *Am. J. Respir. Crit. Care Med.* **182**: 643–51.

Mookerjee, I, Hewitson, TD, Halls, ML, Summers, RJ, Mathai, ML, Bathgate, R a D, *et al.* (2009).

Relaxin inhibits renal myofibroblast differentiation via RXFP1, the nitric oxide pathway, and Smad2. *FASEB J.* **23**: 1219–29.

Nagai, M, Horikoshi, K, Izumi, T, Seki, S, Taniguchi, M, Taniguchi, I, *et al.* (2004).

Cardioprotective action of perindopril versus candesartan in renovascular hypertensive rats. *Cardiovasc. Drugs Ther.* **18**: 353–362.

Ohashi, R, Shimizu, A, Masuda, Y, Kitamura, H, Ishizaki, M, Sugisaki, Y, *et al.* (2002). Peritubular capillary regression during the progression of experimental obstructive nephropathy. *J. Am. Soc. Nephrol.* **13**: 1795–1805.

Patel, JM, Martens, JR, Li, YD, Gelband, CH, Raizada, MK, Block, ER (1998). Angiotensin IV receptor-mediated activation of lung endothelial NOS is associated with vasorelaxation. *Am. J. Physiol.* **275**: L1061-8.

Rehman, A, Leibowitz, A, Yamamoto, N, Rautureau, Y, Paradis, P, Schiffrin, EL (2012).

Angiotensin type 2 receptor agonist compound 21 reduces vascular injury and myocardial fibrosis in stroke-prone spontaneously hypertensive rats. *Hypertension* **59**: 291–299.

Royce, SG, Patel, KP, Mao, W, Zhu, D, Lim, R, Samuel, CS (2019). Serelaxin enhances the therapeutic effects of human amnion epithelial cell-derived exosomes in experimental models of lung disease. *Br. J. Pharmacol.* [Epub ahead of print].

Royce, SG, Shen, M, Patel, KP, Huuskes, BM, Ricardo, SD, Samuel, CS (2015). Mesenchymal stem cells and serelaxin synergistically abrogate established airway fibrosis in an experimental model of chronic allergic airways disease. *Stem Cell Res.* **15**: 495–505.

Royce, SG, Tominaga, AM, Shen, M, Patel, KP, Huuskes, BM, Lim, R, *et al.* (2016). Serelaxin improves the therapeutic efficacy of RXFP1-expressing human amnion epithelial cells in experimental allergic airway disease. *Clin. Sci.* **130**: 2151–2165.

Samuel, CS (2009). Determination of Collagen Content, Concentration, and Sub-types in Kidney Tissue. In *Kidney Research. Methods in Molecular Biology (Methods and Protocols)*, G. Becker, and T.D. Hewitson, eds. (Humana Press), p.

- Samuel, CS, Cendrawan, S, Gao, X-M, Ming, Z, Zhao, C, Kiriazis, H, *et al.* (2011). Relaxin remodels fibrotic healing following myocardial infarction. *Lab. Invest.* **91**: 675–90.
- Sasaki, Y, Iwama, R, Sato, T, Heishima, K, Shimamura, S, Ichijo, T, *et al.* (2014). Estimation of glomerular filtration rate in conscious mice using a simplified equation. *Physiol. Rep.* **2**: 1–10.
- Saura, M, Zaragoza, C, Herranz, B, Grier, M, Diez-Marqués, L, Rodríguez-Puyol, D, *et al.* (2005). Nitric oxide regulates transforming growth factor- β signaling in endothelial cells. *Circ. Res.* **97**: 1115–1123.
- Šebeková, K, Lill, M, Boor, P, Heidland, A, Amann, K (2009). Functional and partial morphological regression of established renal injury in the obese Zucker rat by blockade of the renin-angiotensin system. *Am. J. Nephrol.* **29**: 164–170.
- Tan, JL, Lau, SN, Leaw, B, Nguyen, HPT, Salamonsen, LA, Saad, MI, *et al.* (2018). Amnion Epithelial Cell-Derived Exosomes Restrict Lung Injury and Enhance Endogenous Lung Repair. *Stem Cells Transl. Med.* **7**: 180–196.
- Teerlink, JR, Cotter, G, Davison, BA, Felker, GM, Filippatos, G, Greenberg, BH, *et al.* (2013). Serelaxin, recombinant human relaxin-2, for treatment of acute heart failure (RELAX-AHF): A randomised placebo-controlled trial. *Lancet* **381**: 29–39.
- Tugtepe, H, Sener, G, Biyikli, N, Yuksel, M, Cetinel, S, Gedik, N, *et al.* (2007). The protective effect of oxytocin on renal ischemia/reperfusion injury in rats. *Regul. Pept.* **140**: 101–108.
- Uneimori, E, Lewis, M, Constant, J, Arnold, G, Grove, G, Normand, J, *et al.* (2000). Relaxin induces vascular endothelial growth factor expression and angiogenesis selectively at wound sites. *Wound Repair Regen.* **8**: 367–370.
- Urbanelli, L, Buratta, S, Sagini, K, Ferrara, G, Lanni, M, Emiliani, C (2015). Exosome-based strategies for Diagnosis and Therapy. *Recent Pat CNS Drug Discov* **10**: 10–27.
- Vader, P, Mol, EA, Pasterkamp, G, Schiffelers, RM (2016). Extracellular vesicles for drug delivery. *Adv. Drug Deliv. Rev.* **106**: 148–156.
- Valadi, H, Ekstrom, K, Bossios, A, Sjostrand, M, Lee, JJ, Lotvall, JO (2007). Exosome-mediated

transfer of mRNAs and microRNAs is a novel mechanism of genetic exchange between cells. *Nat. Cell Biol.* **9**: 654–659.

Vinh, A, Widdop, RE, Chai, SY, Gaspari, TA (2008a). Angiotensin IV-evoked vasoprotection is conserved in advanced atheroma. *Atherosclerosis* **200**: 37–44.

Vinh, A, Widdop, RE, Drummond, GR, Gaspari, TA (2008b). Chronic angiotensin IV treatment reverses endothelial dysfunction in ApoE-deficient mice. *Cardiovasc. Res.* **77**: 178–187.

Wang, B, Yao, K, Huuskes, BM, Shen, H, Zhuang, J, Godson, C, *et al.* (2016a). MicroRNA-let7c via Exosomes to Attenuate Renal Fibrosis. *Mol. Ther.* **24**: 1290–1301.

Wang, C, Kemp-Harper, BK, Kocan, M, Ang, SY, Hewitson, TD, Samuel, CS (2016b). The anti-fibrotic actions of relaxin are mediated through a NO-sGC-cGMP-dependent pathway in renal myofibroblasts in vitro and enhanced by the NO donor, diethylamine NONOate. *Front. Pharmacol.* **7**: 1–12.

Wang, D, Luo, Y, Myakala, K, Orlicky, DJ, Dobrinskikh, E, Wang, X, *et al.* (2017). Serelaxin improves cardiac and renal function in DOCA-salt hypertensive rats. *Sci. Rep.* **7**: 9793.

Weir, MR, Fink, JC (2005). Salt intake and progression of chronic kidney disease: An overlooked modifiable exposure? A commentary. *Am. J. Kidney Dis.* **45**: 176–188.

Woessner Jr, J (1995). Quantification of matrix metalloproteinases in tissue samples. *Methods Enzym.* **248**: 510–52.

Yamaguchi, I, Tchao, BN, Burger, ML, Yamada, M, Hyodo, T, Giampietro, C, *et al.* (2012). Vascular endothelial cadherin modulates renal interstitial fibrosis. *Nephron - Exp. Nephrol.* **120**: e20–e31.

Yoshida, T, Kumagai, H, Kohsaka, T, Ikegaya, N (2013). Relaxin protects against renal ischemia-reperfusion injury. *Am. J. Physiol. Physiol.* **305**: F1169–F1176.

Yoshida, T, Kumagai, H, Kohsaka, T, Ikegaya, N (2014). Protective Effects of Relaxin against Cisplatin-Induced Nephrotoxicity in Rats. *Nephron Exp. Nephrol.* **128**: 9–20.

- Yoshida, T, Kumagai, H, Suzuki, A, Kobayashi, N, Ohkawa, S, Odamaki, M, *et al.* (2012). Relaxin ameliorates salt-sensitive hypertension and renal fibrosis. *Nephrol. Dial. Transplant* **27**: 2190–7.
- Zhang, A, Li, M, Wang, B, Klein, JD, Price, SR, Wang, XH (2018). miRNA-23a/27a attenuates muscle atrophy and renal fibrosis through muscle-kidney crosstalk. *J. Cachexia. Sarcopenia Muscle* **9**: 755–770.
- Zhao, B, Zhang, Y, Han, S, Zhang, W, Zhou, Q, Guan, H (2017). Exosomes derived from human amniotic epithelial cells accelerate wound healing and inhibit scar formation. *J. Mol. Histol.* **48**: 121–132.
- Zulli, A, Burrell, LM, Buxton, BF, Hare, DL (2008). ACE2 and AT4R are present in diseased human blood vessels. *Eur. J. Histochem.* **52**: 39–44.

Chapter 6

General Discussion

6.0 General discussion

Fibrosis is a hallmark of CKD, which is caused by a surfeit of conditions including genetic, immune, toxin, diet and/or injury to the kidney, and results in a slow and progressive loss of essential kidney function over time (i.e taking several years to manifest in humans). It is well-recognised that a number of risk factors can contribute to and accelerate disease progression, including ageing, diabetes, obesity and hypertension amongst others (Hill *et al.*, 2016). CKD is a major health concern affecting 13.4% of the global population and is defined by a reduced glomerular filtration rate and an increase in albumin excretion that persists in a patient for more than 3 months (Jha *et al.*, 2013; Hill *et al.*, 2016). With prolonged damage to the kidneys, this can lead to ESRF with patients often requiring lifestyle changes, dialysis or transplantation to maintain some quality of life (Stevens and Farmer, 2012). Although a number of medications are also available, most commonly being ACEi, ARBs, TGF- β 1-, aldosterone- or endothelin-1 receptor-blockers or statins, these therapies largely offer symptomatic management of disease progression without having the capacity to directly reverse kidney damage and related dysfunction (Boor *et al.*, 2007). This is most likely due to the fact that most of these therapies only block one contributing factor to disease progression, which is unlikely to have overall efficacy in attempting to treat a multi-factorial process; while also inducing several side-effects when administered at high concentrations. Hence, new therapies that can more directly reverse established chronic kidney injury and offer broader suppression of the pathways that contribute to disease progression, but also provide safe therapeutic efficacy, are still urgently required.

Whilst fibrogenesis is required for wound healing to occur following injury or insult to the kidney, dysregulated collagen-induced wound repair and/or persistent inflammation induces CKD, by creating a cycle of inflammatory cell recruitment, pro-inflammatory and pro-fibrotic cytokine release and activation, myofibroblast activation and excessive ECM deposition. This aberrant increase in ECM components, primarily collagen, in turn lengthens the distance between tubular cells causing hypoxia and eventual apoptosis of kidney cells, cascading into loss of kidney function (Tanaka, 2017). Currently-used anti-hypertensive treatments such as candesartan (CAND; an ARB) and perindopril (PERIN; an ACEi) are able to provide symptomatic relief by decreasing the impact

of blood pressure on kidney remodeling leading to fibrosis (Shihab, 2007; Dézsi, 2014; Schelbert *et al.*, 2014). However, whether these drugs offer any direct therapeutic efficacy in the absence of blood pressure regulation, when administered to normotensive settings remains poorly understood.

6.1 Summary of thesis

This thesis compared and combined current pharmacological treatments for kidney disease (CAND, PERIN) that target the ACE/AT₁R axis, to several other experimentally and clinically studied or newly-developed treatments that target other receptors such as RXFP1, IRAP or the AT₂R. Additionally, it investigated recently conceived combination therapies involving hAECs+RLX or EXO+RLX (Royce *et al.*, 2019), in the setting of normotensive kidney disease. The central focus of this thesis was the RXFP1 agonist, serelaxin (RLX), which has demonstrated rapid-occurring anti-fibrotic efficacy in several organs including the kidney and independently of disease etiology (reviewed in (Samuel *et al.*, 2016, 2017)), but which has been compared to current standard of care medication in very few studies (Samuel *et al.*, 2014). Chapter 3 compared and combined the ability of RLX to reverse established HS-induced kidney inflammation, fibrosis and related dysfunction with CAND or the AT₂R agonist, CGP42112 (CGP). Chapter 4 compared the ability of RLX to reverse established HS-induced kidney inflammation, fibrosis and related dysfunction to CAND, PERIN and the IRAP inhibitor, HFI-419 (HFI); and also evaluated the combined effects of HFI with CAND, PERIN or RLX. Chapter 5 compared the ability of RLX to prevent rapidly-occurring tubulointerstitial fibrosis to PERIN, the single chain derivative of RLX, B7-33, HFI, the AT₂R agonist, β -pro⁷-Ang III (BPRO), EXO, hAECs+RLX and EXO+RLX.

The key findings from this thesis were: 1) that currently-used anti-hypertensive therapies such as CAND and PERIN (at 1-2mg/kg/day) offered some anti-inflammatory effects in the models studied, while inducing hypotension when administered to normotensive models. However, in the absence of any overt HS- or UUO-induced increases in blood pressure, these therapies failed to exert any marked anti-fibrotic effects, indicating that they more likely ameliorate the impact of high blood pressure on kidney remodeling and fibrosis. Furthermore, when administered at higher concentrations that did induce some anti-remodelling effects in the kidney (i.e

4mg/kg/day of PERIN; Chapter 4), ACE inhibition induced a loss of body weight and exacerbated renal failure. This confirmed the limitations of using ACEi or ARBs as treatments for fibrosis-induced CKD;

2) Therapies that targeted alternative receptors to the AT₁R, including RXFP1, AT₂R or IRAP provide equivalent or greater anti-inflammatory efficacy to that of CAND or PERIN, and more direct anti-fibrotic efficacy compared to these anti-hypertensive medications, when administered to normotensive kidney disease models. While these therapies were able to inhibit mediators of collagen synthesis and augment a mediator of collagen degradation (MMP-2), they were able to induce these effects and alleviate renal dysfunction in the absence of having to regulate blood pressure;

3) Combining RLX with CGP (Chapter 3) or HFI (Chapter 4) did not offer any additive anti-fibrotic effects over either therapy alone, although the combined effects of CGP+RLX or HFI+RLX retained the anti-inflammatory effects of CGP/HFI and the anti-fibrotic effects of HFI/RLX. To a large extent, the therapeutic efficacy of RLX or HFI was diminished when these drugs were co-administered with CAND; but maintained when they were co-administered with PERIN (Chapter 4);

4) On the other hand, combining the anti-fibrotic effects of RLX with the anti-inflammatory and tissue-reparative effects of hAECs or EXO appeared to offer improved anti-inflammatory and anti-fibrotic efficacy over the effects of either treatment alone; and also synergistically inhibited mediators of collagen synthesis while promoting the MMP-2/TIMP-1 ratio to a greater extent than the individual treatments investigated (Chapter 5).

Taken together, this thesis has demonstrated the anti-fibrotic efficacy of a number of treatments that may be further developed and evaluated to replace the effects of ACEi/ARBs as treatments for normotensive kidney disease or that can act as adjunct therapies to ACEi to more broadly treat hypertensive kidney diseases.

6.2 The limited renoprotection offered by candesartan or perindopril in normotensive disease settings.

Although the 5% NaCl (HS)- and UUO-induced models of kidney disease utilised in this thesis undergo an up-regulation of the intrinsic RAS within the kidney (HS) (Yu *et al.*, 1998) and plasma renin (UUO), they fail to undergo large increases in blood pressure in mice. Hence, these models are known to be associated with normotensive disease in mice; with higher levels (8-10%) of HS being required to induce hypertensive kidney disease (Mozaffari and Wyss, 1999; Yoshida *et al.*, 2012). ACEi and ARBs are well known to inhibit specific components of the RAS (ACE and the AT₁R, respectively), resulting in their ability to primarily inhibit the vasoconstricting effects of Ang II, and to a lesser extent, the pro-inflammatory and tissue remodelling effects of the hormone (Nagai *et al.*, 2004; Dézsi, 2014). Interestingly, even in the absence of an elevation in blood pressure in 5% NaCl-fed mice, the ability of CAND or PERIN to suppress Ang II activity or production, respectively, presumably resulted in their ability to induce hypotension after 4 weeks of treatment. Although the effects of CAND were strain-dependent (inducing significant hypotension in the FVB/N mice studied in Chapter 3, but not in the C57B6J mice studied in Chapter 4), these findings highlighted the potential side-effects that can be induced by ACEi and ARBs. At doses of 1-2mg/kg/day (which are commonly-used to induce their anti-hypertensive effects in hypertensive models), both CAND and PERIN were also able to suppress or reduce p-iKB expression levels, which was used as a surrogate marker of NF-κB activity, confirming that these drugs were biologically active at the doses administered. Consistent with this, Yu and colleagues showed in nephrectomised spontaneously hypertensive rats that CAND could dose-dependently ameliorate inflammation (Yu *et al.*, 2007). In humans, CAND also exhibited anti-inflammatory effects when administered to diabetic and non-diabetic hypertensive patients (Derosa *et al.*, 2010).

As demonstrated in Chapters 3 and 5, however, when administered at this same dose range (of 1-2mg/kg/day), neither CAND nor PERIN administration to normotensive models of kidney disease affected renal remodelling or fibrosis. Interestingly, there is not much published on the effects of these drugs in other normotensive models of nephropathy, likely because they are largely known and used for their anti-hypertensive effects. In line with this, a plethora of studies

have shown that CAND (Noda *et al.*, 1999; Brown *et al.*, 2001; Nagai *et al.*, 2004; Jones *et al.*, 2012) or PERIN (Ina *et al.*, 2004; Nagai *et al.*, 2004; Liang and Leenen, 2008; Rafiq *et al.*, 2014) administration can reduce the impact of Ang II on high blood pressure-induced renal remodelling after several weeks of treatment (i.e 4-16 weeks), when administered to hypertensive rodent models of kidney disease. When then administered at high doses (4mg/kg/day of PERIN used in Chapter 4) that do mediate some anti-remodelling and anti-fibrotic effects, PERIN was found to lower body weight, induce hypotension and exacerbate renal failure; suggesting that ACEi at least can induce ECM remodelling within the normotensive kidney, but at doses which induce adverse side-effects. On the other hand, when administered at lower/safer doses that do not induce these side-effects, they do not appear to be able to induce ECM remodelling within the damaged kidney, at least within the 1-4 week treatment period investigated in this thesis.

Even at the *in vitro* level, studies have shown that ARBs and ACEi can induce ECM remodelling, but only by blocking the contribution of the Ang II/AT₁R axis to aberrant remodelling and fibrosis progression. For example, CAND was found to prevent the Ang II-induced increase in fibronectin and collagen I in mouse collecting duct cells, which can undergo mesenchymal cell transition contributing to interstitial renal fibrosis (Cuevas *et al.*, 2014). In rat cardiac myofibroblasts, both CAND and the ACEi, enalapril, were found to abrogate the contribution of hydrogen peroxide to Ang II production that in turn enhanced AT₁R expression in these cells (Anupama *et al.*, 2016). An up-regulation of Ang II can lead to increased IL-6 and ERK phosphorylation/MAP kinase activity (Anupama *et al.*, 2016; Ohkura *et al.*, 2017) in cardiac myofibroblasts, where the promotion of IL-6 can induce cardiac hypertrophy. Taken together, these studies confirm that ARBs and ACEi can safely prevent or reduce aberrant ECM remodelling only in the presence of an elevated Ang II/AT₁R axis. Likewise, several studies have shown that ARBs and ACEi can reduce fibrosis when applied to hypertensive models (Wright *et al.*, 2002; Nagai *et al.*, 2004; Yu *et al.*, 2007; Santos *et al.*, 2009; Jones *et al.*, 2012), which are associated with elevated tissue and/or circulating Ang II levels. Alternatively, it has been suggested that ARBs and ACEi may not have direct anti-fibrotic effects, because some pathways involved in interstitial renal fibrosis may be independent of RAS activity (Debelle *et al.*, 2004).

Although ARBs and ACEi are used as frontline treatments for heart failure, diabetic nephropathy and other metabolic diseases, the findings of this thesis suggest that these drugs are likely to only provide symptomatic management of disease progression, rather than direct anti-fibrotic effects at doses that do not induce any side-effects. As a result of this, clinical evaluation of these drugs such as the ACEi, Ramipril, in hypertensive patients, found that the drug was able to decrease blood pressure but did not slow the progression of sclerotic kidney damage in these patients (Wright *et al.*, 2002). Furthermore, due to their indirect actions on tissue-remodelling, these drugs are likely to be slow-acting, mainly offering anti-hypertensive and anti-inflammatory efficacy. If administered at high doses (that induce side-effects) to normotensive patients who are not overweight, these drugs may induce hypotension and worsen renal function in treated patients. Hence, the need to identify new/other types of drug- or cell-based therapies that can more effectively reduce renal remodelling leading to reduced fibrosis progression.

6.3 Novel treatments with alternative receptor targets provide better anti-fibrotic efficacy.

Throughout this thesis, the one major common finding identified was that those treatments which targeted alternative receptors (RXFP1, AT₂R) or enzymes (IRAP) provided more direct anti-fibrotic efficacy compared to those that targeted the ACE/AT₁R axis. This was evidenced by the lack of anti-fibrotic efficacy offered by CAND or PERIN when administered to normotensive models, at doses that were able to reduce blood pressure and renal inflammation; whereas the anti-fibrotic efficacy of RLX, HFI and CGP at least were shown to be independent of blood pressure regulation. The following additional observations were made:

Although the RXFP1 agonists evaluated (RLX, B7-33) did not inhibit macrophage infiltration to a similar extent as the other treatments evaluated, they significantly lowered P-iKB levels, which was used as a surrogate marker of NF-kB activity. It may be that targeting RXFP1 has an immediate effect on other cells such as neutrophils (Masini *et al.*, 2004) and/or mast cells (Bani *et al.*, 1998), or that targeting RXFP1 has a greater effect on the inhibition of pro-inflammatory cytokine activity. This is evidenced by previous studies showing that RLX inhibits the expression and/or activity of factors such as TGF- β 1 (Heeg *et al.*, 2005; Mookerjee *et al.*, 2009; Yoshida *et*

et al., 2012), TNF- α (Brecht *et al.*, 2011; Yoshida *et al.*, 2013, 2014), IL-1/IL-6 (Wang *et al.*, 2017; Giam *et al.*, 2018) as well as ICAM-1 and VCAM-1 (Brecht *et al.*, 2011; Wang *et al.*, 2017). As RLX does not affect basal matrix turnover when administered to unstimulated myofibroblasts (Samuel *et al.*, 2004), it has been well-documented that RLX mediates its anti-fibrotic actions by inhibiting TGF- β 1 and/or Ang II activity and the pro-fibrotic influence of these factors on fibroblast proliferation and differentiation into myofibroblasts, and hence, myofibroblast-induced ECM production. RLX has also been found to inhibit endothelial cell to mesenchymal cell transition (Zhou *et al.*, 2015; Zheng *et al.*, 2017), which may contribute to its ECM-inhibitory actions.

The ability of RLX to disrupt TGF- β 1 signal transduction was shown to be mediated by its ability to signal through a RXFP1-pERK1/2-nNOS-NO-sGC-cGMP-dependent pathway in rat and human renal fibroblasts, to inhibit the phosphorylation of Smad2 (Heeg *et al.*, 2005; Mookerjee *et al.*, 2009); where Smad2 is an intracellular protein that promotes TGF- β 1 signal transduction. In addition to suppressing the pro-fibrotic influence of TGF- β 1 on ECM/collagen deposition, RLX has also been found to promote collagen-degrading MMPs (collagenases and gelatinases) through the above-mentioned signal transduction pathway (Chow *et al.*, 2012). This is thought to also be achieved via the TGF- β 1-inhibitory actions of RLX, as TGF- β 1 contributes to renal fibrosis by suppressing MMP activity and inducing TIMP activity (Meng *et al.*, 2015). Although B7-33 has only recently been developed (Hossain *et al.*, 2016) and hence, many of the signal transduction mechanisms by which it mediates its anti-fibrotic effects have not been evaluated, it was expected (as demonstrated in Chapter 5) that B7-33 would mimic the anti-fibrotic effects of RLX, given its specificity for the RXFP1 receptor. Although not evaluated in this thesis, RXFP1 activation offers broader renal protection as it also includes anti-hypertrophic (Lekgabe *et al.*, 2005; Moore *et al.*, 2007; Parikh *et al.*, 2013), vasodilatory (Conrad, 2011; Van Drongelen *et al.*, 2013), and anti-oxidant (Sasser *et al.*, 2011; Ng *et al.*, 2018) effects which may have contributed to tissue remodelling.

In comparison to the RXFP1 agonists evaluated, the AT₂ receptor agonists CGP and BRPO both appeared to significantly reduce infiltrating macrophage and P-iKB levels, and hence, it may be

suggested that by activating the AT₂R, these drugs primarily suppressed the contribution of inflammation to fibrosis progression. On the other hand, CGP did not reduce glomerulosclerosis, interstitial fibrosis, renal TGF- β 1 expression levels or myofibroblast accumulation to the same extent as RLX, nor affect the MMP-9/TIMP-1 and MMP-2/TIMP-1 ratio to the same extent as the RXFP1 agonist (Chapter 3). BPRO also did not prevent interstitial fibrosis nor KIM-1 associated renal damage to the same extent as RLX or B7-33; suggesting that these AT₂R agonists did not suppress measures of ECM/collagen synthesis or promote measures of ECM/collagen degradation to the same extent as drugs targeting RXFP1. Consistent with this theory, studies investigating the therapeutic effects of CGP or its non-peptide counterpart, C21, have shown that these AT₂R agonists can broadly inhibit TNF- α , IL-6, and oxidative stress (Rompe *et al.*, 2010; Namsolleck *et al.*, 2014). There is evidence though to suggest that AT₂R activation can inhibit profibrotic TGF- β 1 signal transduction via Smad and MAPK signalling, particularly by dephosphorylating (activating) ERK via the actions of tyrosine phosphatases (Widdop *et al.*, 2003; Murphy *et al.*, 2015). Similar to RXFP1 activation, AT₂R activation also promotes NO bioavailability and NO-cGMP signalling, which are known suppressors of Smad signalling (Widdop *et al.*, 2003; Koulis *et al.*, 2015; Sumners *et al.*, 2019). Hence, taken together with the data shown in Chapters 3 and 5, it can be suggested that stimulating AT₂R activity can consistently lead to suppression of the pro-inflammatory and pro-fibrotic influence of TGF- β 1; resulting in a greater inhibition of inflammation over collagen turnover. Regardless of this, targeting the AT₂R offered similar protection against HS-induced renal dysfunction, to that of targeting RXFP1. Although BPRO demonstrated stronger collagen-inhibitory efficacy to that of CGP, it is unclear whether this was due to the fact that BPRO was evaluated as a preventative therapy (against UUO) whereas CGP was evaluated for its ability to reduce established fibrosis (due to HS), or whether this was due to the higher affinity of BPRO for the AT₂R.

Targeting IRAP with HFI had similar anti-inflammatory efficacy to that of CGP and BPRO, and similar anti-fibrotic efficacy to that of RLX and B7-33, suggesting that the targeting of IRAP offered more broader renoprotection compared to the targeting of RXFP1 or AT₂R. HFI was shown to mediate its anti-fibrotic effects by inhibiting TGF- β 1-induced myofibroblast differentiation and myofibroblast-induced ECM/collagen deposition, while promoting the MMP-2/TIMP-1 ratio that

would likely lead to augmentation of MMP-2-induced ECM/collagen degradation. Due to HFI also being relatively recently developed and several patents being filed on its potential use as a therapy, there is limited information on its anti-fibrotic potential in kidney disease or on other organ disease. Although the mechanistic actions of IRAP inhibition are still to be fully elucidated, it is proposed that IRAP substrates such as lys-bradykinin, vasopressin, oxytocin and Ang III are increased by HFI contributing to its renoprotection (Kakoki *et al.*, 2007; Tugtepe *et al.*, 2007; Albiston *et al.*, 2010; Plante *et al.*, 2015). In particular, oxytocin receptors have been shown to increase in expression during inflammation and once bound with oxytocin, reduce macrophage infiltration and IL-6 (Szeto *et al.*, 2017). Furthermore, oxytocin has been shown to reduce NADPH-dependent and TGF- β 1 P38 MAPK/Smad signalling (Rashed *et al.*, 2011; Jiang *et al.*, 2014). Ang III is a partial agonist for AT₂ receptors and can induce similar inhibition of TGF- β 1 to that of other AT₂ receptor agonists (De Gasparo *et al.*, 2000). Consistent with these data and unpublished findings from our group, to which I contributed, we have demonstrated that the anti-fibrotic effects of HFI in the same UUO model was abrogated by co-administration of oxytocin receptor blockade or AT₂R blockade.

Given the regulatory and manufacturing advantages to using EXO over their parental cells, the effects of hAEC-derived EXO were also evaluated in the UUO model alone. As a preventative therapy, EXO (administered at 25 μ g/mouse; which is thought to provide the therapeutic equivalence of 12.5 million AECs) had a striking ability to suppress renal damage, inflammation and fibrosis to a similar extent as the other mono-therapies (RLX, B7-33, HFI, BPRO) investigated. However, when administered to established fibrosis-induced disease, at least in experimental models of lung disease, this same dose of EXO only had a partial effect in reducing airway/lung inflammation and fibrosis (Royce *et al.*, 2019). This would suggest then that the fibrosis associated with established/chronic disease can hinder the viability and therapeutic efficacy of EXO (as has been found in the case of fibrosis hindering stem cell survival and function) (Lu *et al.*, 2004; Eun *et al.*, 2011).

It has been suggested that exosomes in general can mediate their therapeutic effects by suppressing immune cell infiltration and the pro-inflammatory cytokines (such as TNF- α and IL-6) that are secreted by infiltrating cells into damaged tissues (Urbanelli *et al.*, 2015). Other studies

have shown that exosomes also possess proteasome, glycolytic enzyme, anti-oxidant and ECM-modifying activity once secreted from their parental cells (reviewed in Urbanelli *et al.*, 2015). Consistent with the latter, the findings presented in Chapter 5 demonstrated that hAEC-derived EXO can partially prevent TGF- β 1-induced myofibroblast differentiation and interstitial collagen deposition, while also being able to promote collagen-degrading MMP-2 activity. Bypassing the limitations of stem cells that were discussed in Chapter 1 (Section 1.7.5), exosomes in general have been shown to produce similar if not superior organ-protective effects compared to their parental cells (Lai *et al.*, 2011; Van Balkom *et al.*, 2011; Urbanelli *et al.*, 2015; Wang *et al.*, 2016). Interestingly, exosomes appear to contain tissue-reparative microRNAs or can be engineered to over-express specific microRNAs that can enhance their therapeutic potential (Wang *et al.*, 2016; Ferguson *et al.*, 2018).

In terms of the combination therapies evaluated, mixed results were observed, suggesting that not all drugs/cell-based therapies can be feasibly combined to produce greater outcomes over either therapy alone. Studies had shown that the combined effects of RLX with the corticosteroids, methylprednisolone (Royce *et al.*, 2013) or dexamethasone (Patel *et al.*, 2016), offered enhanced anti-inflammatory effects over that of RLX alone and enhanced anti-remodelling effects over that of the corticosteroids alone in an experimental model of chronic AAD. This resulted in greater protection against chronic AAD-induced airway reactivity over the effects of the corticosteroids alone. Combining RLX with the ACEi, enalapril also demonstrated greater protection of cardiac fibrosis over the effects of enalapril alone, but similar protection to that of RLX alone in an isoproterenol-induced model of cardiomyopathy (Samuel *et al.*, 2014), while combining RLX with hAECs or hAEC-derived EXO offered improved protection over either therapy alone against experimental models of established lung disease (Royce *et al.*, 2016, 2019). These previously published studies offered the encouraging basis for combining RLX or HFI with various other therapies in this thesis.

However, as observed in HS models (Chapters 3 and 4), combining RLX or HFI with CAND resulted in the inhibition or compromise of the renoprotective effects of RLX or HFI alone. In the case of RLX, this was thought to be due to the direct interaction or crosstalk that can occur between RXFP1 and the AT₁R, as RXFP1 has been shown to form heterodimer with AT₂ receptors (Chow *et*

al., 2014). Heterodimerization can also occur between AT₁ receptors and AT₂ receptors (AbdAlla *et al.*, 2001; Miura *et al.*, 2010) which would allow AT₁R blockers such as CAND to inhibit the RXFP1-agonist actions of RLX. In the case of HFI, however, this was thought to be able to occur due to high enough concentrations of the IRAP inhibitor possibly being able to activate the AT₁R, which would allow CAND to then block the renoprotective effects of HFI acting through the AT₁R. Further work is required to validate these theories, and to also determine if other ARBs can achieve similar inhibitory effects when combined with RLX or HFI or with other RXFP1 agonists or IRAP inhibitors, respectively. Based on the findings demonstrated in this thesis, however, it would be suggested not to combine the effects of ARBs with RXFP1 agonists or IRAP inhibitors in a clinical setting.

In the HS model, combining HFI with PERIN appeared to maintain the renoprotective effects of either therapy alone, and somewhat protect from HS-induced renal macrophage infiltration to a greater extent than PERIN alone. As HFI alone offered broader renoprotection over the effects of PERIN alone without regulating blood pressure, it could be suggested that the efficacy of this combination therapy could be further evaluated in hypertensive models of kidney disease, in which the blood pressure-lowering effects of PERIN could be combined with the anti-remodelling and anti-fibrotic effects of HFI. Further work by other members of our Labs is also determining if the combined effects of RLX and PERIN offer greater cardiovascular protection over either therapy alone; as combining RLX with ACEi may be more clinically suited as a combination therapy to retaining (but not compromising) the broader tissue remodelling and blood-pressure lowering effects of these therapies when combined.

Most excitingly, the findings presented in Chapter 5 demonstrated that combining the therapeutic effects of RLX and EXO offered almost full protection (as a preventative therapy) against UUO-induced tubulointerstitial renal disease, which was to a greater extent than either therapy alone. Combining EXO with RLX offered enhanced anti-inflammatory effects over that of RLX alone, enhanced protection against UUO-induced tissue damage compared to EXO alone, and fully prevented the UUO-induced vascular rarefaction. These findings suggest that as a preventative therapy, the anti-remodelling and anti-fibrotic effects of RLX can be effectively combined with the immunomodulatory and tissue-reparative effects of EXO to ablate the

progression of renal injury-induced fibrosis. It is also likely that the effects of this combination therapy are mediated independently of blood-pressure regulation. Further work is now required to validate the therapeutic efficacy of this combination therapy as an intervention strategy, in both normotensive and hypertensive models of renal disease associated with established fibrosis; in which the therapeutic effects of EXO alone may be compromised. In the latter setting, it needs to be determined if RLX can be administered at the same time as EXO (which may be feasible as a preventative therapy administered at the time of injury onset, before fibrosis is established), or whether RLX pre-treatment would further enhance the therapeutic effects of EXO when combined together. Evaluation of the reparative components that are released by these EXO and the mechanisms of action that contribute to the synergistic effects of this combination therapy also require further investigation.

In summary, this thesis has shown that there are several therapies that can effectively inhibit renal injury-induced tissue remodelling, fibrosis and dysfunction without the need to regulate blood pressure. The RXFP1 agonists RLX and B7-33 as well as the IRAP inhibitor, HFI were found to have broad renoprotective effects (which were associated with their ability to inhibit measures of collagen synthesis while promoting measures of collagen degradation), which were mediated via the anti-inflammatory, anti-fibrotic and angiogenic actions of these drugs. Even the AT₂R agonists, CGP and BPRO were found to effectively inhibit the contribution of renal inflammation to fibrosis progression, and along with the RXFP1 agonists and IRAP inhibitor studied, offered greater renoprotection over the effects of the ARB (CAND) and ACEi (PERIN) evaluated. While EXO alone offered similar renoprotection to the above-mentioned therapies as a preventative therapy, it is likely that the anti-fibrotic effects of RLX would need to be combined with EXO to offer some protection against CKD progression, when administered as an intervention therapy. Further evaluation of these therapies may lead to recognition of clinical conditions in which they may be used as stand-alone therapies, or where their tissue remodelling potential may serve as adjunct therapies to the blood pressure lowering effects of current standard of care medication.

6.5 Limitations and future directions

As discussed in Chapters 3-5, there were some limitations to the studies conducted, which may have to be considered and addressed in future experiments. Firstly, for consistency, only two markers of renal inflammation (F4/80 and P-iKB) were measured throughout this thesis. Although macrophages (Tang *et al.*, 2019) and NF- κ B (Declèves and Sharma, 2014) are key contributors to the renal inflammation that eventually contributes to CKD, in reality however, several other cell types (such as neutrophils, leukocytes, T cells, etc) are known to infiltrate the damaged kidney post-injury, and several other factors (such as TNF- α , IL-6, MCP-1, ICAM-1, VCAM-1, etc) are known to contribute to renal inflammation and remodelling (Mene *et al.*, 2003; Sato and Yanagita, 2018). Clearly, the impact of the therapies investigated on other infiltrating and resident cells (such as dendritic cells, epithelial cells, myofibroblasts, etc) as well as other pro-inflammatory and anti-inflammatory cytokines that regulate renal inflammation would need to be investigated in future studies. Secondly, this thesis focused on TGF- β 1 and myofibroblast-induced ECM production as measures of fibrosis, as the proliferation and differentiation of resident fibroblasts into activated myofibroblasts is considered the main contributor (~50%) to renal fibrosis (Loeffler and Wolf, 2015). However, as bone-marrow-derived fibrocyte differentiation (~35%) EndMT (~10%) and EMT (~5%) can also contribute to renal fibrosis (Loeffler and Wolf, 2015), it is clear that future studies should also investigate the extent to which the various therapies examined in this thesis, impact on these other contributors to kidney fibrosis. Thirdly, in terms of the current standard of care therapies studied (CAND, PERIN), dose-response studies evaluating the anti-remodelling and anti-fibrotic effects of these drugs as well as other ARBs and ACEi should be performed over longer-periods of time; and perhaps in larger animals where renal remodelling takes longer than 1-4 weeks to occur. This is due to the fact that renal remodelling in humans take several months to years to occur.

Ageing, sex differences, hypertension and/or diabetes are all risk factors that contribute to CKD, and should also be incorporated into future studies when evaluating the efficacy of the various drugs/treatment strategies studied in this thesis. AT₁R expression is maintained from childhood to adulthood (providing a suitable target for ARBs), whereas AT₂R expression decreases with age (De Gasparo *et al.*, 2000). Only after injury, and in females over males is AT₂R expression

dramatically increased (Carey, 2005), which would allow it to be more appropriately targeted by AT₂R-agonists for the treatment of fibrosis. Female rats have been shown to have higher AT₂ receptor levels in their kidneys compared to their male counterparts, which may result in AT₂R-agonists having higher anti-fibrotic effects in the kidneys of females, which is thought to be estrogen-dependent (Baiardi *et al.*, 2004). Similarly, high doses of estrogen were also found to contribute to higher RXFP1 receptor expression in rodent female organs (Du *et al.*, 2003; Dehghan *et al.*, 2015). Hence, as only male mice were used in this thesis, further examination into age and sex differences are needed to verify if the treatments investigated will have similar therapeutic efficacy in pre-menopausal vs post-menopausal females (the latter being associated with a loss of estrogen and relaxin).

In terms of renal functional measurements, this could only be achieved in the HS model and not in the UUO model, as the unobstructed kidney, although overworked, is known to be able to maintain renal function in the latter model (Hewitson, 2009). Only plasma urea levels were used as a surrogate marker of renal dysfunction (Waikar and Bonventre, 2007). Additionally, other measures such as glomerular filtration rate (GFR) should be included as it is the current “gold standard” measurement (Sasaki *et al.*, 2014) for the detection of renal dysfunction. Other measures such as albuminuria and/or creatine clearance can also be used to measure changes in disease- and treatment-induced changes in renal dysfunction.

As discussed in Chapter 5, the various treatments investigated in the UUO model were all administered as preventative therapies, immediately after UUO was performed; and prior to fibrosis being established. This would not be clinically relevant, as almost all therapies are administered to patients with established disease (Mehta *et al.*, 2015; Bouchard and Mehta, 2016; Hill *et al.*, 2016), and usually when these patients have lost at least half their renal function. Nevertheless, the results provided in that Chapter did provide proof of principle findings, that can be further validated by administering the most efficacious treatments as intervention therapies to established disease.

6.4 Final remarks

This thesis has contributed to evaluation of the direct anti-fibrotic efficacy of the various therapies/combination strategies evaluated in the setting of normotensive kidney disease, which lacked ageing, hypertension or diabetes as risk factors that often contribute to CKD. Although the anti-fibrotic and renoprotective effects, RLX had previously been investigated in rats fed a 8% NaCl diet (Yoshida *et al.*, 2012), which led to elevated blood pressure in those animals; as well as the UUO model (Hewitson *et al.*, 2007), this is the first time, its effects were evaluated in HS-fed mice that did not undergo elevated blood pressure. The findings of this thesis confirmed that RLX was able to maintain its anti-fibrotic effects in the kidney independently of etiology, as its effects are consistently mediated by its ability to inhibit the pro-fibrotic effects of TGF- β 1 and/or Ang II on myofibroblast differentiation and ECM/collagen production, independently of blood-pressure regulation. The findings of this thesis are the first reported on the effects of CGP and HFI in HS-fed mice; and on the effects of B7-33, BPRO, hAECs+RLX, EXO or EXO+RLX in mice subjected to UUO. As previously mentioned, a lack of head-to-head comparisons between these therapies has often contributed to poor translation of their experimental effects to clinical potential. This thesis has demonstrated the rapid-occurring and superior anti-fibrotic efficacy offered by RLX, HFI, HFI+RLX and EXO+RLX, over the effects of CAND or PERIN, in experimental models of normotensive kidney disease. Not only are these therapies worthy of further examination as possible stand-alone treatments for kidneys diseases that are not associated with elevated blood pressure, but they are also worthy of examination for their potential ability to act as suitable adjunct therapies to that of ACEi. On the other hand, it did not appear feasible to combine RLX or HFI with CAND, as the therapeutic effects of the RXFP1-agonist or IRAP inhibitor were compromised in the presence of the ARB. Further evaluation of these therapies/combination strategies may lead to new treatments for CKD, which are urgently needed, given that CAND and PERIN only appeared to inhibit the contribution of hypertension to renal remodelling. As many of these therapies are already being clinically evaluated for other indications, it is envisaged that they may be fast-tracked as treatments for CKD, but only when validation of their therapeutic efficacy over longer-term periods has been substantiated.

6.5 References

- AbdAlla, S, Lothar, H, Abdel-tawab, AM, Quitterer, U (2001). The angiotensin II AT2 receptor is an AT1 receptor antagonist. *J Biol Chem* **276**: 39721–39726.
- Albiston, AL, Fernando, RN, Yeatman, HR, Burns, P, Ng, L, Daswani, D, *et al.* (2010). Gene knockout of insulin-regulated aminopeptidase: Loss of the specific binding site for angiotensin IV and age-related deficit in spatial memory. *Neurobiol. Learn. Mem.* **93**: 19–30.
- Anupama, V, George, M, Dhanesh, SB, Chandran, A, James, J, Shivakumar, K (2016). Molecular mechanisms in H2O2-induced increase in AT1 receptor gene expression in cardiac fibroblasts: A role for endogenously generated Angiotensin II. *J. Mol. Cell. Cardiol.* **97**: 295–305.
- Baiardi, G, Macova, M, Armando, I, Ando, H, Tyurmin, D, Saavedra, JM (2004). Estrogen upregulates renal angiotensin II AT1 and AT2 receptors in the rat. *Regul. Pept.* **124**: 7–17.
- Balkom, BWM Van, Pisitkun, T, Verhaar, MC, Knepper, MA (2011). Exosomes and the kidney: Prospects for diagnosis and therapy of renal diseases. *Kidney Int.* **80**: 1138–1145.
- Bani, D, Masini, E, Bello, MG, Bigazzi, M, Sacchi, TB (1998). Relaxin protects against myocardial injury caused by ischemia and reperfusion in rat heart. *Am. J. Pathol.* **152**: 1367–76.
- Boor, P, Šebeková, K, Ostendorf, T, Floege, J (2007). Treatment targets in renal fibrosis. *Nephrol. Dial. Transplant.* **22**: 3391–3407.
- Bouchard, J, Mehta, RL (2016). Acute Kidney Injury in Western Countries. *Kidney Dis.* **2**: 103–110.
- Brecht, A, Bartsch, C, Baumann, G, Stangl, K, Dschietzig, T (2011). Relaxin inhibits early steps in vascular inflammation. *Regul. Pept.* **166**: 76–82.
- Brown, L, Fenning, A, Shek, A, Burstow, D (2001). Reversal of cardiovascular remodelling with candesartan. *J. Renin-Angiotensin-Aldosterone Syst.* **2**: S141–S147.
- Carey, RM (2005). Cardiovascular and renal regulation by the angiotensin type 2 receptor: The AT2 receptor comes of age. *Hypertension* **45**: 840–844.

Chow, BSM, Chew, EGY, Zhao, C, Bathgate, RAD, Hewitson, TD, Samuel, CS (2012). Relaxin signals through a RXFP1-pERK-nNOS-NO-cGMP-dependent pathway to up-regulate matrix metalloproteinases: The additional involvement of iNOS. *PLoS One* **7**:.

Chow, BSM, Kocan, M, Bosnyak, S, Sarwar, M, Wigg, B, Jones, ES, *et al.* (2014). Relaxin requires the angiotensin II type 2 receptor to abrogate renal interstitial fibrosis. *Kidney Int.* **86**: 75–85.

Conrad, KP (2011). Maternal vasodilation in pregnancy: the emerging role of relaxin. *Am. J. Physiol. Integr. Comp. Physiol.* **301**: R267–R275.

Cuevas, CA, Gonzalez, AA, Inestrosa, NC, Vio, CP, Prieto, MC (2014). Angiotensin II increases fibronectin and collagen I through the β -catenin-dependent signaling in mouse collecting duct cells. *Am. J. Physiol. Physiol.* **308**: F358–F365.

Debelle, FD, Nortier, JL, Husson, CP, Prez, EG De, Vienne, AR, Rombaut, K, *et al.* (2004). The renin-angiotensin system blockade does not prevent renal interstitial fibrosis induced by aristolochic acids. *Kidney Int.* **66**: 1815–1825.

Declèves, AE, Sharma, K (2014). Novel targets of antifibrotic and anti-inflammatory treatment in CKD. *Nat. Rev. Nephrol.* **10**: 257–267.

Dehghan, F, Yusof, A, Muniandy, S, Salleh, N (2015). Estrogen receptor (ER)- α , β and progesterone receptor (PR) mediates changes in relaxin receptor (RXFP1 and RXFP2) expression and passive range of motion of rats' knee. *Environ. Toxicol. Pharmacol.* **40**: 785–791.

Derosa, G, Maffioli, P, Salvadeo, SAT, Ferrari, I, Gravina, A, Mereu, R, *et al.* (2010). Candesartan effect on inflammation in hypertension. *Hypertens. Res.* **33**: 209–213.

Dézsi, CA (2014). Differences in the clinical effects of angiotensin-converting enzyme inhibitors and angiotensin receptor blockers: A critical review of the evidence. *Am. J. Cardiovasc. Drugs* **14**: 167–173.

Drongelen, J Van, Koppen, A Van, Pertijs, J, Gooi, JH, Sweep, FCGJ, Lotgering, FK, *et al.* (2013). Impaired effect of relaxin on vasoconstrictor reactivity in spontaneous hypertensive rats. *Peptides* **49**: 41–48.

Du, X, Du, X, Samuel, CS, Samuel, CS, Gao, X, Gao, X, *et al.* (2003). Increased myocardial collagen and ventricular diastolic dysfunction in relaxin deficient mice: a gender-specific phenotype. *Cardiovasc. Res.* **57**: 395–404.

Eun, LY, Song, H, Choi, E, Lee, TG, Moon, DW, Hwang, D, *et al.* (2011). Implanted bone marrow-derived mesenchymal stem cells fail to metabolically stabilize or recover electromechanical function in infarcted hearts. *Tissue Cell* **43**: 238–245.

Ferguson, SW, Wang, J, Lee, CJ, Liu, M, Neelamegham, S, Canty, JM, *et al.* (2018). The microRNA regulatory landscape of MSC-derived exosomes: a systems view. *Sci. Rep.* **8**: 1–12.

Gasparo, M De, Catt, K, Inagami, T, Wright, J, Unger, T (2000). International Union of Pharmacology . XIII . The Angiotensin II Receptors. *Pharmacol. Rev.* **52**: 415–472.

Giam, B, Chu, PY, Kuruppu, S, Smith, AI, Horlock, D, Murali, A, *et al.* (2018). Serelaxin attenuates renal inflammation and fibrosis in a mouse model of dilated cardiomyopathy. *Exp. Physiol.* **103**: 1593–1602.

Heeg, MHJ, Koziolk, MJ, Vasko, R, Schaefer, L, Sharma, K, Müller, GA, *et al.* (2005). The antifibrotic effects of relaxin in human renal fibroblasts are mediated in part by inhibition of the Smad2 pathway. *Kidney Int.* **68**: 96–109.

Hewitson, TD (2009). Renal tubulointerstitial fibrosis: common but never simple. *AJP Ren. Physiol.* **296**: F1239–F1244.

Hewitson, TD, Mookerjee, I, Masterson, R, Zhao, C, Tregear, GW, Becker, GJ, *et al.* (2007). Endogenous relaxin is a naturally occurring modulator of experimental renal tubulointerstitial fibrosis. *Endocrinology* **148**: 660–669.

Hill, NR, Fatoba, ST, Oke, JL, Hirst, JA, O’Callaghan, CA, Lasserson, DS, *et al.* (2016). Global Prevalence of Chronic Kidney Disease – A Systematic Review and Meta-Analysis. *PLoS One* **11**: e0158765.

Hossain, MA, Kocan, M, Yao, ST, Royce, SG, Nair, VB, Siwek, C, *et al.* (2016). A single-chain derivative of the relaxin hormone is a functionally selective agonist of the G protein-coupled

receptor, RXFP1. *Chem. Sci.* **7**: 3805–3819.

Ina, Y, Yao, K, Ohno, T, Suzuki, K, Sonoka, R, Sato, H (2004). Effects of Benidipine and Candesartan on Kidney and Vascular Function in Hypertensive Dahl Rats. *Hypertens. Res.* **26**: 569–576.

Jha, V, Garcia-Garcia, G, Iseki, K, Li, Z, Naicker, S, Plattner, B, *et al.* (2013). Chronic kidney disease: Global dimension and perspectives. *Lancet* **382**: 260–272.

Jiang, F, Liu, GS, Dusting, GJ, Chan, EC (2014). NADPH oxidase-dependent redox signaling in TGF- β -mediated fibrotic responses. *Redox Biol.* **2**: 267–272.

Jones, ES, Black, MJ, Widdop, RE (2012). Influence of angiotensin II subtype 2 receptor (AT 2R) antagonist, PD123319, on cardiovascular remodelling of aged spontaneously hypertensive rats during chronic angiotensin II subtype 1 receptor (AT 1R) blockade. *Int. J. Hypertens.* **2012**..

Kakoki, M, McGarrah, RW, Kim, H-S, Smithies, O (2007). Bradykinin B1 and B2 receptors both have protective roles in renal ischemia/reperfusion injury. *Proc. Natl. Acad. Sci. U. S. A.* **104**: 7576–81.

Koulis, C, Chow, BSM, Mckelvey, M, Steckelings, UM, Unger, T, Thallas-Bonke, V, *et al.* (2015). AT2R agonist, compound 21, is Reno-protective against type 1 diabetic nephropathy. *Hypertension* **65**: 1073–1081.

Lai, RC, Chen, TS, Lim, SK (2011). Mesenchymal stem cell exosome: a novel stem cell-based therapy for cardiovascular disease. *Regen. Med.* **6**: 481–92.

Lekgabe, ED, Kiriazis, H, Zhao, C, Xu, Q, Moore, XL, Su, Y, *et al.* (2005). Relaxin reverses cardiac and renal fibrosis in spontaneously hypertensive rats. *Hypertension* **46**: 412–418.

Liang, B, Leenen, FHH (2008). Prevention of salt-induced hypertension and fibrosis by AT 1-receptor blockers in Dahl S rats. *J. Cardiovasc. Pharmacol.* **51**: 457–466.

Loeffler, I, Wolf, G (2015). Epithelial-to-Mesenchymal Transition in Diabetic Nephropathy: Fact or Fiction? *Cells* **4**: 631–652.

Lu, L, Zhang, JQ, Ramires, FJ, Sun, Y (2004). Molecular and cellular events at the site of myocardial infarction: From the perspective of rebuilding myocardial tissue. *Biochem. Biophys. Res. Commun.* **320**: 907–913.

Masini, E, Nistri, S, Vannacci, A, Bani Sacchi, T, Novelli, A, Bani, D (2004). Relaxin inhibits the activation of human neutrophils: involvement of the nitric oxide pathway. *Endocrinology* **145**: 1106–12.

Mehta, RL, Cerdá, J, Burdmann, EA, Tonelli, M, García-García, G, Jha, V, *et al.* (2015). International Society of Nephrology's Oby25 initiative for acute kidney injury (zero preventable deaths by 2025): A human rights case for nephrology. *Lancet* **385**: 2616–2643.

Mene, P, Polci, R, Festuccia, F (2003). Mechanisms of repair after kidney injury. *J. Nephrol.* **16**: 186–195.

Meng, XM, Tang, PMK, Li, J, Lan, HY (2015). TGF- β /Smad signaling in renal fibrosis. *Front. Physiol.* **6**: 1–8.

Miura, S, Matsuo, Y, Kiya, Y, Karnik, SS, Saku, K (2010). Molecular mechanisms of the antagonistic action between AT1 and AT2 receptors. *Biochem. Biophys. Res. Commun.* **391**: 85–90.

Mookerjee, I, Hewitson, TD, Halls, ML, Summers, RJ, Mathai, ML, Bathgate, R a D, *et al.* (2009). Relaxin inhibits renal myofibroblast differentiation via RXFP1, the nitric oxide pathway, and Smad2. *FASEB J.* **23**: 1219–29.

Moore, XL, Tan, SL, Lo, CY, Fang, L, Su, YD, Gao, XM, *et al.* (2007). Relaxin antagonizes hypertrophy and apoptosis in neonatal rat cardiomyocytes. *Endocrinology* **148**: 1582–1589.

Mozaffari, M, Wyss, J (1999). Dietary NaCl-Induced Hypertension in Uninephrectomized Wistar-Kyoto Rats: Role of Kidney Function. *J. Cardiovasc. Pharmacol.* **33**: 814–821.

Murphy, AM, Wong, AL, Bezuhly, M (2015). Modulation of angiotensin II signaling in the prevention of fibrosis. *Fibrogenes. Tissue Repair* **8**: 1–7.

Nagai, M, Horikoshi, K, Izumi, T, Seki, S, Taniguchi, M, Taniguchi, I, *et al.* (2004).

Cardioprotective action of perindopril versus candesartan in renovascular hypertensive rats. *Cardiovasc. Drugs Ther.* **18**: 353–362.

Namsolleck, P, Recarti, C, Foulquier, S, Steckelings, UM, Unger, T (2014). AT(2) receptor and tissue injury: therapeutic implications. *Curr. Hypertens. Rep.* **16**: 416.

Ng, HH, Leo, CH, Parry, LJ, Ritchie, RH (2018). Relaxin as a therapeutic target for the cardiovascular complications of diabetes. *Front. Pharmacol.* **9**: 1–10.

Noda, M, Matsuo, T, Fukuda, R, Ohta, M, Nagano, H, Shibouta, Y, *et al.* (1999). Effect of candesartan cilexetil (TCV-116) in rats with chronic renal failure. *Kidney Int.* **56**: 898–909.

Ohkura, SI, Usui, S, Takashima, SI, Takuwa, N, Yoshioka, K, Okamoto, Y, *et al.* (2017). Augmented sphingosine 1 phosphate receptor-1 signaling in cardiac fibroblasts induces cardiac hypertrophy and fibrosis through angiotensin II and interleukin-6. *PLoS One* **12**: 1–19.

Parikh, A, Patel, D, McTiernan, CF, Xiang, W, Haney, J, Yang, L, *et al.* (2013). Relaxin suppresses atrial fibrillation by reversing fibrosis and myocyte hypertrophy and increasing conduction velocity and sodium current in spontaneously hypertensive rat hearts. *Circ. Res.* **113**: 313–321.

Patel, KP, Giraud, AS, Samuel, CS, Royce, SG (2016). Combining an epithelial repair factor and anti-fibrotic with a corticosteroid offers optimal treatment for allergic airways disease. *Br. J. Pharmacol.* **173**: 2016–2029.

Plante, E, Menaouar, A, Danalache, BA, Yip, D, Broderick, TL, Chiasson, JL, *et al.* (2015). Oxytocin treatment prevents the cardiomyopathy observed in obese diabetic male db/db mice. *Endocrinology* **156**: 1416–1428.

Rafiq, K, Nishiyama, A, Konishi, Y, Morikawa, T, Kitabayashi, C, Kohno, M, *et al.* (2014). Regression of glomerular and tubulointerstitial injuries by dietary salt reduction with combination therapy of angiotensin II receptor blocker and calcium channel blocker in Dahl salt-sensitive rats. *PLoS One* **9**:

Rashed, LA, Hashem, RM, Soliman, HM (2011). Oxytocin inhibits NADPH oxidase and P38 MAPK in cisplatin-induced nephrotoxicity. *Biomed. Pharmacother.* **65**: 474–480.

- Rompe, F, Artuc, M, Hallberg, A, Alterman, M, Str??der, K, Th??ne-Reineke, C, *et al.* (2010). Direct angiotensin II type 2 receptor stimulation acts anti-inflammatory through epoxyeicosatrienoic acid and inhibition of nuclear factor ??b. *Hypertension* **55**: 924–931.
- Royce, SG, Patel, KP, Mao, W, Zhu, D, Lim, R, Samuel, CS (2019). Serelaxin enhances the therapeutic effects of human amnion epithelial cell-derived exosomes in experimental models of lung disease. *Br. J. Pharmacol.* [Epub ahead of print]. bph.14666.
- Royce, SG, Sedjatera, A, Samuel, CS, Tang, MLK (2013). Combination therapy with relaxin and methylprednisolone augments the effects of either treatment alone in inhibiting subepithelial fibrosis in an experimental model of allergic airways disease. *Clinical Sci.* **124**: 41–51.
- Royce, SG, Tominaga, AM, Shen, M, Patel, KP, Huuskes, BM, Lim, R, *et al.* (2016). Serelaxin improves the therapeutic efficacy of RXFP1-expressing human amnion epithelial cells in experimental allergic airway disease. *Clin. Sci.* **130**: 2151–2165.
- Samuel, CS, Bodaragama, H, Chew, JY, Widdop, RE, Royce, SG, Hewitson, TD (2014). Serelaxin is a more efficacious antifibrotic than enalapril in an experimental model of heart disease. *Hypertension* **64**: 315–322.
- Samuel, CS, Royce, SG, Hewitson, TD, Denton, KM, Cooney, TE, Bennett, RG (2017). Anti-fibrotic actions of relaxin. *Br. J. Pharmacol.* **174**: 962–976.
- Samuel, CS, Summers, RJ, Hewitson, TD (2016). Antifibrotic Actions of Serelaxin - New Roles for an Old Player. *Trends Pharmacol. Sci.* **37**: 485–497.
- Samuel, CS, Unemori, EN, Mookerjee, I, Bathgate, RAD, Mak, J, Layfield, SL, *et al.* (2004). Relaxin Modulates Cardiac Fibroblast Proliferation, Differentiation, and Collagen Production and Reverses Cardiac Fibrosis in Vivo. *Endocrinology* **145**: 4125–4133.
- Santos, E, Picoli Souza, K de, Silva, E da, Batista, E, Martins, P, D’Almeida, V, *et al.* (2009). Long term treatment with ACE inhibitor enalapril decreases body weight gain and increases life span in rats. *Biochem. Pharmacol.* **78**: 951–958.
- Sasaki, Y, Iwama, R, Sato, T, Heishima, K, Shimamura, S, Ichijo, T, *et al.* (2014). Estimation of

glomerular filtration rate in conscious mice using a simplified equation. *Physiol. Rep.* **2**: 1–10.

Sasser, JM, Molnar, M, Baylis, C (2011). Relaxin ameliorates hypertension and increases NO metabolite excretion in Angiotensin II but not L-NAME hypertensive rats. *Hypertension* **58**: 197–204.

Sato, Y, Yanagita, M (2018). Immune cells and inflammation in AKI to CKD progression. *Am. J. Physiol. Physiol.* **315**: F1501–F1512.

Schelbert, EB, Fonarow, GC, Bonow, RO, Butler, J, Gheorghiade, M (2014). Therapeutic targets in heart failure: Refocusing on the myocardial interstitium. *J. Am. Coll. Cardiol.* **63**: 2188–2198.

Shihab, FS (2007). Do we have a pill for renal fibrosis? *Clin. J. Am. Soc. Nephrol.* **2**: 876–878.

Stevens, PE, Farmer, CKT (2012). Chronic kidney disease and life expectancy. *Nephrol. Dial. Transplant.* **27**: 3014–3015.

Sumners, C, Peluso, A, Haugaard, A, Bertelsen, J, Steckelings, U (2019). Anti-fibrotic mechanisms of angiotensin AT2 -receptor stimulation. *Acta Physiol.* **8**: e13280.

Szeto, A, Sun-suslow, N, Mendez, AJ, Hernandez, RI, Wagner, K V, McCabe, PM (2017). Regulation of the macrophage oxytocin receptor in response to inflammation. *Am J Physiol Endocrinol Metab* **312**: 183–189.

Tanaka, T (2017). A mechanistic link between renal ischemia and fibrosis. *Med. Mol. Morphol.* **50**: 1–8.

Tang, PMK, Nikolic-Paterson, DJ, Lan, HY (2019). Macrophages: versatile players in renal inflammation and fibrosis. *Nat. Rev. Nephrol.* **15**: 144–158.

Tugtepe, H, Sener, G, Biyikli, N, Yuksel, M, Cetinel, S, Gedik, N, *et al.* (2007). The protective effect of oxytocin on renal ischemia/reperfusion injury in rats. *Regul. Pept.* **140**: 101–108.

Urbanelli, L, Buratta, S, Sagini, K, Ferrara, G, Lanni, M, Emiliani, C (2015). Exosome-based strategies for Diagnosis and Therapy. *Recent Pat CNS Drug Discov* **10**: 10–27.

Waikar, SS, Bonventre, J V. (2007). Biomarkers for the diagnosis of acute kidney injury. *Curr.*

Opin. Nephrol. Hypertens. **16**: 557–564.

Wang, B, Yao, K, Huuskes, BM, Shen, H, Zhuang, J, Godson, C, *et al.* (2016). MicroRNA-let7c via Exosomes to Attenuate Renal Fibrosis. *Mol. Ther.* **24**: 1290–1301.

Wang, D, Luo, Y, Myakala, K, Orlicky, DJ, Dobrinskikh, E, Wang, X, *et al.* (2017). Serelaxin improves cardiac and renal function in DOCA-salt hypertensive rats. *Sci. Rep.* **7**: 9793.

Widdop, RE, Jones, ES, Hannan, RE, Gaspari, TA (2003). Angiotensin AT₂ receptors: cardiovascular hope or hype? *Br. J. Pharmacol.* **140**: 809–824.

Wright, JT, Bakris, G, Greene, T, Appel, LJ, Cheek, D, Douglas-baltimore, JG, *et al.* (2002). Effect of Blood Pressure Lowering and Antihypertensive Drug Class on Progression of Hypertensive Kidney Disease. *Jama* **288**: 2421–2432.

Yoshida, T, Kumagai, H, Kohsaka, T, Ikegaya, N (2013). Relaxin protects against renal ischemia-reperfusion injury. *Am. J. Physiol. Physiol.* **305**: F1169–F1176.

Yoshida, T, Kumagai, H, Kohsaka, T, Ikegaya, N (2014). Protective Effects of Relaxin against Cisplatin-Induced Nephrotoxicity in Rats. *Nephron Exp. Nephrol.* **128**: 9–20.

Yoshida, T, Kumagai, H, Suzuki, A, Kobayashi, N, Ohkawa, S, Odamaki, M, *et al.* (2012). Relaxin ameliorates salt-sensitive hypertension and renal fibrosis. *Nephrol. Dial. Transplant* **27**: 2190–7.

Yu, C, Gong, R, Rifai, A, Tolbert, EM, Dworkin, LD (2007). Long-term, high-dosage candesartan suppresses inflammation and injury in chronic kidney disease: nonhemodynamic renal protection. *J. Am. Soc. Nephrol.* **18**: 750–759.

Yu, H, Burrell, L, Black, MJ, Wu, LL, Dilley, RJ, Cooper, ME, *et al.* (1998). Salt Induces Myocardial and Renal Fibrosis in Normotensive and Hypertensive Rats. *Circulation* **98**: 2621–2628.

Zheng, G, Cai, J, Chen, X, Chen, L, Ge, W, Zhou, X, *et al.* (2017). Relaxin Ameliorates Renal Fibrosis and Expression of Endothelial Cell Transition Markers in Rats of Isoproterenol-Induced Heart Failure. *Biol. Pharm. Bull.* **40**: 960–966.

Zhou, X, Chen, X, Cai, JJ, Chen, LZ, Gong, YS, Wang, LX, *et al.* (2015). Relaxin inhibits cardiac

fibrosis and endothelial–mesenchymal transition via the Notch pathway. *Drug Des. Devel. Ther.* **9**: 4599–4611.

7.0 Appendix

Molecular and Cellular Endocrinology 487 (2019) 59–65

Contents lists available at ScienceDirect



Molecular and Cellular Endocrinology

journal homepage: www.elsevier.com/locate/mce



Relaxin and extracellular matrix remodeling: Mechanisms and signaling pathways

Hooi Hooi Ng^{a,1}, Matthew Shen^{b,1}, Chrishan S. Samuel^b, Jens Schlossmann^{c,2}, Robert G. Bennett^{d,*,2}

^a Department of Human and Molecular Genetics, Herbert Wertheim College of Medicine, Florida International University, Miami, FL, USA ^b Cardiovascular Disease Theme, Monash Biomedicine Discovery Institute and Department of Pharmacology, Monash University, Clayton, VIC, Australia ^c Department of Pharmacology and Toxicology, Institute of Pharmacy, University Regensburg, Regensburg, Germany

^d Research Service, VA Nebraska-Western Iowa Health Care System, Departments of Internal Medicine and Biochemistry & Molecular Biology, University of Nebraska Medical Center, Omaha, NE, USA



ARTICLE INFO

Keywords:

Relaxin
Relaxin family peptides
Relaxin family peptidereceptor
Fibrosis Nitric
oxide
cGMP

ABSTRACT

Fibrosis is associated with accumulation of excess fibrillar collagen, leading to tissue dysfunction. Numerous processes, including inflammation, myofibroblast activation, and endothelial-to-mesenchymal transition, play a role in the establishment and progression of fibrosis. Relaxin is a peptide hormone with well-known antifibrotic properties that result from its action on numerous cellular targets to reduce fibrosis. Relaxin activates multiple signal transduction pathways as a mechanism to suppress inflammation and myofibroblast activation in fibrosis. In this review, the general mechanisms underlying fibrotic diseases are described, along with the current state of knowledge regarding cellular targets of relaxin. Finally, an overview is presented summarizing the signaling pathways activated by relaxin and other relaxin family peptide receptor agonists to suppress fibrosis.

Introduction

Throughout its history, the hormone relaxin has been closely associated with the process of extracellular matrix (ECM) remodeling. Indeed, the first description of the effects of relaxin by Hisaw in 1926, was of the softening and lengthening of the pubic ligament (Hisaw, 1926). This effect involved a dramatic change in the structure of collagen in the pubic ligament and other reproductive organs, including a decreased density of the collagen fibre bundles (Zhao et al., 2000), which in turn reduced the rigidity of the ligament whilst increasing its ability to expand and widen. Other early studies suggested that relaxin reduced fibrillar collagen in nonreproductive tissues, including the skin, leading to clinical studies using relaxin to target scleroderma, a painful disorder characterized by fibrosis of the skin and connective tissue (Casten and Boucek, 1958; Evans, 1959). These studies, using partially purified porcine relaxin, generally involved small numbers of subjects, and reported variable degrees of success. Progress on clinical studies of relaxin in fibrotic diseases was hampered until the availability of recombinant human relaxin (now known as serelaxin), leading to a more recent clinical trial of serelaxin for the treatment of scleroderma (Seibold et al., 2000). While this trial was largely unsuccessful, interest remains in targeting the various signaling pathways that are activated by relaxin as a therapeutic approach for the treatment of fibrotic diseases.

Much of what is known about the antifibrotic effects of relaxin (predominantly involving the use of serelaxin) is the result of cell culture studies. Relaxin was shown to decrease pathological collagen production by inhibiting its synthesis and secretion from myofibroblasts (activated fibroblasts that are key fibrosis-producing cells) derived from numerous organs (Bennett et al., 2003; Samuel et al., 2004a; Unemori and Amento, 1990; Unemori et al., 1996). At the same time, relaxin is able to promote the expression and activity of matrix metalloproteinases (MMPs), and/or decrease the levels of their endogenous inhibitors, the tissue inhibitors of metalloproteinases (TIMPs) to facilitate the degradation of aberrant collagen accumulation (Bennett et al., 2003; Heeg et al., 2005; Masterson et al., 2004; Samuel et al., 2004a; Unemori et al., 1996). Similar effects were observed using rodent models of renal, pulmonary, cardiac, and hepatic fibrosis (Bennett et al., 2014; Fallowfield et al., 2014; Garber et al., 2001; Samuel et al., 2004a; Unemori et al., 1996). Finally, mice deficient in either endogenous relaxin or the relaxin receptor, RXFP1, develop age-related fibrosis in numerous organs (Du et al., 2003; Hewitson et al., 2012; KrajncFranken et al., 2004; Samuel et al., 2003, 2004b, 2005, 2009). Therefore, there is considerable *in vitro* and *in vivo* evidence that relaxin is an important factor in the progression and treatment of fibrosis. In addition, there is emerging evidence that additional relaxin family peptides, such as relaxin-3, may also play a role in fibrosis (Hossain et al., 2011; Zhang et al., 2018).

Early studies of the signaling pathways activated by relaxin were hampered by the fact that, until 2002, relaxin was an orphan hormone without an identified cognate receptor. However, it was known early that cellular cAMP and nitric oxide levels were increased in response to relaxin administration in some tissues (Braddon, 1978; Masini et al., 1994). Finally, the discovery in 2002 of the first two receptors capable of activation by relaxin family peptide members began the rapid elucidation of signaling pathways activated by relaxin (Hsu et al., 2002). It is now well established that there are four relaxin family peptide receptors (RXFPs) that are differentially activated by relaxin family peptides, and often have complex signaling mechanisms (Bathgate et al., 2013).

* Corresponding author. VA Nebraska-Western Iowa Health Care System, Research Service (151), 4101 Woolworth Avenue, Omaha, NE, 68105, USA.

E-mail addresses: hoong@fiu.edu (H.H. Ng), matthew.shen@monash.edu (M. Shen), chrishan.samuel@monash.edu (C.S. Samuel), jens.schlossmann@chemie.uni-regensburg.de (J. Schlossmann), rgbennet@unmc.edu (R.G. Bennett).

¹ These authors contributed equally to this work.

² These authors contributed equally to this work.

<https://doi.org/10.1016/j.mce.2019.01.015>

Received 5 November 2018; Received in revised form 15 January 2019; Accepted 16 January 2019 Available online 17

January 2019

0303-7207/ Published by Elsevier B.V.

The purpose of this minireview is to present the current state of knowledge regarding the mechanism of the anti-fibrotic effects of relaxin, and the signaling pathways triggered by relaxin family peptides. The review begins with an overview of the general mechanisms common to the development and progression of fibrosis. This is followed by a summary of the mechanisms by which relaxin acts on the cellular and tissue level to impede fibrotic processes. The final section focuses on the established and emerging signaling pathways triggered by relaxin family peptides that may be involved in mediating their antifibrotic effects.

General processes underlying fibrosis

2.1. Inflammation and fibrogenesis

Fibrosis is characterized by an accumulation of ECM proteins and increased collagen deposition in various organs, as a result of fibrogenesis, whereby a normal wound healing process is overactive in response to tissue injury in order to preserve the native tissue morphological and functional integrity (Lee and Kalluri, 2010; Wynn, 2008). Fibrosis can affect many tissue and organ systems, where it is most apparent in liver cirrhosis, atherosclerosis, scleroderma, vascular dysfunction, lung, kidney and heart diseases. Initiation of the fibrotic process is highly complex, which involves a vast array of stimulatory and inhibitory factors that are pivotal in modulating cells that are involved in regulating fibrosis. In the initial step, the affected organ is in an inflamed state where there is recruitment and activation of immune cells such as macrophages, eosinophils, CD8⁺ T cells, lymphocytes CD4⁺, mast cells and fibroblasts (Gieseck et al., 2018), leading to the secretion of growth factors, proteolytic enzymes and cytokines by these immune cells within the site of injury. These inflammatory products are responsible in the formation of connective tissues that replace normal physiological ones. Major fibrogenic mediators secreted during this process include transforming growth factor- β 1 (TGF- β 1), connective tissue growth factor (CTGF) and platelet-derived growth factor (PDGF) (Wynn, 2008). TGF- β 1 is considered the central mediator of

fibrosis to regulate cellular processes and ECM proteins such as collagen, elastin and fibronectin. It is well known that TGF- β 1 signaling pathway is upregulated in cardiac (Yue et al., 2017), liver (Katz et al., 2016), kidney (Chen et al., 2018) and lung fibrosis (Eser and Janne, 2018), through both canonical (Smad-dependent) and non-canonical (Smad-independent) pathways. These signaling pathways lead to the activation or recruitment of myofibroblasts and overproduction of ECM proteins, as well as impeding the degradation of ECM components (Meng et al., 2016).

2.2. Myofibroblast activation and matrix remodeling

The primary culprit in all fibrotic diseases is the activation of myofibroblasts (Hinz et al., 2012). Myofibroblasts are the main matrix-producing cells that generate ECM proteins such as fibronectin and collagen type I, III and IV (Kisseleva and Brenner, 2008), and remodel the neo-ECM components by producing contractile forces in response to the surroundings of the cells. Myofibroblasts are thought to be formed from a heterogeneous population derived from resident fibroblasts, as well as endothelial cells, epithelial cells, mesothelial cells, and circulating fibrocytes of bone marrow origin (Davis and Molkentin, 2014). Several cellular mechanisms have been proposed to describe the fibroblast-myofibroblast transdifferentiation process. Upon activation of the process, fibroblasts migrate into the site of injury and attain a myofibroblast phenotype. Activated myofibroblasts are capable of producing substantial amounts of ECM proteins to trigger collagen accumulation. As discussed above, fibrogenic mediators such as TGF- β 1 and PDGF produced by activated myofibroblasts and inflammatory cells, as well as angiotensin II (Ang II), which is derived from activation of the renin-angiotensin system (Bataller et al., 2005; Suzuki et al., 2003; Weber et al., 1993), further stimulate the proliferation of myofibroblasts and the production of collagen and fibronectin. The ECM serves as an important scaffold for cells and growth factors, and also provides biomechanical clues that guide myofibroblast activation and activity. The MMPs belong to a multi-gene family of zinc and calcium-dependent endopeptidases secreted by connective tissue cells and inflammatory phagocytes that play pivotal roles in ECM remodeling due to their ability to degrade many matrix components, growth factors and cytokines (Nagase and Woessner, 1999). Under physiological conditions, proteolytic activities of MMPs are tightly controlled by their endogenous protein inhibitors, TIMPs (Gomez et al., 1997). However, under fibrotic conditions, there is an imbalance between MMPs and TIMPs, with suppression of MMP activity and increased TIMP expression, resulting in the protection of ECM and decreased proteolysis. During this period, the synthesis of new collagen from myofibroblasts exceeds its degradation rate following the inflammatory cytokine-driven events at the site of injury (Van Linthout et al., 2014), thus resulting in aberrant collagen deposition over time. This cascade of events will eventually lead to a significant deposition of ECM proteins that outpaces its degradation, resulting in fibrosis and pathological remodeling of target organs. *2.3. Endothelial-to-mesenchymal transition*

In addition to directly stimulating the differentiation of fibroblasts into myofibroblasts, TGF- β 1 can stimulate epithelial and endothelial cells to acquire a mesenchymal phenotype in which they de-differentiate, migrate and subsequently re-differentiate into myofibroblasts to secrete large amounts of matrix proteins to promote wound healing; commonly known as epithelial-to-mesenchymal cell transition (EMT) and endothelial cell-to-mesenchymal cell transition (EndMT), respectively (Barnes and Gorin, 2011; Du et al., 2012; Klahr and Morrissey, 2002). During an aberrant wound healing process, however, these transitioned epithelial and endothelial cells remain as myofibroblasts and continue to produce ECM components such as collagen and fibronectin. In the murine kidney, it was shown that 10% of endothelial cells undergo EndMT and 5% of epithelial cells undergo EMT, contributing to myofibroblast-induced renal fibrosis (LeBleu et al., 2013). Moreover, in a murine model of cardiac fibrosis, it was revealed that 27–33% of all cardiac fibroblasts were of endothelial origin using a Cre-recombinase genetic marking system to identify cells that express Tie1 (an endothelial marker) (Zeisberg et al., 2007). Furthermore in EndMT, phenotypes of endothelial cells, such as CD31 and vascular endothelial (VE)-cadherin expression are often replaced by specific properties of mesenchymal cells like vimentin and α -smooth muscle actin (α -SMA) expression (Kovacic et al., 2012). These studies collectively demonstrated that EndMT plays a critical role in regulating the pathological processes leading to fibrosis.

The antifibrotic effects of relaxin

3.1. Relaxin effects on inflammation and fibrogenesis

Several studies have shown that relaxin inhibits the infiltration of various immune cells into injured/damaged organs, which produce various pro-inflammatory and pro-fibrotic factors to initiate the wound healing response to injury, but which over prolonged periods contribute to the stimulation of excess ECM secretion (Wynn, 2008). Unresolved inflammation, followed by dysregulated wound healing, can lead to fibrosis-induced organ failure. Serelaxin and/or porcine relaxin has been shown to reduce the infiltration of inflammatory cells within several tissues including neutrophils, basophils, mast cells, endothelial cells and macrophages (Bani et al., 1997, 2002; Bei et al., 2018; Garber et al., 2001; Nistri et al., 2003, 2008), the latter being a source of TGF- β 1 production. Furthermore, relaxin decreases granule exocytosis and mast cell degranulation to reduce pro-inflammatory and allergic cytokines such as histamine, leukotrienes and serotonin (Masini et al., 1997). Relaxin can also inhibit the endothelial adhesiveness to neutrophils and the infiltration of macrophages which are crucial for the recruitment and migration of inflammatory cells to the site of injury (Hewitson et al., 2007; Martin et al., 2018; Nistri et al., 2003), inhibit toll-like receptor-4 signaling, and promote tissue-repairing M2 macrophage polarization (Chen et al., 2017). Moreover, relaxin inhibits NLRP3 inflammasome activity, which is known to increase interleukin (IL)-1 β activity (Raleigh et al., 2017), and also plays a role in inhibiting NF κ B signaling, a crucial transcription factor that regulates many inflammatory genes (Martin et al., 2018). Aside from its effects on inflammatory cell infiltration, relaxin has been shown to reduce the pro-fibrotic influence of cytokines or mediators such as TGF- β 1 (Bennett et al., 2014; Heeg et al., 2005; Kocan et al., 2017; Mookerjee et al., 2009; Samuel et al., 2004a; Unemori and Amento, 1990; Unemori et al., 1996; Wang et al., 2016, 2017), IL-1 β (Bei et al., 2017; Pini et al., 2016; Unemori and Amento, 1990), IL-6 (Bei et al., 2017, 2018; Wang et al., 2017; Yoshida et al., 2014), monocyte chemoattractant protein-1 (Brecht et al., 2011; Wang et al., 2017), and tumor necrosis factor- α (Brecht et al., 2011; Yoshida et al., 2013, 2014), amongst others.

3.2. Relaxin effects on myofibroblast activation and matrix remodeling

Serelaxin has been found to consistently inhibit TGF- β 1, IL-1 β and/ or angiotensin (Ang) II-mediated fibroblast proliferation and/or differentiation into myofibroblasts, regardless of etiology (Bennett et al., 2003; Fallowfield et al., 2014; Heeg et al., 2005; Hewitson et al., 2010; Huuskes et al., 2015; Lekgabe et al., 2005; Mookerjee et al., 2009; Samuel et al., 2004a, 2011; Sassoli et al., 2013; Unemori and Amento, 1990; Unemori et al., 1996). Furthermore, serelaxin also inhibited myofibroblast contractility as part of its anti-fibrotic actions (Huang et al., 2011). These combined actions of serelaxin led to reduced myofibroblast-induced ECM (primarily collagen and fibronectin) synthesis and deposition (Bennett et al., 2003; Cernaro et al., 2017; Heeg et al., 2005; Hewitson et al., 2010; Lee et al., 2011; Lekgabe et al., 2005; Royce et al., 2015; Samuel et al., 2004a, 2011; Sassoli et al., 2013; Unemori and Amento, 1990; Unemori et al., 1996). Furthermore, serelaxin promoted MMP expression and activity and/or inhibited TIMP activity to induce the degradation of aberrant ECM protein accumulation (Heeg et al., 2005; Hewitson et al., 2010; Huuskes et al., 2015; Kang et al., 2017; Lekgabe et al., 2005; Royce et al., 2015; Samuel et al., 2011; Sassoli et al., 2013; Unemori and Amento, 1990; Unemori et al., 1996; Williams et al., 2001).

Mechanistically, serelaxin has been shown to signal through RXFP1 on myofibroblasts to suppress TGF- β 1 signal transduction and activity at the level of Smad2 phosphorylation (Chow et al., 2014; Kocan et al., 2017; Mookerjee et al., 2009; Sarwar et al., 2015; Wang et al., 2016). This then resulted in a decrease in TGF- β 1-induced myofibroblast differentiation and hence, myofibroblast-mediated ECM/collagen synthesis; a decrease in TGF- β 1-induced suppression of MMP (MMP-2, MMP9, MMP-1/-13) activity (Chow et al., 2012); and a decrease in TGF- β 1-induced TIMP activity and inhibition of ECM degradation. In cardiac myofibroblasts, serelaxin signaled through Notch-1 and suppressed Smad3 phosphorylation to inhibit the pro-fibrotic actions of TGF- β 1 (Kocan et al., 2017; Sassoli et al., 2013).

3.3. Relaxin effects on endothelial-to-mesenchymal transition

Recent studies showed that serelaxin inhibits EndMT within the heart and kidney of isoprenaline-induced cardiomyopathy in rodents (Cai et al., 2017; Zheng et al., 2017). Zhou et al. found that serelaxin improves cardiac function in rats with myocardial fibrosis, by reducing EndMT and interstitial collagens I and III, while increasing the microvascular density of the heart (Zhou et al., 2015). Similar to cardiac myofibroblasts, serelaxin also inhibited TGF- β 1-induced mobility of endothelial cells through a Notch-1-dependent pathway, and increased expression of CD31 while decreasing vimentin content of human umbilical vein endothelial cells (HUVECs) *in vitro* (Zhou et al., 2015). In a separate study, serelaxin was capable of reducing cardiac fibrosis *in vivo* via the inhibition of EndMT, and by increasing VE-cadherin and CD31 levels while suppressing vimentin and α -SMA levels in HUVECs *in vitro* (Cai et al., 2017). While these combined findings suggest that relaxin inhibits myofibroblast-mediated aberrant ECM synthesis and deposition at multiple levels, further studies are required to fully understand the detailed mechanisms underlying its potent antifibrotic actions in various tissues and organs for future therapeutic applications.

Relaxin family peptide signaling in fibrosis

4.1. Relaxin family peptides and receptors

The peptides of the relaxin/insulin-like super family exhibit a variety of functions, including antifibrotic activity in diverse organs, e.g. kidney, heart, lung and liver (Samuel et al., 2017). These peptides bind to the Gprotein coupled receptors RXFP1-4, which induce diverse signaling cascades (Bathgate et al., 2013). The most well-studied pathways activated by these receptors involve modulation of cAMP production. For example, RXFP1 and RXFP2 activation initially leads to Gs stimulation and thereby enhanced cAMP synthesis. Depending on the cell type, RXFP1 can also couple to Go and Gi to promote a biphasic pattern of cAMP production. In contrast, RXFP3 and 4 are coupled to Gi/o, leading to a reduction in cAMP levels. Of the receptors, only RXFP1 has thus far demonstrated antifibrotic effects. However, as discussed below, most of the signaling pathways that have been tied to antifibrotic effects involve different signaling pathways (summarized in Table 1).

4.2. RXFP1 signaling through the nitric oxide-cGMP and ERK pathways

The most important receptor for the suppression of fibrosis in different organs is RXFP1. The physiological ligands that bind to this receptor are relaxin-2, its human recombinant form serelaxin, and relaxin-1 (in other species). In myofibroblasts, (se)relaxin binding to RXFP1 stimulates Gs and G β proteins (Mookerjee et al., 2009), and through an extracellular signal-regulated kinase phosphorylation (pERK1/2) and neuronal NO synthase (nNOS)-mediated NO-soluble guanylate cyclase (sGC)-cyclic guanosine monophosphate (cGMP)-dependent pathway to suppress TGF- β 1 signal transduction and activity at the level of Smad2 phosphorylation (Chow et al., 2014; Kocan et al., 2017; Mookerjee et al., 2009; Sarwar et al., 2015; Wang et al., 2016) (Fig. 1). Relaxin also directly stimulated cGMP synthesis independent of ERK1/2 activation (Kocan et al., 2017). Furthermore, it was established that signaling via cGMP and the cGMP-activated protein kinase-1 (PKG1) mediates the suppressive effects of serelaxin in unilateral ureter obstruction (UUO)-induced interstitial renal fibrosis (Wetzel et al., 2016). In this model, serelaxin treatment strongly enhanced plasma cGMP. Using PKG1-deficient mice, it was observed that the reduction in pSmad2 and pERK1 in response to serelaxin treatment was dependent on PKG1 (Wetzel et al., 2016). In comparison, the phosphodiesterase-5 (PDE5) inhibitor, zaprinast, acts as an antifibrotic agent via suppression of ERK1/2 signaling, but this effect was independent from PKG1. The combination of serelaxin with this PDE5 inhibitor does not reveal additional benefits against kidney fibrosis (Wetzel et al., 2017).

Table 1

Selected signaling pathways activated by relaxin family peptides and their receptors in fibrosis.

Agonist	Receptor	Cells/Disease Model	Signaling Pathway	Targets	Reference
Serelaxin	RXFP1 RXFP1/AT2R	Renal, cardiac, dermal fibroblasts, Renal fibrosis	pERK1/2-nNOsGcGMP-PKG1	TGFβ pSmads SMA Collagen Fibronectin MMPs TIMPs	(Chow et al., 2012, 2014; Mookerjee et al., 2009; Sarwar et al., 2015; Wang et al., 2016; Wetzl et al., 2016, 2017)
ML290	RXFP1	Cardiac and hepatic myofibroblasts	NOSeNO-sGC-cGMP	TGFβ pSmads SMA MMPs	Kocan et al. (2017)
B7-33	RXFP1	Renal myofibroblasts Cardiac and lung fibrosis	pERK1/2	pSmads Collagen MMPs	(Hossain et al., 2016; Praveen et al., 2017)
Relaxin-3	RXFP1, RXFP3?	Cardiac fibrosis	unknown	NLRP3-inflammasome Collagen MMPs	(Hossain et al., 2011; Zhang et al., 2017, 2018)
InsL6	unknown	Cardiac fibrosis	unknown	TGFβ collagen	Maruyama et al. (2018)

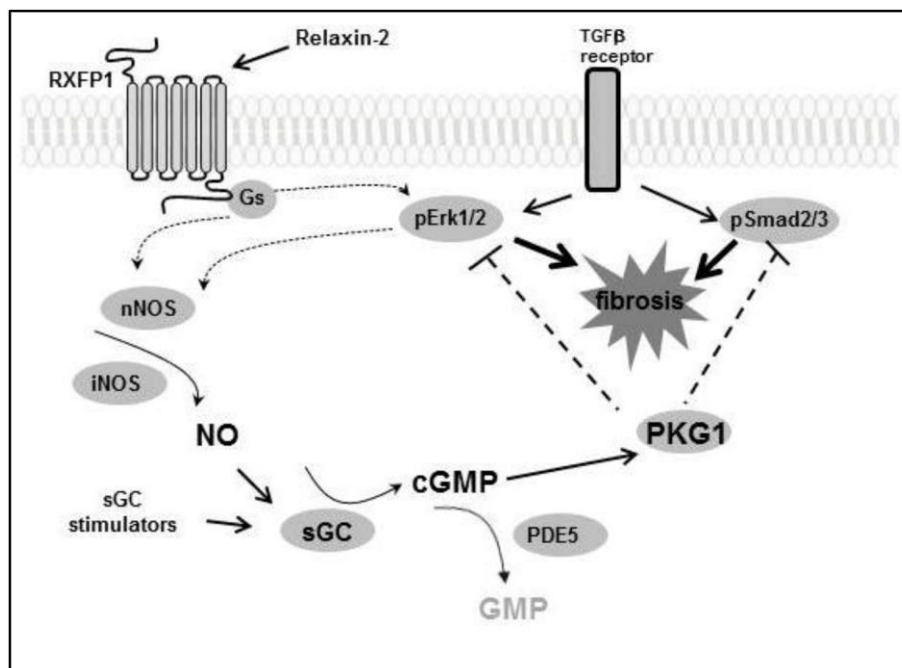


Fig. 1. : Scheme for antifibrotic signaling of relaxin2. Relaxin-2 activates RXFP1, which stimulates NO/ cGMP/PKG1 signaling. Activation of the relaxinRXFP1 axis subsequently leads to the inhibition of pERK1/2 and pSmad2/3, which ultimately suppresses TGFβ-induced fibrosis. PKG1 – cGMP-dependent protein kinase 1, sGC – soluble guanylyl cyclase, cGMP – cyclic guanosine monophosphate, ERK – extracellular-signal regulated kinase, GMP – guanosine monophosphate, NOS – nitric oxide synthase, PDE5 – phosphodiesterase 5, RXFP1 – relaxin family peptide receptor 1, Smad – small mothers against decapentaplegic protein, TGFβ – transforming growth factor-β

In summary, the diverse effects of relaxin peptides on signaling systems upon cAMP, cGMP, ERK1/2 and Smad2/3 are important parameters to elucidate their (patho)physiological functions. Interestingly, these effects are also time-dependent. The level of cAMP can be enhanced upon short exposure with relaxin via G_s signaling, but it is reduced upon chronic exposure via activation of G_{0B} (Halls et al., 2006). These differential effects can be also observed in the ERK1/2-system which is activated in the short term to enhance NO and thereby cGMP synthesis (Chow et al., 2012). However, ERK1/2 phosphorylation is reduced by serelaxin upon chronic treatment which might be important *inter alia* for suppression of kidney fibrosis (Schinner et al., 2017).

4.3. Crosstalk and heterodimerization between RXFP1 and AT₂R

Many of the signal transduction pathways activated by serelaxin in myofibroblasts require the presence of the Ang II type 2 receptor (AT₂R), which appears to occur through an interaction between RXFP1 and the AT₂R (Chow et al., 2014). As a result of this interaction, the anti-fibrotic effects of serelaxin can be abrogated by co-administration of an AT₂R antagonist (PD123319) or when serelaxin is administered to AT₂R knockout mice (Chow et al., 2014). As the AT₂R can inhibit both the expression and activation of the AT₁R, serelaxin may also signal through the RXFP1:AT₂R axis to indirectly inhibit the pro-fibrotic effects of Ang II via the Ang II–AT₁R–TGF-β1 interaction (Nakajima et al., 1995; Yang et al., 2012).

4.4. Emerging potential relaxin-based antifibrotic therapies

There is evidence that other relaxin family peptides may also have antifibrotic effects. Human relaxin-3 (also known as H3 relaxin) reduced the fibrotic properties of rat ventricular fibroblasts, acting through RXFP1, and decreased collagen expression in a mouse model of cardiomyopathy (Hossain et al., 2011). Relaxin-3 treatment in cardiac fibroblasts also inhibited reactive oxygen species- and inflammasome-mediated collagen synthesis under high glucose conditions, and there was evidence of both RXFP1 and RXFP3 expression in cardiac tissue in a rat model of diabetic cardiomyopathy (Zhang et al., 2017, 2018). Hence, relaxin-3 (acting via RXFP1, and possibly via RXFP3) might be therapeutically relevant for the treatment of diabetic cardiomyopathy. A recent study showed that mice lacking insulin-like peptide 6 (Insl6), a member of the relaxin family, exhibit cardiac dysfunction and enhanced cardiac fibrosis, suggesting the role of Insl6 in suppressing cardiac fibrosis and its potential to be used for the treatment of heart failure (Maruyama et al., 2018). Further studies are needed to determine if relaxin-3 or Insl6 can be used to treat established models of tissue fibrosis.

In addition to the endogenous ligands of RXFP1, a recently identified non-peptide agonist of the human relaxin receptor, ML290, shows promising effects in ameliorating fibrosis in cell culture studies. For example, ML290 treatment induces profound antifibrotic effects in human hepatic stellate cell line, LX-2, by down-regulating the gene expression of collagens, α -SMA, PDGF, and up-regulating MMP1 (McBride et al., 2017). In human cardiac fibroblasts, ML290 effectively suppresses TGF- β 1-induced myofibroblast activation through a reduction in Smad2/3 phosphorylation and up-regulation of MMP2 (Kocan et al., 2017). The biased signaling of ML290 compared to relaxin might be a powerful tool to evaluate the specific antifibrotic properties of relaxin. Another RXFP1 agonist, B7-33, is a peptide analogue of the B-chain of relaxin which reduces fibrosis in heart and kidney of rodent models (Hossain et al., 2016; Praveen et al., 2017). Its affinity for RXFP1 is lower, but its specificity for RXFP1 is higher than that of (se)relaxin. The peptide mimetic B7-33 acts via preferential activation of pERK1/2 and cGMP in (myo)fibroblast cells compared to cAMP activation (Hossain et al., 2016; Praveen et al., 2017).

One critical requirement for the development of new relaxin analogues/agonists is high throughput bioassay systems for screening potential compounds. One important readout for the activity of candidate compounds is cAMP measurement. Bioluminescence resonance energy transfer (BRET) biosensors provide dynamic real-time measurement of cAMP levels. One such system, the CAMYEL assay (cAMP sensor using YFP-Epac.Rlu) has been validated as an assay for all RXFPs in HEK cells (Valkovic et al., 2018). In addition, cGMP sensor mice might be valuable for cGMP measurements and for screening *in vivo* (Paolillo et al., 2018); the latter which is more relevant for investigating the anti-fibrotic effects of (se)relaxin in myofibroblasts.

Conclusion

Since the development of the relaxin and RXFP1 knockout mice, it has become clear that endogenous relaxin plays a critical role in the protection of organs from age-related fibrosis. As the cellular mechanisms and signaling pathways by which (se)relaxin exerts its antifibrotic effects become clearer, additional therapeutic options are expected to emerge. Furthermore, numerous studies utilizing preclinical *in vivo* models are underway that support the use of (se)relaxin and relaxin mimetics for the treatment of fibrotic diseases. However, clinical trials using (se)relaxin or mimetics are needed to determine if this pathway can be exploited to treat human fibrotic disease.

Conflicts of interest

The authors declare that they have no conflict of interest.

Funding

This work was supported by a National Health & Medical Research Council (NHMRC) of Australia Senior Research Fellowship GNT10417660 (C.S.S), Australia; Novartis Pharma GmbH, the Bavarian State and Sonderforschungsbereich SFB699 (J.S.), Germany; and the U.S. Department of Veterans Affairs Merit Review BX000849 (R.G.B), USA.

References

- Bani, D., Ballati, L., Masini, E., Bigazzi, M., Sacchi, T.B., 1997. Relaxin counteracts asthma-like reaction induced by inhaled antigen in sensitized Guinea pigs. *Endocrinology* 138, 1909–1915.
- Bani, D., Baronti, R., Vannacci, A., Bigazzi, M., Sacchi, T.B., Mannaioni, P.F., Masini, E., 2002. Inhibitory effects of relaxin on human basophils activated by stimulation of the Fc epsilon receptor. The role of nitric oxide. *Int. Immunopharm.* 2, 1195–1204.
- Barnes, J.L., Gorin, Y., 2011. Myofibroblast differentiation during fibrosis: role of NAD(P) H oxidases. *Kidney Int.* 79, 944–956.
- Bataller, R., Sancho-Bru, P., Gines, P., Brenner, D.A., 2005. Liver fibrogenesis: a new role for the renin-angiotensin system. *Antioxidants Redox Signal.* 7, 1346–1355.
- Bathgate, R.A., Halls, M.L., van der Westhuizen, E.T., Callander, G.E., Kocan, M., Summers, R.J., 2013. Relaxin family peptides and their receptors. *Physiol. Rev.* 93, 405–480.
- Beiert, T., Knappe, V., Tiyerili, V., Stockigt, F., Effelsberg, V., Linhart, M., Steinmetz, M., Klein, S., Schierwagen, R., Trebicka, J., Roell, W., Nickenig, G., Schrickel, J.W., Andrie, R.P., 2018. Chronic lower-dose relaxin administration protects from arrhythmia in experimental myocardial infarction due to anti-inflammatory and antifibrotic properties. *Int. J. Cardiol.* 250, 21–28.
- Beiert, T., Tiyerili, V., Knappe, V., Effelsberg, V., Linhart, M., Stockigt, F., Klein, S., Schierwagen, R., Trebicka, J., Nickenig, G., Schrickel, J.W., Andrie, R.P., 2017. Relaxin reduces susceptibility to post-infarct atrial fibrillation in mice due to antifibrotic and anti-inflammatory properties. *Biochem. Biophys. Res. Commun.* 490, 643–649.
- Bennett, R.G., Heimann, D.G., Singh, S., Simpson, R.L., Tuma, D.J., 2014. Relaxin decreases the severity of established hepatic fibrosis in mice. *Liver Int.* 34, 416–426.
- Bennett, R.G., Kharbanda, K.K., Tuma, D.J., 2003. Inhibition of markers of hepatic stellate cell activation by the hormone relaxin. *Biochem. Pharmacol.* 66, 867–874.
- Braddon, S.A., 1978. Relaxin-dependent adenosine 6',5'-monophosphate concentration changes in the mouse pubic symphysis. *Endocrinology* 102, 1292–1299.
- Brecht, A., Bartsch, C., Baumann, G., Stangl, K., Dschietzig, T., 2011. Relaxin inhibits early steps in vascular inflammation. *Regul. Pept.* 166, 76–82.

- Cai, J., Chen, X., Chen, X., Chen, L., Zheng, G., Zhou, H., Zhou, X., 2017. Anti-fibrosis effect of relaxin and spironolactone combined on isoprenaline-induced myocardial fibrosis in rats via inhibition of endothelial-mesenchymal transition. *Cell. Physiol. Biochem.* 41, 1167–1178.
- Casten, G.G., Boucek, R.J., 1958. Use of relaxin in the treatment of scleroderma. *J. Am. Med. Assoc.* 166, 319–324.
- Cernaro, V., Medici, M.A., Bianco, F., Santoro, D., Lacquaniti, A., Romeo, A., Lucisano, S., Buemi, A., Buemi, M., 2017. Opposite actions of urotensin II and relaxin-2 on cellular expression of fibronectin in renal fibrosis: a preliminary experimental study. *Clin. Exp. Pharmacol. Physiol.* 44, 1069–1071.
- Chen, L., Sha, M.L., Li, D., Zhu, Y.P., Wang, X.J., Jiang, C.Y., Xia, S.J., Shao, Y., 2017. Relaxin abrogates renal interstitial fibrosis by regulating macrophage polarization via inhibition of Toll-like receptor 4 signaling. *Oncotarget* 8, 21044–21053.
- Chen, L., Yang, T., Lu, D.W., Zhao, H., Feng, Y.L., Chen, H., Chen, D.Q., Vaziri, N.D., Zhao, Y.Y., 2018. Central role of dysregulation of TGF- β /Smad in CKD progression and potential targets of its treatment. *Biomed. Pharmacother.* 101, 670–681.
- Chow, B.S., Chew, E.G., Zhao, C., Bathgate, R.A., Hewitson, T.D., Samuel, C.S., 2012. Relaxin signals through a RXFP1-pERK-nNOS-NO-cGMP-dependent pathway to upregulate matrix metalloproteinases: the additional involvement of iNOS. *PLoS One* 7, e42714.
- Chow, B.S., Kocan, M., Bosnyak, S., Sarwar, M., Wigg, B., Jones, E.S., Widdop, R.E., Summers, R.J., Bathgate, R.A., Hewitson, T.D., Samuel, C.S., 2014. Relaxin requires the angiotensin II type 2 receptor to abrogate renal interstitial fibrosis. *Kidney Int.* 86, 75–85.
- Davis, J., Molkentin, J.D., 2014. Myofibroblasts: trust your heart and let fate decide. *J. Mol. Cell. Cardiol.* 70, 9–18.
- Du, X.-J., Samuel, C.S., Gao, X.-M., Zhao, L., Parry, L.J., Tregear, G.W., 2003. Increased myocardial collagen and ventricular diastolic dysfunction in relaxin deficient mice: a gender-specific phenotype. *Cardiovasc. Res.* 57, 395–404.
- Du, X., Shimizu, A., Masuda, Y., Kuwahara, N., Arai, T., Kataoka, M., Uchiyama, M., Kaneko, T., Akimoto, T., Iino, Y., Fukuda, Y., 2012. Involvement of matrix metalloproteinase-2 in the development of renal interstitial fibrosis in mouse obstructive nephropathy. *Lab. Invest.* 92, 1149–1160.
- Eser, P.O., Janne, P.A., 2018. TGF β pathway inhibition in the treatment of non-small cell lung cancer. *Pharmacol. Ther.* 184, 112–130.
- Evans, J.A., 1959. Relaxin (releasin) therapy in diffuse progressive scleroderma; a preliminary report. *AMA Arch. Derm.* 79, 150–158.
- Fallowfield, J.A., Hayden, A.L., Snowden, V.K., Aucott, R.L., Stutchfield, B.M., Mole, D.J., Pellicoro, A., Gordon-Walker, T.T., Henke, A., Schrader, J., Trivedi, P.J., Princivalle, M., Forbes, S.J., Collins, J.E., Iredale, J.P., 2014. Relaxin modulates human and rat hepatic myofibroblast function and ameliorates portal hypertension in vivo. *Hepatology* 59, 1492–1504.
- Garber, S.L., Mirochnik, Y., Brecklin, C.S., Unemori, E.N., Singh, A.K., Slobodskoy, L., Grove, B.H., Arruda, J.A., Dunea, G., 2001. Relaxin decreases renal interstitial fibrosis and slows progression of renal disease. *Kidney Int.* 59, 876–882.
- Gieseck 3rd, R.L., Wilson, M.S., Wynn, T.A., 2018. Type 2 immunity in tissue repair and fibrosis. *Nat. Rev. Immunol.* 18, 62–76.
- Gomez, D.E., Alonso, D.F., Yoshiji, H., Thorgeirsson, U.P., 1997. Tissue inhibitors of metalloproteinases: structure, regulation and biological functions. *Eur. J. Cell Biol.* 74, 111–122.
- Halls, M.L., Bathgate, R.A., Summers, R.J., 2006. Relaxin family peptide receptors RXFP1 and RXFP2 modulate cAMP signaling by distinct mechanisms. *Mol. Pharmacol.* 70, 214–226.
- Heeg, M.H., Koziol, M.J., Vasko, R., Schaefer, L., Sharma, K., Muller, G.A., Strutz, F., 2005. The antifibrotic effects of relaxin in human renal fibroblasts are mediated in part by inhibition of the Smad2 pathway. *Kidney Int.* 68, 96–109.
- Hewitson, T.D., Ho, W.Y., Samuel, C.S., 2010. Antifibrotic properties of relaxin: in vivo mechanism of action in experimental renal tubulointerstitial fibrosis. *Endocrinology* 151, 4938–4948.
- Hewitson, T.D., Mookerjee, I., Masterson, R., Zhao, C., Tregear, G.W., Becker, G.J., Samuel, C.S., 2007. Endogenous relaxin is a naturally occurring modulator of experimental renal tubulointerstitial fibrosis. *Endocrinology* 148, 660–669.
- Hewitson, T.D., Zhao, C., Wigg, B., Lee, S.W., Simpson, E.R., Boon, W.C., Samuel, C.S., 2012. Relaxin and castration in male mice protect from, but testosterone exacerbates, age-related cardiac and renal fibrosis, whereas estrogens are an independent determinant of organ size. *Endocrinology* 153, 188–199.
- Hinz, B., Phan, S.H., Thannickal, V.J., Prunotto, M., Desmouliere, A., Varga, J., De Wever, O., Mareel, M., Gabbiani, G., 2012. Recent developments in myofibroblast biology: paradigms for connective tissue remodeling. *Am. J. Pathol.* 180, 1340–1355.
- Hisaw, F.L., 1926. Experimental relaxation of the pubic ligament of the Guinea pig. *Proc. Soc. Exp. Biol. Med.* 23, 661–663.
- Hossain, M.A., Chow Suet Man, B., Zhao, C., Xu, Q., Du, X.-J., Wade, J.D., Samuel, C.S., 2011. H3 relaxin demonstrates antifibrotic properties via the RXFP1 receptor. *Biochemistry* 50, 1368–1375.
- Hossain, M.A., Kocan, M., Yao, S.T., Royce, S.G., Nair, V.B., Siwek, C., Patil, N.A., Harrison, I.P., Rosengren, K.J., Selemidis, S., Summers, R.J., Wade, J.D., Bathgate, R.A., Samuel, C.S., 2016. A single-chain derivative of the relaxin hormone is a functionally selective agonist of the G protein-coupled receptor. *Chem. Sci.* RXFP1. <https://doi.org/10.1039/C5SC04754>.
- Hsu, S.Y., Nakabayashi, K., Nishi, S., Kumagai, J., Kudo, M., Sherwood, O.D., Hsueh, A.J.W., 2002. Activation of orphan receptors by the hormone relaxin. *Science* 295, 671–674.
- Huang, X., Gai, Y., Yang, N., Lu, B., Samuel, C.S., Thannickal, V.J., Zhou, Y., 2011. Relaxin regulates myofibroblast contractility and protects against lung fibrosis. *Am. J. Pathol.* 179, 2751–2765.
- Huuskens, B.M., Wise, A.F., Cox, A.J., Lim, E.X., Payne, N.L., Kelly, D.J., Samuel, C.S., Ricardo, S.D., 2015. Combination therapy of mesenchymal stem cells and serelaxin effectively attenuates renal fibrosis in obstructive nephropathy. *FASEB J.* 29, 540–553.
- Kang, Y.M., Lee, H.M., Moon, S.H., Kang, H., Choi, Y.R., 2017. Relaxin modulates the expression of MMPs and TIMPs in fibroblasts of patients with carpal tunnel syndrome. *Yonsei Med. J.* 58, 415–422.
- Katz, L.H., Likhter, M., Jogunoori, W., Belkin, M., Ohshiro, K., Mishra, L., 2016. TGF- β signaling in liver and gastrointestinal cancers. *Cancer Lett.* 379, 166–172.
- Kisseleva, T., Brenner, D.A., 2008. Mechanisms of fibrogenesis. *Exp. Biol. Med.* 233, 109–122.
- Klahr, S., Morrissey, J., 2002. Obstructive nephropathy and renal fibrosis. *Am. J. Physiol. Renal. Physiol.* 283, F861–F875.
- Kocan, M., Sarwar, M., Ang, S.Y., Xiao, J., Marugan, J.J., Hossain, M.A., Wang, C., Hutchinson, D.S., Samuel, C.S., Agoulnik, A.I., Bathgate, R.A.D., Summers, R.J., 2017. ML290 is a biased allosteric agonist at the relaxin receptor RXFP1. *Sci. Rep.* 7, 2968.
- Kovacic, J.C., Mercader, N., Torres, M., Boehm, M., Fuster, V., 2012. Epithelial-to-mesenchymal and endothelial-to-mesenchymal transition: from cardiovascular development to disease. *Circulation* 125, 1795–1808.
- Krajnc-Franken, M.A.M., van Disseldorp, A.J.M., Koenders, J.E., Mosselman, S., van Duin, M., Gossen, J.A., 2004. Impaired nipple development and parturition in LGR7 knockout mice. *Mol. Cell Biol.* 24, 687–696.
- LeBleu, V.S., Taduri, G., O'Connell, J., Teng, Y., Cooke, V.G., Woda, C., Sugimoto, H., Kalluri, R., 2013. Origin and function of myofibroblasts in kidney fibrosis. *Nat. Med.* 19, 1047–1053.
- Lee, S.B., Kalluri, R., 2010. Mechanistic connection between inflammation and fibrosis. *Kidney Int. Suppl.* S22–S26.
- Lee, W.J., Kim, Y.O., Choi, I.K., Rah, D.K., Yun, C.O., 2011. Adenovirus-relaxin gene therapy for keloids: implication for reversing pathological fibrosis. *Br. J. Dermatol.* 165, 673–677.
- Lekgabe, E.D., Kiriazis, H., Zhao, C., Xu, Q., Moore, X.L., Su, Y., Bathgate, R.A., Du, X.J., Samuel, C.S., 2005. Relaxin reverses cardiac and renal fibrosis in spontaneously hypertensive rats. *Hypertension* 46, 412–418.
- Martin, B., Gabris-Weber, B.A., Reddy, R., Romero, G., Chattopadhyay, A., Salama, G., 2018. Relaxin reverses inflammatory and immune signals in aged hearts. *PLoS One* 13, e0190935.

- Maruyama, S., Wu, C.L., Yoshida, S., Zhang, D., Li, P.H., Wu, F., Parker Duffen, J., Yao, R., Jardin, B., Adham, I.M., Law, R., Berger, J., Di Marchi, R., Walsh, K., 2018. Relaxin family member insulin-like peptide 6 ameliorates cardiac fibrosis and prevents cardiac remodeling in murine heart failure models. *J Am Heart Assoc* 7.
- Masini, E., Bani, D., Bello, M.G., Bigazzi, M., Mannaioni, P.F., Sacchi, T.B., 1997. Relaxin counteracts myocardial damage induced by ischemia-reperfusion in isolated Guinea pig hearts: evidence for an involvement of nitric oxide. *Endocrinology* 138, 4713–4720.
- Masini, E., Bani, D., Bigazzi, M., Mannaioni, P.F., Bani-Sacchi, T., 1994. Effects of Relaxin on Mast Cells: in vitro and in vivo studies in rats and Guinea pigs. *J. Clin. Invest.* 94, 1974–1980.
- Masterson, R., Hewitson, T.D., Kelyack, K., Martic, M., Parry, L., Bathgate, R., Darby, I., Becker, G., 2004. Relaxin down-regulates renal fibroblast function and promotes matrix remodelling in vitro. *Nephrol. Dial. Transplant.* 19, 544–552.
- McBride, A., Hoy, A.M., Bamford, M.J., Mossakowska, D.E., Ruediger, M.P., Griggs, J., Desai, S., Simpson, K., Caballero-Hernandez, I., Iredale, J.P., Pell, T., Aucott, R.L., Holmes, D.S., Webster, S.P., Fallowfield, J.A., 2017. In search of a small molecule agonist of the relaxin receptor RXFP1 for the treatment of liver fibrosis. *Sci. Rep.* 7, 10806.
- Meng, X.M., Nikolic-Paterson, D.J., Lan, H.Y., 2016. TGF-beta: the master regulator of fibrosis. *Nat. Rev. Nephrol.* 12, 325–338.
- Mookerjee, I., Hewitson, T.D., Halls, M.L., Summers, R.J., Mathai, M.L., Bathgate, R.A., Tregear, G.W., Samuel, C.S., 2009. Relaxin inhibits renal myofibroblast differentiation via RXFP1, the nitric oxide pathway, and Smad2. *FASEB J.* 23, 1219–1229.
- Nagase, H., Woessner Jr., J.F., 1999. Matrix metalloproteinases. *J. Biol. Chem.* 274, 21491–21494.
- Nakajima, M., Hutchinson, H.G., Fujinaga, M., Hayashida, W., Morishita, R., Zhang, L., Horiuchi, M., Pratt, R.E., Dzau, V.J., 1995. The angiotensin II type 2 (AT2) receptor antagonizes the growth effects of the AT1 receptor: gain-of-function study using gene transfer. *Proc. Natl. Acad. Sci. U. S. A.* 92, 10663–10667.
- Nistri, S., Chiappini, L., Sassoli, C., Bani, D., 2003. Relaxin inhibits lipopolysaccharide-induced adhesion of neutrophils to coronary endothelial cells by a nitric oxide-mediated mechanism. *FASEB J.* 17, 2109–2111.
- Nistri, S., Cinci, L., Perna, A.M., Masini, E., Bani, D., 2008. Mast cell inhibition and reduced ventricular arrhythmias in a swine model of acute myocardial infarction upon therapeutic administration of relaxin. *Inflamm. Res.* 57 (Suppl. 1), S7–S8.
- Paolillo, M., Peters, S., Schramm, A., Schlossmann, J., Feil, R., 2018. Real-time imaging reveals augmentation of glutamate-induced Ca(2+) transients by the NO-cGMP pathway in cerebellar granule neurons. *Int. J. Mol. Sci.* 19.
- Pini, A., Boccalini, G., Lucarini, L., Catarinichia, S., Guasti, D., Masini, E., Bani, D., Nistri, S., 2016. Protection from cigarette smoke-induced lung dysfunction and damage by H2 relaxin (serelaxin). *J. Pharmacol. Exp. Therapeut.* 357, 451–458.
- Praveen, P., Bathgate, R.A., Hossain, M.A., Patil, N.A., 2017. A single-chain derivative of the relaxin hormone is a functionally selective agonist of the G protein-coupled receptor. In: *RXFP1, 6th Modern Solid Phase Peptide Synthesis & its Applications Symposium*. Queensland, Australia, pp. 55.
- Raleigh, J.V., Mauro, A.G., Devarakonda, T., Marchetti, C., He, J., Kim, E., Filippone, S., Das, A., Toldo, S., Abbate, A., Salloum, F.N., 2017. Reperfusion therapy with recombinant human relaxin-2 (Serelaxin) attenuates myocardial infarct size and NLRP3 inflammasome following ischemia/reperfusion injury via eNOS-dependent mechanism. *Cardiovasc. Res.* 113, 609–619.
- Royce, S.G., Shen, M., Patel, K.P., Huuskens, B.M., Ricardo, S.D., Samuel, C.S., 2015. Mesenchymal stem cells and serelaxin synergistically abrogate established airway fibrosis in an experimental model of chronic allergic airways disease. *Stem Cell Res.* 15, 495–505.
- Samuel, C.S., Cendrawan, S., Gao, X.-M., Ming, Z., Zhao, C., Kiriazis, H., Xu, Q., Tregear, G.W., Bathgate, R.A.D., Du, X.-J., 2011. Relaxin remodels fibrotic healing following myocardial infarction. *Lab. Invest.* 91, 675–690.
- Samuel, C.S., Royce, S.G., Chen, B., Cao, H., Gossen, J.A., Tregear, G.W., Tang, M.L.K., 2009. Relaxin family peptide receptor-1 protects against airway fibrosis during homeostasis but not against fibrosis associated with chronic allergic airways disease. *Endocrinology* 150, 1495–1502.
- Samuel, C.S., Royce, S.G., Hewitson, T.D., Denton, K.M., Cooney, T.E., Bennett, R.G., 2017. Anti-fibrotic actions of relaxin. *Br. J. Pharmacol.* 174, 962–976.
- Samuel, C.S., Unemori, E.N., Mookerjee, I., Bathgate, R.A., Layfield, S.L., Mak, J., Tregear, G.W., Du, X.J., 2004a. Relaxin modulates cardiac fibroblast proliferation, differentiation, and collagen production and reverses cardiac fibrosis in vivo. *Endocrinology* 145, 4125–4133.
- Samuel, C.S., Zhao, C., Bathgate, R.A., Bond, C.P., Burton, M.D., Parry, L.J., Summers, R.J., Tang, M.L., Amento, E.P., Tregear, G.W., 2003. Relaxin deficiency in mice is associated with an age-related progression of pulmonary fibrosis. *FASEB J.* 17, 121–123.
- Samuel, C.S., Zhao, C., Bathgate, R.A., Du, X.J., Summers, R.J., Amento, E.P., Walker, L.L., McBurnie, M., Zhao, L., Tregear, G.W., 2005. The relaxin gene-knockout mouse: a model of progressive fibrosis. *Ann. N. Y. Acad. Sci.* 1041, 173–181.
- Samuel, C.S., Zhao, C., Bond, C.P., Hewitson, T.D., Amento, E.P., Summers, R.J., 2004b. Relaxin-1-deficient mice develop an age-related progression of renal fibrosis. *Kidney Int.* 65, 2054–2064.
- Sarwar, M., Samuel, C.S., Bathgate, R.A., Stewart, D.R., Summers, R.J., 2015. Serelaxin-mediated signal transduction in human vascular cells: bell-shaped concentration-response curves reflect differential coupling to G proteins. *Br. J. Pharmacol.* 172, 1005–1019.
- Sassoli, C., Chellini, F., Pini, A., Tani, A., Nistri, S., Nosi, D., Zecchi-Orlandini, S., Bani, D., Formigli, L., 2013. Relaxin Prevents Cardiac Fibroblast-Myofibroblast Transition via Notch-1-Mediated Inhibition of TGF- β /Smad3 Signaling. *PLoS One* 8, e63896.
- Schinner, E., Wetzl, V., Schramm, A., Kees, F., Sandner, P., Stasch, J.P., Hofmann, F., Schlossmann, J., 2017. Inhibition of the TGF β signalling pathway by cGMP and cGMP-dependent kinase I in renal fibrosis. *FEBS Open Bio* 7, 550–561.
- Seibold, J.R., Korn, J.H., Simms, R., Clements, P.J., Moreland, L.W., Mayes, M.D., Furst, D.E., Rothfield, N., Steen, V., Weisman, M., Collier, D., Wigley, F.M., Merkel, P.A., Csuka, M.E., Hsu, V., Rocco, S., Erikson, M., Hannigan, J., Harkonen, W.S., Sanders, M.E., 2000. Recombinant human relaxin in the treatment of scleroderma. A randomized, double-blind, placebo-controlled trial. *Ann. Intern. Med.* 132, 871–879.
- Suzuki, Y., Ruiz-Ortega, M., Lorenzo, O., Ruperez, M., Esteban, V., Egido, J., 2003. Inflammation and angiotensin II. *Int. J. Biochem. Cell Biol.* 35, 881–900.
- Unemori, E.N., Amento, E.P., 1990. Relaxin modulates synthesis and secretion of procollagenase and collagen by human dermal fibroblasts. *J. Biol. Chem.* 265, 10681–10685.
- Unemori, E.N., Pickford, L.B., Salles, A.L., Piercy, C.E., Grove, B.H., Erikson, M.E., Amento, E.P., 1996. Relaxin induces an extracellular matrix-degrading phenotype in human lung fibroblasts in vitro and inhibits lung fibrosis in a murine model in vivo. *J. Clin. Invest.* 98, 2739–2745.
- Valkovic, A.L., Leckey, M.B., Whitehead, A.R., Hossain, M.A., Inoue, A., Kocan, M., Bathgate, R.A.D., 2018. Real-time examination of cAMP activity at relaxin family peptide receptors using a BRET-based biosensor. *Pharmacol Res Perspect* 6, e00432.
- Van Linthout, S., Miteva, K., Tschöpe, C., 2014. Crosstalk between fibroblasts and inflammatory cells. *Cardiovasc. Res.* 102, 258–269.
- Wang, C., Kemp-Harper, B.K., Kocan, M., Ang, S.Y., Hewitson, T.D., Samuel, C.S., 2016. The anti-fibrotic actions of relaxin are mediated through a NO-sGC-cGMP-Dependent pathway in renal myofibroblasts in vitro and enhanced by the NO donor, diethylamine NONOate. *Front. Pharmacol.* 7, 91.
- Wang, D., Luo, Y., Myakala, K., Orlicky, D.J., Dobrinskikh, E., Wang, X., Levi, M., 2017. Serelaxin improves cardiac and renal function in DOCA-salt hypertensive rats. *Sci. Rep.* 7, 9793.
- Weber, K.T., Brilla, C.G., Campbell, S.E., Guarda, E., Zhou, G., Sriram, K., 1993. Myocardial fibrosis: role of angiotensin II and aldosterone. *Basic Res. Cardiol.* 88 (Suppl. 1), 107–124.
- Wetzl, V., Schinner, E., Kees, F., Faerber, L., Schlossmann, J., 2017. Differences in the renal antifibrotic cGMP/cGKI-dependent signaling of serelaxin, zaprinast, and their combination. *Naunyn-Schmiedeberg's Arch. Pharmacol.* 390, 939–948.
- Wetzl, V., Schinner, E., Kees, F., Hofmann, F., Faerber, L., Schlossmann, J., 2016. Involvement of cyclic guanosine monophosphate-dependent protein kinase I in renal antifibrotic effects of serelaxin. *Front. Pharmacol.* 7, 195.
- Williams, E.J., Benyon, R.C., Trim, N., Grove, B.H., Arthur, M.J., Unemori, E.N., Iredale, J.P., 2001. Relaxin inhibits effective collagen deposition by cultured hepatic stellate cells and decreases rat liver fibrosis in vivo. *Gut* 49, 577–583.

- Wynn, T.A., 2008. Cellular and molecular mechanisms of fibrosis. *J. Pathol.* 214, 199–210.
- Yang, J., Chen, C., Ren, H., Han, Y., He, D., Zhou, L., Hopfer, U., Jose, P.A., Zeng, C., 2012. Angiotensin II AT(2) receptor decreases AT(1) receptor expression and function via nitric oxide/cGMP/Sp1 in renal proximal tubule cells from Wistar-Kyoto rats. *J. Hypertens.* 30, 1176–1184.
- Yoshida, T., Kumagai, H., Kohsaka, T., Ikegaya, N., 2014. Protective effects of relaxin against cisplatin-induced nephrotoxicity in rats. *Nephron Exp. Nephrol.* 128, 9–20.
- Yoshida, T., Kumagai, H., Kohsaka, T., Ikegaya, N., 2013. Relaxin protects against renal ischemia-reperfusion injury. *Am. J. Physiol.* 305, F1169–F1176 Renal physiology.
- Yue, Y., Meng, K., Pu, Y., Zhang, X., 2017. Transforming growth factor beta (TGF-beta) mediates cardiac fibrosis and induces diabetic cardiomyopathy. *Diabetes Res. Clin. Pract.* 133, 124–130.
- Zeisberg, E.M., Tarnavski, O., Zeisberg, M., Dorfman, A.L., McMullen, J.R., Gustafsson, E., Chandraker, A., Yuan, X., Pu, W.T., Roberts, A.B., Neilson, E.G., Sayegh, M.H., Izumo, S., Kalluri, R., 2007. Endothelial-to-mesenchymal transition contributes to cardiac fibrosis. *Nat. Med.* 13, 952–961.
- Zhang, X., Fu, Y., Li, H., Shen, L., Chang, Q., Pan, L., Hong, S., Yin, X., 2018. H3 relaxin inhibits the collagen synthesis via ROS- and P2X7R-mediated NLRP3 inflammasome activation in cardiac fibroblasts under high glucose. *J. Cell Mol. Med.* 22, 1816–1825.
- Zhang, X., Pan, L., Yang, K., Fu, Y., Liu, Y., Chen, W., Ma, X., Yin, X., 2017. Alterations of relaxin and its receptor system components in experimental diabetic cardiomyopathy rats. *Cell Tissue Res.* 370, 297–304.
- Zhao, L., Samuel, C.S., Tregear, G.W., Beck, F., Wintour, E.M., 2000. Collagen studies in late pregnant relaxin null mice. *Biol. Reprod.* 63, 697–703.
- Zheng, G., Cai, J., Chen, X., Chen, L., Ge, W., Zhou, X., Zhou, H., 2017. Relaxin ameliorates renal fibrosis and expression of endothelial cell transition markers in rats of isoproterenol-induced heart failure. *Biol. Pharm. Bull.* 40, 960–966.
- Zhou, X., Chen, X., Cai, J.J., Chen, L.Z., Gong, Y.S., Wang, L.X., Gao, Z., Zhang, H.Q., Huang, W.J., Zhou, H., 2015. Relaxin inhibits cardiac fibrosis and endothelial-mesenchymal transition via the Notch pathway. *Drug Des. Dev. Ther.* 9, 4599–4611.